Open Research Online

The Mechanistic Role of Long Non-coding RNAs in Advanced Prostate Cancer Response to Therapy

Thesis

oro.open.ac.uk

School of Life, Health and Chemical Sciences

The mechanistic role of long non-coding RNAs in advanced prostate cancer response to therapy

Perla Pucci

A Thesis submission to the Open University for the degree of

Doctor of Philosophy

December 2019

DECLARATION

I declare that the work presented in this thesis is my own and acknowledgements to other researchers who contributed in relevant parts of the text are included. This work does not contain any material submitted for awards or other degree.

ABSTRACT

Prostate cancer is one of the most common malignancies and the fifth leading cause of cancer related deaths in males, worldwide. It is commonly treated using androgen deprivation therapy (ADT), but around 25% develop ADT resistance and are called Castration-Resistant Prostate Cancers (CRPCs). Therapies currently used for CRPC treatment include: the new generation anti-androgen enzalutamide, the taxane cabazitaxel and carboplatin. Despite the prolonged survival resulting from these treatments, CRPC is still incurable. Recent evidence suggests that long non-coding RNAs (lncRNAs) promote drug resistance. The lncRNA *HORAS5* (i.e. *linc00161*) regulates drug response in different cancers and is upregulated in CRPC versus hormone-sensitive patient-derived xenografts (PDXs), thereby stimulating pro-survival mechanisms. This project has investigated whether *HORAS5* has a role in CRPC response to therapy. CRPC cells have been treated with different concentrations of cabazitaxel, carboplatin and enzalutamide. Cabazitaxel exposure increases *HORAS5* expression, in androgen receptor-positive (AR^+) and -negative (AR^-) prostate cancer cells and *HORAS5* overexpression decreases cabazitaxel sensitivity and cell apoptosis. *HORAS5* RNA interference (RNAi) increases cabazitaxel sensitivity and cell apoptosis. Next-generation RNA sequencing and real time qPCR have shown that the anti-apoptotic factor *BCL2A1* is significantly upregulated upon *HORAS5* overexpression in AR^- prostate cancer cells exposed to cabazitaxel. *BCL2A1* silencing decreases cell count and increases apoptosis of prostate cancer cells exposed to cabazitaxel. *HORAS5* and *BCL2A1* upregulation is associated with decreased survival in prostate cancer patients and *HORAS5* is upregulated in clinical samples from prostate cancer patients exposed to taxanes. Transfection of CRPC cells with *HORAS5*-targeting antisense oligonucleotides (ASOs) efficiently reduces *HORAS5* expression, thereby decreasing cabazitaxel IC_{50} when tested in combination with this drug. Overall, this project shows that *HORAS5* stimulates *BCL2A1* expression in prostate cancer cells, thereby reducing caspase-mediated apoptosis. This leads to increased cabazitaxel resistance. The clinical relevance of *HORAS5* expression and the effect of *HORAS5*-targeting ASOs shown in this thesis highlight the translational potential of *HORAS5* modulation. This work sheds light on the relevance of lncRNAs in cancer drug resistance and proposes the use of *HORAS5* as a future therapeutic target to increase therapy efficacy in CRPC.

ACKNOWLEDGMENTS

Table of Contents

List of Figures

List of Tables

ABBREVIATIONS

AA: abiraterone acetate

ABCB1: ATP binding cassette subfamily B member 1

ABCC1: ABC Subfamily C Member 1

ADT: androgen deprivation therapy

AKT: protein kinase B

ANRIL: Antisense Noncoding RNA In The INK4 Locus

AR: androgen receptor

AR$^-$: androgen receptor-negative

AR$^+$: androgen receptor-positive

ARE: androgen response elements

AR-V7: Androgen receptor spice variant-7

ASO: antisense oligonucleotide

Bax: bcl-2-associated X protein

BCL2: B-cell lymphoma 2

BCL2A1: Bcl2-Related Protein A1

BIK: Bcl2-interacting killer

bp: base pairs

BRCA: Breast Cancer Susceptibility Protein

BSA: bovine serum albumin

CAB: combined androgen blockade

CCAT1: Colon Cancer Associated Transcript 1

ceRNA: competing endogenous RNA

CHGA: chromogranin A

CMV: cytomegalovirus

CRPC: Castration-Resistant Prostate Cancer

Ct: cycle threshold

CTCs: circulating tumour cells

DMSO: dimethyl sulfoxide

DNA: Deoxyribonucleic acid

DsiRNA: Dicer-Substrate siRNA

EDTA: ethylenediaminetetraacetic acid

EMT: Epithelial to mesenchymal transition

ER: oestrogen receptor

EZH2: enhancer of zeste homolog 2

FDA: Food and Drugs Administration

FSCN1: fascin actin-bundling protein 1

GalNAc: N-acetylgalactosamine

GAPDH: glyceraldehyde 3-phosphate dehydrogenase

GAS5: growth arrest specific 5

GEA: gene expression assay

H3K27: lysine 27 on histone 3

HBSS: Hanks' Balanced Salt Solution

HCC: hepatocellular carcinoma

HORAS: hormone resistance associated non-coding sequences

HOTAIR: HOX Transcript Antisense RNA

HPRT1: hypoxanthine phosphoribosyltransferase 1

HRR: homologous recombination repair

HSP: Heat shock protein

IC$_{50}$: half-maximal inhibitory concentration

IFIT2: Interferon Induced Protein with Tetratricopeptide Repeats 2

KD: knockdown

LH: luteinizing hormone

LHRH: luteinizing hormone-releasing hormone

lincRNAs: intergenic lncRNAs

LNA: locked nucleic acids

LncRNA: long non-coding RNA

LTR: long terminal repeat

mAb: monoclonal antibody

MALAT1: Metastasis Associated Lung Adenocarcinoma Transcript 1

MAPK: mitogen-activated protein kinase

mCRPC: metastatic CRPC

MDR: multi-drug resistance protein

MGB: minor groove binder

MIAT: myocardial infarction associated transcript

miRNA: microRNA

mTOR: mammalian target of rapamycin

NC: negative control

ncRNA: noncoding RNA

NE: neuroendocrine

NEC: neuroendocrine cell

NEPC: neuroendocrine prostate cancer

NF-kβ: nuclear factor kappa-light-chain-enhancer of activated B cells

NHEJ: non-homologous end joining

NOS: reactive nitrogen species

PANDA: P21-associated noncoding RNA DNA damage-activated

PCAT: prostate cancer-associated transcript

PCGEM: Prostate Cancer Gene Expression Marker 1

Pdcd5: programmed cell death protein 5

PDXs: patient-derived xenografts

PFS: progression-free survival

PI3K: phosphoinositide 3-kinases

PIN: prostatic intra-epithelial neoplasia

PRC: polycomb repressive complex

PSA: prostate specific antigen

PS-ASO: Phosphorothioate ASO

PTEN: phosphatase and tensin homologue

RISC: RNA-induced silencing complex

RNA: Ribonucleic acid

RNAi: RNA interference

ROS: reactive oxygen species

RT-qPCR: quantitative reverse transcription polymerase chain reaction

SDS: sodium dodecyl sulfate

siRNA: small interfering RNAs

SNHG12: Small Nucleolar RNA Host Gene 12

snoRNA: small nucleolar RNA

STAT3: signal transducer and activator of transcription 3

TBS: Tris-Buffered Saline

TDRG1: testis developmental related gene 1

TEAD1: Transcriptional Enhancer Factor 1

TF: transcription factor

TFBS: transcription factor binding site

UCA1: urothelial cancer associated 1

WT: wild-type

ZEB1-AS1: Zinc Finger E-Box Binding Homeobox 1- Antisense RNA 1

DEGs: differentially expressed genes

TCGA: The Cancer Genome Atlas

PUBLICATIONS AND CONFERENCE ITEMS

Publications

Perla Pucci, Erik Venalainen, Ilaria Alborelli, Luca Quagliata, Pasquale Rescigno, Rebecca Mather, Cheryl Hawkes, Ignacio Romero, Sushila Rigas, Yuzhuo Wang, Francesco Crea (2019). The long non-coding RNA *HORAS5* promotes cabazitaxel resistance in castration resistant prostate cancer via a BCL2A1-dependent survival mechanism. Epigenomics (under review).

Rebecca L. Mather, Erik Venalainen, Ilaria Alborelli, Dong Lin, Elena Jachetti, Mario P Colombo, Hui Xue, Perla Pucci, Xinpei Ci, Cheryl Hawkes, Hardev Pandha, Igor Ulitsky, Luca Quagliata, Wei Jiang, Ignacio Romero, Yuzhuo Wang, Francesco Crea (2019). The evolutionarily conserved long non-coding RNA *NEAR1* activates the FOXA2 transcriptional programme and promotes neuroendocrine prostate cancer proliferation. Clinical Cancer Research (under review).

Perla Pucci, Wallace Yuen, Erik Venalainen, David Roig Carles, Yuzhuo Wang, Francesco Crea (2019). Long non-coding RNAs and cancer cells' drug resistance: an unexpected connection. Chapter for the Springer book THE CHEMICAL BIOLOGY OF LONG NONCODING RNAs (Accepted).

Roberto Silvestri, Perla Pucci, Erik Venalainen, Chrysanthi Matheou, Rebecca Mather, Stephen Chandler, Romina Aceto, Sushilaben H Rigas, Yuzhuo Wang, Katja Rietdorf, Martin David Bootman, Francesco Crea (2019). T-type calcium channels drive the proliferation of androgen-receptor negative prostate cancer cells. Prostate, 79, pp.1580-1586.

Jasmine Cassar White, Perla Pucci, Francesco Crea (2019). The role of histone lysine demethylases in cancer cells' resistance to tyrosine kinase inhibitors. Cancer Drug Resistance, 2:326-334.

Parolia Abhijit, Venalainen Erik, Xue Hui, Mather Rebecca, Lin Dong, Wu Rebecca, Pucci Perla, Rogalski Jason, Evans Joseph, Feng Felix, Collins Colin, Wang Yuzhuo, Crea Francesco (2019). The long non-coding RNA *HORAS5* mediates castration-resistant prostate cancer survival by activating the androgen receptor transcriptional program. Molecular Oncology, 13(5), pp. 1121-1136.

Perla Pucci, Pasquale Rescigno, Semini Sumanasuriya, Johann de Bono, Francesco Crea (2018). Hypoxia and Noncoding RNAs in Taxane Resistance. Trends in Pharmacological Sciences, 39(8), pp. 695-709.

Chiara De Santi, Perla Pucci, Alessandra Bonotti, Ombretta Melaiu, Monica Cipollini, Elisa Barone, Elisa Paolicchi, Alda Corrado, Irene Lepori, Irene Dell'Anno, Lucia Pelle', Luciano Mutti, Rudy Foddis, Alfonso Cristaudo, Federica Gemignani and Stefano Landi (2017). Mesothelin promoter variants are associated with increased Soluble-Mesothelin Related Peptide (SMRP) levels in asbestos-exposed individuals. Occupational Environmental Medicine, 74 (6), pp.456-463.

Perla Pucci (2017). Genomic "dark matter": a key to understand cancer biology? Article available on OpenLearn platform, The Open University.

Conference items

Perla Pucci, Erik Venalainen, Ilaria Alborelli, Luca Quagliata, Pasquale Rescigno, Rebecca Mather, Cheryl Hawkes, Ignacio Romero, Sushila Rigas, Yuzhuo Wang, Francesco Crea (2019). 1986PD *HORAS5* promotes cabazitaxel resistance in castration resistant prostate cancer via a BCL2A1-dependent survival mechanism. Annals of Oncology, 30 (Supplement_5) and Conference poster, selected also for poster discussion: ESMO Congress 2019.

Rebecca Mather, Erik Venalainen, Perla Pucci, Dong Lin, Hui Xue, Yuzhuo Wang, Francesco Crea (2017). The long non-coding RNA *NEAR1* promotes neuroendocrine prostate cancer cell proliferation and survival. Conference poster: 3rd International Cancer Symposium, CRCL.

Perla Pucci, Erik Venalainen, Rebecca Mather, Sushila Rigas, Ignacio Romero, Yuzhuo Wang, Francesco Crea (2017). Identification of a long non-coding RNA that mediates response to therapy in castration-resistant prostate cancer. Conference poster: 3rd International Cancer Symposium, CRCL.

CHAPTER 1: INTRODUCTION

1.1. Prostate cancer: overview and progression

Prostate cancer is a neoplasm arising in the prostate, which is a small, walnut-shaped organ that represents the most common site of neoplastic transformation in the male human body (Antony *et al.*, 2014). The prostate is a gland of the male reproductive system (fig.1.1A), located around the urethra, at the base of the bladder where it exerts its main function, i.e. secreting proteins into the seminal fluid to provide protection and nourishment to sperm (Crea, Venalainen, *et al.*, 2016). Histologically it is composed by a pseudo-stratified epithelium constituted by luminal, basal and neuroendocrine cells (NECs) (fig.1.1B) (Crea, Venalainen, *et al.*, 2016). Luminal cells represent the most abundant cell type; their main function is to produce keratins and secretory proteins, such as the prostate specific antigen (PSA). Basal cells express different kinds of keratins and other proteins; NECs represent the least frequent component (<1%) of the prostate normal epithelium and express neuroendocrine (NE)-specific markers (Crea, Venalainen, *et al.*, 2016).

A
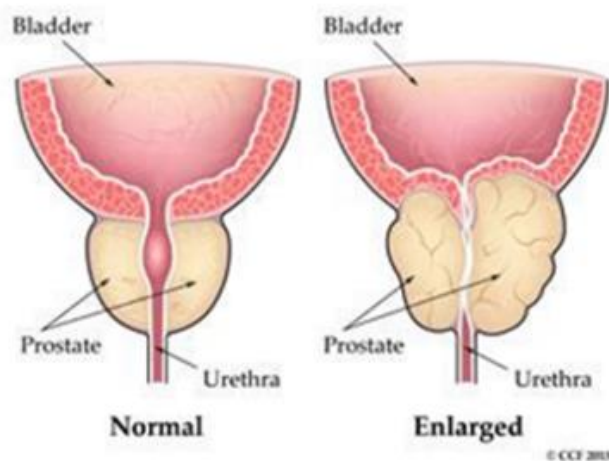
B
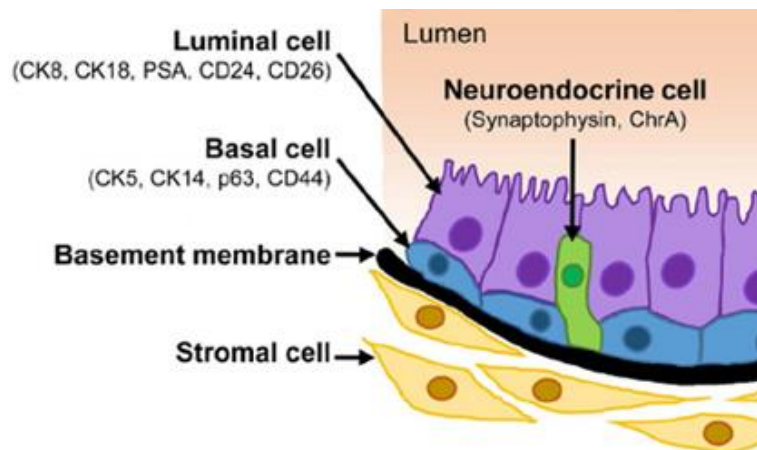
Figure1.1| Representation of prostate`s location in the human body and schematic representation of the cellular structure of prostate epithelium.
A. The prostate is a small gland of the male reproductive system, which becomes bigger with age (The Cleveland Clinic Foundation, 2017). **B.** The cellular structure of prostate epithelium consists of an inner layer with secretory luminal cells surrounded by a layer of basal cells in contact with the basement membrane that separates stromal cells from the epithelium. NECs spread throughout the epithelium and form just the 1% of it. Each cell type has specific characteristics and expresses specific proteins (*in brackets*); modified from Rybak et al., 2014 (Rybak, Bristow and Kapoor, 2014).

The neoplastic transformation of the prostate epithelium is more frequent in older

individuals. Prostate cancer is a heterogeneous disease (Crea, Quagliata, *et al.*, 2016)

which represents the most commonly diagnosed malignancy worldwide (Fan Liancheng,

Wang Yanqing, Chi Chenfei, Pan Jiahua, Shangguan Xun, Xin Zhixiang, Hu Jianian, Zhou Lixin, Dong Baijun, 2017) and the second cause of cancer-related deaths among men in western countries. Worldwide, the incidence of prostate cancer is rising and this is partially attributable to the increasing life expectancy (Lin *et al.*, 2017). The majority of prostate cancers are driven by the activation of the androgen receptor (AR) signalling (fig.1.2), triggered by the interaction of AR with androgens, mainly produced by the testis, which stimulates pathways involved in proliferation and survival (Stice *et al.*, 2017). Prostate cancers have been suggested to originate from the luminal lineage with an over-activation of AR, which triggers epithelial proliferation and favours the accumulation of genetic mutations (Xin, 2013). A second theory suggests that basal cells can also originate prostate cancer, via acquisition of luminal lineage features (Xin, 2013). Prostate cancer is a heterogeneous disease, since it can be characterized by various phenotypical, histological and molecular characteristics. Some stages of cellular and molecular transformation of the prostate epithelium have been recognised and often associated with prostate cancer progression:

1. Prostatic intra-epithelial neoplasia (PIN) is characterized by hyperplasia of the luminal epithelium, decrease in the number of basal cells that are still present and enlargement of nuclei and nucleoli. Although PIN has not been clinically demonstrated to be a precursor of prostate cancer, some PIN cases are at the initial stage of the malignant transformation, especially when high grade PIN is identified. High grade PIN has an increase in the expression of proliferation markers and of telomerase activity. In PIN it is possible to find some mutations such as loss of function of *PTEN*, loss of heterozygosity in the *NKX3.1* homeobox gene and upregulation of nuclear MYC protein;

2. Localized adenocarcinoma has a luminal phenotype characterized by the total absence of p63 and other markers of basal cells. It is characterized by some mutations like the loss of PTEN and the *TMPRSS2-ERG* fusion, occurring in 50% of adenocarcinoma cases;

3. Metastatic prostate cancer is a phenotypically heterogeneous stage but molecular and cytogenetic analyses have shown that multiple metastases in the same patient are clonally related and that it could originate from selective pressure such as therapeutic intervention, promoting selective proliferation of these clones during the tumour progression. Some molecular features of this stage are *MYC* overexpression, ETS activation and deletion of *PTEN* (Shen and Abate-Shen, 2010; Shtivelman, Beer and Evans, 2014).

In most cases, prostate cancer is initially hormone-dependent and can be effectively treated with androgen deprivation therapy (ADT, i.e. chemical castration). It has been shown that after prolonged ADT, a substantial fraction (25%) of adenocarcinomas develops resistance to this therapy, mainly as a consequence of genetic and epigenetic alterations that allow for a ligand-independent activation of AR. These cancers are therefore called castration-resistant prostate cancer (CRPC).

Despite the development of new therapies, CRPC is still incurable. Therefore, the identification of more effective therapeutic targets is of paramount importance and can help explain the origin and evolution of CRPC. In the next sections, the clinical progression of prostate cancer from the most common form to the most aggressive subtypes is outlined (fig.1.2).
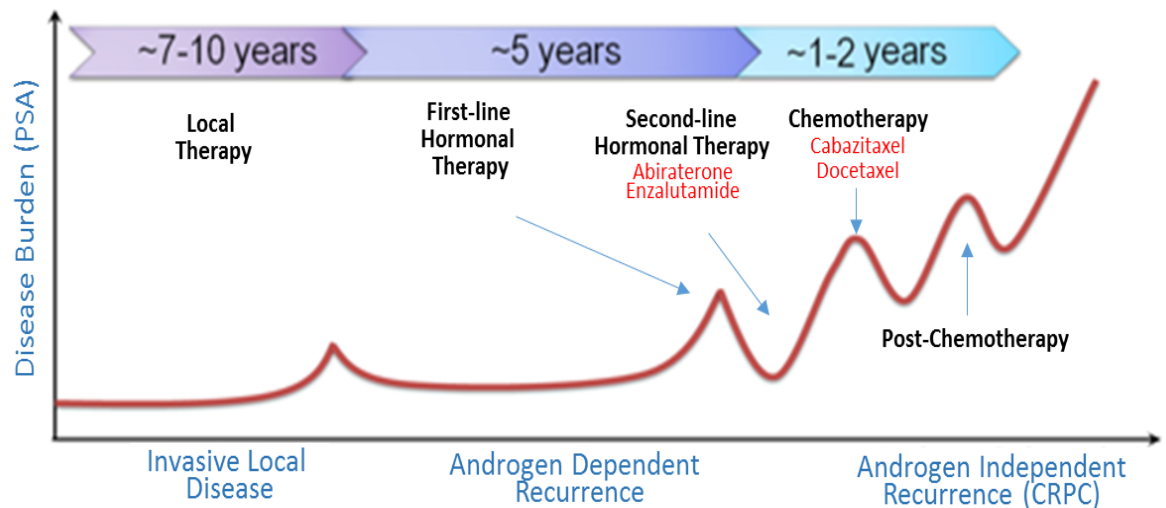
Figure1.2| The clinical progression of prostate cancer from the hormone-dependent forms treated with local and hormonal therapy to the most aggressive forms after the acquisition of castration resistance.
Most common therapies for CRPC are shown in red.

1.1.1. Hormone-dependent Prostate cancer

In 1941 Huggins established that prostate cancer was a hormone-dependent disease and could regress after castration. For this discovery, he won the Nobel Prize in 1966 (Toledo-pereyra, 2001). Male sex hormones are called androgens; testosterone and dihydrotestosterone are the most abundant androgens. Testosterone is mainly produced in the testes and its production is stimulated by luteinizing hormone (LH) produced in the pituitary gland, which is stimulated by luteinizing hormone-releasing hormone (LHRH), released by the hypothalamus (fig.1.3). The adrenal gland produces the remaining testosterone. Once produced, androgens are secreted into the prostate where they bind and activate the AR (National Cancer Institute, 2014), a member of the nuclear steroid receptor superfamily of ligand-dependent transcription factors (TFs) (Lu *et al.*, 2006). When inactive, the AR is located inside the cytoplasm of prostate cells, but upon binding to androgens, it changes its conformation and translocates into the

nucleus (Hsu *et al.*, 2017). Here, the AR creates homodimers, which recruit co-regulators to bind specific elements of the DNA, called androgen response elements (AREs); the AREs are located in the transcription regulation regions (e.g. promoters) of AR-target genes such as PSA. With this mechanism, androgens trigger the expression of several genes, thereby promoting the growth and function of the prostate that can result in uncontrolled proliferation. When this process is uncontrolled, it triggers the development and progression of hormone-dependent prostate cancers and it is therefore an ideal target to inhibit prostate cancer growth (National Cancer Institute, 2014; Shtivelman, Beer and Evans, 2014).
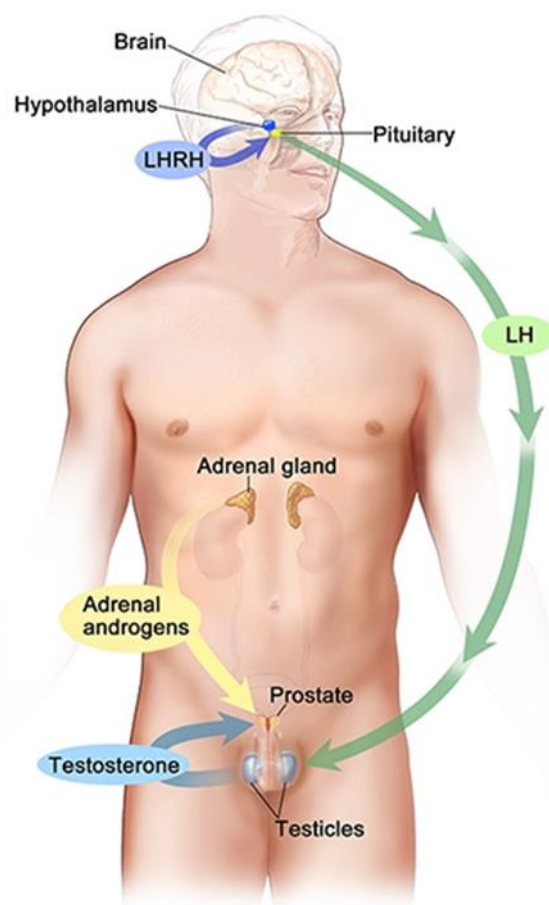
Figure1.3| Process of hormone production and activation to regulate androgens-AR interaction, thereby promoting prostate growth.
When this signalling pathway is uncontrolled prostate cells can initiate a malignant transformation.

Hormone-dependent prostate cancer is first diagnosed based on abnormally increased level of circulating PSA. PSA levels of 3 ng/ml or higher are considered critical for further investigation (Pezaro, Woo and Davis, 2014). Since elevated levels of PSA are frequently associated with non-neoplastic conditions, several areas of the prostate are biopsied, in order to confirm the presence of neoplastic cells. Subsequently, confirmed prostate cancers are graded based on Gleason Score. Higher scores are associated with less differentiation and worse prognosis. Different imaging techniques (MRI, CT scans) are used to visualize the neoplasm and determine the stage (local vs. metastatic prostate cancer). The most common sites of prostate cancer metastasis are pelvic lymph nodes, bones, liver and lung.

Localized hormone-dependent prostate cancers are commonly treated with surgery (prostatectomy) and/or radiotherapy (Toledo-pereyra, 2001; National Cancer Institute, 2014); when prostate cancer spreads to different sites and becomes metastatic, ADT is commonly employed; ADT reduces the levels of androgens, blocking the signalling pathway described above (fig.1.3). The main hormonal treatments in prostate cancer are: LHRH agonists, LHRH antagonists and reversible AR antagonists.

LHRH agonists reduce the levels of testosterone produced by the testicles. LHRH agonists can be injected under the skin from once a month to once a year, according to the specific drug used. At the beginning of the treatment LHRH agonists produce a brief and very low increase of testosterone that is called *flare* and can give side effects such as pain in bones if the tumour has spread to there (American Cancer Society, 2016). Subsequently, the LHRH agonists saturate the LHRH receptors and permanently inhibit testosterone production.

LHRH antagonists reduce testosterone levels more quickly and do not produce tumour flare like LHRH agonists. They are given once a month per injection under the skin and this is connected to some side effects such as pain, redness and swelling at the injection site. LHRH agonists and antagonists can stop the testicles from producing androgens, but other cells in the body, including prostate cancer cells themselves, can still produce small amounts, which can fuel cancer growth (American Cancer Society, 2016).

Other drugs stop androgens from working rather than suppressing androgen levels. They are called anti-androgens and prevent the interaction between androgens and AR, by competing with androgens for binding the AR (Lu *et al.*, 2006). Examples of anti-androgen are bicalutamide, apalutamide and darolutamide. Anti-androgens are taken daily as pills.

An anti-androgen can also be combined with orchiectomy or with an LHRH agonist as first-line hormone therapy. This is called combined androgen blockade (CAB) and has shown just small incremental benefits for patients (American Cancer Society, 2016).

There are also newer types of anti-androgens, such as abiraterone acetate (AA) and enzalutamide, which can be helpful when prostate cancer develops resistance to chemical castration and is therefore able to grow even in low or undetectable levels of androgens. This will be discussed in further detail later in this thesis (section 1.2.1).

1.1.2. Castration-resistant Prostate Cancer

CRPC is an incurable form of prostate cancer due to the ability of cancer cells to evade ADT-dependent growth inhibition. CRPC is often metastatic and associated with poor prognosis (Fan Liancheng, Wang Yanqing, Chi Chenfei, Pan Jiahua, Shangguan Xun, Xin

Zhixiang, Hu Jianian, Zhou Lixin, Dong Baijun, 2017). In the next sections are described the main characteristics of hormone resistant prostate cancers.

1.1.2.1. CRPC

After several cycles of ADT, some prostate cancers start to become resistant to castration therapy, since they need very low or undetectable levels of androgens to proliferate (National Cancer Institute, 2014). CRPC cells acquire this potential mainly through genetic and epigenetic alterations that increase the production or the activity of AR molecules (fig.1.4). This is possible via several processes:

1) The overexpression or genetic amplification of the *AR* gene.

2) *AR* mutations that increase AR affinity to androgens, or production of splice variants that lack the ligand-binding domain.

3) It is also possible that the hormone-independent phenotype occurs without any direct change in the *AR locus*; for example, the emergence of CRPC can be ascribed to alterations in signalling pathways that modulate the activity or expression of the AR (Schroder, 2008). An example is the capacity of CRPC cells to induce AR expression via NF-kB, a TF activated by the phosphoinositide 3-kinases (PI3K)/protein kinase B (AKT) signalling pathway (Y. Kim *et al.*, 2017).

4) CRPC cells can independently produce androgens, thereby self-sustaining neoplastic proliferation.

Hence, most CRPCs maintain AR expression and are still classified as adenocarcinomas.

CRPCs are associated with poorer prognosis and shorter survival (from around 10 years to around 1 year) than the hormone-sensitive prostate cancers and the mortality rate is still high (Lin *et al.*, 2017). Even if CRPC remains currently an incurable disease, chemotherapeutics (e.g. cabazitaxel) and second-generation hormonal therapies (e.g.

enzalutamide and AA) can effectively increase CRPC patient survival (de Bono *et al.*, 2010; Scher *et al.*, 2012; Ryan *et al.*, 2013, 2015; Crea, Venalainen, *et al.*, 2016; de Wit *et al.*, 2019). Since the hormone-resistance is often due to the alteration of the AR pathway, some of these new strategies to treat CRPC aim to inhibit AR signalling (Y. Kim *et al.*, 2017). They will be discussed in the next sections of this thesis.

However, these new therapies can also have a role in the further clinical progression of prostate cancer. Despite not clinically proven, there are studies suggesting that enzalutamide may exert a selective pressure that can promote the selection of AR negative (AR⁻) prostate cancer cells, which can further evolve in anaplastic prostate cancers such as NEPC (Aggarwal *et al.*, 2018; Y. Zhang *et al.*, 2018), a prostate cancer subtype, which is resistant to all hormone therapies, particularly aggressive and rapidly lethal, which will be described in the next section (X. Xu *et al.*, 2017).
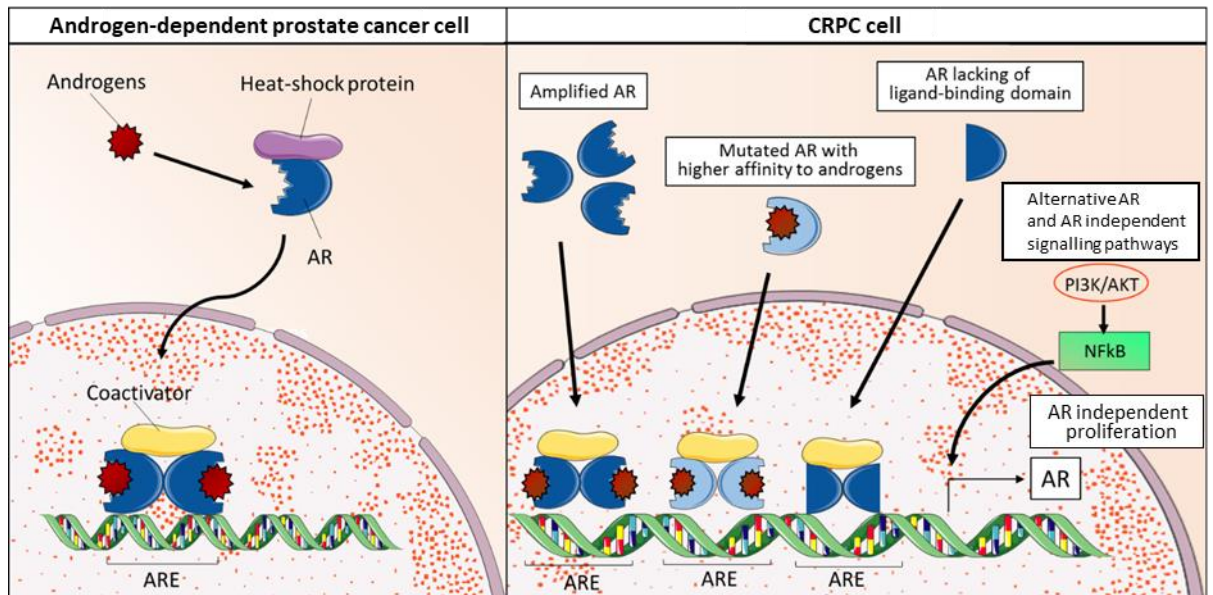
Figure1.4 | Mechanisms of prostate cancer proliferation in androgen-dependent prostate cancer and CRPC cells.
Left panel: activation of AR via binding with androgens and release from the heat-shock protein which binds the inactive form in the cytoplasm. The androgen-AR complex migrates into the nucleus where it dimerizes and interacts with coactivators to bind AREs to activate the transcription of AR-target genes. Right panel: mechanisms that trigger the proliferation of CRPC cells with low or undetectable levels of androgens: amplification of *AR* gene; mutations that increase the affinity of AR to androgens; production of constitutively active AR due to the lack of ligand-binding domains; activation of alternative pathways to upregulate AR or to stimulate cancer proliferation in AR independent manner.

1.1.2.2. Anaplastic prostate cancer

A minority of prostate cancers are resistant to all types of hormonal therapies, highly metastatic and characterized by low levels of *AR* expression with low or undetectable PSA and/or NE phenotype (Beltran *et al.*, 2016; Tsaur *et al.*, 2019). These characteristics fall within the classification of "anaplastic" CRPC (Tsaur *et al.*, 2019). When anaplastic CRPC has clear NE differentiation, with expression of NE markers and phenotype, the tumour is called NEPC (Tsaur *et al.*, 2019). NEPCs represent around the 0.5-2% of newly diagnosed prostate cancers, but almost 50% of CRPCs (Crea, Venalainen, *et al.*, 2016). NEPCs are composed of small NE–like cells with big nucleus and small cytoplasm

(Clermont *et al.*, 2015). Most NEPCs are AR[-] (X. Xu *et al.*, 2017) (fig.1.5A), even if some studies show that a fraction of NEPCs retain some AR expression (Crea, Venalainen, *et al.*, 2016). In any case, NEPC cells do not rely on AR activation for proliferation and survival. Moreover NEPC does not express adeno-prostate cancer markers such as PSA (Lin *et al.*, 2014; Zaffuto *et al.*, 2017) (fig.1.5A). The absent PSA expression hinders diagnosis at an early stage and monitoring of the progression of the tumour. NEPC cells express several NE proteins, such as synaptophysin, chromogranin A (CHGA), neural specific enolase and a variety of neuropeptides (Nouri *et al.*, 2017) (fig. 1.5A). Due to this molecular and phenotypic heterogeneity, several studies focused on the cellular origin of NEPC. The two main models postulate that NEPC can be created via malignant transformation of normal NEC or via transdifferentiation of adeno-prostate cancer cells into NEPC cells. These models are discussed below.

1) <u>Transformation of non-neoplastic NECs</u> (Crea, Venalainen, *et al.*, 2016): NECs, luminal and basal prostatic cells are the main components of the normal prostatic epithelium. Here, NECs regulate epithelial cell growth and differentiation. Unlike the other cell types, NECs do not require the presence of androgens to function properly and to proliferate (X. Xu *et al.*, 2017). Hence, it has been hypothesized that several cycles of ADTs can induce the proliferation and subsequently the neoplastic transformation of NECs, which would generate NEPCs.

2) <u>Transdifferentiation from adeno-prostate cancer cells into NEPC cells</u> (Lin *et al.*, 2014; Crea, Venalainen, *et al.*, 2016; Lee *et al.*, 2017)(fig.1.5B): Under particular conditions, adeno-prostate cancer cells could transdifferentiate into NEPC by losing AR expression and by acquiring NEC markers, via a mechanism that is still not completely elucidated. DNA Sequencing studies from clinical samples indicate that some NEPC clones derive

28

from CRPC-Adeno cells (Lee *et al.*, 2017). Pre-clinical experimental data support this model: AR+ LNCaP cells are capable of transdifferentiating into NEPC cells after prolonged androgen depletion, if other growth factors are supplemented (Beltran *et al.*, 2014; X. Xu *et al.*, 2017). According to this hypothesis, a study shows that adeno-prostate cancer patient-derived xenograft (PDX) develops NEPC relapse upon chemical castration therapy (Crea, Venalainen, *et al.*, 2016).

NE transdifferentiation, emerging from increasing treatment of advanced prostate cancer, is more common than transformation of non-neoplastic NECs ("*de novo* NEPC") (Crea, Venalainen, *et al.*, 2016; Tsaur *et al.*, 2019). NEPCs are usually diagnosed in individuals already affected by adeno-prostate cancers (Lin *et al.*, 2014). It is therefore conceivable that first and second-line hormonal therapies increase the chances of developing NEPC. After repeated cycles of hormonal therapy, NEPC cells can become the dominant population (Clermont *et al.*, 2015) since these cells can easily adapt to AR signalling suppression therapy and are highly proliferative (Crea, Venalainen, *et al.*, 2016). NEPC is often diagnosed at a metastatic stage and does not respond to any hormonal therapy and is therefore associated with very short average survival time (6-8 months) (Clermont *et al.*, 2015; J. Kim *et al.*, 2017; Lee *et al.*, 2017; Yadav *et al.*, 2017; Zaffuto *et al.*, 2017). Since according to the most accredited theories NEPC could originate from CRPC-Adeno, there is an urgent need to find new therapies (Clermont *et al.*, 2015) to both treat this neoplasm and to prevent the transdifferentiation of CRPC-Adeno into NEPC.
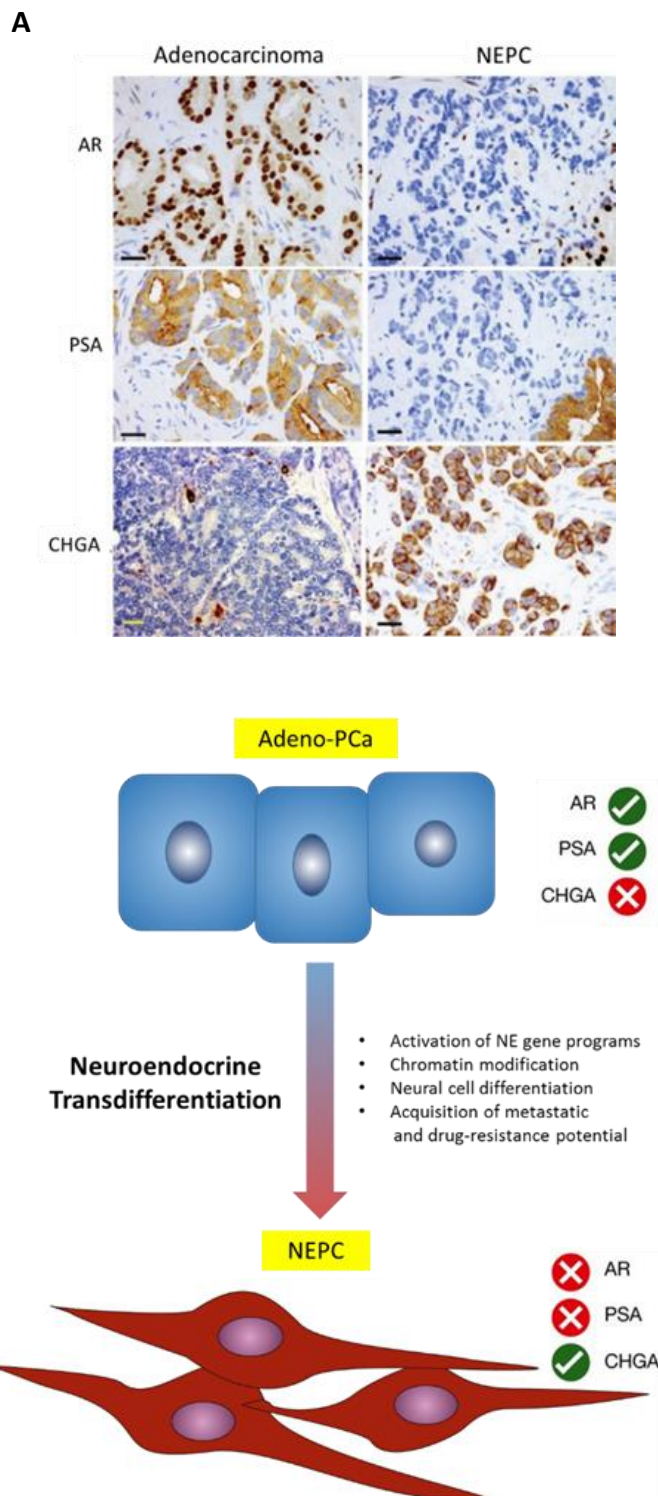
Figure1.5 | NEPC can originate from the transdifferentiation of adeno-prostate cancer.
A. Immunohistochemistry of adeno-prostate cancer vs NEPC. Adeno-prostate cancers express AR and PSA and are negative for NE markers such as CHGA. NEPCs lack the expression of AR and PSA but are positive for NE markers staining (CHGA); *Modified by Lipianskaya et al., 2014* (Lipianskaya *et al.*, 2014)*.* **B.** Schematic representation of the transdifferentiation from adeno-prostate cancer into NEPC. Under particular conditions, (e.g. prolonged androgen depletion), adeno-prostate cancer cells could lose AR expression and acquire NE markers, via a mechanism that is still not completely elucidated.

1.2. Drugs for the treatment of CRPC

After 18-24 months of ADT, 25% of patients can develop CRPC, which is currently incurable (Nouri *et al.*, 2017; X. Xu *et al.*, 2017). Hence, there is an urgent need to discover new compounds to target this disease. Despite the emergence of hormone-resistance, the expression and activity of AR is retained in most CRPC cases and most of the new therapeutic strategies aim to target this signalling pathway with higher efficacy (Fan Liancheng, Wang Yanqing, Chi Chenfei, Pan Jiahua, Shangguan Xun, Xin Zhixiang, Hu Jianian, Zhou Lixin, Dong Baijun, 2017).

Effective therapeutic options for CRPC include:

1) The use of immunotherapy with the antigen-presenting cell-based vaccine sipuleucel-T.

2) Internal radiotherapy with radium-223 chloride.

3) New generation hormone therapies: AA, enzalutamide.

4) Chemotherapy (taxanes and platinum agents).

In addition to these therapies, other options are available, such as the checkpoint inhibitor pembrolizumab, which showed antitumor activity in docetaxel-refractory metastatic CRPC (mCRPC) patients (Antonarakis *et al*., 2020). Moreover, these treatments are not all effective and each of these drugs has a variable response depending on the patient which underlines the heterogenicity of prostate cancer.

The next sections will examine in further detail new generation hormone therapies and chemotherapeutic agents, which are the focus of this research project.

These treatments, and their therapeutic indication, are summarized in table 1.1.

Table 1.1 | Drugs used for the treatment of CRPC examined in this research project.

Drug	Mechanism of action	Clinical indication
Enzalutamide	Irreversible AR antagonist	CRPC
Cabazitaxel	Microtubule disruption	CRPC, anaplastic prostate cancer
Carboplatin	DNA damage	Anaplastic prostate cancer

1.2.1. New generation hormonal treatments

The new generation hormonal treatments for CRPC include compounds that can block androgens biosynthesis or AR activity, thereby arresting AR$^+$ CRPC proliferation. In particular, several clinical trials have shown that AA and enzalutamide are highly effective in mCRPC, and that these drugs successfully prolong the survival of CRPC patients (National Cancer Institute, 2014; Sissung *et al.*, 2014; X. Xu *et al.*, 2017).

Abiraterone acetate (AA)

As discussed before, first line ADT blocks the production of testosterone by the testis. However, the adrenal gland and prostate cancer cells themselves can still produce androgens, which can drive the proliferation of CRPCs. AA is an inhibitor of adrenal gland and intra-tumour androgen synthesis (National Cancer Institute, 2014; Stice *et al.*, 2017; X. Xu *et al.*, 2017). AA can effectively promote androgen-deprivation, thereby resulting in survival benefits for CRPC patients (Sissung *et al.*, 2014). Phase III clinical trials have shown that AA in combination with prednisone can improve the overall survival of mCRPC patients pre-treated or not with chemotherapeutics (Ryan *et al.*, 2013, 2015). AA exerts its action by blocking CYP-17 lyase and hydroxylase, an enzyme which is

essential for the biosynthesis of androgens and adrenal hormones, resulting in undetectable levels of testosterone (Fan Liancheng, Wang Yanqing, Chi Chenfei, Pan Jiahua, Shangguan Xun, Xin Zhixiang, Hu Jianian, Zhou Lixin, Dong Baijun, 2017) (fig.1.6A).

Despite the effective inhibition of testosterone production, AA's effects on patients are very heterogeneous and around the 30% of patients are inherently resistant to this drug. Moreover, since CYP-17 affects also the androgen biosynthesis in healthy cells and is involved in the production and accumulation of other hormones (e.g. mineralocorticoids), there are doubts on the overall benefits of AA on CRPC patients (Sissung *et al.*, 2014; Fan Liancheng, Wang Yanqing, Chi Chenfei, Pan Jiahua, Shangguan Xun, Xin Zhixiang, Hu Jianian, Zhou Lixin, Dong Baijun, 2017). Indeed, common side effects include fluid retention, oedema, hypertension, and hypokalaemia, which are usually due to mineralocorticoid excess (Bedoya and Mitsiades, 2012).

Enzalutamide

Enzalutamide is a non-steroidal anti-androgen that interferes with the binding between androgens and AR (National Cancer Institute, 2014; Guo *et al.*, 2017). It has a high efficacy thanks to its strong binding affinity with AR and it can also block the translocation of AR to the nucleus and reduce the efficacy of the binding with AREs, thereby blocking proliferation and activating apoptosis in prostate cancer cells (Tran, 2009) (fig.1.6B). Despite enzalutamide showing efficacy in prostate cancer growth suppression, its effect is reduced in some prostate cancer cells and patients. Moreover, several cycles of treatment with this drug can result in the failure of AR inhibition in

CRPC, due the acquisition of AR mutations and alternative splice variants, which lack the androgen-binding domain (Lin *et al.*, 2013).

Mutations and alternative splicing can confer constitutive activity to the receptor, thereby rendering CRPC cells insensitive to enzalutamide. AR variant AR-V7 detection in circulating tumour cells from CRPC patients correlates with resistance to new-generation hormonal treatments, including enzalutamide (Antonarakis *et al.*, 2014). In particular, patients with expression of the variant AR-V7 have lower PSA response rates and shorter progression-free survival and overall survival (Antonarakis *et al.*, 2014).

Additionally, *in vitro*, *in vivo* and clinical studies have shown that prostate cancer prolonged enzalutamide treatment can promote NEPC differentiation and decrease overall survival in NEPC patients (Aggarwal *et al.*, 2018; Y. Zhang *et al.*, 2018).
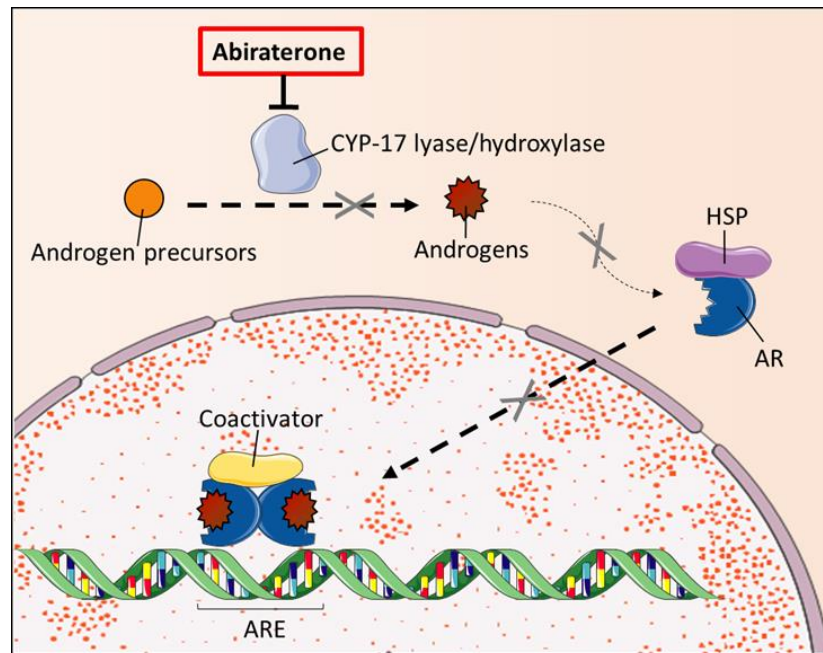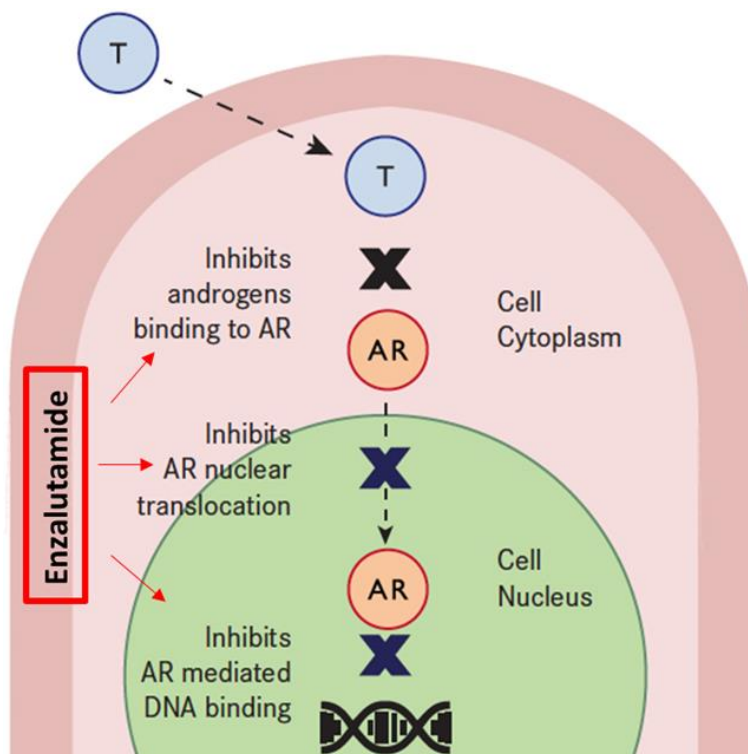
Figure1.6 | Mechanisms of action of AA and enzalutamide.
A. AA exerts its action by blocking CYP-17 lyase and hydroxylase, an enzyme which is essential for the biosynthesis of androgens and adrenal hormones, resulting in undetectable levels of testosterone. **B.** Enzalutamide blocks prostate cancer cells proliferation and induces cell death by interfering with AR function. Enzalutamide can interfere with the androgens-AR binding, block AR nuclear translocation or inhibit the interaction of AR with ARE. HSP: heat shock protein. T: testosterone. Modified from *Ammannagari and George, 2015* (Ammannagari and George, 2014).

As reported above, the use of both AA and enzalutamide can lead to resistance mechanisms such as mutations and the appearance of AR splice variants, which are constitutively active. The obstacles in targeting AR receptor underline the need of novel compounds to target CRPC, downstream the AR (Stice *et al.*, 2017). Considering that the response rate to these treatments is relatively short, that new mechanisms of resistance can rapidly occur and that some CRPC are AR⁻, other therapeutic options, such as chemotherapy, are used to treat CRPC patients (Stice *et al.*, 2017).

1.2.2. Taxanes

Taxanes are a family of chemotherapeutic agents employed for the treatment of a variety of tumours. They all derive from paclitaxel, a plant diterpenoid, which was extracted in 1967 from the Pacific yew tree (*Taxus brevifolia*) (Wani *et al.*, 1971). Paclitaxel was the first natural compound showing an action on microtubule stabilization (Wani *et al.*, 1971). Taxanes were introduced in the clinical use more than 30 years ago and, since then, the use of taxanes has increased, with improvements in their effects. In fact, since the discovery of the original compound, novel taxanes have been synthetized by chemical modification (Ojima *et al.*, 1999) such as docetaxel and cabazitaxel, which are characterized by improved mechanisms of actions, as described in more detail in the next paragraphs. Moreover, the development of novel taxane-based formulations can improve the clinical profile of these drugs. An example is the case of albumin-bound paclitaxel, also called Abraxane or nab-paclitaxel, which permits the transport and accumulation of paclitaxel in tumour areas, via the reversible binding of albumin

(Gradishar, 2006). This method increases paclitaxel efficacy and reduces its side effects, with consequent increase in patient response rate and survival (Gradishar, 2006; Stinchcombe, 2007; Takashima *et al.*, 2018). Except for albumin-bound paclitaxel, several clinical trials have demonstrated that taxanes, either alone or in combination with other agents, can improve cancer patient outcome of different cancers, including prostate (de Bono *et al.*, 2010; Quoix *et al.*, 2011; Pignata *et al.*, 2014; Muro *et al.*, 2016). Taxanes mainly interact with beta (β)-tubulin that, together with alpha (α)-tubulin constitutes microtubules (fig.1.7). The molecules of α- and β-tubulin form heterodimers that constitute the parallel protofilaments of microtubules, which are dynamic components. Microtubules dynamics is due to their continuous polymerization and depolymerisation via the use of energy from GTP-hydrolysis and interaction with several motor proteins and microtubule-associated proteins (Needleman *et al.*, 2005). Microtubule dynamics is essential for fundamental cellular processes such as mitosis and meiosis, to support and preserve cell shape and for correct molecular trafficking (Wang *et al.*, 1999; Needleman *et al.*, 2005; Churchill, Klobukowski and Tuszynski, 2015). As mentioned at the beginning of this section, taxanes are microtubules stabilizing agents, therefore via their binding with β-tubulin they inhibit microtubule depolymerisation, thereby disrupting microtubule dynamics and functions (Churchill, Klobukowski and Tuszynski, 2015). In particular taxane action on mitotic cells affects chromosome separation and blocks cell division, thereby hindering cell cycle progression and triggering apoptosis (Abal, Andreu and Barasoain, 2003; Weaver, 2014). Taxane involvement in microtubule instability damages many other cancer-specific functions in CRPC cells, such as secretion, intracellular signalling and migration (Smiyun, Azarenko, Miller, Rifkind, Lapointe, *et al.*, 2017). In addition to the evidence on taxanes

microtubule-binding functions, they have been suggested to have roles in processes that do not directly affect mitotic disruption. So far, taxanes mechanism of action has not been fully elucidated.

Previous work has shown that taxanes are involved in molecular trafficking, cell signalling and transport, and in interphase cancer cells death (Ganansia-Leymarie *et al.*, 2003; Herbst and Khuri, 2003; Weaver, 2014). Boundny and Nakano have shown that taxane-mediated apoptosis can be triggered via B-cell lymphoma 2 protein (bcl2) phosphorylation that inhibits this anti-apoptotic factor, thereby activating cell death signalling (Boudny and Nakano, 2002). Vice versa, antiapoptotic members of the bcl2 family , have been found involved in decreased response to taxanes in cancer cells (Xia *et al.*, 2006).

Different studies have proposed taxanes as regulators of other cellular functions such as mitochondrial activity, via alteration in their membrane features (Gabor Varbiro *et al.*, 2001) or ROS production, via taxane-mediated inhibition of antioxidant enzymes (Kosaka *et al.*, 2017). According to this evidence, taxanes seem to interact with several pathways, thereby affecting different cellular processes. This results in a broad anticancer effect (de Bono *et al.*, 2010; Lorch *et al.*, 2011; Quoix *et al.*, 2011; Pignata *et al.*, 2014; Muro *et al.*, 2016; Vogel *et al.*, 2016; Zielinski *et al.*, 2016).

In prostate cancer, taxanes seem to be active in both the nucleus and the cytoplasm of cancer cells, due to their action in both androgen-dependent (interfering with the correct production of regulators of the expression of androgen-dependent genes) and -independent mechanisms (Acharya *et al.*, 2017). Docetaxel and cabazitaxel are the most studied taxanes in CRPC and they have shown strong effects on prostate tumour growth (Smiyun, Azarenko, Miller, Rifkind, Lapointe, *et al.*, 2017).
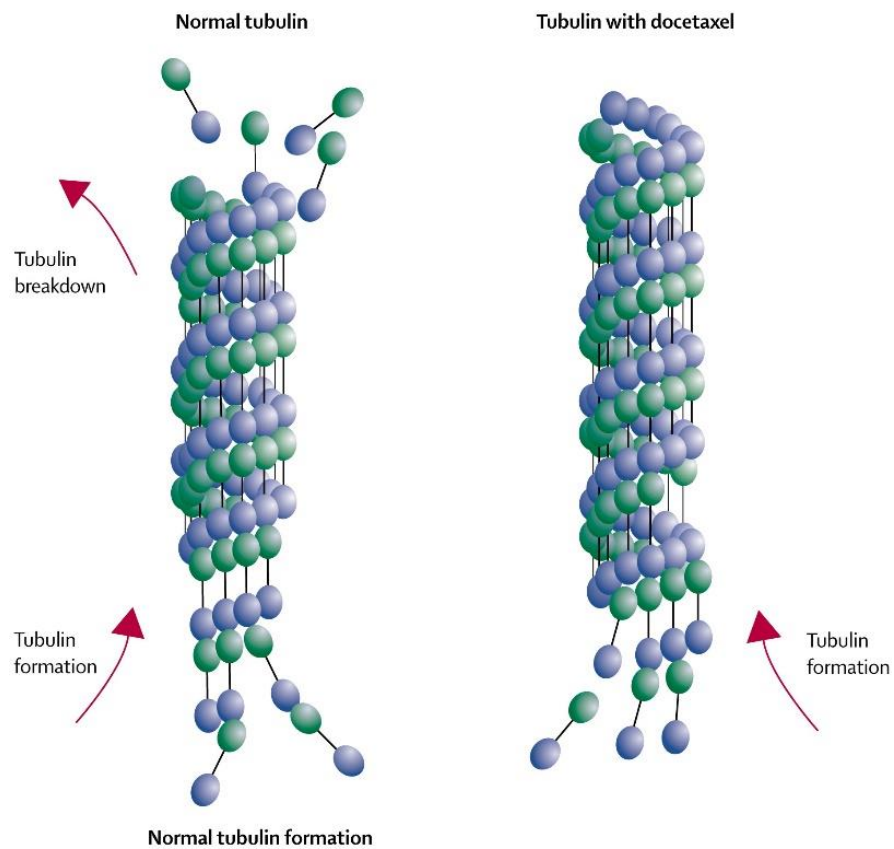
Figure1.7 | Mechanism of action of taxanes on microtubule function.
Taxanes are anticancer agents that target tubulin to disrupt microtubule function during cell division. Taxanes interact and stabilize β subunit of tubulin thereby preventing tubulin heterodimer depolymerisation. This event leads to the inhibition of cell division, thereby inducing cell-cycle arrest and apoptosis; from *Montero et. Al., 2005* (Montero *et al.*, 2005).

Docetaxel

Docetaxel, also called Taxotere (Smiyun, Azarenko, Miller, Rifkind, Lapointe, *et al.*, 2017), is one of the most well characterized and used taxanes in cancer chemotherapy. It is a semisynthetic analogue of paclitaxel. It has been well studied for the treatment of many malignant neoplasms such as breast, stomach, lung and prostate cancers. A phase

III clinical trial has shown that docetaxel increases overall survival in hormone sensitive prostate cancer patients treated with hormone therapy (James *et al.*, 2016).

Docetaxel has also been shown to increase CRPC patients mean global quality of life and median survival in a phase II clinical trial (Petrioli *et al.*, 2003). Moreover, in this study, weekly administration of docetaxel has shown very low side effects (neutropenia and anemia) (Petrioli *et al.*, 2003). .

Despite its efficacy in aggressive forms of CRPC, patients can develop resistance to docetaxel and treatment failure (Rosenberg *et al.*, 2007; Harland *et al.*, 2013). This could be due to the action of ABCB1 (ATP binding cassette subfamily B member 1) (Sissung *et al.*, 2014; Mizokami *et al.*, 2017), which is a membrane glycoprotein acting as efflux pump and excluding the drug from the cancer cells. Docetaxel has a high affinity for ABCB1 and this results in easy release of the drug from the cells. In cases of prostate cancer resistance to docetaxel, the second generation taxane cabazitaxel can be used (Mizokami *et al.*, 2017).

Cabazitaxel

Cabazitaxel (i.e. Jevtana, commercial name) is a semisynthetic taxane, analogue of paclitaxel, approved by the Food and Drugs Administration (FDA) in 2010 and by the European Medicines Agency (EMA) in 2011. Cabazitaxel has been recently introduced for the treatment of CRPC patients resistant to docetaxel (National Cancer Institute, 2014; Sissung *et al.*, 2014; Smiyun, Azarenko, Miller, Rifkind, Lapointe, *et al.*, 2017).

Cabazitaxel has a low affinity for ABCB1, therefore it cannot be captured and released outside the cell (Mizokami *et al.*, 2017) as easily as docetaxel, resulting in higher intracellular activity, especially in docetaxel-resistant CRPCs (Sissung *et al.*, 2014).

Phase III and phase IV clinical trials have demonstrated cabazitaxel efficacy in improving the clinical outcome of prostate cancer patients, either alone or in combination with other treatments (de Bono *et al.*, 2010; de Wit *et al.*, 2019). One of the most recent study on cabazitaxel role on prostate cancer patients clinical outcome has shown that mCRPC patients previously treated with docetaxel or new generation hormonal treatments (i.e. AA or enzalutamide) show improved progression-free survival (PFS) when treated with cabazitaxel compared to new generation hormonal treatments (de Wit *et al.*, 2019).

1.2.3. Platinum agents

Platinum agents are compounds derived from platinum and used in cancer chemotherapy. They act via formation of crosslinks between complementary strands of DNA. The result of this interaction causes multiple errors in the DNA replication. This results in several DNA double-strand breaks that rapidly accumulate inside the cancer cells, resulting in activation of apoptosis. Some studies have shown efficacy of cisplatin and carboplatin in CRPC, and particularly in anaplastic CRPC as described in the following paragraphs.

Cisplatin

Cisplatin is a platinum agent approved by the FDA in 1978 and used as an anti-neoplastic chemotherapeutic for the treatment of several cancers since it inhibits cell proliferation and induces cancer cell death (Guo *et al.*, 2017). Its effective action has been shown in several studies both alone and in combination with other treatments. *In vitro* studies indicate that Cisplatin could suppress the growth of cells resistant to enzalutamide,

becoming useful in the treatment of CRPC resistant to second-line hormone therapy (Guo *et al.*, 2017).

Carboplatin

Carboplatin is a chemotherapeutic drug that interferes with the cell cycle and binds DNA strands, thereby creating cross-links between complementary strands. It is a second-generation platinum agent. Carboplatin has been shown to be effective against a large variety of solid cancers (e.g. lung, bladder, stomach) and both pre-clinical and clinical evidence has shown its role in anaplastic prostate cancer (McPherson, Galettis and de Souza, 2009; Aparicio *et al.*, 2013). In particular, a phase II clinical trial has shown that carboplatin, in combination with docetaxel, increases PFS of anaplastic prostate cancer patients, compared to etoposide-cisplatin combination treatment (Aparicio *et al.*, 2013). As mentioned before, carboplatin is used in combination with taxanes (Aparicio *et al.*, 2013; Gillessen S., 2016). Moreover it has been used in a triple combination study with the taxane paclitaxel and estramustine phosphate in 310 CRPC patients and it has induced ≥50% PSA reduction in 69% of cases and significantly prolonged the survival of treated patients (Regan *et al.*, 2010). Another study has shown that the treatment of CRPC patients with or without a NE differentiation using carboplatin in combination with etoposide (a topoisomerase II inhibitor used in the treatment of several cancers) results in a significant reduction in PSA and NE markers, but in a minority of patients (Gillessen S., 2016).

Despite the activity of these drugs, 50% of patients initially responding to these therapies develop resistance within 2 years (Yadav *et al.*, 2017). Therefore, the

characterization of the mechanisms that drive cancer drug resistance is fundamental to hinder it and increase patient survival.

1.3. Cancer drug resistance

Unsuccessful cancer treatments are caused by the onset of therapy resistance that determines tumour progression and relapse, with dramatic consequences for patient survival. This section is focussed on cancer drug resistance, particularly chemotherapy (platinum agents and taxanes) and targeted therapies (hormonal treatment) since they are currently employed to treat CRPC. Malignant cells can be intrinsically resistant to specific therapies, determining absence of response since the initial treatment or can become resistant after initial sensitivity, in consequence of adaptive mechanisms.

Cancer drug resistance is commonly a multifactorial phenomenon, ascribed to alterations in various molecular pathways in the singular cell and in the surrounding microenvironment (Das *et al.*, 2015; Němcová-Fürstová *et al.*, 2016; Galletti *et al.*, 2017). Moreover, single factors or a variety of molecular events can determine resistance to one or more drugs and drug types. The latter phenomenon is called multidrug resistance. An example of well-known factors associated with multidrug resistance are the multidrug resistance transmembrane cellular transporters (MDR proteins). In this case, the multidrug resistance effect is due to the action of these transporters in preventing drugs from accumulation in the cytosol (Nikolaou *et al.*, 2018). The next paragraphs focus on the well-characterized factors and pathways that promote drug resistance, from ABC transporters to apoptosis.

ABC transporters

ABC proteins are the best characterized MDR proteins in cancer drug resistance, as they determine the efflux of hydrophobic compounds which can be cytotoxic for the cells, such as anticancer drugs (Sarkadi *et al.*, 2006; Higgins, 2007; Matsunaga *et al.*, 2016). Therefore, ABC transporter upregulation often increases cancer drug resistance. An example is ABCB1, a well characterized member of this family, which is involved in prostate cancer resistance to different agents, including taxanes and platinum agents (Narita *et al.*, 2012; Lombard *et al.*, 2017, 2019). In particular, a study has shown that ABCB1 is up-regulated in docetaxel-resistant prostate cancer and that pre-treatment of these cells with ABCB1 inhibitors restores taxane sensitivity (Matsunaga *et al.*, 2016).

DNA damage repair

Other factors that have been linked to drug resistance are members of the DNA damage repair system (Nikolaou *et al.*, 2018). Cancer cells can hyper-activate DNA damage repair systems, becoming insensitive to the action of DNA-damaging drugs. In fact, some drugs act by damaging DNA, which is hardly repaired by cancer cells, which lack of many control mechanisms, due to their uncontrolled and fast proliferation. For example, taxanes cytotoxic action induces DNA damage that causes cell apoptosis if not repaired (Iida, Shimada and Sakagami, 2013; Poruchynsky *et al.*, 2015). Nevertheless, cancer cells can induce specific molecular mechanisms via which they stimulate DNA repair factors expression and function, thereby repairing DNA damage and evading cell death (Swanton *et al.*, 2009). DNA damage repair proteins have been linked to drug response. *BRCA1* and *BRCA2* are two genes involved in double strand homologous recombination repair (HRR). These genes are frequently mutated in breast and ovarian cancers and the

expression of *BRCA1* and *BRCA2* has been shown to predict breast cancer patients response to neoadjuvant anthracycline and taxane-based chemotherapy (Xu *et al.*, 2018). Moreover *BRCA2* germline variants have been associated with metastatic advanced prostate cancer response to platinum agents, taxanes and new generation hormonal treatments (Pomerantz MM, Spisák S, Jia L, Cronin AM, Csabai I, Ledet E, Sartor AO, Rainville I, O'Connor EP *et al.*, 2017; Castro *et al.*, 2019).

Pim-1, a serine/threonine kinase constitutively expressed in human cells and involved in cell cycle progression, inhibits apoptosis and triggers non-homologous end joining (NHEJ) DNA repair (Hsu *et al.*, 2012). In human CRPC cells, *Pim-1* silencing increases taxane-induced apoptosis, by impairing the DNA repair system (Hsu *et al.*, 2012).

Antioxidant response

Oxidative stress, often induced by some drugs via release of reactive oxygen (ROS) and nitrogen (NOS) species, can induce cell death by damaging DNA proteins and other macromolecules (Jaiyesimi *et al.*, 1995). Cancer cells can evade this death-inducing mechanism, by activating the antioxidant response, reducing oxidative stress and enhancing cancer cell survival (Crea, Serrat and Hurt, 2011; Datta *et al.*, 2017). This results in increased drug resistance, as reported for docetaxel in prostate cancer (Crea, Serrat and Hurt, 2011).

Autophagy

Cancer cells can also react to drug treatment using autophagy as defence. Autophagy is a cellular mechanism leading to degradation of cellular components, which is physiologically important in cellular recycling, homeostasis and stem cell differentiation

and self-renewal (Lyakhovich and Lleonart, 2016). This process normally stimulates cells to be healthy and to avoid cell death, thereby promoting cell survival (Peng *et al.*, 2014). In cancer cells, especially under stress conditions such as drug treatment, autophagy promotes tumourigenesis and plays important roles in the plastic response of cancer cells to therapy (Lyakhovich and Lleonart, 2016). Cancer cells can use autophagy to evade chemotherapy-induced cell death (Pan *et al.*, 2014). Autophagy-associated pathways and markers are increased in taxane resistant cancer cell lines and in neoplastic tissues resistant to taxanes (Peng *et al.*, 2014).

In prostate cancer cells, autophagy is associated with increased survival upon treatment with anti-androgens and taxanes (Bennett *et al.*, 2013). The use of 3-methylalanine to pharmacologically inhibit autophagy enhances cell sensitivity to this combination treatment (Bennett *et al.*, 2013). Other studies have associated increased autophagy with decreased sensitivity to taxanes and platinum agents (J. Liu *et al.*, 2019; Jia *et al.*, 2019).

Apoptosis

The mechanisms described so far, as other mechanisms that promote cancer drug resistance, are strictly connected to apoptosis. This can be easily explained considering that the last event of cancer cell sensitivity to treatments is commonly cell death. For this reason, apoptosis is a fundamental process for cancer response to therapy and is often decreased as a mechanism of cancer defence from drug-induced stress.

For this reason, several apoptotic factors and pathways have been associated to increased drug response and their inhibition has been shown to increase drug resistance.

46

In prostate cancer cells programmed cell death protein 5 (Pdcd5) stimulates caspase-induced apoptosis and decreases the expression of anti-apoptotic factors such as Bcl2 and (bcl-2-associated X protein) increases the pro-apoptotic Bax, thereby promoting platinum-agents sensitivity (Zhu, Li and Gao, 2015). Hence, increased apoptosis stimulated by Pdcd5 has been proposed in combination with platinum-agents to treat prostate cancer with reduced initial response to the drug (Zhu, Li and Gao, 2015). Increase of apoptosis via inhibition of anti-apoptotic factors such as Bcl-xl and Mcl-1 has also been associated with increased taxane response in CRPC (Hwang *et al.*, 2012). Another study has shown that alteration of Bcl2 members signalling affects CRPC cells apoptosis (Pilling and Hwang, 2019). In particular, Pilling and Hwang have shown that Bcl-xL and Mcl-1 inhibit apoptosis via repression of pro-apoptotic factors such as Bim and Bax, in CRPC cells treated with enzalutamide (Pilling and Hwang, 2019). This mechanism results in increased cancer cell survival in response to enzalutamide, thereby promoting resistance to this therapeutic agent (Pilling and Hwang, 2019). Moreover, it has been shown that Bcl-xL and Mcl-1 inhibitors affect this mechanism and promote enzalutamide sensitivity (Pilling and Hwang, 2019). These findings underline the importance of apoptosis escape for cancer cells as defence from drug treatments in advanced prostate cancer and pave the way for the inhibition of anti-apoptotic pathways to sensitize prostate cancer cells to treatment. Moreover, the inhibition of these pathways can cross react with other drug-resistance drivers to increase drug sensitivity since, as already mentioned, apoptosis is often altered in cancer and drug resistance cancers.

Overall, these studies highlight that several mechanisms can contribute to prostate cancer drug resistance, especially in CRPC cells that normally develop resistance to

several treatments. Since CRPC is molecularly and clinically a heterogeneous disease (Acharya *et al.*, 2017) it is very hard to find a therapeutic option that is durably effective. Hence, there is an urgent need to find compounds to treat CRPC and to prevent the development of further resistance (Acharya *et al.*, 2017).

Moreover, lack of knowledge on the molecular features of hormone-independent prostate cancer such as CRPC and NEPC, prevents the early diagnosis and effective treatment of these aggressive diseases (Beltran *et al.*, 2016). For this reason, the study of long non-coding RNAs (lncRNAs) could pave the way for innovative and effective cancer therapies.

1.4. Long non-coding RNAs

This section describes lncRNAs and their roles in health and disease, with a particular focus on cancer and treatment resistance.

1.4.1. Definition and mechanisms of action

The "central dogma" of molecular biology states that genetic information flows from nucleic acids to proteins and that it cannot be transferred back (fig.1.8 left panel). In particular, according to this theory, the information goes from DNA to RNA via transcription and eventually to protein via translation (Crick, 1970). Proteins were considered the only molecules able to directly affect cellular phenotypes.

The human genome is constituted by thousands of protein-coding genes but in the era of next generation sequencing, it has been shown that they represent a minor portion of the human transcriptome. Indeed, almost 99% of the human genome lacks the potential to encode proteins while it is transcriptionally active and estimated to play a wide range of biological functions (Poller *et al.*, 2017). These non-coding regions were initially called "junk DNA" and their derived transcripts were considered non-functional "transcriptional noise" (Ponjavic, Ponting and Lunter, 2007; Pennisi, 2012). Nevertheless, it is currently known that the "non-coding" transcriptome includes different RNA types (fig.1.8 right panel). So far, the best characterized include lncRNAs, microRNAs (miRNAs) and small nucleolar RNAs (snoRNAs).
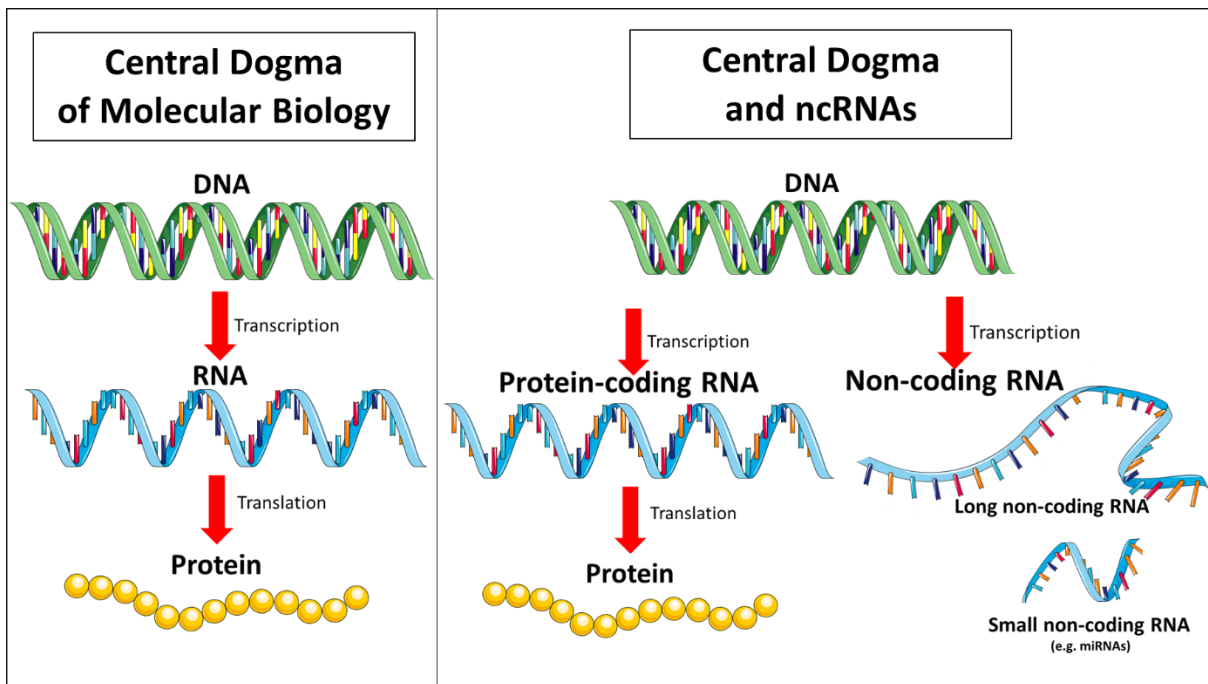
Figure1.8 | "Central dogma" of molecular biology and noncoding RNAs (ncRNAs).
Left panel shows the "central dogma" of molecular biology: the genetic information flows from DNA to RNA via transcription and eventually to protein via translation. Right panel includes in the model ncRNAs that are functional transcripts despite lacking protein-coding potential. There are two main groups of ncRNAs: long and small ncRNAs.

LncRNAs are the most abundant class of ncRNAs. They are defined as transcripts longer than 200 nucleotides, without protein-coding potential (Sun and Wong, 2016). Similarly to the protein coding genes, lncRNAs have exons and introns, which are spliced to produce one or more variants (Cathcart *et al.*, 2015; Sun and Wong, 2016).

A minority of lncRNAs are transcribed by RNA polymerase III while most of them are transcribed by RNA polymerase II from more than 50,000 unique *loci* (Mohanty, Badve and Janga, 2014; Crea, Venalainen, *et al.*, 2016). They have a cap at the 5` end and some of them are polyadenylated. Upon transcription and post-transcriptional modifications, lncRNAs can fold in tri-dimensional structures, which enable their cellular functions, via interaction with TFs, epigenetic effectors, splicing factors, other ncRNAs and many other macro-molecules (Crea, Clermont, *et al.*, 2014) (fig.1.9). These functions make lncRNAs

important in several cellular key processes such as gene expression regulation, homeostasis, cell proliferation and tumourigenesis.

LncRNAs have been classified based on their location in the human genome in:

1) Intergenic lncRNAs (lincRNAs), which are transcribed by RNA polymerase II from *loci* that are between protein-coding genes but quite far from them, i.e. >5000 base pairs (bp);

2) Intronic lncRNAs, located inside the intronic regions of other genes. They can be transcribed either in sense or anti-sense directions;

3) Antisense lncRNAs, derived from protein-coding genes transcribed in the opposite direction. Notably, it has been estimated that around 70% of protein-coding *loci* produces antisense lncRNAs (Sun and Wong, 2016).

These categories of lncRNAs are estimated to act in a wide range and variety of biological processes (Bayoumi *et al.*, 2016). According to their subcellular localization, lncRNAs can be classified as predominantly nuclear, cytoplasmic or present in both compartments (Sun and Wong, 2016). In the nucleus, they act mainly in the transcriptional regulation of gene expression by binding epigenetic complexes and TFs, in order to regulate chromatin modifications and transcriptional gene expression, respectively (fig.1.9). Some of the most characterized nuclear lncRNAs are HOX Transcript Antisense RNA (*HOTAIR*) and Antisense Noncoding RNA In The INK4 Locus (*ANRIL*), which interact with polycomb repressive complexes (PRCs) (Crea, Clermont, *et al.*, 2014), thereby controlling histone methylation and tissue-specific gene silencing (Sun and Wong, 2016). Nuclear lncRNAs can also act as decoys for proteins and protein complexes such as TFs or splicing complexes (Crea, Clermont, *et al.*, 2014), thereby controlling transcriptional and post-transcriptional modulation of gene expression respectively (Bayoumi *et al.*,

2016). Metastasis Associated Lung Adenocarcinoma Transcript 1 (*MALAT1*), for example, is a well-studied lncRNA that acts in the cell nucleus regulating transcriptional gene expression by binding of many complexes (e.g. polycomb proteins) (Crea, Clermont, *et al.*, 2014) (fig.1.9). As mentioned above, lncRNAs play roles also in alternative splicing: Gonzalez and collaborators have identified an antisense lncRNA transcribed from the *FGFR2 locus*. They have shown that this lncRNA can recruit polycomb-group proteins and histone demethylases to impair binding of a repressive chromatin splicing adaptor complex, via modulation of chromatin signatures, in human normal prostate cells and mesenchymal stem cells (Gonzalez *et al.*, 2015).

LncRNAs located in the cell cytoplasm have been mainly studied as competing endogenous RNAs (ceRNAs). In fact they can interfere with miRNA functions (Sun and Wong, 2016), simply binding and sequestering them (fig.1.9). They are also called miRNA sponges and one of the first discovered has been *PTENP1*, a pseudogene acting as an oncosuppressor in many malignancies (Poliseno *et al.*, 2010). In particular, *PTENP1* retains many miRNA binding sites of the original *PTEN* transcript and competes for the binding with expressed miRNAs. In this way it can increase PTEN levels by sequestering *PTEN*-targeting miRNAs such as *miR-19b* and *miR-20a*; both *PTEN* and *PTENP1* are downregulated in human cancers and when they are upregulated they promote tumour-suppression (Poliseno *et al.*, 2010). Many other lncRNAs act as miRNA sponges in health and disease and in the next sections, they will be described in more detail, in relation to cancer and drug resistance (1.4.3 and 1.4.4).

Cytoplasmic lncRNAs can also be precursors of mature miRNAs (fig.1.9). It has been estimated that lncRNAs can be involved in many other functions inside the cells by binding other molecules and subcellular structures like the cytoskeleton, the

endoplasmic reticulum or proteasome complexes, thereby participating in fundamental cellular events, such as protein secretion, cytoskeleton remodelling and protein degradation, respectively (Crea, Clermont, *et al.*, 2014).
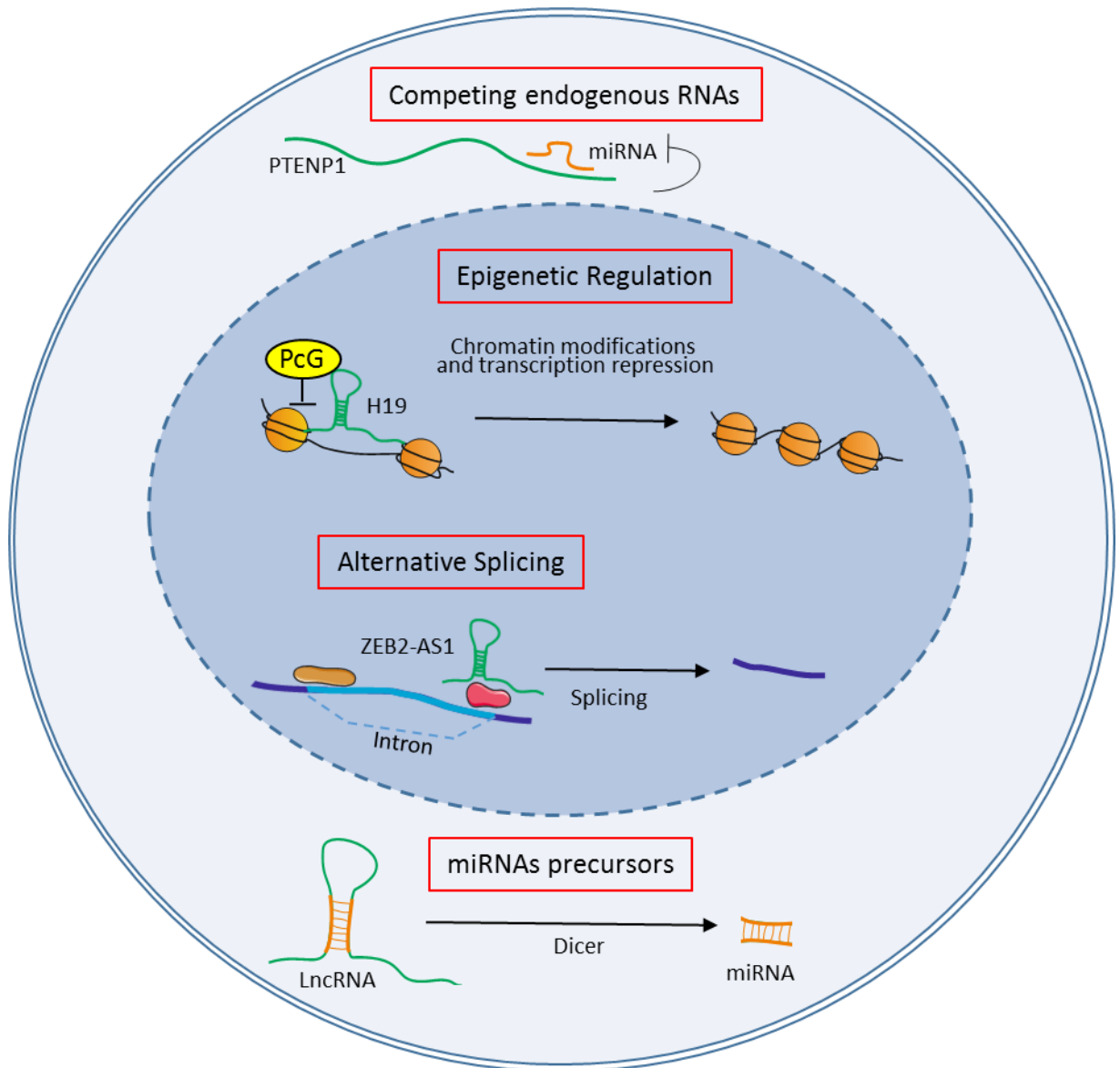
Figure1.9 | Main mechanisms of action of lncRNAs.
Processes involving lncRNAs in the regulation of many phenomena in both nucleus and cytoplasm. The main functions of lncRNAs in the nucleus are associated with epigenetic regulation by interaction with epigenetic effectors such as proteins of the PRCs (e.g. H19 in figure) and with the recruitment of splicing complexes in order to promote alternative splicing (e.g. ZEB2-AS1 in figure). In the cytoplasm, lncRNAs exert their main functions by sequestering miRNAs, acting as ceRNAs (e.g. *PTENP1*) and by being processed to produce mature miRNAs. Nucleus is represented as the space in darker blue; cytosol is in lighter blue. LncRNAs are in green.

Despite lncRNAs being expressed at a relatively low level compared to protein coding genes, they are often expressed in a tissue- and cell-specific manner, and several lncRNAs have shown a disease-specific expression pattern (Sun and Wong, 2016).

1.4.2. LncRNAs in health and disease

LncRNAs have been studied in many processes, from organogenesis to the malignant transformation of the cell, and they act in both physiological and pathological conditions. For example, heart development involves some lncRNAs such as *Bvht* and *Fendrr* which modulate the expression of TFs to promote heart development in humans, rats and mice (Bayoumi *et al.*, 2016).

LncRNAs seem to be important also for brain development, where they play roles in homeostasis and plasticity thanks to their elevated expression in the central nervous system (Qureshi and Mehler, 2010; Clark and Blackshaw, 2014). Recent evidence suggests that the lncRNA myocardial infarction associated transcript (*MIAT*) is a key player in mice retinal cell specification, since it promotes the survival of retinal cells. In keeping with this evidence, *MIAT* inactivation leads to progressive neurodegeneration (Rapicavoli, Poth and Blackshaw, 2010; Jiang *et al.*, 2016). Therefore, some lncRNAs could play roles in neurological disorders such as Parkinson disease. *MALAT1* induces apoptosis in dopaminergic neurons by the interaction with *miR-124*, both *in vitro* and *in vivo* (W. Liu *et al.*, 2017); many other lncRNAs have been correlated with neurodegeneration, suggesting that lncRNA-based drugs may represent a novel therapeutic strategy for the treatment of neurodegenerative pathologies (Carrieri *et al.*, 2015; Majidinia *et al.*, 2016). LncRNAs have been also studied in cardiovascular diseases (Poller *et al.*, 2017) and in diabetes (Sun and Wong, 2016). Additionally, the majority of

54

disease-and trait-associated single nucleotide polymorphisms have been found in non-coding regions of the genome (Maurano *et al.*, 2012). This evidence suggests that lncRNAs play key roles in many pathologies, including cancer.

1.4.3. LncRNAs in cancer

The role of lncRNAs in cancer has been well studied during the last years, showing the importance of these molecules in several human malignancies (Parolia *et al.*, 2015).

LncRNAs can act in cancer both as oncogenes and oncosuppressors.

For example, the knockdown (KD) of the lncRNA *GAS5* promotes the proliferation of leukaemia and breast cancer cells, suggesting that this lncRNA plays a role in anti-tumoural pathways (Mohanty, Badve and Janga, 2014). Another oncosuppressor lncRNA is *Bm743401* whose down regulation increases aggressiveness of gastric cancer (Crea, Clermont, *et al.*, 2014).

Despite this evidence, most of the characterized lncRNAs have shown ability to act as oncogenes. Many metastatic neoplasms have higher expression of specific lncRNAs when compared to primary tumour sites. *MALAT1* and *HOTAIR* are two lncRNAs promoting cell motility and invasion in several cancers (Mohanty, Badve and Janga, 2014), thereby inducing the activation of metastatic pathways in cancer cells.

In particular, *MALAT1* was originally found over-expressed in non-small cell lung cancer metastases and it has been associated with poor survival and high tissue-invasion potential in clinical samples (Ji *et al.*, 2003). In breast cancer, *MALAT1* has been shown to inhibit metastasis both via miRNA suppression and via interaction and direct

inhibition of the prometastatic TF Transcriptional Enhancer Factor 1 (TEAD1) (Kim *et al.*, 2018).

HOTAIR is highly associated with lymph-node metastases, lymph-vascular invasion and shorter recurrence-free survival in different types of cancer (Crea, Clermont, *et al.*, 2014).

This lncRNA can recruit PRC2 factors in order to induce epigenetic repression of oncosuppressor genes via trimethylation of the amino acid lysine 27 on histone 3 (H3K27), in different tumours, such as breast cancer, lung cancer and gastric cancer (Tang and Hann, 2018).

Another interesting lncRNA expressed in cancer cells is *H19* that can have different functions, depending on the splicing isoform expressed in the specific malignancy. *H19* can have oncosuppressive or oncogenic roles, and can act both at transcriptional and post-transcriptional level, by binding epigenetic effectors and miRNAs respectively, in several tumours such as bladder, colon and breast cancer (Yoshimizu *et al.*, 2008; Crea, Clermont, *et al.*, 2014; Z. Li *et al.*, 2017). Hao and collaborators have showed the tumour-suppressor activity of *H19* in embryonic tumour cell lines; Indeed after transfection with a *H19*-expression construct these cells show slower growth, impaired clonogenicity in soft agar and reduced tumorigenicity in nude mice (Elizabeth Newcomb, 1993). Moreover, *H19* seems to reduce the size of experimental teratocarcinomas and the number of colorectal adenomas in murine models (Yoshimizu *et al.*, 2008). In contrast, Zhen Li and collaborators have observed that *H19* stimulates breast cancer cell proliferation and invasion via sponging miR-152 (Z. Li *et al.*, 2017). This suggests that lncRNAs can play multiple roles in cancer and the same lncRNA can act in different ways according to the organ and the tissue where it is expressed. For example, *MIAT* is a non-

coding transcript associated with myocardial infarction but it has been also found to promote neural cell activation and possibly NEPC cell survival (Crea, Venalainen, *et al.*, 2016).

Some lncRNAs have been studied also in the clinical setting to assess their possible use as biomarkers. *SChLAP1* is a lncRNA well validated in the clinics as prognostic biomarker of advanced prostate cancer (Parolia *et al.*, 2015) and *PCA3* is used in FDA-approved diagnostic tests for early prostate cancer. Zhu and collaborators have recently studied the relation between *TUBA4B*, a lncRNA previously identified as a key player in non-small cell lung cancer, and ovarian cancer progression, suggesting a possible role as novel biomarker for diagnosis of this tumour (Zhu *et al.*, 2017).

Several lncRNAs (e.g. *PCAT1*, *PCAT18*, *PCGEM1*) promote metastasis and other traits of aggressiveness such as drug resistance in prostate cancer cells. As mentioned before, *ANRIL* is involved in epigenetic regulation of chromatin and can recruit PRCs to downregulate oncosuppressors like p16^{INK4a} or p14^{ARF} in prostate cancer (Yap *et al.*, 2010; Crea, Clermont, *et al.*, 2014). *PCGEM1* has been one of the first cancer-associated transcripts described in prostate and it is highly tissue specific; *PCAT18* has been described as a driver of prostate cancer AR-dependent metastatic progression (Crea, Watahiki, *et al.*, 2014; Parolia *et al.*, 2015). After this general introduction on the multifaceted roles of lncRNAs in cancer, the main pathways where lncRNAs play important roles in carcinogenesis and progression will be described: proliferation, apoptosis evasion, and metastasis.

Proliferation

Several lncRNAs have been found to be involved in cancer cell proliferation such as Colon Cancer Associated Transcript 1 (*CCAT1*), which is highly expressed in colorectal cancers, where it recruits enhancers to the oncogene *MYC* promoter, thereby facilitating and increasing *MYC* expression (Schmitt and Chang, 2016). Moreover, the fact that Myc can determine *CCAT1* upregulation suggests the existence of a positive feedback mechanism resulting in strong activation of proliferative pathways in the cancer cells (N. Wang *et al.*, 2019). In prostate cancer, different studies have shown that many lncRNAs promote cell proliferation via acting as ceRNAs, thereby influencing important signalling pathways. Some examples are: *SChLAP1*, which sequesters *miR-198* thereby promoting the MAPK1 signaling pathway, which promotes proliferation (Y. Li *et al.*, 2018); *SNHG7*, which sponges *miR-503*, thereby enhancing prostate cancer cell proliferation via stimulation of cyclin D1 that controls cell cycle progression (Qi *et al.*, 2018); Small Nucleolar RNA Host Gene 12 (*SNHG12*), which promotes activation of the Wnt/β-catenin signaling in prostate cancer via sponging *miR-195* (Song *et al.*, 2019).

Other lncRNAs regulate prostate cancer cell proliferation via other mechanisms. Examples are: Zinc Finger E-Box Binding Homeobox 1- Antisense RNA 1 (*ZEB1-AS1*), which is involved in the epigenetic regulation of *ZEB1*; *HORAS5*, which stabilizes *AR* mRNA, thereby enhancing the AR-dependent signalling pathway that promotes cancer cells proliferation and survival (Su *et al.*, 2017; Parolia *et al.*, 2019).

PlncRNA-1 is another lncRNA upregulated in prostate cancer cells and its silencing determines significant decrease in cell proliferation and increase in apoptosis via regulation of the AR signalling (Cui *et al.*, 2013).

Notably, some of these lncRNAs can also regulate other cancer-associated pathways such as metastasis (Y. Li *et al.*, 2018) and cell death (Parolia *et al.*, 2019), underlining again the multifaceted roles and mechanisms of action of this complex class of molecules.

Apoptosis

Several studies in prostate and many other tumours have shown that lncRNAs act in cell death control, mostly via inhibition of the death signalling, such as the already mentioned *HORAS5* and *PlncRNA-1* and many others (Cui *et al.*, 2013; Parolia *et al.*, 2019). *TUG1* is a diagnostic factor in lung adenocarcinoma and suppresses apoptosis via epigenetic silencing of *BAX* expression (H. Liu *et al.*, 2017). *PVT1* inhibits renal cancer cell apoptosis by up-regulating Mcl-1(Q. Wu *et al.*, 2017).

Although other lncRNAs can also stimulate apoptosis (Ling Li *et al.*, 2017; Q. Wang *et al.*, 2019), the majority of them enhance pro-survival pathways in cancer cells, thereby contributing to increased proliferation and other aggressive phenotypes (e.g. metastasis, drug resistance).

Moreover, as already mentioned, the same lncRNAs can have different roles depending on the cancer site where they are expressed and according to the molecular pathways where they interact. In this context, some lncRNAs can function as inhibitor of apoptosis in some cases while stimulating it in others. An example is P21-associated noncoding RNA DNA damage-activated (*PANDA*), which reduces apoptosis by inactivating the TF NF-YA in osteosarcoma (Kotake *et al.*, 2017), while it inhibits apoptosis by inactivating the MAP/ERK signalling pathway, in diffuse large B-cell lymphoma (Wang *et al.*, 2017).

Metastasis

Metastasis is a key step of tumour progression characterized by the ability of cancer cells of crossing the barrier of basement membrane and spread to other sites distant from where the primary tumor originated. Epithelial to mesenchymal transition (EMT) is fundamental for cancer cells metastasis since it enables epithelial cells to acquire mesenchymal stem cell characteristics, thereby gaining ability to invade the basement membrane and migrate to secondary sites. Metastasis happens when cancer cells acquire the two properties of invasion and migration and several lncRNAs are involved in these processes, thereby regulating cancer metastasis, mostly as oncogenes. The oncogenic role of *HORAS5* in prostate cancer progression has been mentioned before; *HORAS5* is also upregulated in hepatocellular carcinoma (HCC) where it promotes cell migration and invasion (Sun *et al.*, 2018). Several other lncRNAs are involved in metastasis, such as *MALAT1* and *HOTAIR*. *MALAT1* promotes EMT in esophageal cancer via stimulation of Notch1 pathway (Ying *et al.*, 2012). Notably, this lncRNA is also involved in the same process in bladder cancer where it stimulates EMT, via the regulation of another well-known pathway, the Wnt signalling (M. Chen *et al.*, 2018). According to another study, *MALAT1* can also repress metastasis in breast cancer cells and animal models (Kim *et al.*, 2018).

Ren and collaborators have found a multifunctional role of *MALAT1* in prostate cancer where this lncRNA stimulates growth, cell cycle progression, invasion and migration of CRPC cells (Ren *et al.*, 2013). Indeed *MALAT-1* silencing inhibits these pathways in the cancer cells and reduces tumour growth and metastasis *in vivo* in CRPC models (Ren *et al.*, 2013).

60

HOTAIR is another important lncRNA in metastasis. The upregulation of *HOTAIR* in breast cancer cells, induced via ectopic overexpression, stimulates the activity of PRC2 leading to epigenetic chromatin remodeling that confers to the malignant cells metastasis properties such as cell motility and invasiveness, while its silencing inhibits the cancer cells invasive potential (Gupta *et al.*, 2010).

According to different studies, *HOTAIR* seems to promote prostate cancer aggressiveness, fundamentally contributing to the castration resistant phenotype (Ling *et al.*, 2017; SunnyHanna, 2018). Notably, as described for breast cancer, *HOTAIR* is also involved in epigenetic regulation of prostate cancer cells, where this lncRNA recruits PRC2 complex to the *AR* promoter, thereby inhibiting *AR* expression and promoting metastasis (Li *et al.*, 2015).

LncRNAs have therefore been implicated in several hallmarks of cancer, mostly playing oncogenic roles, though some lncRNAs have also been shown to inhibit cancer progression and metastasis, and to activate apoptosis.

LncRNAs can influence one or more of the pathways described above and many others. By doing so, some of them have been found to affect cancer cell drug response.

1.4.4. LncRNAs and cancer cell drug resistance

Drug resistance is one of the main processes driving aggressive phenotypes in cancer. As mentioned before, there are well-characterized mechanisms by which cancer cells are intrinsically resistant or acquire this phenotype in consequence of stress-induced adaptive responses. Examples of classical mechanisms of cancer drug resistance are over-activation of efflux pumps or loss and inactivation of apoptotic pathways. However,

most times cancer drug resistance arises in consequence of several factors and molecular changes. Based on the fact that lncRNAs play multifaceted roles in health and disease and especially in cancer-associated pathways, it is comprehensible that these molecules participate in regulation of cancer response to several treatments, including radiotherapy, chemotherapy and hormonal treatments. The next sections will describe lncRNA roles in resistance to taxanes, platinum agents and hormonal therapies, with a particular focus on lncRNAs regulation of miRNAs, pro-survival mechanisms and prostate cancer drug response.

<u>LncRNAs regulate drug resistance via *miRNAs* inhibition</u>

LncRNAs have been recently shown to play roles in drug resistance by interacting with miRNAs. In lung adenocarcinoma, linc-ROR KD has been shown to increase sensitivity to docetaxel and to reduce proliferation and invasion in docetaxel-resistant cells (Pan *et al.*, 2017). Lin-ROR acts by sponging *miR-145* and indirectly activating fascin actin-bundling protein 1 (FSCN1); FSCN1 organizes F-actin into parallel bundles and contributes to the formation of actin-based cellular protrusions, thereby playing important roles in cell migration, motility and adhesion of multiple types of cancer (Pan *et al.*, 2017). Similarly, in the same tumour type, *CCAT1* has been shown to sequester miRNA *let-7c* thereby promoting resistance to docetaxel via increase of *Bcl-xl* expression, which reduces docetaxel-induced apoptosis (Chen *et al.*, 2016) (fig.1.10).

LncRNAs also participate in cancer drug response to platinum agents and hormonal treatments via miRNA regulation (fig1.10 and 1.11). In osteosarcoma, a lncRNA (*linc00161*, i.e. *HORAS5*) has been discovered as a critical component of the pro-apoptotic signals induced by cisplatin; according to this study, *HORAS5* silencing has

been shown to induce cisplatin resistance in osteosarcoma cells by interacting with *mir-645* (Wang *et al.*, 2016). Wang and collaborators have shown that upon cisplatin treatment, *HORAS5* is up-regulated and sequesters mir645, which normally inhibits the translation of *IFIT2* (Interferon Induced Protein with Tetratricopeptide Repeats 2) mRNA (Wang *et al.*, 2016). Once IFIT2 is translated, it activates osteosarcoma cells apoptosis (Wang *et al.*, 2016) (fig.1.10). The same lncRNA has been recently found associated to cisplatin resistance also in ovarian cancer, showing a clear role of *HORAS5* in drug response, particularly upon cisplatin (Xu *et al.*, 2019). According to this study, *HORAS5* sequesters *miR-128* thereby releasing *MAPK1* mRNA, with consequent MAPK1 protein increase which promotes cisplatin resistance in ovarian cancer cells (Xu *et al.*, 2019) (fig.1.10) .

H19 has also been associated with increased cisplatin resistance via miRNA inhibition. In fact *H19* can sponge *miR-106b-5p* in seminoma cells and reactivate *TDRG1* (testis developmental related gene 1) expression (Wei *et al.*, 2018). The *TDRG1* oncogene encodes for a nc-RNA that determines upregulation of the PI3K/Akt/mammalian target of rapamycin (mTOR) signalling, thereby promoting cancer progression that confers to the cancer cells the resistant phenotype (Wei *et al.*, 2018) (fig.1.10).

The hormonal treatment tamoxifen has been correlated to lncRNA urothelial cancer associated 1 (*UCA1*) upregulation in oestrogen receptor (ER)-positive breast cancer cells that increases tamoxifen resistance by sequestering *miR-18a*, with consequent increase of HIF1α (Li *et al.*, 2016) (fig.1.11). According to the same study *miR-18a* in turn increases sensitivity to tamoxifen via regulation of cell cycle proteins (Li *et al.*, 2016). Moreover the inhibition of *miR-18a* increases breast cancer cells resistance to tamoxifen, while the miRNA induction mimics re-sensitizes them to the treatment (Li *et*

al., 2016). *UCA1* has also been found upregulated in tamoxifen resistant breast cancer cells according to another study where it has been also found in the cancer-associated exosomes released by these cells (Xu *et al.*, 2016). This evidence suggests that *UCA1* might also be involved in a signalling mechanism to propagate drug resistance between cells using exosomes.

LncRNAs regulate drug resistance via other survival mechanisms

LncRNAs are involved in cancer drug resistance via different mechanisms and molecular interactions, other than directly interacting with miRNAs. *MALAT1* has been shown to inhibit autophagy-related pathways, thereby decreasing chemotherapeutics sensitivity in diffuse large B-cell lymphoma (Li-juan Li *et al.*, 2017).

Other lncRNAs affect survival pathways in response to drug treatment, acting in the regulation of expression and activity of apoptotic factors. For example, *H19* is involved in *BIK* and *NOXA* epigenetic regulation, two proteins that promotes apoptosis (Si et al., 2016). This role of *H19* is explicated in breast cancer cells resistant to paclitaxel where the lncRNA recruits enhancer of zeste homolog 2 (EZH2) in the nucleus of the cancer cells to epigenetically repress the expression of BIK and NOXA (Si et al., 2016). This mechanism results in inhibition of paclitaxel-mediated apoptosis and therefore in reduced drug response (Si et al., 2016) (fig. 1.10). Another lncRNA directly involved in response to paclitaxel-induced apoptosis is lncRNA *MA-linc1* (Bida *et al.*, 2015). *MA-linc1* has been shown to repress in cis *Purα* a gene located not distant from the lncRNA *locus* (Bida *et al.*, 2015). *Purα* encodes for a protein that is involved in DNA replication and transcription with inhibitory effects on cell cycle progression (Bida *et al.*, 2015).

Therefore *MA-linc1* seems to induce paclitaxel resistance via apoptotic evasion induced by hyper-activation of cell cycle (Bida *et al.*, 2015) (fig.1.10).

UCA1 is described in several publications in the context of cancer drug resistance. Wu and Luo have shown that *UCA1* activates mTor signalling in response to tamoxifen treatment, thereby promoting anti-apoptotic functions in breast cancer cells (Wu and Luo, 2016) (fig.1.11). Other studies have also confirmed the connection between the AKT/mTOR signalling pathway and tamoxifen resistance, in breast cancer cells (Block *et al.*, 2012) and also between this pathway and *UCA1* in other tumours (Li *et al.*, 2014; Cheng *et al.*, 2015).

LncRNAs regulate drug resistance in prostate cancer

Several lncRNAs have been shown to modulate drug response in prostate cancer.

UCA1 promotes docetaxel resistance via inhibition of *miR-204* in prostate cancer cells (Wang, Yang and Ma, 2016). This mechanism of action causes apoptosis evasion, thereby promoting cancer cell survival against docetaxel-induced cell death (Wang, Yang and Ma, 2016).

LncRNAs can regulate AR signalling and this has consequences in the context of prostate cancer response to hormonal treatments (Aird *et al.*, 2018). *PCGEM1* has been described in prostate cancer as a key regulator of ADT resistance by promoting the expression of AR splice variants which are clinically relevant, thereby inducing therapy resistance and metastasis (Smolle *et al.*, 2017) (fig.1.11). Hence, the inhibition of *PCGEM1* in combination with ADT may increase the efficacy of the drug treatment. The function of another lncRNA, *HOTAIR*, has been analysed in prostate cancer since it has shown oncogenic functions via induction of drug resistance. According to this, *HOTAIR* is

upregulated in CRPC compared to hormone sensitive prostate cancer, and *HOTAIR* levels increase in LNCaP cells upon treatment with enzalutamide (Ali Zhang, Jonathan C. Zhao, Jung Kim, Ka-wing Fong and Debabrata Chakravarti, Yin-Yuan Mo, 2015). Interestingly another lncRNA has been studied in the context of prostate cancer response to enzalutamide, in particular in the involvement of promotion of cancer aggressiveness to aggressive prostate cancer phenotypes such as CRPC and NEPC (Luo *et al.*, 2019). In this study, the authors have shown that Enzalutamide treatment affects AR binding with AREs thereby indirectly promoting *lncRNA-P21* expression. This mechanism seems to be involved in changes in EZH2 functions (from histone-methyltransferase to non-histone methyltransferase) that determines signal transducer and activator of transcription 3 (*STAT3*) promoter methylation, thereby inducing a signalling to activate NE differentiation (NED) (fig.1.11). In vivo evidence has also confirmed the importance of lncRNA-P21 in this context (Luo *et al.*, 2019).

According to the evidence described, several lncRNAs have been shown to regulate drug response, particularly to chemotherapeutics (fig.1.10) and hormonal treatments (fig.1.11). Since some lncRNAs can be involved in resistance to different treatments, even in different cancer types, the targeting of these transcripts could increase drug response in different cancers and overcome drug resistance.

The described lncRNAs, and many others, are promising targets for novel cancer treatments, alone or in combination with other compounds. This could reduce drug resistance in many aggressive cancers in the not too distant future (Ayers and Vandesompele, 2017).
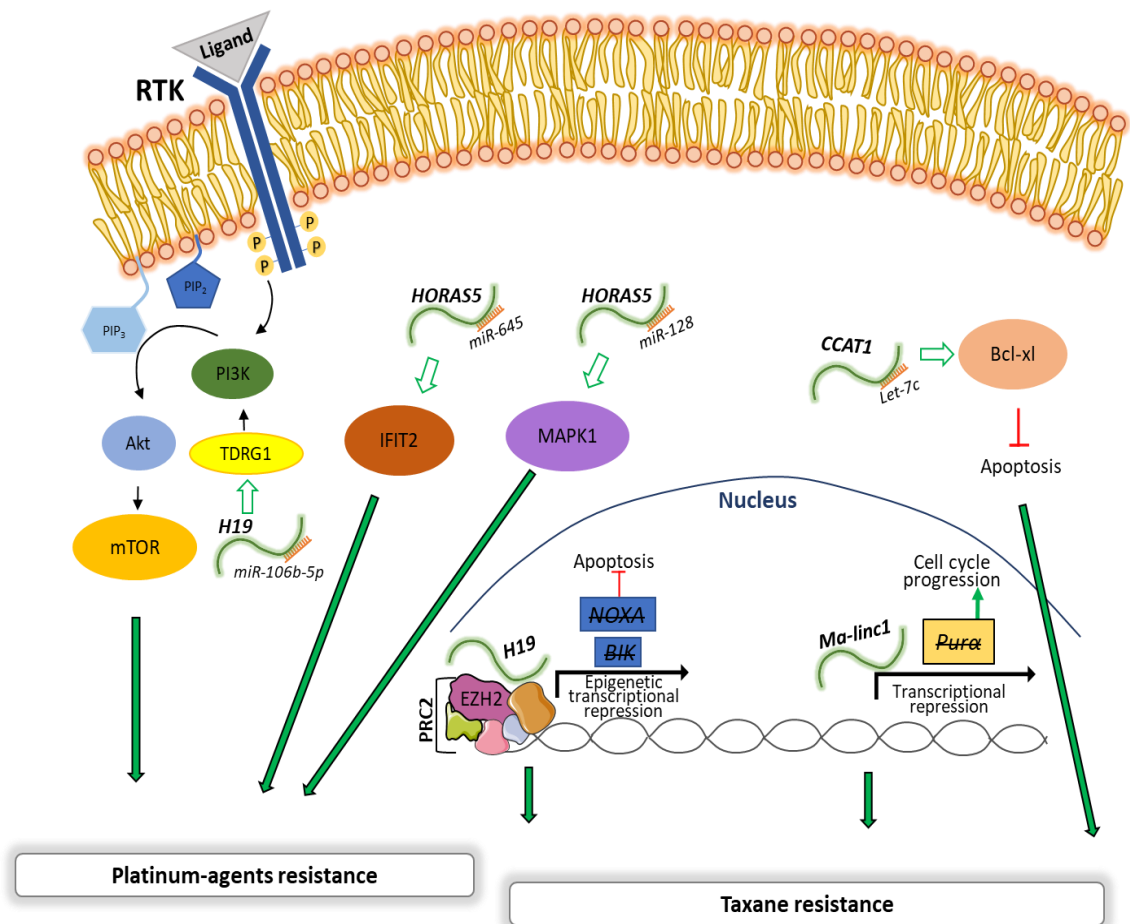
Figure1.10 | LncRNAs play key roles in chemoresistance.
This figure represents some of the lncRNAs reported to promote chemoresistance in this Chapter, focussing on platinum-agents and taxanes resistance. LncRNAs can sponge miRNAs, thereby inhibiting their suppressive functions on survival associated proteins or they can recruit epigenetic effectors or act via other possible functions, participating in the regulation of critical pathways that drive drug resistance. On the left side are represented some lncRNAs that have been reported to promote resistance to platinum-agents: *H19* sequesters miR-106b-5p, thereby releasing the block on TDRG1 expression that promotes cisplatin resistance via stimulation of the PI3K/Akt/mTOR pathway; *HORAS5* can inhibit different miRNAs according to the cancer type where it is expressed, thereby increasing the expression of proliferation and pro-survival proteins (i.e. IFIT2 and MAPK1). On the right side of this figure are represented some lncRNAs that promote taxane resistance: *CCAT1* acts in the cytosol via sponging *Let-7c* and releasing the block on the expression of the anti-apoptotic *BCL2-XL* while *H19* and *Ma-linc1* act in the nucleus, suppressing the transcription of genes involved in apoptosis (*NOXA, BIK*) and cell cycle inhibition (*PURα*), respectively. Modified from (Perla Pucci, Wallace Yuen, Erik Venalainen, David Roig Carles, Yuzhuo Wang, 2019).
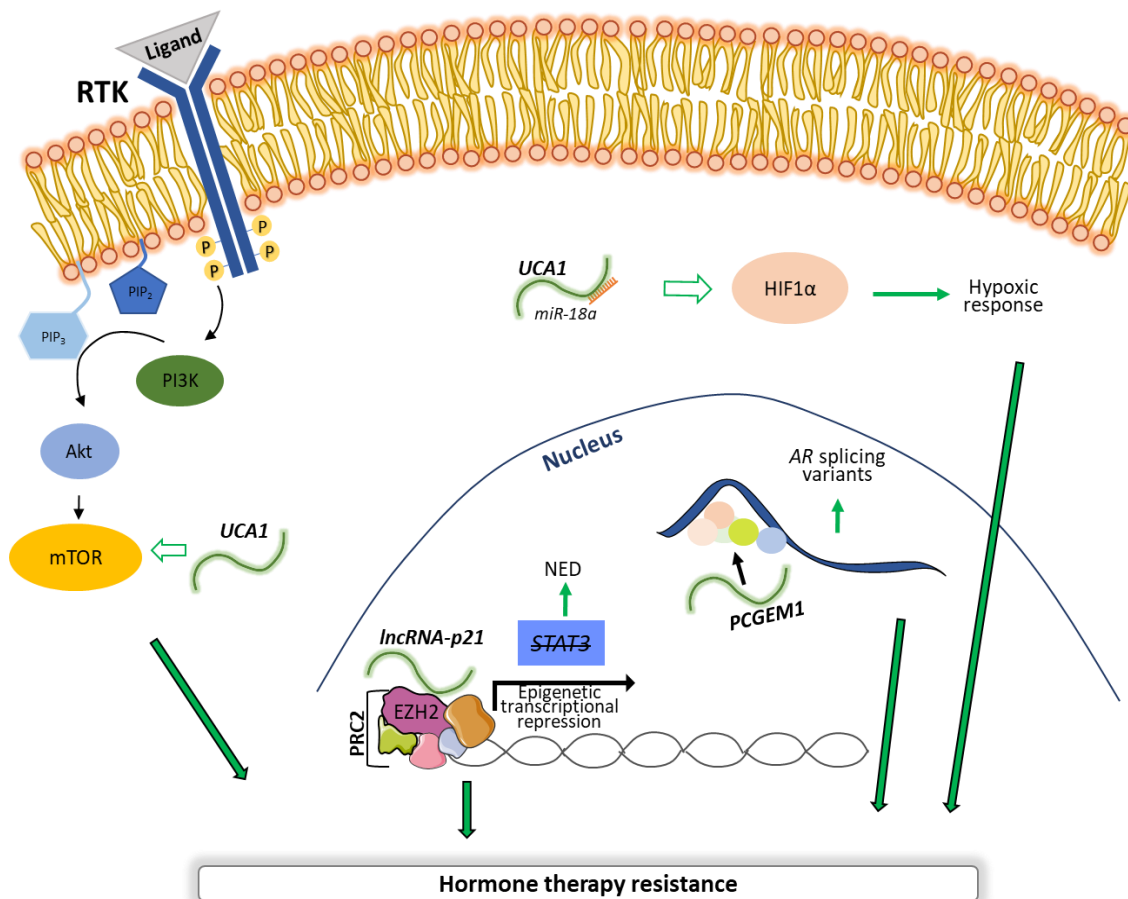
Figure1.11 | LncRNAs play key roles in hormone therapy resistance.

This figure represents some of the lncRNAs reported to promote resistance to hormonal treatments in this Chapter. LncRNAs can sponge miRNAs, thereby inhibiting their suppressive functions on survival associated proteins such as HIF1α involved in hypoxic response, or they can recruit epigenetic effectors or act via other mechanisms, thereby regulating pathways involved in drug resistance. On the left side of this figure are represented some lncRNAs that have been reported to promote resistance to tamoxifen and enzalutamide: *UCA1* is proposed to increase *mTOR* expression thereby enhancing this pro survival pathway and to sequester *miR-18a* thereby promoting the expression of *HIF1α* that drives hypoxia; *lncRNA-P21* influences EZH2 functions, thereby promoting NE differentiation (and therefore enzalutamide resistance) of prostate cancer via STAT3 inhibition; PCGEM1 is involved in expression of AR splice variants expression thereby increasing prostate cancer resistance to hormone treatment Modified from (Perla Pucci, Wallace Yuen, Erik Venalainen, David Roig Carles, Yuzhuo Wang, 2019).

1.4.5. LncRNAs-targeting approaches to overcome drug resistance

LncRNAs have key roles in health and disease, particularly in pathways that regulate cancer progression and drug resistance. Most lncRNAs promote resistance to different antitumour agents, by coordinating numerous molecular mechanisms.

According to recent findings, preclinical studies have recently aimed to inhibit lncRNAs as combination therapeutic approach to increase drug sensitivity and overcome drug resistance. Since lncRNAs do no encode for proteins, it is conceivable that small inhibitors or antibodies cannot affect lncRNAs. This leads to the need for DNA or RNA molecules to bind the complementary lncRNA sequence and induce its degradation.

Nowadays it is known that lncRNAs can be targeted using different systems but the use of antisense oligonucleotides (ASOs) is the most-developed method so far, closer to a clinical use.

These approaches target oncogenic lncRNAs but can also be used to target inhibitors of oncosuppressor lncRNAs, in order to re-activate these lncRNAs and orchestrate anticancer responses.

ASOs are used to transiently modulate lncRNAs but other methods exist for both stable and transient lncRNAs targeting.

Stable upregulation or depletion of lncRNAs can be achieved using lentiviral transduction (B. Zhang *et al.*, 2018; Panda *et al.*, 2018) and CRISPR-Cas9-dependent genome editing (Lavalou *et al.*, 2019). Notably, there are not *in vivo* findings supporting the use of these approaches and no clinical data are currently reliable, suggesting unpredictability on the future employment of these stable lncRNAs-targeting methods in cancer.

Transient modulation of lncRNA expression has been optimized in the last years, showing successful results *in vitro* and *in vivo*. LncRNA silencing using small interfering RNAs (siRNAs) represents one of these techniques (Chery, 2016). This method works via transfection of short sequences (around 20bp) of synthetic double strand RNAs. These duplexes are processed to single strand, able to target complementary RNA sequences, via the interaction with a protein complex called RISC (RNA-induced silencing complex) (Pratt and MacRae, 2009), thereby forming a complex recognised and degraded from cellular endonucleases. While cytoplasmic RNAs can efficiently be silenced using this method (Mahmoodi Chalbatani *et al.*, 2019), nuclear targets are hard to silence, due to the RISC cytoplasmic location (Pratt and MacRae, 2009). Moreover, siRNA transfection needs lipid reagents that increase *in vivo* toxicity, making them difficult to be used in the clinical setting. Additionally, siRNAs tent to be rapidly degraded upon injection and have not shown high target and tissue specificity, although there are studies addressing this limitations in order to improve siRNAs stability and reduce their off-target effects (Mahmoodi Chalbatani *et al.*, 2019).

The most promising lncRNA-targeting molecules seem to be ASOs.

ASOs are DNA or RNA molecules whose length is more varied than siRNAs, since they can measure 13-200nts. They are synthetized as single strand DNAs or RNAs which bind complementary target RNAs, without the interaction with any complex. ASOs recruit RNase-H enzyme, which degrades the ASO-RNA duplex formed (Chery, 2016). Notably, RNase-H is an enzyme expressed in both the cell nucleus and cytoplasm (Liang *et al.*, 2017), thereby allowing ASO mediated silencing to work in both cell compartments. Several studies have shown that ASOs successfully silence genes involved in cancer cell proliferation and metastasis (Crea, Quagliata, *et al.*, 2016; Gordon *et al.*, 2019). The use

of ASOs in clinical cancer trials has been successful, with some of them reaching phase III (Beer *et al.*, 2017; Bellmunt *et al.*, 2017; Yu *et al.*, 2018), although there are still no clinical trials on lncRNA-targeting ASOs.

Nevertheless, several studies have shown that it is possible to increase ASOs cellular uptake and stability via a series of chemical modifications, such as locked nucleic acids (LNAs) and Phosphorothioate (PS) ASOs (Shen and Corey, 2018). LNAs are ASOs with increased stability and strength of hybridization due to a 2',4'-methylene linkage in the ribose ring between the 2'-O and 4'-C atoms, which in this way "locks" the ribose in the ideal conformation for Watson-Crick binding (Shen and Corey, 2018). PS ASOs have increased molecular stability due to the substitution of one oxygen of the phosphodiester bond between two ribose molecules with a sulphur that creates a phosphorothioate bond (Shen and Corey, 2018). This gives protection from digestion by nucleases and stronger serum protein binding, thereby increasing PS ASOs stability in the circulation as well as their tissue and cellular uptake (Shen and Corey, 2018). Other modifications can be done to increase ASOs stability and uptake using nanoparticles or targeting ligands (e.g. N-acetylgalactosamine (GalNAc)) instead of chemically modifying ASO structure (Shen and Corey, 2018); this evidence suggests that important improvements can reasonably be expected in the use of these molecules in preclinical studies and in their clinical use, in the near future.

Overall, antisense therapies using ASOs and their modified variants seem to be the most promising lncRNA-targeting approach to treat cancer and drug resistant malignancies. Nevertheless, further research needs to be done in order to improve their potential for clinical trials and clinical approval.

1.5 Hypothesis and Aims

Treatment resistance is a major cancer hallmark for CRPC. LncRNAs can play key roles in cancer and drug resistance and lncRNA-targeting approaches could increase drug response in aggressive cancers, such as CRPC. This study is focussed on one specific lncRNA that seems particularly promising in the landscape of cancer drug response: *HORAS5*.

Therefore, the hypothesis of this project is that *HORAS5* affects CRPC response to therapy acting via specific mechanisms of action.

In order to test this hypothesis, the following aims have been addressed:

1 To establish a CRPC model of *HORAS5* overexpression in DU145 cells, which endogenously express undetectable levels of *HORAS5*; to characterize the effect of *HORAS5* overexpression on the lncRNA subcellular localization and on cell proliferation.

2 To determine the levels of *HORAS5* in prostate cancer cell lines after treatment with different drugs (AR antagonist/chemotherapeutics), with the aim of selecting one specific drug to be tested for the further aims.

3 To test the effect of *HORAS5* modulation, via lentiviral-mediated overexpression and RNAi, on prostate cancer cell response to treatment.

4 To study one mechanism of action by which *HORAS5* mediates prostate cancer cell response to therapy.

5 To analyse the expression and prognostic value of *HORAS5* in clinical samples and investigate its possible future use as *in vivo* therapeutic target with preclinical tests on *HORAS5* inhibition with ASOs in combination with drug treatment.

CHAPTER 2: MATERIALS AND METHODS

2.1. Cell lines and cell culture reagents

DU145 cells were used in this study as a model of AR⁻ hormone-independent epithelial prostate cancer cells and they derive from brain metastases. LNCaP cells were used in this study as a model of AR⁺ hormone-independent prostate cancer cells and they derive from left supraclavicular lymph node metastases. LNCaP express a mutated *AR* gene and can grow in androgen deprivation conditions (i.e. castrate conditions) (Sedelaar and Isaacs, 2009). Both DU145 and LNCaP have been purchased from the American Type Culture Collection (ATCC, Burlington, ON, Canada). Additionally, DU145 have been stably transduced with *HORAS5*-lentiviral particle (fig.2.1) and sent to the Open University from Experimental Therapeutics, British Columbia (BC) Cancer Agency (Vancouver, Canada). DU145 transduced cells will be named DU145-NC when the lentiviral particle does not carry the *HORAS5* gene and DU145-OE when *HORAS5* is overexpressed. The cells have been kept at 20 passages or lower and *HORAS5* overexpression has always been confirmed via quantitative reverse transcription-polymerase chain reaction (RT-qPCR).

DU145 cells (both DU145-NC and DU145-OE) have been cultured in RPMI-1640 (Gibco, Loughborough, UK) and LNCaP cells have been cultured in RPMI-1640 ATCC modification (Gibco, Loughborough, UK), both supplemented with 10% of heat-inactivated FBS (Thermo Fisher, Loughborough, UK) and 1% antibiotics (penicillin and streptomycin) (Thermo Fisher, Loughborough, UK) (tab.2.1). ATCC protocols have been followed for culture passage and cells storage. Cells have been cultured at 37°C in a 5% CO_2 humidified incubator.

Table 2.1 | Reagents used for cell culture maintenance in this project.

Reagents	Supplier	Cat.No
RPMI 1640 Medium-phenol red	GIBCO®	21875034
RPMI 1640 Medium (ATCC modification)	GIBCO®	A1049101
Fetal Bovine Serum (FBS)	Thermo Fisher	10099141
Hank`s balanced salt solution (HBSS)	Sigma-Aldrich	H6648
Trypsin-EDTA (0.25%)Phenol Red	Thermo Fisher	11570626
Penicillin-Streptomycin (pen/strep) (10,000 U/mL)	Thermo Fisher	15140122

All the cell lines have been conserved in liquid nitrogen in cryo-tubes.

Mycoplasma screening has been tested routinely using the MycoAlert Detection Kit (Lonza, UK) with the MycoAlert assay control set (Lonza, UK).

2.2. *HORAS5* overexpression

A lentivirus-derived particle that carries the *HORAS5* gene was transduced into DU145 in order to induce the exogenous expression of *HORAS5*. The plasmid was purchased from Genecopoeia (Cat.No LPP-GS266B-Lv105-050) by collaborators at the BC Cancer Agency in Vancouver; they transduced and sent us the cells. This plasmid is a 3rd generation HIV lentiviral particle, replication-defective and able to transduce and integrate the genomic host sequence flanked by the long terminal repeat (LTR) sequences, identical sequences of DNA found in most eukaryotic cells at the end of retrotransposons and used by viruses to integrate their genetic material into the host

genome. *HORAS5*-lentiviral particle contains the Puromycin and Ampicillin resistance cassettes that permit antibiotic selective pressures, the cytomegalovirus (CMV) promoter to drive strong transgene expression, upstream *HORAS5*, a bacteria replication start (pUC Ori) and a 3` and 5` long terminal repeats (LTRs) and packaging elements (fig. 2.1).
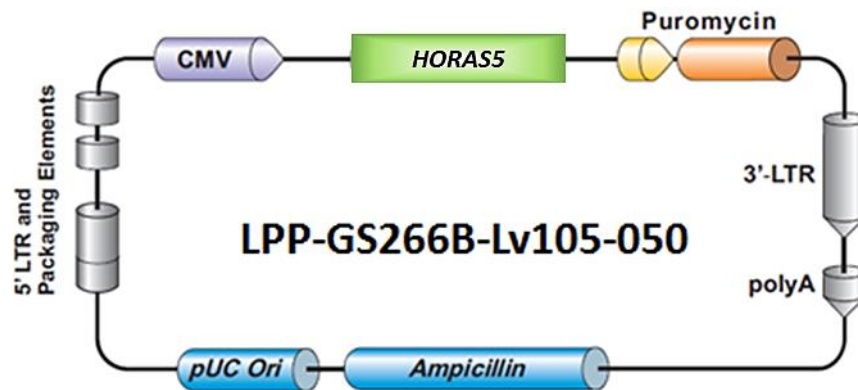
Figure2.1| *HORAS5*-lentiviral plasmid.
Schematic representation of the vector LPP-GS266B-Lv105-050 used to induce the expression of *HORAS5* in the transduced cells. The plasmid contains the LTR packaging elements the CMV strong promoter, the pUC Ori bacteria-start replication site and the antibiotic resistance cassettes to select the cells transduced and containing *HORAS5*.

For the overexpression procedure, 7×10^4 DU145 cells were seeded in 24-well plates and incubated overnight at 37°C in 5% CO_2 incubator. Thereafter, old media was removed and replaced by media with addition of polybrene (i.e. Hexadimethrine Bromide, Sigma Aldrich, Gillingham, UK) at a final concentration of 8 μg/mL. Polybrene was used to increase the transduction efficiency (Denning *et al.*, 2013). After media replacement, the purified human *HORAS5* lentiviral particles (Titer: 1.37×10^8 TU/mL where 1TU=100 copies of viral genomic RNA) were added to the cells which were incubated overnight. After the incubation time, cells were washed three times with RPMI-1640 containing 10% FBS three times and let grow for two days. After 48h-72h, the cells were passaged into 6-well plates (1:2 concentration) and let grow for 5-6 hours in order to reach cell

adhesion to the plate thereby allowing antibiotic selection using puromycin (Gibco, Cat# A1113803). The cells were treated with puromycin for two weeks, changing media every three-four days. To achieve high copy number, 3 μg/mL puromycin was selected. All overexpression experiments were normalized to DU145 transduced with the empty vector (DU145-NC control cells).

2.3. MTS cell viability assay

Cell viability was examined at various time-points (Days 1, 3, 5, and 7) in Du145 cells stably overexpressing *HORAS5*. Cells were harvested at a confluency between 80-90%, counted and seeded in 96-well plates at a final volume of 100μL. Seeding densities corresponding to days 1, 3, 5, and 7 are 1.0×10^3, 6.0×10^3, 4.0×10^3, 2.0×10^3 and 5.0×10^3, 2.0×10^3, 1.0×10^3, 5.0×10^2 respectively. Six replicates for both control (WT) and DU145-OE were performed. After the selected time-points, cell viability was assessed using the colorimetric CellTiter 96® Aqueous One Solution Cell Proliferation Assay (MTS) (Promega, Southampton, UK). Following the manufacturer's protocol, the 96® AQueous One Solution Reagent was thawed and 20μl of it was added to each well of the 96-well assay plate containing the samples in 100μl of culture medium. The cells were incubated at 37°C in a 5% CO_2 incubator for 1 hour and 30 minutes prior to absorbance measurements using a spectrophotometer set to 490nm. A media blank was used to remove background absorbance before plotting data values normalized to the WT Day 1 reading for each respective line. To account for variations in seeding densities, a correction factor was applied as below:

$$Normalization = \left(\frac{Abs.\,for\,Samp_x}{Abs.\,for\,Day1\,WT} \right) \times \left(\frac{\#\,of\,cells\,used\,for\,Day1\,WT}{\#\,of\,cells\,used\,for\,DayX\,samp_x} \right)$$

2.4. Drugs and treatment

In order to analyse a possible influence of drug treatment on the expression of *HORAS5* in prostate cancer cell, three drugs were used (tab.2.2):

- Enzalutamide (MDV3100, Selleckchem) was purchased from Selleckchem as powder and solubilized in sterile DMSO to obtain a stock solution of 50 mM which was stored at -80°C. The stock was serially diluted to obtain the final concentrations: 1 µM, 10 µM in gene expression experiments.

- Cabazitaxel (Jevtana, Selleckchem) was purchased from Selleckchem as powder. It was solubilized in sterile dimethyl sulfoxide (DMSO) to obtain a stock solution of 5 mM, which was stored at -80°C. The stock was serially diluted in complete media to obtain the final concentrations: 5 nM, 50 nM in gene expression experiments, caspase assays and RNA sequencing and [0.00005, 0.0005, 0.05, 0.5, 5, 50, 100] nM in the Trypan blue-based cell counting and IC_{50} calculation experiments.

- Carboplatin was purchased from Sigma-Aldrich (Gillingham, UK) as powder and solubilized in distilled water to obtain a stock solution of 10mg/ml. The solution was sterilized using a 0.22 µm filter and stored at -20°C. The stock solution was serially diluted to obtain the final concentrations: 1 µM, 10 µM and 100 µM in gene expression experiments.

Table 2.2 | Drugs used in this project and specifications.

Drugs Name	Supplier	Cat.No	Solubility
Enzalutamide (MDV3100)	Selleckchem	S1250	DMSO
Cabazitaxel	Selleckchem	S3022	DMSO
Carboplatin	Sigma-Aldrich	C2538	H_2O

The concentrations tested in these experiments were selected based on the range of concentrations used in the literature for prostate cancer cells (McPherson, Galettis and de Souza, 2009; Mukhtar *et al.*, 2016; Yadav *et al.*, 2016; Ríos-Colón *et al.*, 2017) (tab.2.3). Inside this range, concentrations distant $\log_{10}$ from each other were chosen, in order to select a range of concentration wide enough to be able to see changes in expression and phenotypes.

The initial timepoint of 72h was selected based on literature evidence (McPherson, Galettis and de Souza, 2009; Yadav *et al.*, 2016; Ríos-Colón *et al.*, 2017).

All drugs were thawed at room temperature and diluted in cell culture media to treat the cells at different concentrations and timepoints, according to the experiments (see next methods of this chapter).

Table 2.3 | Reported drug concentration range based on the literature for prostate cancer cells and concentrations selected for this project.

Treatments	Reported concentrations in AR⁻ cells	Reported concentrations in AR⁺ cells	Concentrations employed for initial experiments	References
Enzalutamide	-	1-10 µM	• 1 µM • 10 µM	(Yadav *et al.*, 2016) (Zhang *et al.*, 2019)
Cabazitaxel	0.1-100 nM	0.1-50 nM	• 5 nM • 50 nM	(Machioka *et al.*, 2018)(Sekino *et al.*, 2019)(Mukhtar *et al.*, 2016)(Ríos-Colón *et al.*, 2017)
Carboplatin	1-100 µM	-	• 1 µM • 10 µM • 100 µM	(McPherson, Galettis and de Souza, 2009)

2.5. *HORAS5* confirmation of expression and subcellular localization

To determine RNA expression, total RNA extraction was performed. To determine the cellular localization of *HORAS5*, the Nuclear/Cytoplasmic Fractionated RNA extraction was performed. In both the total and fractionated RNA extractions the cells were harvested after medium removal and one wash in HBSS.

2.5.1. Total RNA extraction

Total RNA was isolated from cultured cells using the RNeasy plus mini Kit (Qiagen, Manchester, UK).

For RNA extraction, cells were seeded in 6-well plates, incubated and treated according to the specific experiment.

After medium removal and wash with HBSS, 350 µL of lysis buffer RLT (supplemented with β-mercaptoethanol) was added directly into each well of the 6-well plate. In order to remove genomic DNA (gDNA) which could alter the results of downstream analysis, the cells were collected into a gDNA RNeasy mini column (supplied in the kit) using a cell-scraper and centrifuged for 30 seconds at 8000 x g.

After centrifuge, 350 µl of 70% ethanol was added to the flow-through, mixed well and the solution was transferred into a RNeasy Mini spin column (supplied), placed in a 2 ml collection tube.

Samples were then centrifuged for 15 seconds at 8000 x g and then the flow-through was discarded. Thereafter, 700 µl of buffer RW1 was added to the column which was centrifuged for 15 seconds at 8000 x g. The flow-through was discarded again and 500 µl of buffer RPE was added to the column.

Samples were centrifuged for 15 seconds at 8000 x g and then the flow-through was discarded. This last step was repeated by adding again 500 µl of buffer RPE to the column and centrifuging 2 minutes at 8000 x g, instead of 15 seconds.

After discarding again the flow-through, the column was placed into a new 2 ml tube and centrifuged 1 minute at 13000 x g, in order to dry the membrane.

The column was then placed into a new 1.5 ml Eppendorf tube and 30-50 µl of DNase/RNase-free water was added. The samples were centrifuged 1 minute at 8000 x g in order to elute the RNA.

2.5.2. Nuclear/Cytoplasmic Fractionated RNA extraction

In order to investigate the subcellular localization of *HORAS5*, the cells were detached with 1 ml trypsin and counted with the haemocytometer, in order to obtain 10^6-10^7 cells; within this range the protocol should work with a high efficiency. The cells were then centrifuged for 5 minutes at 1500 rpm. The pellet was washed in HBSS. From this step, the cells were kept on ice and used for nuclear- and cytoplasmic-fractionated RNA extraction, performed on cultured cells using the PARIS™ kit (Ambion, Loughborough, UK). This protocol does not include a DNAse digestion step. Hence, after the fractionated RNA isolation, the TURBO DNA-free™ Kit was used for DNA removal (Ambion, Loughborough, UK, Cat# AM1907) (section 2.8).

According to the protocol, initial reagents were prepared by adding 415 µl of 2-mercaptoethanol to the 2X Lysis/Binding Solution and mixing well.

Wash Solution 2/3 was supplemented with 64 mL of absolute ethanol up to a final volume of 144 mL and they were mixed thoroughly.

Cell Disruption Buffer and Cell Fractionation Buffer were placed on ice while 2X Lysis/Binding Solution and Wash Solution 1 were placed at room temperature, before starting the procedure.

After completing these preparations, 500 μl of Cell Fractionation Buffer was added to the pelleted cells and used to resuspend it.

The cell suspension was incubated on ice for 10 minutes and then centrifuged for 4 minutes at 500 x g at 4° C, using a pre-cooled centrifuge.

The supernatant containing the cytoplasmic lysate was transferred into a new Eppendorf tube.

In the meantime, the nuclear fraction can be obtained after some additional steps. In fact, 500 μl of ice-cold Cell Fractionation buffer was added to the pellet.

The tube was flicked and centrifuged for 1 minute at 500 x g at 4° C. Supernatant was removed and 500 μl of ice-cold Cell Disruption Buffer was added to the pellet, which was vortexed vigorously to homogenize the nuclear lysate.

After these steps to obtain the nuclear fraction, 500 μl of 2X Lysis/Binding Solution was added to both the cytoplasmic and nuclear lysates and the samples were gently mixed by pipetting 4 times.

The nuclear lysate might appear viscous and can be passed through a syringe needle (needle gauge 20) 2 times in order to address this problem. Thereafter, 500 μl of 100% ethanol was added to both nuclear and cytoplasmic fraction and samples were mixed gently by pipetting. Samples were then transferred into a Filter Cartridge (maximum volume 700 μl) placed in a collection tube and centrifuged for 1 minute at 13000 x g at room temperature.

The flow-through was discarded and the last steps were repeated with the rest of the sample if some exceeded the filter cartridge volume of 700 µl.

When all the sample volume had been passed through the filter cartridge and flow-through discarded, 700 µl of Wash Solution 1 was added to the Filter Cartridge and centrifuged for 1 minute at 13000 x g at room temperature.

The flow-through was discarded and 500 µl of Wash Solution 2/3 was added and centrifuged for 1 minute at 13000 x g at room temperature.

This last step was repeated, flow-through was discarded and samples were centrifuged again for 30 seconds at 13000 x g at room temperature, in order to remove the last traces of wash solution.

The Filter Cartridge was placed into a new collection tube and 98°C preheated Elution Solution was added, in two separate aliquots: elution of the RNA in 40 µl of solution and centrifuge for 30 seconds; elution in 10 µl of solution into the same tube and centrifuge for 30 seconds.

After the fractionated RNA extraction, the samples were kept on ice, quantified and purified, according to the TURBO DNA-free ™ procedure, described in section 2.7.

2.6. RNA quantification with Nano Drop

The RNA extracted was quantified using Thermo Scientific™ NanoDrop™ OneC Microvolume UV-Vis Spectrophotometer. Before the quantification, both the arms of the Nano Drop were cleaned with H_2O. Once cleaned, 2µl of DNase/RNase-free water was loaded as blank. Then the nanodrop's arms were cleaned and the samples were loaded; the arms were cleaned after each loading. The instrument measures the

concentration of the RNA samples in ng/µl, recorded for the further steps of the experiments.

2.7. RNA purification with gDNA removal

After quantification, the RNA extracted with the PARIS procedure was treated to remove DNA residue, following the TURBO DNA-free (Invitrogen, Loughborough, UK) procedure.

Samples were diluted to 100 ng/µl in order to obtain the same concentration for each sample. At this concentration efficient removal of contaminating DNA is possible, as the protocol suggests to use a concentration ≤ 500 ng/µl.

After dilution, 4.5 µl of 10X TURBO DNase Buffer (typically ~0.1 volume of total sample) and 1 µl of TURBO DNase were added to 45 µl of sample.

The solution was mixed gently and incubated at 37° C for 30 minutes.

After the incubation time, 5µl of DNase Inactivation Reagent was added and sample was incubated at room temperature for 5 minutes. Samples were transferred into a centrifuge tube and centrifuged at 10000 x g for 1.5 minutes.

The supernatant contains the purified RNA and was transferred into a new tube for further analysis.

2.8. RT-qPCR

Upon extraction and quantification, the purified RNA was converted into cDNA using the High-Capacity cDNA Reverse Transcription Kit (Applied Biosystems, Loughborough, UK). All the components of the kit were thawed on ice. For each sample, 10 µL of RT mix was prepared on ice using the following reagents and volumes:

- 10X RT Buffer, 2 µL

- 25X d NTP Mix (100mM), 0.8 µL

- 10X RT Random Primers, 2 µL

- Multiscribe Reverse Transcriptase, 1 µL

- Nuclease Free H_2O, 4.2 µL

After the preparation, the reagents were mixed gently and 10 µl of mix in each 0.2 ml tube was added.

In each tube with prepared RT mix, 10 µl of RNA sample (100 ng/µl) was added, in order to obtain a final quantity of 1 µg of RNA. The reagents in the tubes were mixed and the tubes were placed into a thermal cycler, selecting the following steps, without cycles:

- 10 minutes at 25°C

- 120 minutes at 37°C

- 5 minutes at 85°C

- Hold at 4°C

After the RT the cDNA samples were diluted 10 times before the real time q-PCR. For each sample the reaction was prepared with the following components:

- TaqMan® Universal PCR Master Mix (2X), 10 µl

84

- TaqMan® gene expression assay (GEA) (20X), 1 µl

- cDNA (1:10), 5 µl

- H$_2$O, 4 µl

The gene expression assays (GEAs) (Applied Biosystems, Loughborough, UK) used in the experiments contain sequence-specific unlabelled primers and the TaqMan® MGB (minor groove binder) probe. The probes used have a 5` FAM reporter dye and a 3` non-fluorescent quencher used to reduce the background signal and increase precision. The TaqMan GEAs used are *LINC00161* (Hs00863167_g1) and *BCL2A1* (Hs00187845_m1). *HPRT1* (Hs02800695_m1) was used as housekeeping control in all the RT-qPCR experiments. For subcellular localisation RT-qPCR experiments, the probes *MALAT1* (Hs00273907_s1) and *GAPDH* (Hs02786624_g1) were also used as nuclear and cytoplasmic control respectively.

20 µl of reaction was loaded into each well of a PCR 96-well plate. The RT-qPCR was performed using the MJ Opticon real time qPCR system, using the following parameters:

- 10 minutes at 95°C for DNA polymerase activation

- 15 seconds at 95°C for denaturation

- 1 minute at 60°C for annealing-extension

X 39 times (40 cycles)

Each sample was run in triplicate and the data analysis was performed by calculating the relative expression ($2^{-\Delta\Delta Ct}$) of the target gene (i.e. *HORAS5* and *BCL2A1*) normalized to the house-keeping genes. The Cts describe the number of cycles necessary to detect a specific expression of a gene, measured as signal produced by the GEAs.

2.9. RNA interference with siRNAs

Gene KD was carried out using the reverse transfection method (Hattori *et al.*, 2017). The cells were seeded in 6-well or 96-well plates, according to the experiments performed, and lipid-siRNA mixture was added. The mixture was prepared using the RNAiMAX reagent (Invitrogen, Loughborough, UK) according to the manufacturer's protocol. Two preliminary experiments were performed using Lipofectamine 3000 as transfection reagent (Invitrogen, Loughborough, UK) according to the manufacturer's protocol. The siRNA treatment was performed using 2nM siRNA as final concentration. All duplexes were purchased from Integrated DNA Technologies (IDT) (Leuven, Belgium): anti-*HORAS5* (*Linc00161*) Dicer-Substrate siRNA (DsiRNA) hs.Ri.LINC00161.13.2, anti-BCL2A1 DsiRNAs hs.Ri.BCL2A1.13.1 and hs.Ri.BCL2A1.13.2 and non-targeting negative control (scramble) DS NC1. DsiRNAs are 27mer RNA duplexes processed by the enzyme Dicer into the conventional, 21mer siRNA product; this gives to them increased potency in RNA target cleavage. In this thesis they will be simply called siRNAs, in order to avoid confusion. After 48- or 72-hours post-transfection, treated cells were harvested for total RNA and/or total protein extraction or used for drug treatment experiments.

2.10. Trypan blue exclusion cell count and IC$_{50}$ calculation

As a measure of cell response to cabazitaxel, cell count was assessed via Trypan blue-based method.

Cell metabolic assays (e.g. MTS assay) are not recommended in these experiments since they can give altered results because taxanes interfere with mitochondria metabolism (G Varbiro *et al.*, 2001).

For this procedure, 2 x 10^5 DU145-NC and DU145-OE cells were seeded in 6-well plates and treated with DMSO as control or cabazitaxel in the concentrations specified above (see "Drugs and treatments", par. 2.5).

For analysis of drug treatment in combination with siRNAs, 2.5 x 10^5 LNCaP cells and 5 x 10^5 DU145-OE cells were seeded in a 6-well plate and reverse transfected using 2nM of either the control siRNA or anti-*HORAS5* siRNA or anti-*BCL2A1* siRNAs. 48h post transfection, the cells were treated with DMSO/cabazitaxel in the concentrations specified above (see drug treatments) for 72h (LNCaP) and 48h (DU145-OE) (fig.2.2).

HORAS5 is indeed significantly induced by cabazitaxel in LNCaP cells after 72h and in DU145-OE after 48h. Since efficient KD at 48h post-transfection was observed, cabazitaxel treatment was started at this timepoint. The result is a 5 days experiment for LNCaP and 4 days experiment for DU145-OE (fig.2.2).
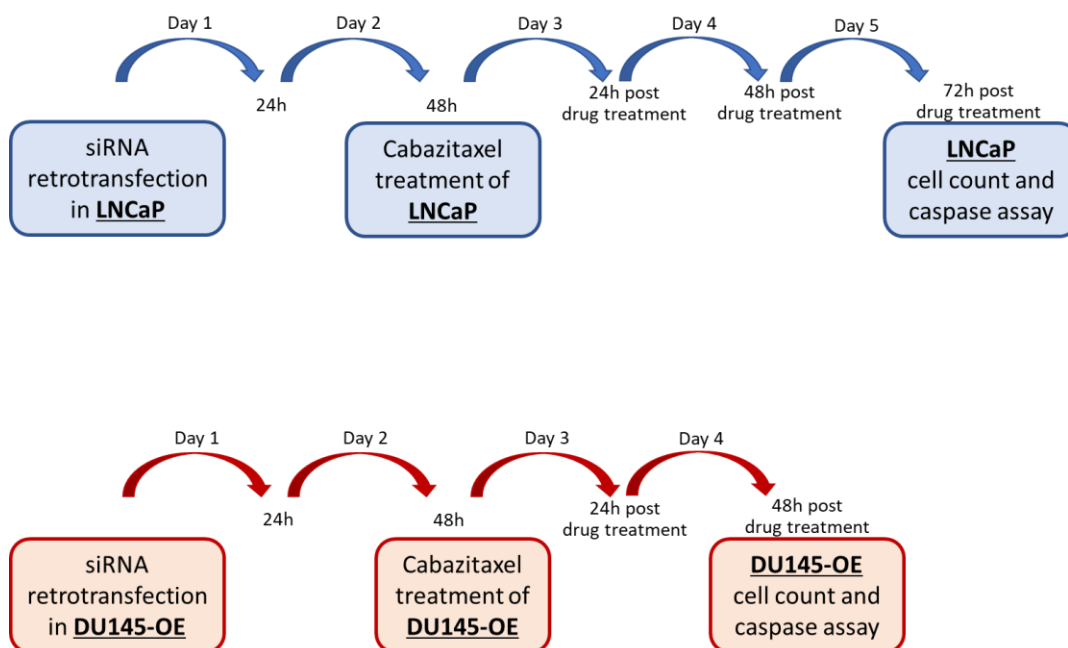
Figure2.2 | Diagram explaining drug treatment procedure in combination with siRNA-mediated KD in LNCaP and DU145-OE cells.

For all the cells, after the drug treatment, cell count has been performed using the trypan blue-based method in order to obtain the fraction of viable cells. The cells were detached using trypsin and collected in a 2 mL Eppendorf tube. 200 µL of cell suspension was mixed with 200 µL of trypan blue and incubated five minutes at room temperature. 10 µL of cell suspension mixed with trypan blue was counted using a haemocytometer. IC_{50} has been calculated using non-linear regression analysis (variable-slope inhibitor fitting), after normalization to untreated (DMSO) cells.

2.11. Caspase 3/7 assay

Caspase-mediated cell apoptosis was measured by Caspase-Glo® 3/7 Assay (Promega, Southampton, UK). 10^4 DU145-NC and DU145-OE cells were seeded in a white, flat-bottom 96-well plate and treated with either DMSO or 5nM of cabazitaxel.

1.25×10^4 LNCaP cells and 2.5×10^4 DU145-OE cells were seeded in a white, flat-bottom 96-well plate and reverse transfected with 2nM of either the control siRNA or anti-

88

HORAS5 siRNA or anti-BCL2A1 siRNAs. 48h after the transfection the cells were treated with DMSO, 5nM or 50nM of cabazitaxel for 72h (LNCaP) and 48h (DU145-OE).

For all the cells, after the drug treatment, 100µl of Caspase-Glo 3/7 Reagent (Promega, Southampton, UK) was prepared and added to each well of a white-walled 96-well plate containing 100µl of cells or blank. The plate was then covered, gently mixed using a plate shaker at 300–500 rpm for 30 seconds and incubated at room temperature for 1 hour and 30 minutes. After incubation, total luminescence was quantified using a BMG Optima polarSTAR plate reader (BMG Labtech, Aylesbury, UK) and normalized to time-matched and treatment-matched cell counts.

2.12.   RNA sequencing and analysis

RNA samples were isolated from DU145-NC and DU145-OE cells untreated (DMSO) vs treated with 5nM of cabazitaxel for 48h. RNA Sequencing Ion Torrent Semiconductor technology (Thermo Fisher Scientific, Loughborough, UK) was carried out at the Institute of Pathology of the University Hospital Basel, Switzerland together with bioinformatics analysis. RNA sequencing data were normalized as reads per million mapped reads (RPM) calculated as: (number of reads mapped to a gene x 10^6)/(total number of mapped reads from given library). The resulting dataset was analysed in order to determine the protein-coding differentially expressed genes (DEGs) upregulated when *HORAS5* is overexpressed (DU145-OE) compared to the negative control (DU145-NC), upon treatment with cabazitaxel (cabazitaxel-driven genes in figure 5.1). The expression threshold was set as RPM fold-change higher than 2 and P value lower than 0.01 for the cells overexpressing *HORAS5* (DU145-OE). 87 genes satisfied these criteria in the cells overexpressing *HORAS5* (DU145-OE) but not in the control cells (DU145-NC). For this

reason, they were shortlisted and filtered based on DU145-NC P value, by sorting in P value descending order (top 25 genes in figure 5.1). The 25 genes shortlisted were selected for pathway analysis, using the Reactome software. The final shortlist of 3 genes was obtained as explained in the results (Chapter 5.1).

2.13.   Cell lysis for protein analysis

Cells were cultured and treated according to the specific experimental protocol. For total protein isolation, cells were lysed using RIPA buffer, prepared using the following components for 100 mL: 0.2422g of Tris pH 8.0 (Sigma Aldrich, Gillingham, UK); 0.877g of NaCl (Sigma Aldrich, Gillingham, UK); 0.0372g of EDTA (Sigma Aldrich, Gillingham, UK); 1 mL of Igepal (Sigma Aldrich, Gillingham, UK); 1 mL of 10% SDS (Sigma Aldrich, Gillingham, UK), 0.21g of NaF (Sigma Aldrich, Gillingham, UK); 0.018g of $NaVO_3$ (Sigma Aldrich, Gillingham, UK); distilled water up to 100 mL.

The cells were placed on ice and washed twice with ice-cold HBSS. After washes, 15-50-100 µL of ice-cold RIPA buffer (volume depending on the number of cells used) were supplemented immediately before use with 1:100 protease and phosphatase inhibitors (Merk Millipore, UK) and added to the cells in order to induce cell lysis. The protease and phosphatase inhibitor cocktail is specially formulated with different concentrations of six protease inhibitors:

100mM of AEBSF, hydrochloride

80µM of aprotinin, bovine lung, crystalline

5mM of Bestatin

1.5 mM of E-64, Protease inhibitor

2mM of Leupetin, Hemisulfate

1mM of Pepstatin A

90

The cells were incubated in RIPA buffer + protease and phosphatase inhibitor cocktail on ice for 5 minutes with occasional swirling.

Cells were harvested using cell scrapers and transferred into pre-cooled Eppendorf tubes. The next stages are carried out keeping the cell lysates in ice.

The samples were sonicated for 10 seconds at 20% amplitude, using ultrasound sonication (Fisherbrand™ Model 120 Sonic Dismembrator, Fisher Scientific, Loughborough, UK) and then centrifuged at 14,000 g for 15 minutes at 4°C.

The pellet contains cell debris while the supernatant contains cell lysate with proteins. Hence, the supernatant was collected for protein quantification and further analyses. The remaining supernatant was aliquoted in order to avoid freeze-thaw cycles in subsequent experiments and stored at -20ºC.

2.14. Protein quantification

Protein content was quantified using the Thermo Scientific Pierce™ BCA Protein assay kit (Thermo Fisher Scientific, Loughborough, UK).

The BCA assay is a colourimetric test to detect and quantify total proteins. This assay couples two reactions: the biuret reaction constituted by protein reduction of Cu^{2+} to Cu^{1+} in alkaline medium that results in a complex with a light-blue colour; and the colourimetic detection of Cu^{1+} using a reagent constituted by bicinchoninic acid (BCA), giving a purple colour. The resulting complex is soluble in water and has and absorbance at 562 nm that increases with a linear trend with increased protein concentrations.

In the laboratory practice, the three steps of this assay are: Preparation of dilutions of the standard, preparation of the BCA working reagent and microplate procedure.

The preparation of dilutions of the standard is necessary since some protein features such as the number of peptide bonds determines color formation with BCA.

For this reason, protein concentrations are normally determined with reference to standards of a common protein such as bovine serum albumin (BSA) in a series of dilutions of known concentrations to build a standard curve in order to be able to estimate the unknown concentrations of the samples.

The standard dilutions were obtained with a BSA stock vial, concentrated 2000µg/mL, included in the kit and the same lysis buffer (RIPA) used to isolate protein, where the protein is suspended in the volumes reported in table 2.4.

The measures of the standards were used to generate the protein standard curve.

The BCA working reagent was prepared using reagent A (bicinchoninic acid) and reagent B (copper (II) sulphate) of the kit in a 50:1 ratio: 50 parts of reagent A for 1 part of reagent B.

The microplate procedure consists of adding 10µL of the standards and the samples in triplicates into the wells of a 96-well plate with clear flat bottom and adding to all the wells 200µL of working reagent, mixing the plate on a plate shaker for 30 seconds, covering and incubating the plate in the dark at 37°C for 30 minutes.

After 30 minutes, the plate was cooled down to room temperature and absorbance was measured at 562nm on a BMG Optima polarSTAR plate reader (BMG Labtech, Aylesbury, UK).

Table 2.4 | Dilutions of BSA protein standards used in the BCA assay to create the standard curve used to determine the total concentration of proteins in this project.

Protein standard	Volume of diluent (RIPA lysis buffer) (µL)	Volume and source of BSA (µL)	Final concentration of BSA (µL/mL)
A	0	300 of stock (2 mg/mL BSA)	2000
B	125	375 of stock	1500
C	325	325 of stock	1000
D	175	175 of vial B dilution	750
E	325	325 of vial C dilution	500
F	325	325 of vial E dilution	250
G	325	325 of vial F dilution	125
H	400	100 of vial G dilution	25
I	400	0	0

2.15.   Western Blot

Gene expression at the protein level was analysed by western blot.

Cells were seeded in cell culture flasks, incubated and treated according to the specific experiment.

After the required incubation period, the cells were lysed, and protein concentration was determined as described above (2.13 and 2.14).

For this analysis, 15 µg of proteins were resolved via gel electrophoresis on reducing SDS-polyacrylamide gels (Tricine 10-20%, Thermo Fisher, Loughborough, UK).

Proteins were prepared as 10µl of 20µg protein diluted in water in order to obtain the same quantity in each well. Novex Tricine SDS Sample Buffer (2X) (Thermo Fisher,

Loughborough, UK) was mixed with 1:250 of β-mercaptothanol. β-mercaptothanol breaks down disulphide bonds which can cause dimers formation. 10μL of β-mercaptothanol + sample buffer was mixed with the 10 μl of protein. In order to allow proteins to run linearly in the polyacrylamide gel, the samples were heated for 2 minutes at 85°C.

While heating proteins, 500ml of 1X Novex Tricine SDS Running Buffer (1:10 dilution from 10X buffer) (Thermo Fisher, Loughborough, UK) containing 500μl of antioxidant (Invitrogen, Loughborough, UK) was prepared and poured into the tank where the gel had been previously inserted. Wells were washed with running buffer in order to remove any possible gel obstruction or bubbles. After proteins were heated, 15μL, containing 15μg of total protein, were loaded into the gel wells. Additionally, 5μL Novex Sharp Pre-stained Protein Standard (Invitrogen, Loughborough, UK) were loaded next to the protein samples. The gel was run for around 2 hours at 110 constant Volts.

During the run, 300 ml of 1X transfer buffer (from 10X tricine running buffer) with 20% methanol was prepared and used to soak sponges, blotting paper and membrane that will be used for the transfer:

   5 x sponges per gel

   2 x blotting paper per gel

   1 x membrane per gel (0.2um nitrocellulose)

After the run, the gel was removed from the rig and placed to equilibrate into transfer buffer.

Proteins were transferred from the gel onto the membrane using the sandwich method with 2 sponges, blotting paper, membrane, gel, blotting paper and 3 sponges. The

sandwich was rolled out to remove bubbles between the different components. The rack was inserted into the transfer chamber and topped up with transfer buffer.

The area outside of the rack was topped up with cold water in order to keep the protein transfer at cold temperatures. Proteins were transferred at constant 300mA for 2 hours and 30 minutes.

After the transfer, the membrane was blocked in 8% skimmed milk dissolved in tris buffered saline (TBS; 0.2 mM Trizma base; 1.4 mM sodium chloride; pH 7.6) supplemented with 0.1% tween-20 (TBST), at room temperature for 1h, with gentle rocking. This step is necessary to reduce the amount of background and non-specific antibody binding.

The membrane was incubated overnight at 4°C on a platform shaker with protein-specific primary antibodies dissolved in 5% BSA diluted in TBS-T for anti-BCL2A1 (310µg/ml stock concentration) (1:100 dilution) (Cell Signalling Technology, A1/Bfl-1 (D1A1C) Rabbit mAb, Cat# 14093) and in 5% milk diluted in TBST for anti-GAPDH (1mg/ml stock concentration) (1:50000 dilution) (Sigma Aldrich, Gillingham, UK). The membrane was washed 3 times with TBST for ten minutes each. The blots were Incubated with HRP-conjugated anti-rabbit secondary antibody (1µg/ml stock concentration) (Fisher, cat#31460) dissolved in 8% milk diluted in TBST, at room temperature for 1h (1:2000 dilution). After the incubation, blots were washed 4 times in TBST for 10 minutes each. After washing, ECL western blotting substrate kit was used (Millipore, Watford, UK) to visualise blot chemiluminescence, using Syngene Gbox with GeneTools software (Syngene, Bangalore, India).

2.16. CbioPortal analysis of clinical evidence

This analysis tested whether *HORAS5* and *BCL2A1* gene expression correlates with prostate cancer survival in order to understand the clinical relevance of the genes. This analysis was conducted using CBioPortal (http://www.cbioportal.org), a genomic platform with publicly available cancer studies. A dataset from The Cancer Genome Atlas (TCGA), with available PFS analyses from patients with high and low expression of *HORAS5* and *BCL2A1*, was queried. Significant association (p<0.05) between gene expression and PFS is expressed in terms of percentage of cases that show relapse on total cases, after initial treatment (radical prostatectomy). *HORAS5* expression was also analysed in an Agilent microarray dataset (Kumar *et al.*, 2016) consisting of a single study with 63 patients, of whom 15 patients were not exposed to chemotherapy treatment and 10 were treated with taxanes. The remaining 38 patients were treated with other drugs and were not considered for this comparison. The samples from metastatic sites, of these 25 total patients, were analysed by comparing no chemotherapy versus taxane-only treatment.

2.17.   ASO-mediated knockdown

In ASO-mediated KD experiments, 1.5 x 10^5 LNCaP cells were seeded in 6-well plates and after 24h the cells were transfected with 75nM of the negative control ASO (Eurofins genomics, ASO-NC: 5'- CCT TCCCTGAAGGTTCCTCC -3' and *HORAS5*-ASOs (Eurofins Genomics):

ASO1: 5'- GGAGACACCATTCAGCCCAC -3'

ASO2: 5'- GACAGGATCCCGGCATATGA -3'

ASO 3: 5'- GGCTGCTGCATGTCTACAGT -3'

ASO4: 5'- GGCTCTTCCCTCATATCCAC -3'

ASO5: 5'- GGTTCATTCAGTAGCTCCAC -3'

ASO6: 5'- CCATCTGAATGCCCACACAC -3'

ASO7: 5'- CTGGCAATTTCCCCACACTC -3'

ASO8: 5'- CAATTCACACCTCCATCAGC -3'

RNAiMAX (Invitrogen, Loughborough, UK) was used as transfection reagent, according to the manufacturer`s protocol. 48h after ASO treatment, the RNA was extracted in gene expression experiments while for cell count, the cells were treated with DMSO or cabazitaxel at the concentrations specified above (see Drugs and treatment, 2.5). 72h after drug treatment, the cells were counted using the trypan blue-based method and IC_{50} was calculated (fig.2.3).
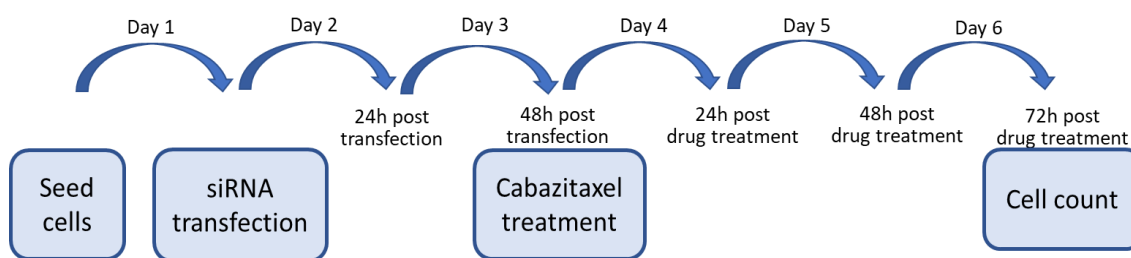
Figure2.3 | Diagram explaining drug treatment procedure in combination with ASO-mediated KD in LNCaP cells.

2.18.   Statistical analysis

Data were analysed using GraphPad-Prism 7 and subsequent update software. Results are presented as mean ± standard deviation (SD) from two or three independent experiments, according to the type of analysis (see figure legends in the next Chapters). An Unpaired Student`s t-test was performed to investigate statistically significant differences between the means of two groups tested.

One-way analysis of variance (ANOVA) was performed to investigate statistically significant differences among the means of three or more groups tested; the difference between groups was investigated using Tukey`s and Dunnett`s multiple comparison test. A post-test for linear trend was used to investigate if the effect of cabazitaxel on *HORAS5* expression is linearly dose dependent.

A two-way ANOVA with Sidak`s multiple comparison post-test was used for statistical analysis when 2 variables were considered and Two-way ANOVA with non-linear fit (log inhibitor vs. normalized response-Variable slope) for IC_{50} analysis. An outlier test was carried out to identify extreme experimental replicates for the IC_{50} calculation.

Unless otherwise stated, P value<0.05 was set as threshold for statistical significance.

CHAPTER 3: THE ROLE OF DRUGS ON HORAS5 EXPRESSION

Current clinical therapies for CRPC can extend patient survival, but are still characterized by short remission times (Nabavi *et al.*, 2017). Wang and collaborators have shown the involvement of the lncRNA *linc00161* (alias *HORAS5*) in osteosarcoma cell response to cisplatin (Wang *et al.*, 2016). They have observed that cisplatin can induce the expression of *HORAS5* and that this lncRNA activates pro-apoptotic pathways. Based on recent findings (Parolia *et al.*, 2019), *HORAS5* promotes CRPC cell growth via inhibition of apoptosis.

It is well known that lncRNAs are characterized by tissue-specific expression and functions. For example *H19* is up-regulated in specific tumours and down-regulated in others (Crea, Clermont, *et al.*, 2014) (Z. Li *et al.*, 2017)(Yoshimizu *et al.*, 2008). In fact, *H19* is downregulated in colorectal adenomas where it acts as an oncosuppressor (Yoshimizu *et al.*, 2008). On the other hand, this lncRNA is highly expressed in breast cancer, where it acts via other mechanisms to promote the proliferation and invasion of cancer cells (Z. Li *et al.*, 2017).

It is therefore conceivable that *HORAS5* plays opposite roles in different cancers. Moreover, other findings have confirmed the role of *HORAS5* in tumour-related pathways (L.-C. Xu *et al.*, 2017), showing key functions in the context of drug response, in ovarian cancer where *HORAS5* promotes cisplatin resistance (Xu *et al.*, 2019).

Based on this evidence, *HORAS5* has emerged as a driver of drug resistance in different malignancies. This paves the way for the discovery of an emerging role of this lncRNA, which could be of paramount importance to overcome drug resistance in CRPC and in other aggressive cancers, where *HORAS5* is dysregulated.

Based on all these findings, *HORAS5* could affect drug response in CRPC. This hypothesis will be further tested and functional and mechanistic studies will be performed on the role of *HORAS5* in CRPC cell response to therapy. The aim of this chapter is to measure the expression levels of *HORAS5* in CRPC cells exposed to clinically relevant drugs in order to investigate if this lncRNA could be involved in CRPC drug resistance phenotypes.

With this purpose, a panel of drugs clinically relevant for the treatment of CRPC have been selected and tested in prostate cancer cells. These drugs are: the AR inhibitor enzalutamide, used in AR$^+$ CRPC (Scher *et al.*, 2012; Beer *et al.*, 2014; Hussain *et al.*, 2018); the microtubule inhibitor cabazitaxel, effective against both AR$^+$ and AR$^-$ CRPCs (Sissung *et al.*, 2014; Smiyun, Azarenko, Miller, Rifkind, LaPointe, *et al.*, 2017); the platinum agent carboplatin, active in anaplastic CRPCs, which are generally AR$^-$ or AR-indifferent (Fléchon *et al.*, 2011; Aparicio *et al.*, 2013) (tab. 3.1). Based on these clinical indications, enzalutamide has been used in LNCaP cells, carboplatin in DU145-OE cells and cabazitaxel in both cell lines (tab. 3.1).

Table 3.1 |Treatment selection based on clinical and in vitro evidence.

Cancer Type	Clinical treatment used	*In vitro* evidence	Cell line selected for experiments	Treatment selected	References
AR^+ CRPC	Hormonal (Abiraterone, Enzalutamide)	Active in AR^+ CRPC cells	LNCAP (AR^+)	Enzalutamide	(Scher *et al.*, 2012; Beer *et al.*, 2014; Hussain *et al.*, 2018)
	Chemotherapy (Docetaxel, cabazitaxel)	Active in both AR^+ and AR^- CRPC cells		Cabazitaxel	(Sissung *et al.*, 2014; Smiyun, Azarenko, Miller, Rifkind, LaPointe, *et al.*, 2017)
AR^- CRPC	Chemotherapy (Docetaxel, cabazitaxel, platinum agents)	Active in both AR^+ and AR^- CRPC cells	DU145-OE and DU145-NC (AR^-)	Cabazitaxel	(Sissung *et al.*, 2014; Smiyun, Azarenko, Miller, Rifkind, LaPointe, *et al.*, 2017)
		Platinum agents active in AR^- CRPC cells		Carboplatin	(Fléchon *et al.*, 2011; Aparicio *et al.*, 2013)

Experiments and results reported in this chapter are discussed in the next sections and

summarized in table 3.2.

Table 3.2 | Summary of specific experiments, methods and results reported in this Chapter.

Experiments	Methods	Results
Overexpression of *HORAS5*	Lentiviral transduction + RNA extraction and RT-qPCR	The lentivector LPP-GS266B-Lv105-050 induces efficient *HORAS5* expression in DU145-OE cells
Subcellular localization	RNA fractionation (PARIS kit) + RT-qPCR	*HORAS5* overexpression retains the endogenous subcellular localization. *HORAS5* is mostly located in DU145-OE cells' cytoplasm. This observation suggests that it can be targetable with siRNAs without increasing efficiency for nuclear transfection. This cytoplasmic location also suggests a main role of *HORAS5* in this compartment with possible interactions with cytoplasmic molecules, complexes and subcellular components
Effect of *HORAS5* overexpression on cells properties	Observation of cells via optic microscope + MTS assay	*HORAS5* overexpression does not induce alterations in cellular morphology and proliferation.
Effects of drug treatment on *HORAS5* expression	Drug treatment at different concentrations + RNA extraction and RT-qPCR	Cabazitaxel induces a concentration-dependent increase in *HORAS5* expression in both AR$^-$ and AR$^+$ CRPC cells. Enzalutamide and carboplatin do not result in such an effect. Cabazitaxel was selected for further investigations.
Cabazitaxel selection and investigation of its role in *HORAS5* induction	Cabazitaxel treatment at different concentrations and timepoints + RNA extraction and RT-qPCR	Cabazitaxel induces a time-dependent increase in *HORAS5* expression in AR$^-$ (48h and 72h post-treatment) and AR$^+$ (72h post-treatment) CRPC cells. This has allowed us to select the optimal timepoints for *HORAS5* increase upon cabazitaxel treatment in each cell line (48h for DU145-OE, 72h for LNCaP) fur further analyses

3.1. *HORAS5* overexpression and subcellular localization

For this work, it has been necessary to select a model of CRPC cells with undetectable *HORAS5* expression in which to induce its overexpression and a model of CRPC cells with constitutive *HORAS5* expression, in which to analyse the effect of silencing this lncRNA. Based on a previous publication (Parolia *et al.*, 2019), LNCaP cells express *HORAS5* and have been used as a model for *HORAS5* KD. On the contrary, DU145 do not express *HORAS5.* Therefore, at the BC Cancer Agency (Vancouver, Canada), a model of *HORAS5* stable overexpression in DU145 (i.e. DU145-OE) has been produced and a model with no *HORAS5* detectable expression is used as control (DU145-NC).

DU145-NC and DU145-OE were sent from the BC Cancer Agency to the Open University and were used in further experiments, in order to investigate the role of *HORAS5* in CRPC cells` response to therapy. For this reason, the expression of *HORAS5* has been quantified in these cells via RT-qPCR. The results obtained show that the lentiviral transduction system works efficiently and DU145-OE cells show significantly higher expression of *HORAS5* than the wild type cell lines (fig. 3.1).
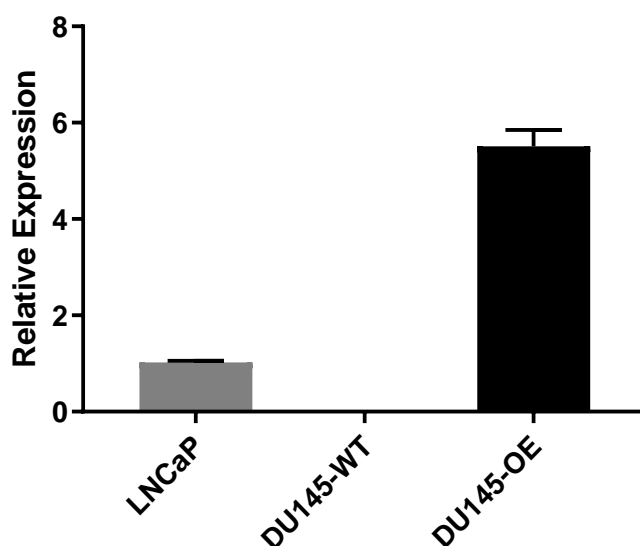
Figure 3.1 | *HORAS5* overexpression in DU145-OE.
Expression of *HORAS5* in LNCaP, DU145-WT and DU145-OE. Expression measured via RT-qPCR and represented as mean expression normalized for *HPRT1* control gene and relative to expression in LNCaP cells ± S.D. Results shown are representative of 3 independent experimental replicates. All RT-qPCR samples reported in this thesis were run in technical triplicate.

Since the *HORAS5* lentiviral transduction induces an artificial expression of the lncRNA, the subcellular localization of the transcript was analysed in DU145-OE cells, in order to identify possible discrepancies with cell lines that constitutively express *HORAS5* (e.g. LNCaP cells). A different localization of the lncRNA could alter its molecular function, thereby impairing the use of the Du145-OE cells to study the functions and mechanisms of action of *HORAS5*. These experiments have shown that *HORAS5* is mainly localized in the cytoplasm of DU145-OE (fig. 3.2). This is in keeping with the results from the cell lines that constitutively express *HORAS5* (Parolia *et al.*, 2019). Hence, the lentiviral system maintains a "normal" sub-cellular distribution of the *HORAS5* transcript in DU145-OE.
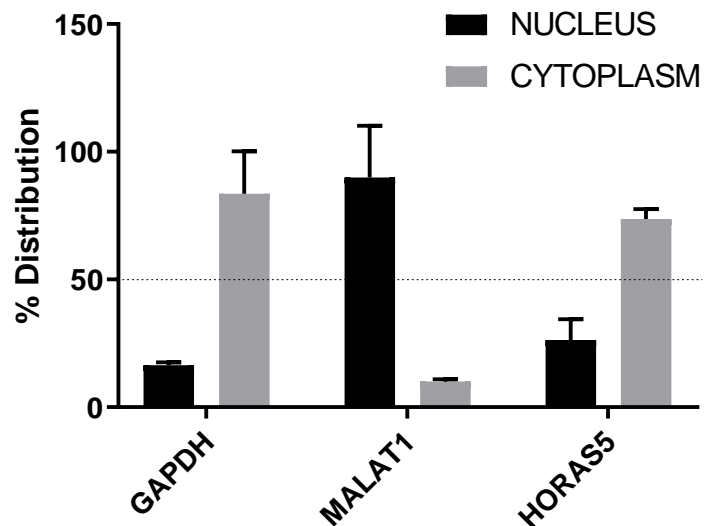
FIGURE 3.2 | *HORAS5* **overexpression preserves endogenous** *HORAS5* **subcellular localization.**
Quantitative expression of *HORAS5* in the nuclear and cytoplasmic fraction of DU145-OE cells, measured via RT-qPCR. *HPRT1* expression has been used for the normalization of the data and *GAPDH* has been used as cytoplasmic control; MALAT1 has been used as nuclear control. The results are shown as the means ± S.D. and are representative of two experimental replicates.

3.2 *HORAS5* overexpression does not affect AR⁻ CRPC cells morphology and proliferation

After the confirmation of *HORAS5* overexpression, it was analysed whether this genetic manipulation has phenotypic effects on DU145-OE cells. *HORAS5* overexpression does not determine changes in cell morphology (fig.3.3A). Moreover, the MTS assay has shown that *HORAS5* overexpression does not affect cell proliferation (fig.3.3B).

A

| DU145-WT | DU145-NC | DU145-OE |

B
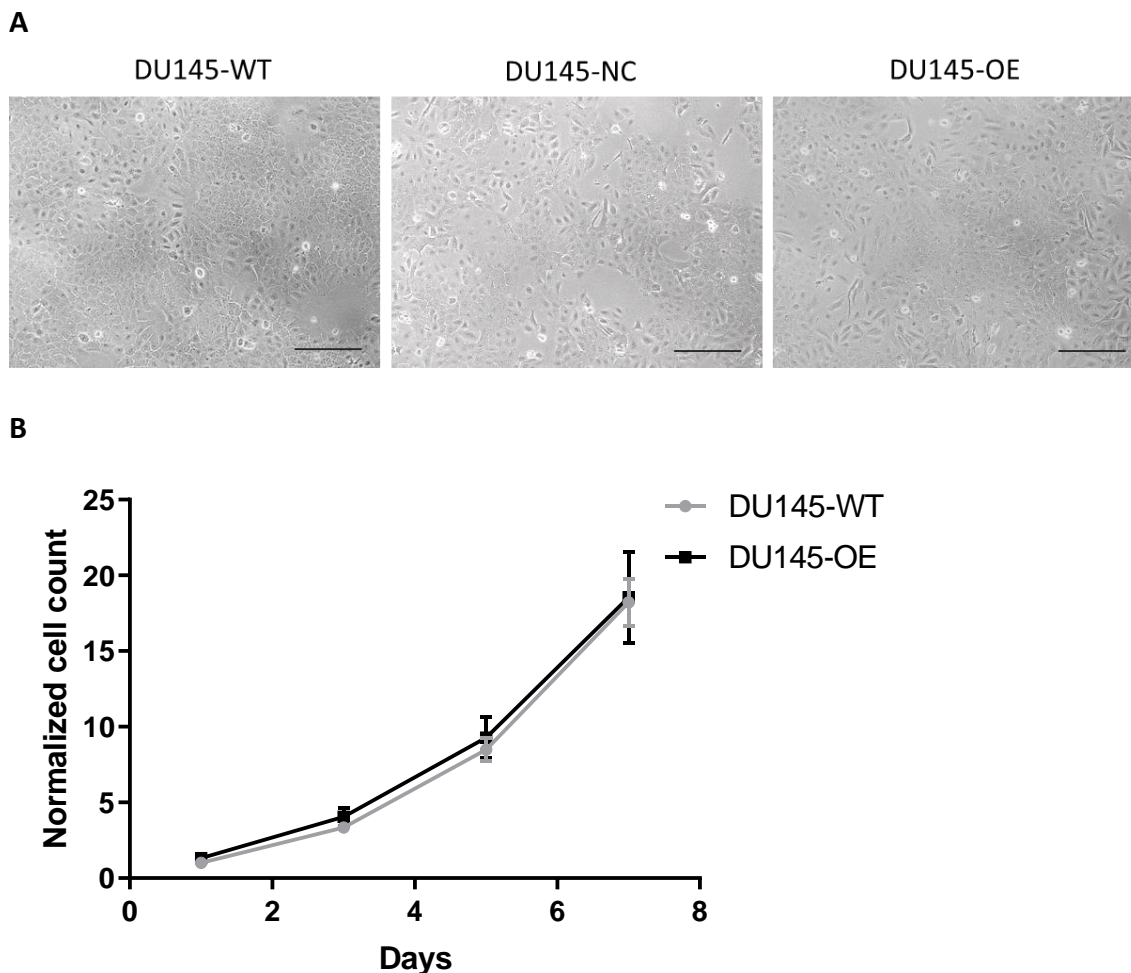
Figure 3.3 | *HORAS5* overexpression does not affect CRPC cell proliferation and morphology.
Pictures of DU145-WT, DU145-NC and DU145-OE cells` morphology (A) and MTS proliferation curves of DU145-OE vs DU145-WT (B). The size bars in figure A represent 100μm. Results expressed as means ± S.D. from two independent replicates. Two-way ANOVA with Sidak`s post-test was performed for statistical comparison in B.

3.3 *HORAS5* is induced by cabazitaxel in a concentration-dependent manner in both AR⁻ and AR⁺ CRPC cells

In order to assess whether there is a correlation between drug treatment and *HORAS5* expression in CRPC cells, LNCaP and DU145-OE cells have been exposed to specific concentrations of each of the different drugs tested. These concentrations have been selected according to the range of concentrations tested in prostate cancer cells, in

106

published studies (McPherson, Galettis and de Souza, 2009; Mukhtar *et al.*, 2016; Yadav *et al.*, 2016; Ríos-Colón *et al.*, 2017) (Chapter 2.4, tab.2.3).

The drug treatment has been done according to the clinicopathological features of each cell line (tab. 3.1). After 72h of drug treatment, the total RNA was extracted and analysed via RT-qPCR. As observed in figure 3.4, enzalutamide treatment does not result in consistent changes in *HORAS5* expression. In fact, despite the statistical analysis showing a significant increase in *HORAS5* expression at the lower concentration compared to the control, this increase is less than 1.5 fold and cells treated with enzalutamide at the higher concentration (10µM) did not show the same response (fig.3.4). The C_{max} represented is the the maximum serum concentration that a drug achieves after drug first administration and is a standard pharmacokinetic measurement. Drug concentrations below C_{max} can considered clinically achievable.
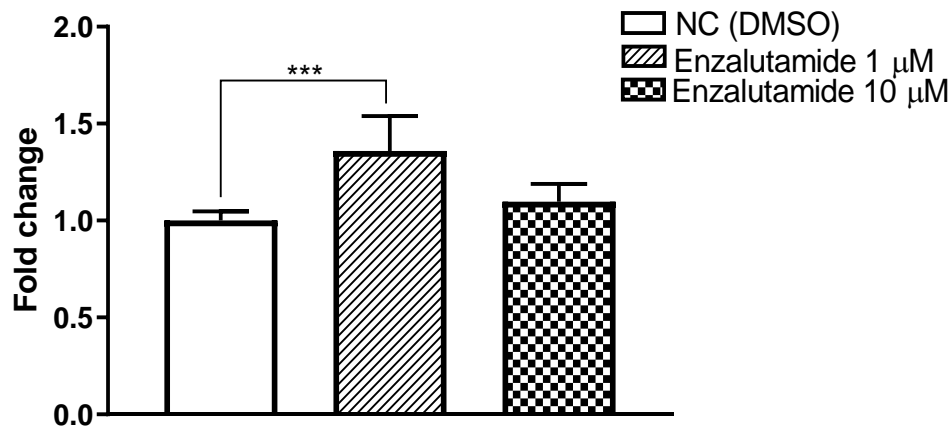
Clinically achievable C_{max} in literature study → 0.3-27.9 µg/mL

Highest concentration used in our experiments → 4.64 µg/mL (10µM)

Figure 3.4 | Effect of enzalutamide treatment on HORAS5 expression in LNCaP cells.
The graph shows *HORAS5* expression in LNCaP cells after treatment with different concentrations of enzalutamide. Below the graph is shown enzalutamide C_{max} from a clinical study (Gibbons *et al.*, 2015) and the highest drug concentration used in these experiments. The cells were treated with 1 µM and 10 µM of enzalutamide and DMSO as negative control (NC). Both the concentrations used are clinically achievable as underlined in the square under the graph. The RNA was extracted 72 h after treatment and was analysed via RT-qPCR. The data show the mean fold changes relative to the negative control (DMSO) ± the S.D. from two independent experimental replicates. Statistical analysis: one-way ANOVA with Dunnett's multiple comparisons test, ***p=0.0008.

Moreover, carboplatin treatment did not result in a statistically significant increase in *HORAS5* expression in DU145-OE cells, except that at the highest concentration tested (fig.3.5). In this case, the highest drug concentration employed resulted in a significant increase in *HORAS5* expression. Notably this concentration (100μM) is not clinically achievable. The additional 100μM concentration was included in these experiments, since it was tested in different studies and represents the closest $\log_{10}$ value to the highest IC_{50} found for AR^- prostate cancer cells in the literature (Yang, Hsu and Yang, 2000; Budman, Calabro and Kreis, 2002; McPherson, Galettis and de Souza, 2009).
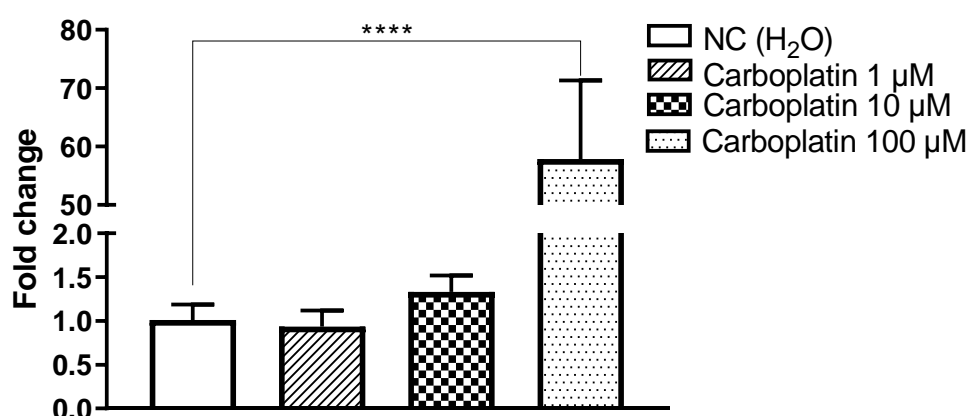
Clinically achievable C_{max} in literature studies → 14.30-26.70 μg/mL

Highest concentration used in this thesis experiments → 37.13 μg/mL (100 μM)

Figure 3.5 | Effect of carboplatin on HORAS5 expression in DU145-OE.
Expression of *HORAS5* in DU145-OE upon carboplatin treatment, measured via RT-qPCR. Below the graph is shown carboplatin C_{max} according to clinical studies (Fukuda *et al.*, 1999)(Kern *et al.*, 2001) and the highest drug concentration used in these experiments. The cells were treated with 1 μM, 10 μM and 100 μM of carboplatin and H_2O as negative control, since carboplatin was dissolved in water. Total RNA was extracted 72 h after treatment. Data show the mean fold change relative to the negative control (H_2O) ± the S.D. from two independent experiments. Statistical analysis: one-way ANOVA with Dunnett's multiple comparisons test, ****$P < 0.0001$.

When treated with cabazitaxel, both DU145-OE and LNCaP showed statistically significant increase in *HORAS5* expression. The increase is significant in both cell lines at the highest concentration of cabazitaxel used (P<0.0001 in DU145-OE, P=0.0001 in LNCaP) and is significant for LNCaP at the lower concentration used (P=0.0079) but not in DU145-OE. Although the statistical analysis does not show significance in DU145-OE cells treated with 5nM of cabazitaxel, the expression of *HORAS5* in cabazitaxel treated cells increased of 18.33 fold change compared to the DMSO treatment. Additionally, the effect shown in DU145-OE is particularly strong, possibly due to the up-regulation of the CMV promoter that controls *HORAS5* expression in this cell line. Nevertheless, since the same trend is observed in LNCaP cells, cabazitaxel simulates *HORAS5* expression by acting also on regulation of the endogenous gene.

Moreover, the average FC observed in both cell lines upon cabazitaxel treatment, of 18.33 and 125.38 in DU145-OE and 2.33 and 3.13 in LNCaP, are higher than the ones observed for the other drugs used. For this reason, in order to confirm the relevance of *HORAS5* upregulation upon cabazitaxel treatment and that this increase is dose dependent, data was additionally analysed using the one-way ANOVA linear trend test (fig.3.6). This analysis showed that *HORAS5* expression increases linearly using the concentrations of 5 nM and 50 nM in both DU145-OE (R square=0.72, P<0.0001) and LNCaP cells (R square=0.65, P<0.0001) (fig.3.6).

A

DU145-OE

Clinically achievable C_{max} in literature study → 0.441 µg/mL
Highest concentration used in this thesis experiments → 0.043 µg/mL (50 nM)

B   **LNCaP**

Clinically achievable C_{max} in literature study → 0.441 µg/mL
Highest concentration used in this thesis experiments → 0.043 µg/mL (50 nM)
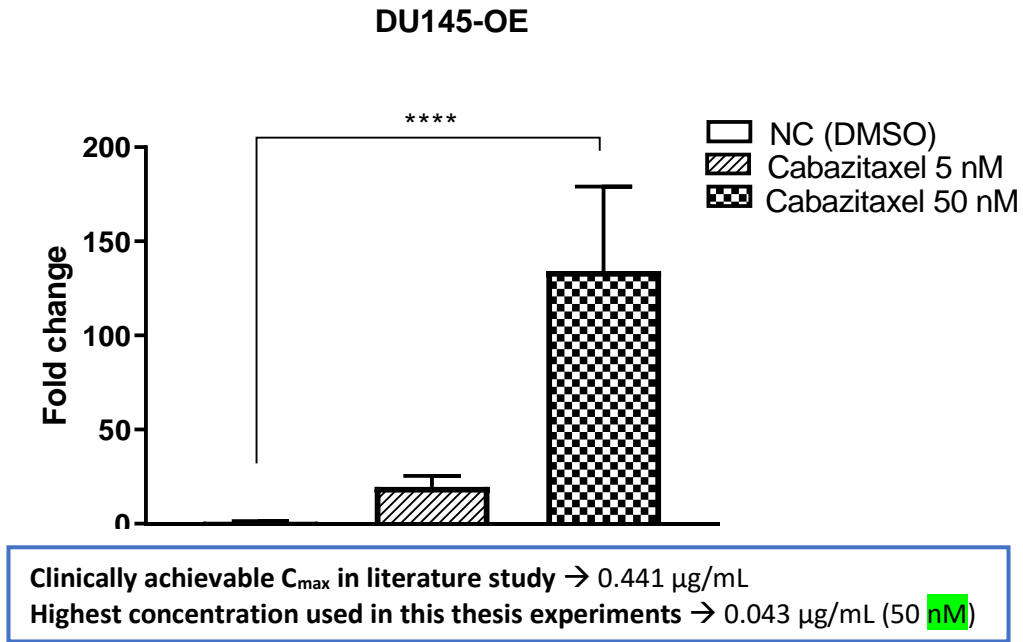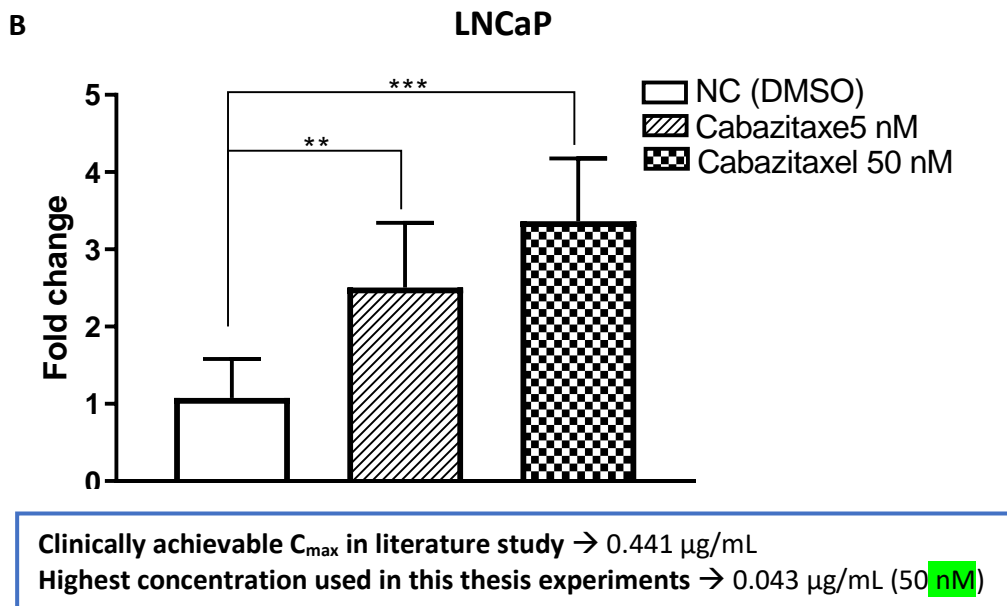
Figure 3.6 | Effects of cabazitaxel treatment on HORAS5 in both DU145-OE and LNCaP in a concentration-dependent manner.

Expression of *HORAS5* in DU145-OE (A) and LNCaP (B) cells, upon cabazitaxel treatment, measured via RT-qPCR. Below the graph are shown cabazitaxel C_{max} (Diéras *et al.*, 2013) and the highest drug concentration used in these experiments. Cabazitaxel induces a significant increase of *HORAS5* expression in both DU145-OE (A) and LNCaP (B) cells. Cells were treated with 5 nM and 50 nM of drug and DMSO as a negative control, since cabazitaxel was dissolved in DMSO; all cabazitaxel concentrations are clinically achievable as underlined in the boxes under the graphs. The RNA was extracted 72 h after treatment. Data are shown as mean fold increase relative to the negative control ± the S.D. from two independent experiments. One-way ANOVA with Dunnett's multiple comparisons test was used for statistical comparison, **P=0.0079, ***P=0.0001, ****P<0.0001. One-way ANOVA.

Taken together, these results indicate that the relation between cabazitaxel treatment and *HORAS5* expression is significant in both the cell lines tested, showing that cabazitaxel induces a concentration-dependent increase in *HORAS5* expression, in both LNCaP and DU145-OE.

3.4 *HORAS5* expression is induced by cabazitaxel treatment in a time-dependent manner in AR⁻ and AR⁺ CRPC cells

So far, based on the described results, cabazitaxel has been selected to investigate the role of *HORAS5* in drug response in CRPC. After determining the correlation between *HORAS5* expression and cabazitaxel concentration, it was also assessed whether this correlation is time-dependent. For this reason, *HORAS5* expression was measured via RT-qPCR after cabazitaxel treatment with 5nM and 50nM at 3 different time points: 24h, 48h, 72h.

The results show that *HORAS5* is up regulated upon cabazitaxel treatment and this up regulation increases with time (fig.3.7 A-B). Moreover, this analysis suggests that *HORAS5* induction is particularly significant 48h post treatment in DU145-OE (fug.3.7A) and 72h post treatment in LNCaP (fig.3.7B). Therefore, these two time points have been respectively selected for further experiments in this context.
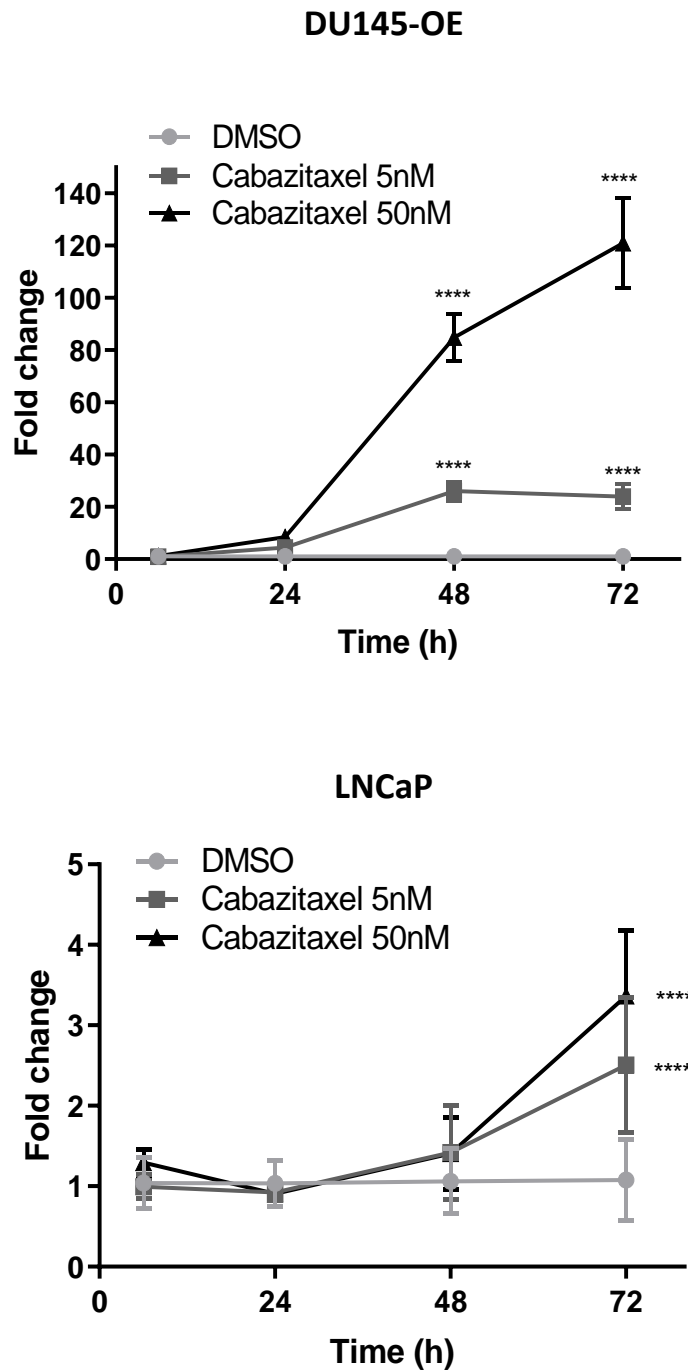
DU145-OE

LNCaP

Figure 3.7 | Cabazitaxel induces HORAS5 time-dependent expression in DU145-OE and LNCaP cells.
Expression of *HORAS5* in DU145-OE (A) and LNCaP (B), measured via RT-qPCR, at different concentrations and different time-points of cabazitaxel treatment. Results represented as mean fold increase relative to the negative control (DMSO) ± S.D. from two independent replicates. Two-way ANOVA with Sidak`s post-test was performed for statistical comparison ****P<0.0001.

3.5 Discussion of Chapter 3

Several studies have investigated the modulation of lncRNAs in cancer in order to assess if they could be involved in tumour-related pathways and therefore used as targets for novel therapies (Crea, Clermont, *et al.*, 2014; Mohanty, Badve and Janga, 2014; Parolia *et al.*, 2015). In order to select the most suitable lncRNA for further studies in CRPC cells, in a previous publication the expression of several transcripts was analysed via RNA sequencing in CRPC vs. hormone sensitive PDX models. From the 136 lncRNAs up regulated in the CRPC PDX, *HORAS5* was selected based on RT-qPCR analyses, showing that this lncRNA is the most consistently up regulated in all CRPC PDX models used and that *HORAS5* favours cell proliferation and inhibits apoptosis in LNCaP and C4-2 cells (Parolia *et al.*, 2019). As already mentioned in this chapter, *HORAS5* has been also characterized in HCC (L.-C. Xu *et al.*, 2017), osteosarcoma (Wang *et al.*, 2016) and ovarian cancer (Xu *et al.*, 2019) and the last two studies have also shown that *HORAS5* is involved in drug response.

According to this evidence, further studies on *HORAS5* role in CRPC drug resistance phenotypes, could lead to the discovery of a possible novel target for the therapy of CRPC. Based on this hypothesis, the goal of this project is to study the correlation between *HORAS5* expression and drug treatment and the mechanistic role of *HORAS5* in CRPC cell response to drug treatment. To this aim, a panel of CRPC cells has been studied. This panel includes:

- LNCaP cells that are AR$^+$ and constitutively express *HORAS5*;
- AR$^-$ DU145-NC that lack detectable expression of *HORAS5*; these cells have been transduced with lentiviral particles without *HORAS5* gene under control of a strong promoter (empty vector). Hence these cells do not express *HORAS5*.

- AR⁻ DU145-OE that are transduced with lentiviral particles containing *HORAS5* under control of a strong promoter, able to induce high expression of the gene.

The quantification of the gene expression has revealed a high expression of *HORAS5* in DU145-OE compared to the DU145-NC control. The use of the lentiviral particles has been possible thanks to the size of *HORAS5* transcript. The *HORAS5 locus* can generate two different transcripts: a short transcript and a long one. From previous studies, it has been found that, in prostate cancer cells, the long variant is the most abundant one (Parolia *et al.*, 2019). Despite this, the size of the longer *HORAS5* transcript remains short enough to be effectively cloned inside the vector: 880 nt, which corresponds to the transcript variant 1 on NCBI-Nucleotide. A similar system to overexpress *HORAS5* has been already effectively used by Wang and collaborators, using the expression lenti-vector pCDH (Wang *et al.*, 2016).

Once it was confirmed that the lentiviral system could induce the expression of *HORAS5*, the subcellular localization of the transcript was analysed in DU145-OE compared to LNCaP cells, the latter reported in previous study (Parolia *et al.*, 2019). From these experiments, it has emerged that *HORAS5* is mostly a cytoplasmic transcript in AR⁻ prostate cancer cells as it has been shown in LNCaP cells when it is endogenously expressed (Parolia *et al.*, 2019). This suggests that both AR⁺ and AR⁻ prostate cancer cells can be studied to predict functions and mechanisms of action of *HORAS5* in similar subcellular compartments (nucleus/cytoplasm). The cytoplasmic localization of *HORAS5* suggests that it can be targeted via RNAi without the use of specific carriers for nuclear transfection, since cytoplasmic RNAs are much easier to silence using siRNAs or ASOs than nuclear ones (Ozcan *et al.*, 2015). Furthermore, the study of lncRNAs subcellular localization can predict the compartment where the transcript exerts most of its

functions. LncRNAs have been shown to act in the nucleus of cells mostly via interactions with epigenetic and splicing factors (Chen *et al.*, 2019; Miao *et al.*, 2019; Zong *et al.*, 2019), but also in the cytoplasm via translational control, modulation of RNA stability and signal transduction (Mercer and Mattick, 2013; Parolia *et al.*, 2019). In particular, increasing evidence is showing that cytoplasmic lncRNAs interact with miRNAs, often inhibiting their functions (Shan *et al.*, 2018; Xu *et al.*, 2019) (Chapter 1.4.1 and 1.4.4). Therefore, the prevalent cytoplasmic subcellular localization of *HORAS5* may also suggest that this lncRNA can interact with cytoplasmic molecules and complexes and may help us predict a possible mechanism of action in this context, which will be discussed in Chapter 5.

From the findings reported in this thesis, *HORAS5* overexpression does not affect AR$^-$ CRPC cell morphology and proliferation.

Given these findings, *HORAS5* modulation could be relevant in response to treatment. Therefore, the focus of this chapter has been to assess whether *HORAS5* expression is altered by drug treatment.

First, *HORAS5* expression stimulation was assessed upon enzalutamide treatment in CRPC cells. The results show that enzalutamide treatment does not result in a significant increase of *HORAS5* expression in the AR$^+$ LNCaP cells.

Carboplatin is widely studied in several cancers and has demonstrated activity in AR$^-$ CRPC cells and patients (Yang, Hsu and Yang, 2000; Budman, Calabro and Kreis, 2002; Fléchon *et al.*, 2011; Aparicio *et al.*, 2013; Corn *et al.*, 2019). For this reason, AR$^-$ DU145-OE cells were treated with different concentrations of carboplatin and *HORAS5*

expression was assessed. Carboplatin does not induce significant changes of *HORAS5* expression when tested at clinically achievable concentrations.

Both DU145-OE and LNCaP showed a statistically significant increase in *HORAS5* expression upon treatment with clinically achievable concentrations of cabazitaxel treatment. Moreover, statistical analysis has shown that *HORAS5* expression increases in a concentration-dependent manner in both AR^- and AR^+ cells treated with cabazitaxel.

Notably, despite some studies having shown that lncRNAs are involved in docetaxel resistance (Chen *et al.*, 2016; Pan *et al.*, 2017; Xue *et al.*, 2018), the role of lncRNAs in cabazitaxel response is still unknown.

Amstrong and collaborators have reported the effect of miRNAs on cabazitaxel resistance (G. Wu *et al.*, 2017). They obtained C4-2 cells resistant to docetaxel and have observed that *miR-181a* was significantly upregulated in these cells compared to the parental ones. *miR-181a* overexpression could also induce cabazitaxel resistance and its KD could restore sensitivity to both docetaxel and cabazitaxel (G. Wu *et al.*, 2017). As mentioned, there is no similar evidence for lncRNAs.

All the concentrations used in these experiments are clinically achievable, except for the highest carboplatin concentration. According to studies in CRPC and other advanced solid tumours in patients, the maximum plasma concentration (C_{max}) for enzalutamide ranges between 0.4±0.1 µg/ml and 27.9 µg/ml and the highest concentration used in the experiments (10 µM) corresponds to 4.64 µg/ml (Gibbons *et al.*, 2015). Carboplatin C_{max} is between 14.30 µg/mL and 26.70 µg/mL (Fukuda *et al.*, 1999; Kern *et al.*, 2001) and the highest concentration used in the current study is 100 µM (37.13 µg/mL). As already mentioned this additional concentration has been tested for carboplatin since it

has been tested in several studies and includes the highest literature reported IC_{50} for AR$^-$ prostate cancer cells (Yang, Hsu and Yang, 2000; Budman, Calabro and Kreis, 2002; McPherson, Galettis and de Souza, 2009). Finally, for cabazitaxel the C_{max} is 0.441 μg/ml, which is much higher than the max concentration used in the experiments (since 50 nM corresponds to 0.043 μg/ml) (Diéras *et al.*, 2013). Hence, these results could be translated into the clinical setting.

The same cabazitaxel clinically achievable concentrations used in the previous experiment have been tested at different time points. These experiments aim to assess if *HORAS5* is induced upon cabazitaxel in a time-dependent manner. The drug experiments were initially performed at 72h, as suggested by previous studies (McPherson, Galettis and de Souza, 2009; Yadav *et al.*, 2016). Thereafter, the most reliable time point was selected for further analysis. The results indicate that cabazitaxel induces a time-dependent increase in *HORAS5* in both LNCaP and DU145-OE cells with highest induction tested after 72h in LNCaP and particularly increasing for both the concentrations tested after 48h in DU145-OE. Hence, the experiments reported in the following chapters of this thesis will be set at these time points.

CHAPTER 4: EFFECTS OF *HORAS5* MODULATION ON PROSTATE CANCER RESPONSE TO CABAZITAXEL

Cabazitaxel treatment was shown to enhance *HORAS5* expression in both AR⁻ (DU145-OE) and AR⁺ (LNCaP) prostate cancer cells. This evidence suggests that the stimulation of *HORAS5* could determine a specific cellular response to the drug treatment. For this reason, this Chapter focuses on how experimental modulation of *HORAS5* via KD and overexpression, affects the cellular response to cabazitaxel.

From the experiments on *HORAS5* subcellular localization, it emerged that it is mostly a cytoplasmic transcript in AR⁻ prostate cancer cells, as had been shown previously in AR⁺ cells (Parolia *et al.*, 2019). Therefore, as already discussed in the previous section, it can be efficiently downregulated using RNAi.

Based on these findings, the KD procedure was optimized (in AR⁺ prostate cancer cells) and then used with *HORAS5* stable overexpression (in AR⁻ prostate cancer cells) to investigate the role of this transcript in cabazitaxel cellular response.

Therefore, a range of concentrations of cabazitaxel was selected based on the IC_{50} reported in published studies and the cellular response was analysed as cell count and survival. Moreover, the specific cabazitaxel IC_{50} was determined in CRPC cells with *HORAS5* modulation.

Experiments and results reported in this chapter are discussed below and summarized in table 4.1.

Table 4.1 | Summary of specific experiments, methods and results reported in this Chapter.

Experiments and analyses	Methods	Results
HORAS5 KD in AR$^+$ CRPC cells (LNCaP)	IDT siRNA transfection with RNAiMax + RNA extraction and RT-qPCR + phase contrast micrographs (LNCaP)	*HORAS5* KD determined a highly effective reduction in expression and reduction in AR$^+$ cells growth as observed in a previous study (Parolia *et al.*, 2019).
Analysis of the effect of *HORAS5* overexpression on AR$^-$ CRPC cell response to cabazitaxel	Cabazitaxel treatment + trypan blue exclusion cell count + phase contrast micrographs (DU145-NC and DU145-OE)	Cell pictures and count show that *HORAS5* overexpression reduces the growth inhibitory effect of cabazitaxel.
IC$_{50}$ measurment	Non-linear fit from cell count, outlier test and comparison between *HORAS5* overexpression and control (DU145-NC and DU145-OE)	This calculation shows that there is a significant increase in cabazitaxel IC$_{50}$ when *HORAS5* is overexpressed in AR$^-$ CRPC cells, compared to the control. *HORAS5* seems to be protective for the cancer cells against the drug treatment.
Analysis of the effect of *HORAS5* KD on AR$^+$ CRPC cell response to cabazitaxel	IDT siRNA transfection + cabazitaxel treatment + trypan blue exclusion cell count + phase contrast micrographs (LNCaP)	Cell pictures and count show significant reduction in cell count upon cabazitaxel treatment, when *HORAS5* is knocked down, compared to the control.
IC$_{50}$ calculation	Non-linear fit from cell count, outlier test and comparison between *HORAS5* KD and control (LNCaP)	This analysis shows that there is a significant decrease in cabazitaxel IC$_{50}$ when *HORAS5* is downregulated in AR$^+$ CRPC cells, compared to the control. This suggests that *HORAS5* KD increases cells' sensitivity to cabazitaxel and confirms the drug-resistance role of *HORAS5*.

Study of the effect of *HORAS5* overexpression on cell death in response to cabazitaxel	Cabazitaxel treatment + caspase 3/7 activity assay (DU145-NC and DU145-OE)	Caspases 3/7 activity, which drives apoptotic stages, increases in response to cabazitaxel but is significantly reduced when *HORAS5* is overexpressed, compared to the control. This suggests that *HORAS5* promotes cabazitaxel resistance by inhibiting CRPC cells' apoptosis.
Study of the effect of *HORAS5* KD on cell death in response to cabazitaxel	IDT siRNA transfection + cabazitaxel treatment +Caspase 3/7 Assay (LNCaP)	Caspases 3/7 activation significantly increased in response to cabazitaxel when *HORAS5* was knocked down, compared to the control. *HORAS5* is therefore confirmed to act in a cytoprotective way in response to cabazitaxel in CRPC cells via inhibition of caspase-mediated apoptosis.

4.1. Optimization of *HORAS5* knockdown

RNAi efficiently silences cytoplasmic transcripts and has been successfully used to silence *HORAS5* in LNCaP cells (Parolia *et al.*, 2019).

In this project, new siRNAs were ordered, compared to the ones employed in the previously published study (Parolia *et al.*, 2019), since the siRNA company had recently changed the available sequences. Hence, it was necessary to optimize the lncRNA silencing procedure in LNCaP cells with the new siRNAs. Moreover, *HORAS5* silencing was validated 5 days after siRNA transfection (Chapter2, fig. 2.2). This was necessary because *HORAS5* is significantly induced by cabazitaxel in LNCaP cells after 72h. Since the KD is 84% 48h post-transfection (fig. 4.2A), cabazitaxel treatment was started at this

timepoint, for 72h. The result is a 5 day experiment (fig.2.2, Chapter2). Hence, it was necessary to confirm *HORAS5* silencing up to 5 days after transfection.

With this aim, two different *HORAS5*-targeting siRNAs were first tested, using two different transfection reagents: lipofectamine 3000 and RNAiMax. As shown in figure 4.1 and 4.2A, lipofectamine 3000 resulted in less efficient KD than RNAiMax, respectively. For this reason, RNAiMax was selected for further KD experiments performed in this thesis.

Then, the two different *HORAS5*-targeting siRNAs were compared in order to select the most efficient for *HORAS5* KD. As shown in figure 4.2A efficient *HORAS5* KD (84%) was confirmed at 48h post transfection using siRNA2 (called from now on simply *HORAS5*-siRNA) which also maintained the phenotypic alteration on the cells observed in the previous study (Parolia *et al.*, 2019). Indeed, *HORAS5* KD, with *HORAS5*-siRNA, decreases cell number 48h post-transfection, as shown in figure 4.2 B and D. Since KD with siRNA1 was much lower than with *HORAS5*-siRNA (fig.4.2A) and did not result in an evident decrease in the cell number (figure 4.2C), this siRNA has not been tested in further experiments, and *HORAS5*-siRNA has been selected.
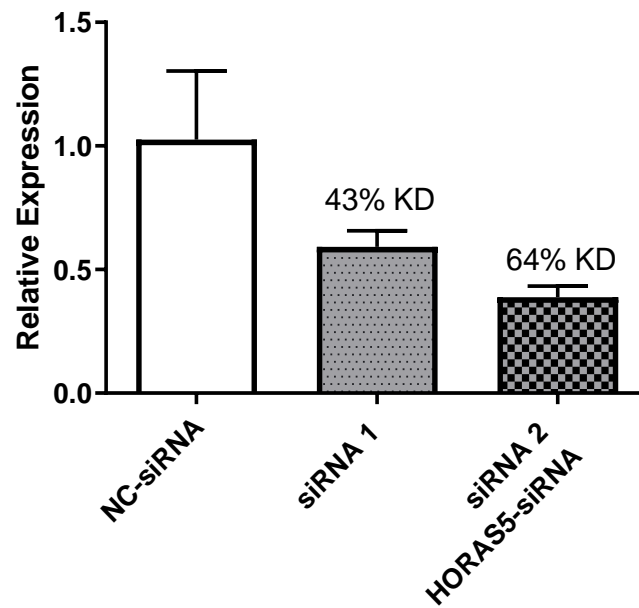
Figure 4.1 | *HORAS5* KD after 48h using lipofectamine 3000.
Expression of *HORAS5* measured via RT-qPCR and normalized for the control *HPRT1* expression in LNCaP cells 48h post-treatment with lipofectamine-transfected siRNAs, either *HORAS5*-siRNAs or negative control (NC-siRNA). Results represented as mean expression relative to negative control (NC-siRNA) ± S.D. from two independent experimental replicates.
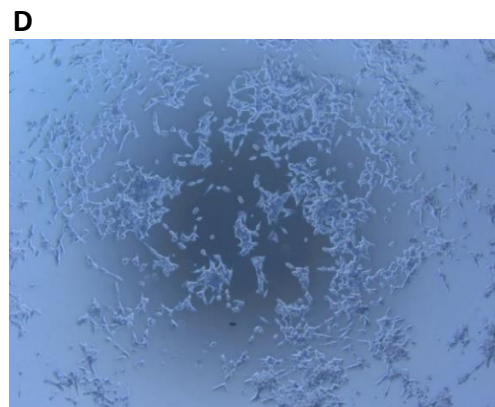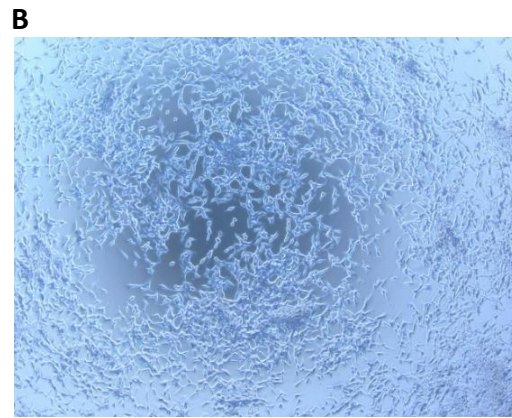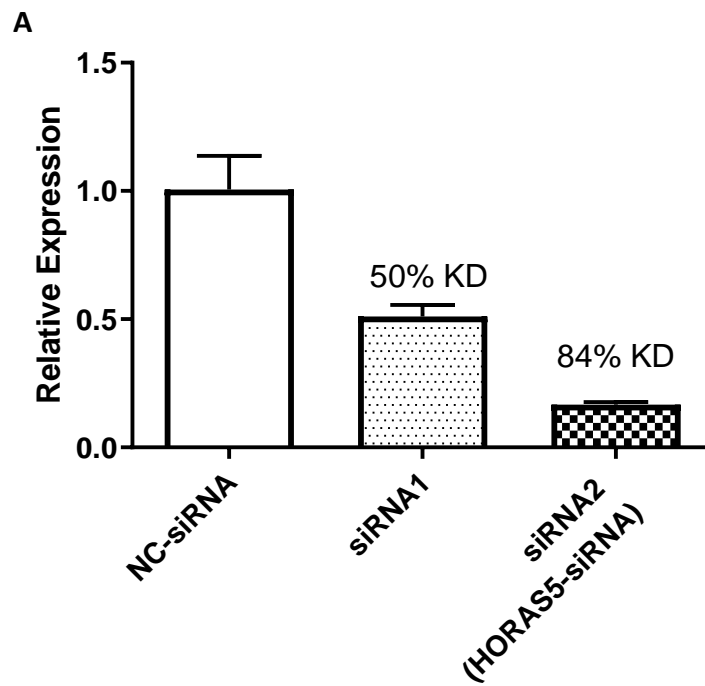
Figure 4.2 | *HORAS5* KD after 48h and selection of HORAS5-siRNA.
A. Expression of *HORAS5* normalized for the control *HPRT1* expression in LNCaP cells 48h post-treatment with RNAiMax-transfected *HORAS5*-siRNAs and negative control (NC-siRNA) measured via RT-qPCR. **B-D.** Images showing LNCaP cells 48h after treatment with NC-siRNA (B), siRNA1 (C) and HORAS5-siRNAs (siRNA2) (D). Results represented as mean expression relative to the negative control ± S.D. from two independent experimental replicates.

As already mentioned, it is also necessary in this context to validate the KD stability 5 days post transfection (fig.4.3A). Five days after *HORAS5*-siRNA transfection there is still 77% of KD that maintains the cell growth inhibition (fig. 4.3B-C).
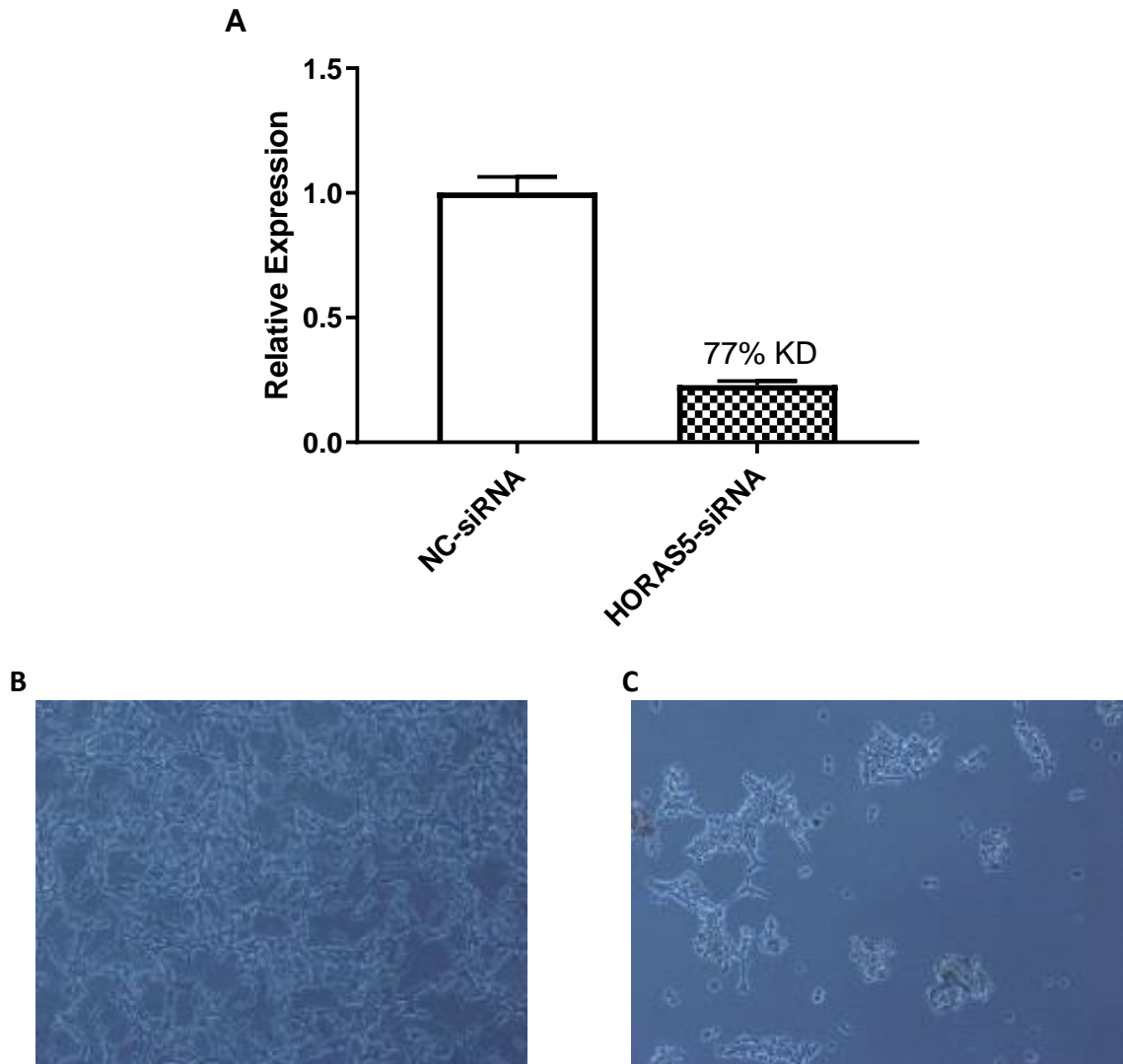
Figure 4.3 | KD of *HORAS5* in LNCaP cells and effect on cells.
A. Expression of *HORAS5* normalized for the expression of the control gene *HPRT1* in LNCaP (A), measured via RT-qPCR, five days after KD. **B-C.** Images show LNCaP cells 5 days after treatment with NC-siRNA (B) or HORAS5-siRNA (C). The results are represented as mean expression relative to the negative control (NC-siRNA) ± S.D. from two independent experimental replicates.

4.2. Effect of *HORAS5* overexpression and knockdown on cell count and cabazitaxel IC$_{50}$

After optimization of the procedures to modulate *HORAS5* via overexpression (section 3.1) and KD (section 4.1), *HORAS5* influence on cell response to cabazitaxel has been assessed. With this aim, DU145 cells (-NC and -OE) were treated with DMSO control or cabazitaxel at one of 6 different concentrations. Cabazitaxel concentrations were selected to span the IC$_{50}$ for DU145 cells predicted from the literature.

 Cells were counted 48h after treatment, using the trypan blue exclusion method. A reduction in cell count has been observed upon cabazitaxel treatment in both cell lines but *HORAS5* overexpression rescues DU145-OE cells from this trend, resulting in protection for DU145-OE exposed to cabazitaxel treatment (fig.4.4A). This significant reduction in the growth inhibitory effect of cabazitaxel is also illustrated in the pictures in figure 4.4 B-C.

A

B
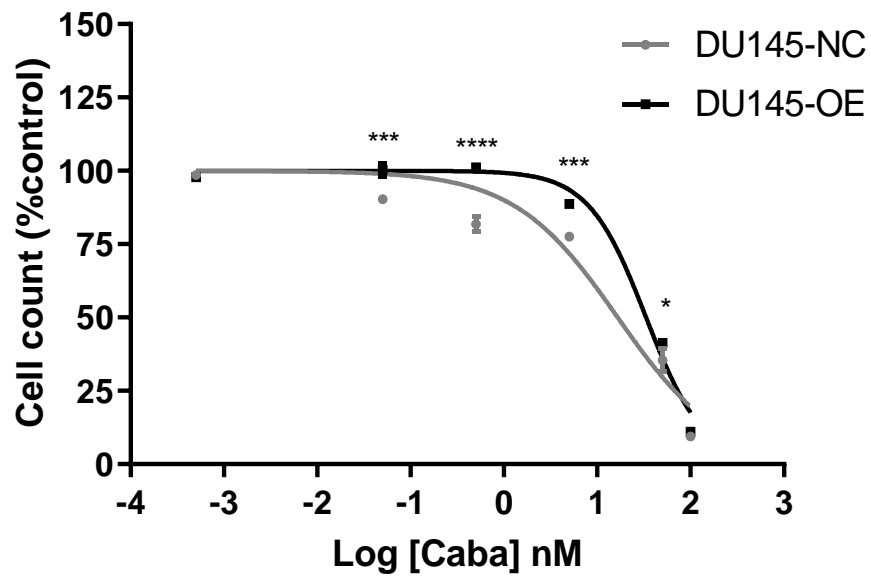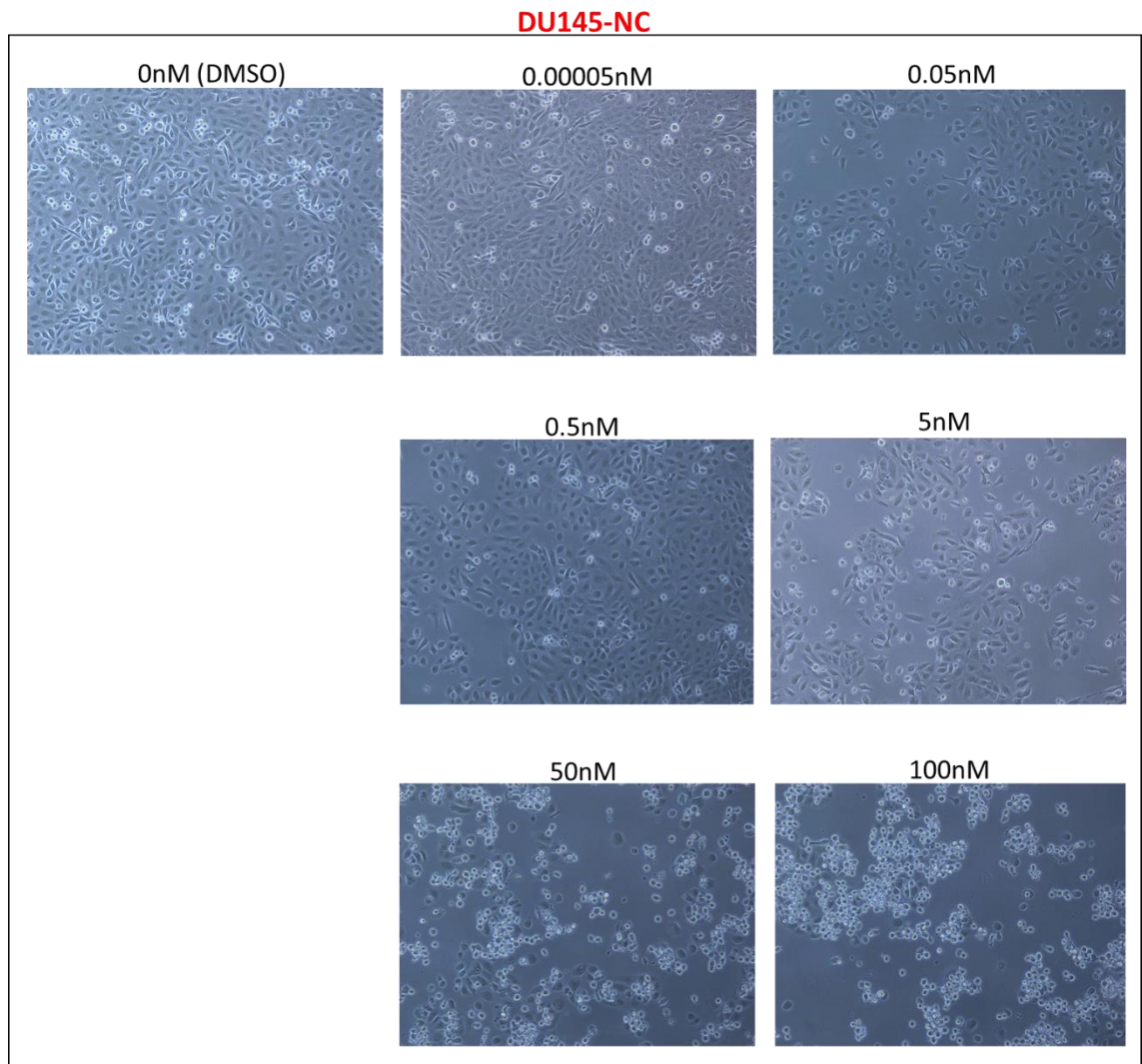
DU145-NC

C
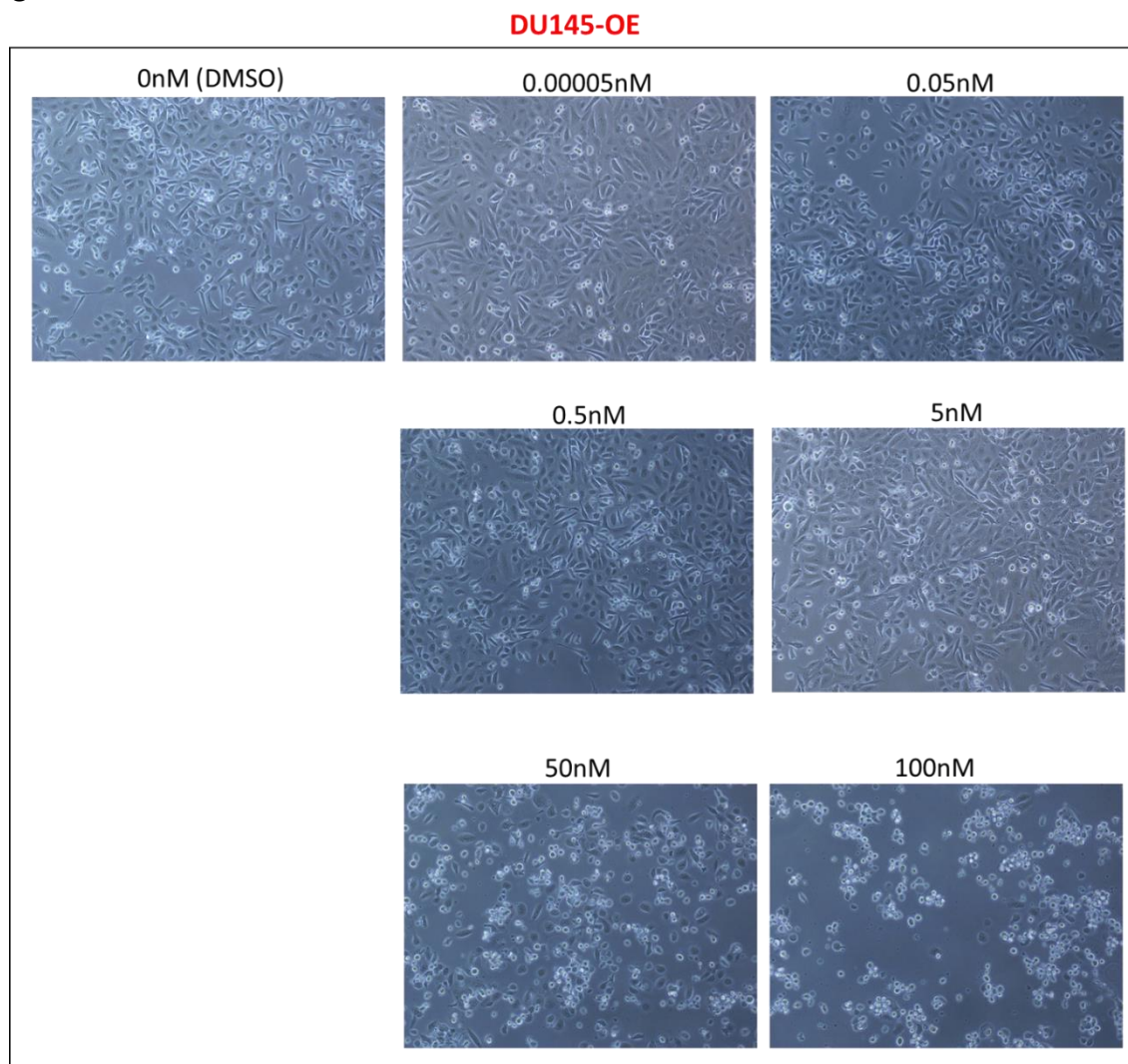
Figure 4.4 | Effect of HORAS5 overexpression on cell count under cabazitaxel exposure.

A. DU145 cell count upon cabazitaxel treatment for 48h, with *HORAS5* overexpression (DU145-OE) compared to the negative control (DU145-NC). Cell count is expressed as nonlinear fit curves of the cell number as a percentage of that in the untreated (DMSO) control. Two-way ANOVA with Sidak`s post-test was performed for statistical comparison *P= 0.0230, ***P< 0.0005, ****P<0.0001. **B-C**. Images showing the cells under cabazitaxel exposure in DU145-NC compared to DU145-OE.

Similarly, for LNCaP, cell count is significantly altered upon *HORAS5* modulation (fig.4.5A). LNCaP cells were also treated with DMSO control or cabazitaxel at one of 6 different concentrations, 48h post transfection for *HORAS5* KD. Cabazitaxel concentrations were selected to span the IC_{50} for LNCaP cells predicted from the literature. LNCaP cells were counted 72h after cabazitaxel treatment. Reduction in cell count upon cabazitaxel treatment is still observed and this effect is significantly enhanced by *HORAS5* KD in LNCaP cells (fig.4.5A-C). These results confirm that *HORAS5* promotes cabazitaxel resistance in CRPC cells.

A
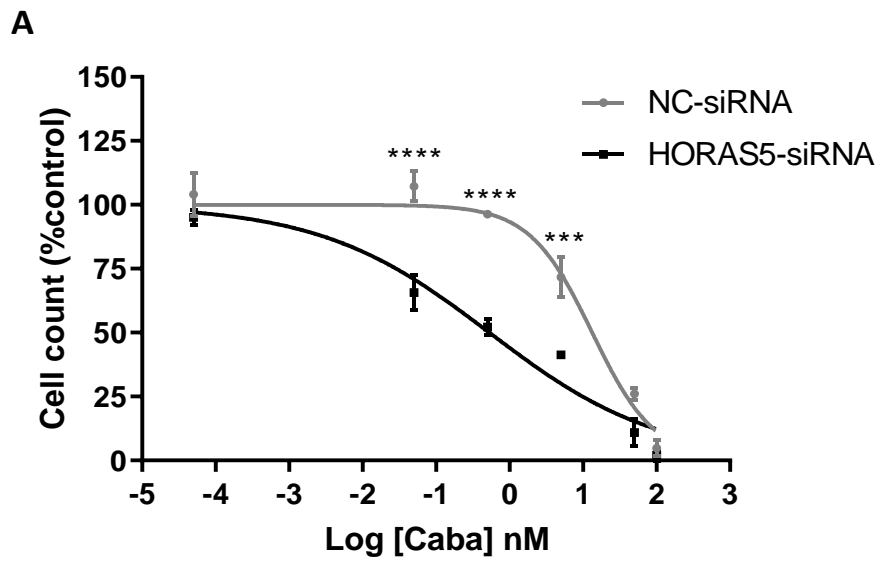
B
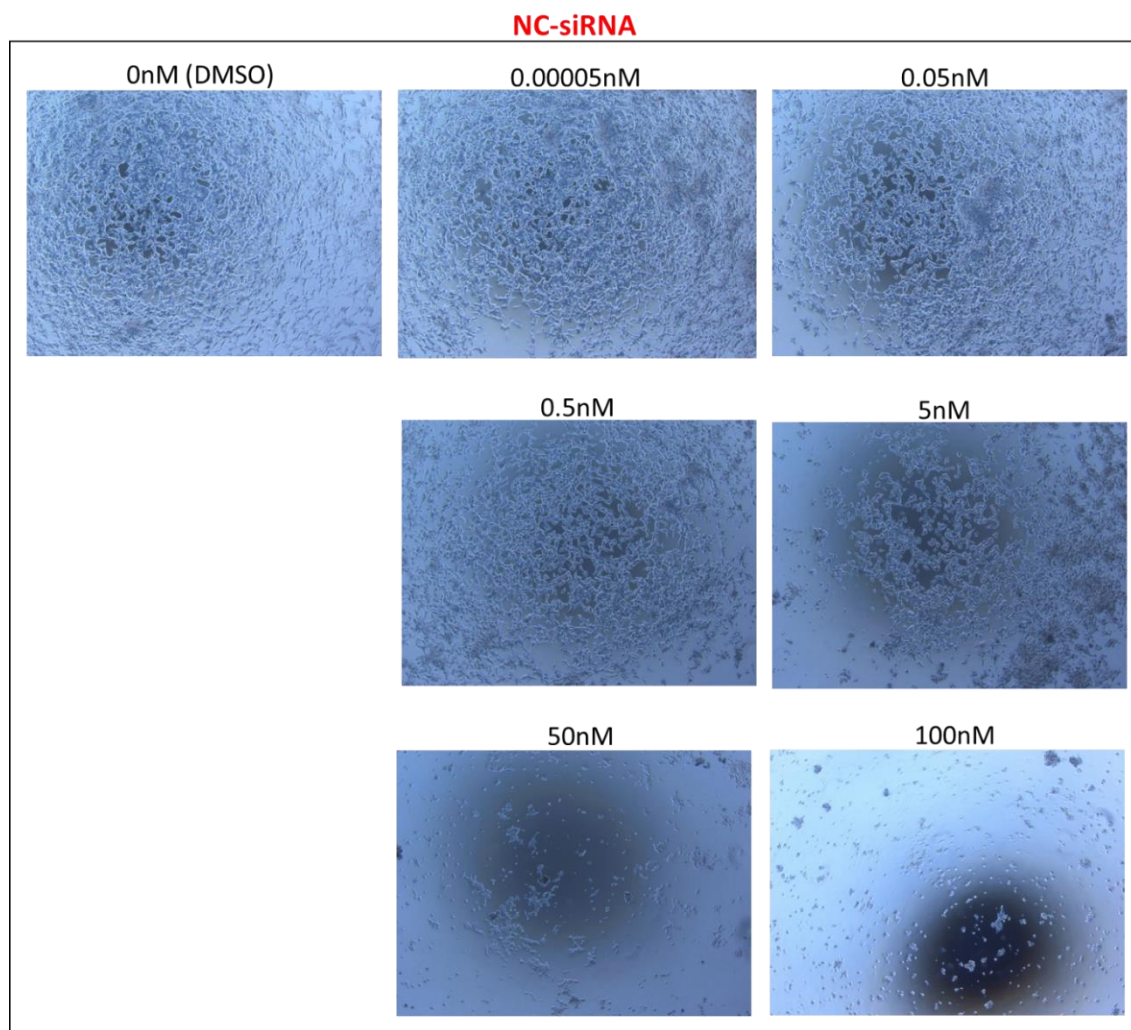
C
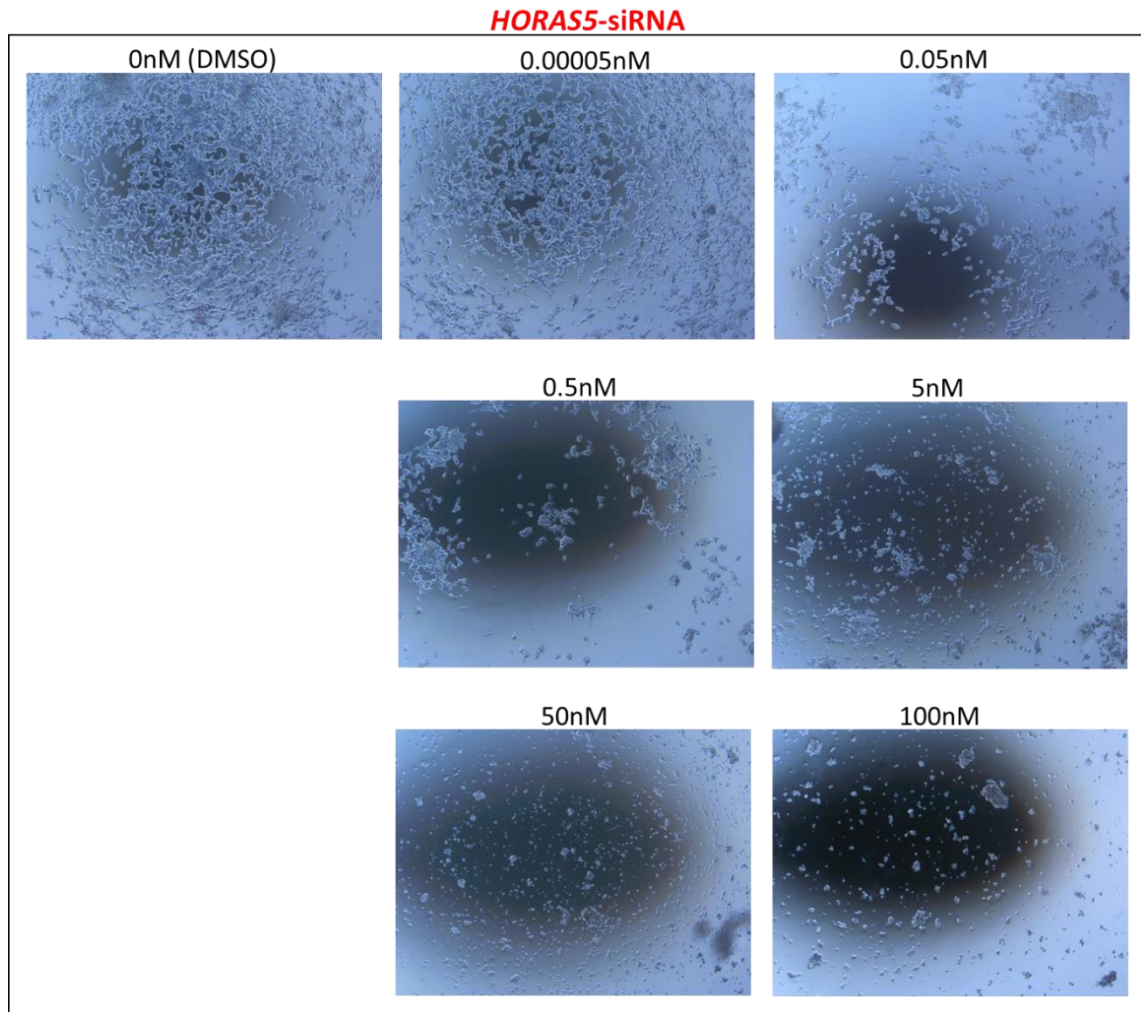
Figure 4.5 | Effect of *HORAS5* KD on cell count under cabazitaxel exposure.
A. LNCaP cell count 2 days post-transfection of *HORAS5*-siRNA + 3 days after cabazitaxel treatment compared to the negative control (NC-siRNA). Cell count is expressed as nonlinear fit curves of the cell number as a percentage of that in the untreated (DMSO) control. Two-way ANOVA with Sidak`s post-test is performed for statistical comparison ***P< 0.0003, ****P<0.0001. **B,C** Images showing effect of cabazitaxel exposure in LNCaP cells treated with NC-siRNA compared to LNCaP treated with *HORAS5*-siRNA.

The findings reported in this section show that cabazitazel IC_{50} is significantly altered by *HORAS5* modulation (fig.4.4 and 4.5). Indeed, *HORAS5* overexpression causes a significant increase in cabazitaxel IC_{50} from 3.11±1.48 nM to 30.55±3.9 (fig.4.6) and vice versa, *HORAS5* KD significantly decreases cabazitaxel IC_{50} from 20.80±0.74 nM to 2.59±0.77 (fig.4.7).

Overall, these findings show that *HORAS5* increases cabazitaxel resistance in both AR⁻

(DU145-OE) and AR⁺ (LNCaP) prostate cancer cells.

Cell type	IC_{50}
DU145-NC	3.11 ± 1.48 nM
DU145-OE	30.55 ± 3.9 nM
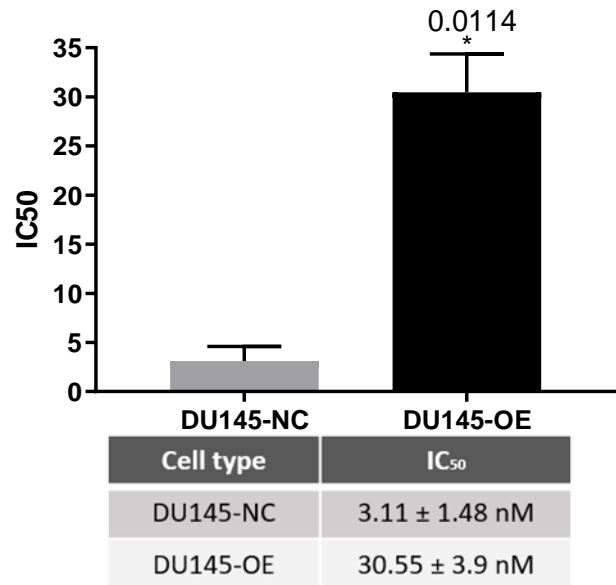
Figure 4.6 | Cabazitaxel IC_{50} in DU145 cells with/without *HORAS5* overexpression.
In figure are cabazitaxel IC_{50s} of DU145-NC and DU145-OE, calculated from the cell count
nonlinear fit graph (fig.4.3A). Outlier values were removed using GraphPad outlier
calculator. The results are expressed as means ± S.D. from independent replicates as
also shown in the table on the right. Student t-test was used for statistical comparison
*P=0.0114.

Cell type	IC_{50}
NC-siRNA	20.80 ± 0.74 nM
HORAS5-siRNA	2.59 ± 0.77 nM
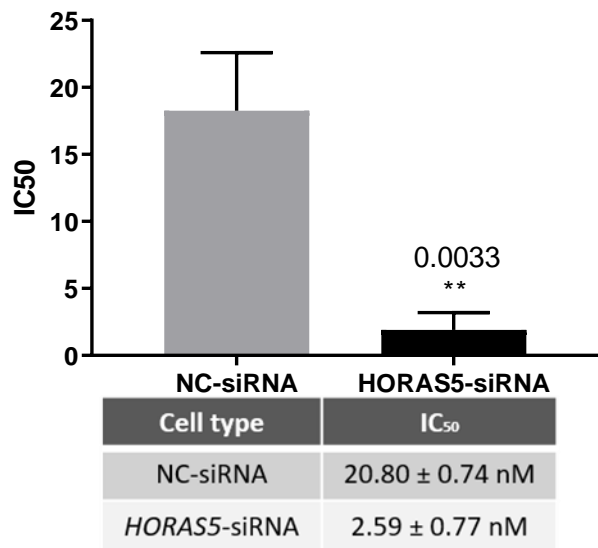
Figure 4.7 | Cabazitaxel IC50 in LNCaP cells with/without HORAS5 KD.
Cabazitaxel IC50s of LNCaP cells transfected with *HORAS5*-siRNA compared to the
negative control (NC-siRNA), calculated from the cell count nonlinear fit graph (fig.4.3A).
Outlier values were removed using GraphPad outlier calculator. Results expressed as
means ± S.D from independent replicates as also shown in the table on the right. Student
t-test was used for statistical comparison *P=0.0114.

4.3. Effect of *HORAS5* overexpression and knockdown on cabazitaxel-induced apoptosis

The observed function of *HORAS5* in promoting cabazitaxel resistance might be a consequence of several biological processes and molecular pathways. A crucial point in this context is to evaluate if the *HORAS5*-driven increase in drug resistance observed via cell count and IC_{50} calculation is a result of cell death inhibition. For this reason, changes in the apoptotic response were analysed in the cells treated with cabazitaxel, with/without *HORAS5* modulation. Caspase 3/7 assay was performed as a measure of early apoptotic response. These experiments showed that *HORAS5* overexpression results in a decrease in the apoptotic response induced by cabazitaxel (fig.4.8). Indeed, while caspases 3/7 activity increases in response to cabazitaxel, DU145-OE cells have a significant reduction in this activity compared to DU145-NC. A similar phenomenon is observed in LNCaP cells treated with cabazitaxel, where *HORAS5* silencing increases the cabazitaxel-induced activation of caspase 3/7 (fig.4.9). Overall, these data show that *HORAS5* promotes cabazitaxel resistance by hampering caspase-mediated apoptosis.
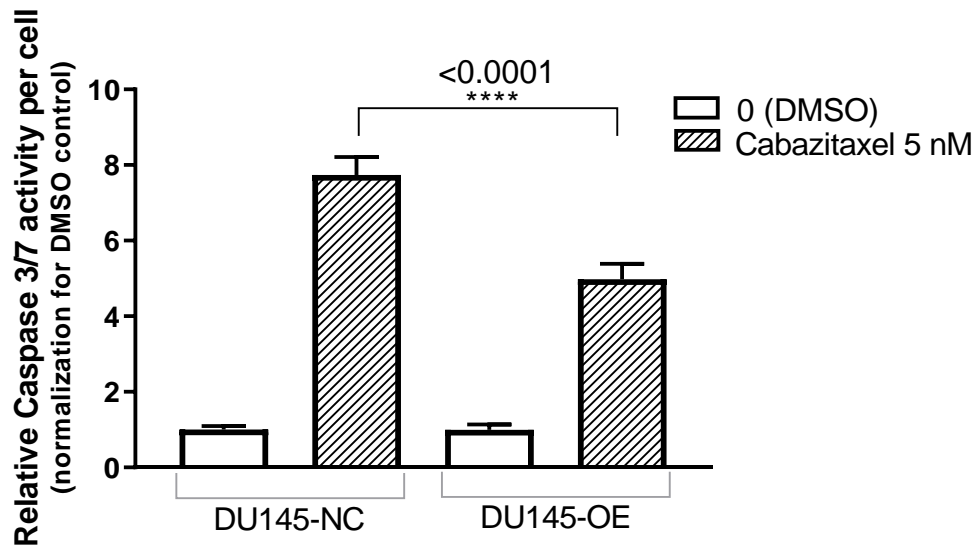
Figure 4.8 | HORAS5 overexpression affects prostate cancer cells apoptosis under cabazitaxel exposure.

The graph shows DU145 caspase 3/7 activity per cell 48h after cabazitaxel treatment, as a measure of early apoptosis. Data were normalized for DMSO control. One-way ANOVA with Tukey`s post-test is used for statistical comparison ****$P<0.0001$. The results are expressed as means ± S.D. from three independent replicates.
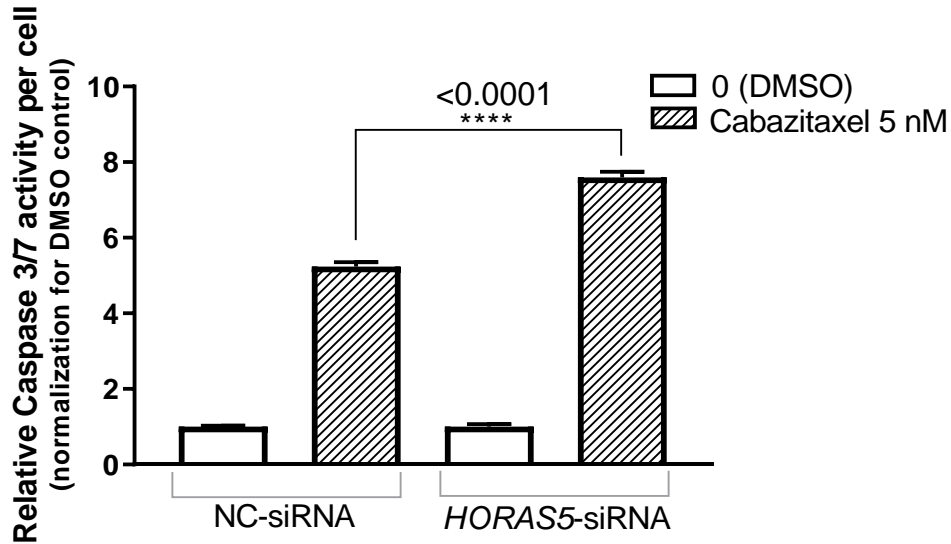
Figure 4.9 | Effect of HORAS5 KD on prostate cancer cell apoptosis under cabazitaxel exposure.

The graph shows LNCaP caspase 3/7 activity per cell 48h after *HORAS5* KD (or NC-siRNA treatment) + 72h of cabazitaxel treatment. Caspase 3/7 assay is used as measure of early apoptosis. Data were normalized for DMSO control. One-way ANOVA with Tukey`s post-test is used for statistical comparison ****$P<0.0001$. The results are expressed as means ± S.D. from three independent replicates.

4.4. Discussion of Chapter 4

This Chapter presented the effects of the modulation of *HORAS5* expression on cabazitaxel response in AR$^-$ and AR$^+$ prostate cancer cells.

HORAS5 can be silenced using siRNAs in prostate cancer cells (Parolia *et al.*, 2019). Therefore, the KD has been confirmed and shown stable for 5 days, which is the length of further experiments in LNCaP cells (see section 4.1).

HORAS5 KD experiments have been performed in only LNCaP as the lentiviral particle causes an upregulation in DU145-OE cells that it is not efficiently silenced by the siRNAs used (data shown in Appendix, fig.8.1). Moreover, *HORAS5* modulation in different cell lines can comprehensively show the effects of *HORAS5* in the context of prostate cancer resistance to cabazitaxel.

However, 7 different concentrations (including the DMSO control) have been chosen, encompassing the IC$_{50}$s found in the literature for both DU145 and LNCaP cells (McPherson, Galettis and de Souza, 2009; Yadav *et al.*, 2016). After the DMSO control (0nM cabazitaxel) and the lower cabazitaxel concentration used, each concentration increases by a log$_{10}$ unit from the previous one as a wide range of concentrations needs to be included in order to be sure to observe a complete cellular response, from no cell count inhibition (0.0005nM in DU145 and 0.00005 nM in LNCaP) to ~100% inhibition (100nM in both cell lines).

The trypan blue exclusion assay used for cell count, has shown the effects of *HORAS5* modulation on cell response to cabazitaxel showing that *HORAS5* overexpression increases cell resistance to cabazitaxel.

Other lncRNAs have been studied to affect drugs IC_{50} in cancer (An, Zhou and Xu, 2018; Wu *et al.*, 2018; Yang, Pan and Deng, 2019; Zheng *et al.*, 2019). In particular, a study on breast cancer has characterized a specific lncRNA that increases taxane IC_{50} (Zheng *et al.*, 2019). According to this study, CASC2 KD decreases resistance of paclitaxel-resistant breast cancer cells (MCF-7/PTX and MDA-MB-231/PTX) with significant IC_{50} reduction, while the overexpression has the opposite effect (Zheng *et al.*, 2019). Interestingly, although the cited studies are relevant in this context, there is no similar evidence specifically for cabazitaxel response.

Furthermore, cell metabolic assays such as MTT and MTS have not been used to determine the effect of *HORAS5* modulation on cabazitaxel cellular response, since taxanes have been reported to affect mitochondrial function (Gabor Varbiro *et al.*, 2001; Pucci *et al.*, 2018; Jiang *et al.*, 2019) and this could have altered the results.

Therefore cell count was used and suggests that *HORAS5* drives cabazitaxel resistance in CRPC cells by increasing the drug IC_{50}. In order to further investigate whether this role of *HORAS5* is just associated with promotion of proliferation or also with inhibition of cell death pathways, a caspase assay was performed. These results suggest that *HORAS5* regulates caspase activity in response to cabazitaxel treatment, thereby inhibiting apoptosis.

Several studies have characterized lncRNAs as regulators of cell apoptosis (Misawa *et al.*, 2017; Huang *et al.*, 2019) and in some cases this role has shown effects on drug response (Deng *et al.*, 2019; Han *et al.*, 2019; Li *et al.*, 2019).

Additionally, *HORAS5* pro-survival phenotype has been observed in both AR^{+} cells with *HORAS5* endogenous expression and AR^{-} cells with lentivirus-induced *HORAS5*

expression. In this regard, the *HORAS5* mechanism of action has been already studied in AR$^+$ cells; in fact, *HORAS5* can increase *AR* mRNA stability, thereby stimulating the AR transcriptional program and targeted genes, such as the oncogenic KIAA0101 and increase cancer cell survival (Parolia *et al.*, 2019). Since *HORAS5* can drive cabazitaxel resistance via this mechanism of action in LNCaP but not in DU145, because they do not express the *AR*, the next Chapter will focus on the study of *HORAS5* mechanism of action in the context of cabazitaxel response in AR$^-$ DU145 cells.

CHAPTER 5: MECHANISM OF *HORAS5*-DEPENDENT CABAZITAXEL RESISTANCE

HORAS5 stimulates cabazitaxel resistance in AR$^+$ and AR$^-$ prostate cancer cells via modulation of cell survival, but the mechanisms determining these effects still need to be investigated.

While I was working on this project, two studies have been published on *HORAS5* mechanism of action in cancer drug response (Wang *et al.*, 2016; Xu *et al.*, 2019). Although these studies consider different cancers and drug response effects, both of them suggest that *HORAS5* acts in the cytoplasm of cancer cells as ceRNA and sequesters specific miRNAs, thereby restoring the downstream pathways. In osteosarcoma, *HORAS5* sponges *miR-645* and activates the interferon-induced gene *IFIT2* expression, thereby sensitising osteosarcoma cells to cisplatin (Wang *et al.*, 2016). In ovarian cancer it sequesters *miR-128* and stimulates *MAPK1* expression, thereby promoting cisplatin resistance (Xu *et al.*, 2019). As discussed before, lncRNAs have different functions based on the tissues and cells where they are expressed and the pathways where they interact.

Despite this evidence, the mechanism of action of *HORAS5* in prostate cancer drug resistance has never been characterized. Moreover, there are no studies suggesting mechanisms of action of lncRNAs in cabazitaxel resistance.

In a previous study, *HORAS5* has been shown to promote prostate cancer cell growth and survival via stabilization of *AR* mRNA, thereby stimulating AR-mediated downstream pathways (Parolia *et al.*, 2019). Additionally, in the same study *HORAS5* has been selected from PDXs and found upregulated in CRPC vs hormone sensitive models. This result suggests that *HORAS5* is involved in treatment resistance phenotypes (Parolia *et al.*, 2019). Notably, the AR signalling pathway directly contributes to taxane resistance

in CRPC cells (Shiota *et al.*, 2013; Martin *et al.*, 2015). For this reason, this mechanism of action could account for *HORAS5* effect on cabazitaxel response in AR$^+$ cells but not in AR$^-$ cells, since they lack the *AR* expression. This suggests that *HORAS5* acts via a different mechanism to stimulate cabazitaxel resistance in AR$^-$ DU145-OE cells.

Having said that, this chapter aims to unravel one possible mechanism of action via which *HORAS5* promotes cabazitaxel resistance in AR$^-$ CRPC cells.

For this reason, RNA sequencing was performed on cells treated with cabazitaxel vs control, in order to investigate if *HORAS5* stimulates a specific protein-coding gene or pathway. The reason why protein-coding genes only have been analysed is that most of these molecules have been functionally characterised and the goal of this project is to investigate *HORAS5* involvement in established pathways. The RNA sequencing has been conducted at the University Hospital Basel, Switzerland, using the Ion AmpliSeq™ from ThermoFisher, with a Human Gene Expression Core Panel that provides gene-level expression information from a single multiplexed panel targeting over 20,000 protein-coding genes.

This specific RNA sequencing method has been used in several other recent publications to successfully determine interactions and mechanisms of action of different molecules (H. Chen *et al.*, 2018; Beinse *et al.*, 2019).

Experiments and results reported in this chapter are discussed in the next sections and summarized in table 5.1.

Table 5.1 | Summary of experiments, methods and results reported in this Chapter.

Experiments	Methods	Results
RNA Sequencing and bioinformatic analysis	Ion AmpliSeq™ ThermoFisher	87 genes are significantly upregulated upon cabazitaxel in DU145-OE that overexpress *HORAS5*, but not in DU145-NC. 25 of these genes are selected based on statistical significance and among them, *SOX9*, *CCL20* and *BCL2A1* are the top 3 genes upregulated upon cabazitaxel treatment and *HORAS5* overexpression (DU145-OE), but not when *HORAS5* is not overexpressed (DU145-NC).
Analysis of pathways regulated by *HORAS5* overexpression upon cabazitaxel treatment	Reactome software	The top 25 genes upregulated upon *HORAS5* overexpression and cabazitaxel treatment are mostly involved in Immune response and apoptosis.
Validation of expression of top 3 genes from RNA Sequencing	Drug treatment + total RNA extraction and RT-qPCR	*SOX9* is not validated via qPCR, *CCL20* and *BCL2A1* are validated via qPCR. BCL2A1 is the most significantly upregulated gene tested via qPCR and has been therefore selected for further experiments.
Validation of expression of BCL2A1 protein	Drug treatment + total protein extraction and WB	BCL2A1 protein is upregulated upon cabazitaxel treatment in cells that overexpress *HORAS5* (DU145-OE)
BCL2A1 KD at mRNA and protein level	siRNA mediated KD + total RNA extraction and RT-qPCR or protein extraction and WB	BCL2A1 is efficiently silenced at both mRNA and protein levels
Effects of BCL2A1 KD on cell count in response to cabazitaxel when HORAS5 is overexpressed	siRNA mediated KD + drug treatment+ Trypan blue exclusion method for cell count	BCL2A1 KD decreases cell count in response to cabazitaxel in cells that overexpress *HORAS5* (DU145-OE)
Effects of BCL2A1 KD on cell caspase-induced apoptosis in response to cabazitaxel when HORAS5 is overexpressed	siRNA mediated KD + drug treatment + 3/7 caspase assay	BCL2A1 KD decreases caspase-mediated apoptosis in response to cabazitaxel in cells that overexpress *HORAS5* (DU145-OE)

5.1. RNA sequencing and selection of *BCL2A1*

The RNA Sequencing has been conducted on DU145 cells in order to investigate *HORAS5* mechanism of action in the AR⁻ CRPC cell response to cabazitaxel. For this reason, the transcriptomic profile of CRPC cells exposed to cabazitaxel has been analysed on the following samples: DU145-NC, untreated; DU145-NC, exposed to cabazitaxel; DU145-OE, untreated; DU145-OE exposed for 48h to 5nM of cabazitaxel.

The approach used for the RNA Sequencing analysis is summarized in figure 5.1. First, 87 genes have been found significantly upregulated (FC>2, P value<0.01) in DU145-OE treated with cabazitaxel vs untreated cells but not in DU145-NC exposed to the same drug (fig.5.1) (tab.8.1). This evidence suggests that these 87 genes are specifically upregulated in response to cabazitaxel in *HORAS5* overexpressing cells. From these 87 genes, the first 25 genes with the highest P value in DU145-NC have been shortlisted. This criteria was chosen in order to focus on the genes that are most probably not regulated by cabazitaxel in DU145-NC cells but which, based on the analysis of response of DU145-OE cells, we know to be up- or down- regulated by cabazitaxel in *HORAS5* overexpressing cells (fig. 5.1 and 5.2 and tab.5.2).

The characterized functions of these 25 genes have been investigated via both *in silico* cell pathway analysis, using the Reactome publicly available database and literature research (fig.5.1).

Following *in-silico* analysis, figure 5.3 shows the most relevant pathways sorted by P value. Two phenomena seem to be particularly represented: immunity regulation and apoptosis (fig.5.3), where two of the 25 genes, *CCL20* and *BCL2A1*, are respectively involved.

Based on the literature, *CCL20 and BCL2A1* have been reported to be involved in cancer and drug resistance in different studies (Haq *et al.*, 2013; Champa *et al.*, 2014; Zhang *et al.*, 2015; Song *et al.*, 2016; W. Chen *et al.*, 2018) (fig.5.1). Notably, another gene particularly emerged from literature research since it has been reported to promote taxane resistance in mCRPC: *SOX9*.

Based on this evidence, the interaction between the *HORAS5* and these three genes, *SOX9*, *CCL20* and *BCL2A1*, was validated via RT-qPCR.
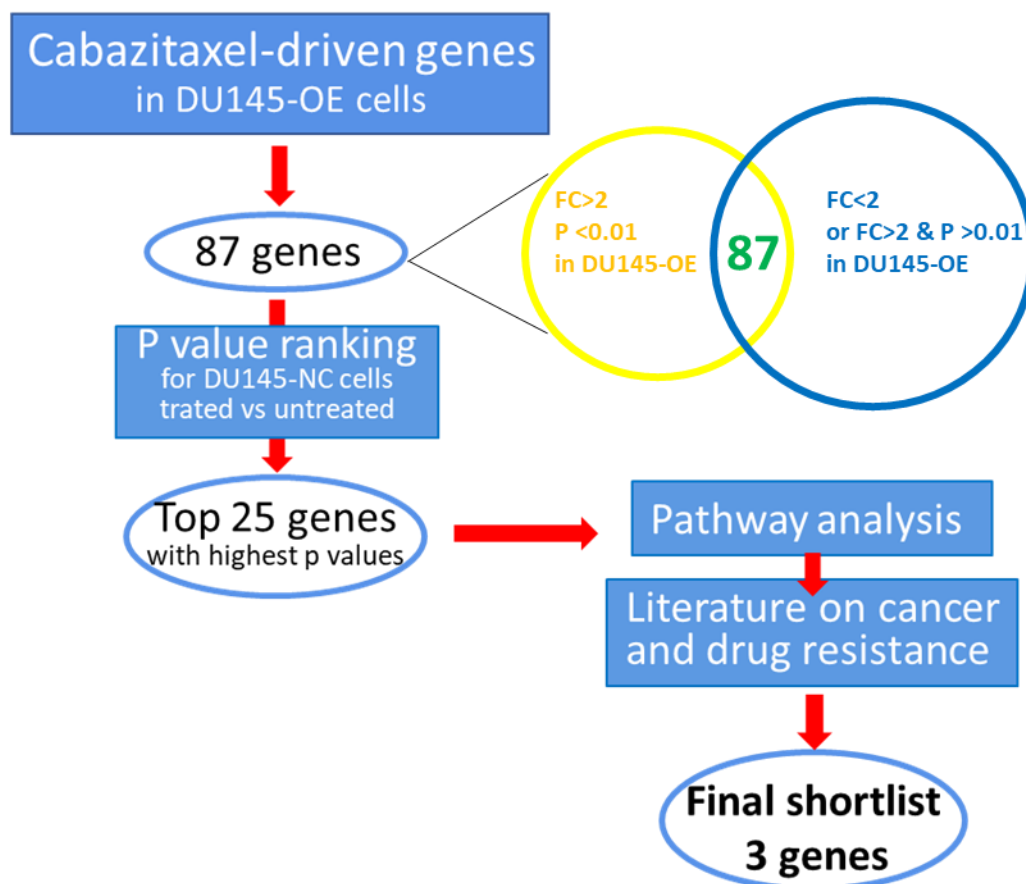
Figure 5.1 | Selection of top 3 genes from RNA sequencing analysis.
The Flow chart shows the method used to shortlist cabazitaxel-driven genes in prostate cancer cells that overexpress *HORAS5* (DU145-OE vs DU145-NC) from RNA sequencing. 87 genes were found up-regulated upon cabazitaxel treatment in DU145-OE cells (P value<0.01) but not in DU145-NC cells (P value>0.01). 25 of these 87 genes were shortlisted as the genes with the highest P value in DU145-NC treated vs untreated, to focus on the genes that are more probably not regulated by cabazitaxel in DU145-NC, among the ones regulated by the drug in DU145-OE (the 87 genes). The final shortlist was obtained by choosing the 3 genes with the highest number of *HORAS5 and* cabazitaxel-related pathways they regulate and/or literature evidence on cancer and drug resistance.

DEGs for NC-DMSO vs OE-DMSO

A

Up 0.12%
Down 0.05%

No Change

Total = 20809 genes

Total DEGs — 35
Up-regulated — 25
Down-regulated — 10
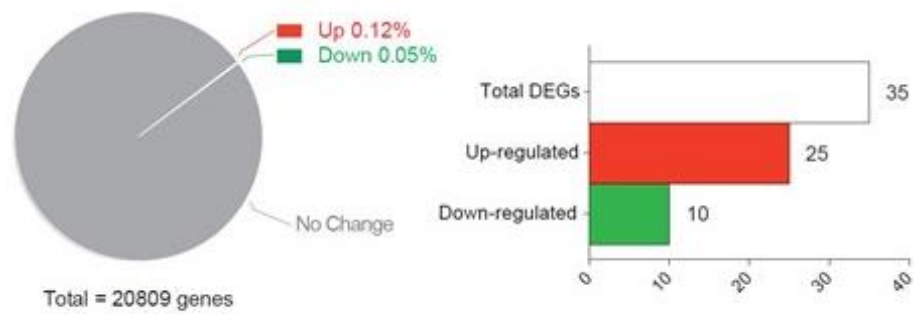
DEGs for OE-DMSO vs OE-CABA

B

Up 1.41%
Down 0.16%

No Change

Total = 20809 genes

Total DEGs — 326
Up-regulated — 293
Down-regulated — 33
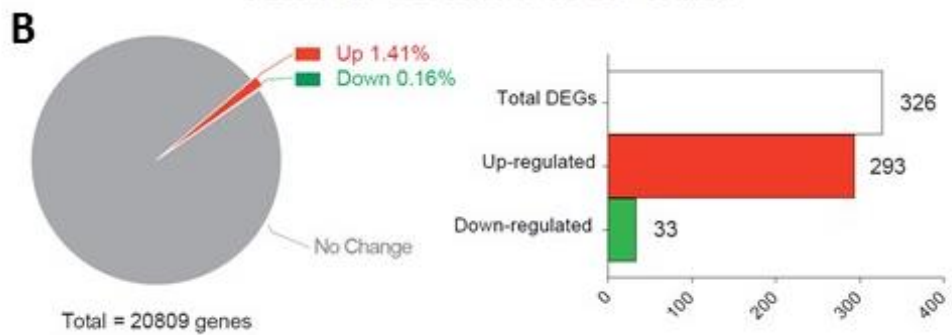
DEGs for NC-DMSO vs NC-CABA

C

Up 1.2%
Down 0.18%

No Change

Total = 20809 genes

Total DEGs — 287
Up-regulated — 249
Down-regulated — 38
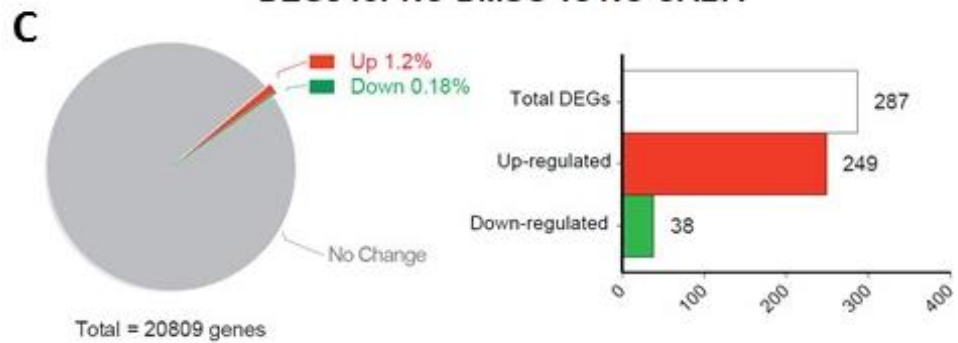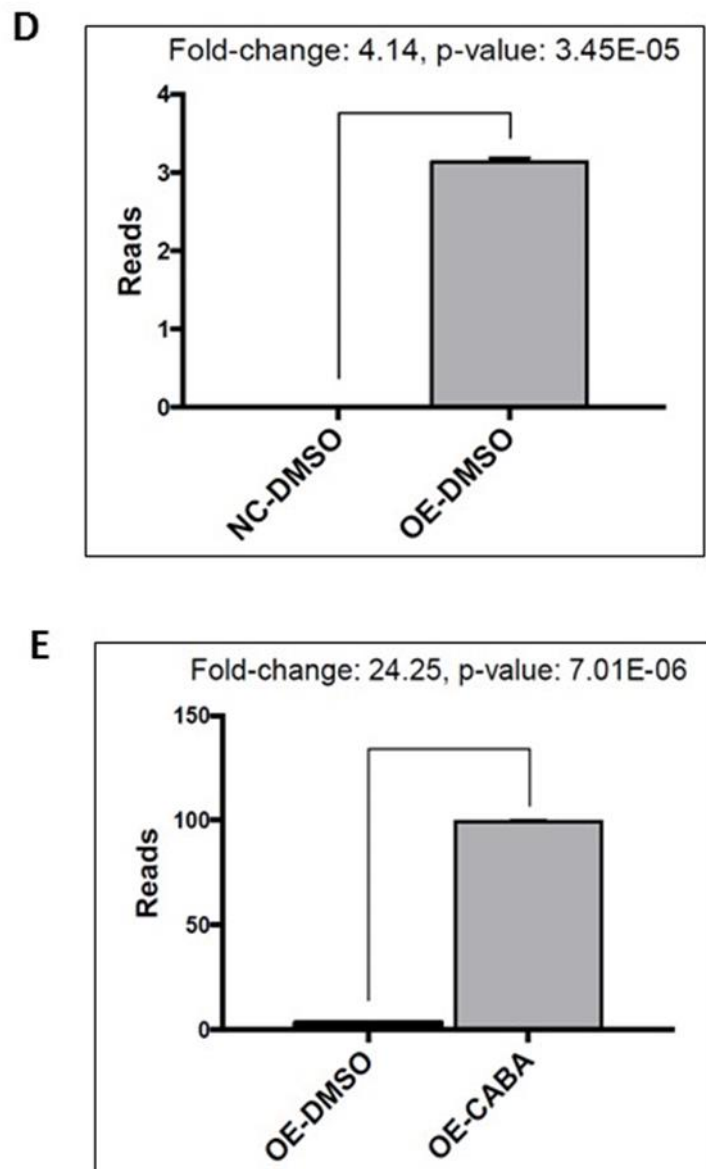
Figure 5.2 |Summary of RNA sequencing analysis.
A,B,C. DEGs upon *HORAS5* overexpression without cabazitaxel treatment (A) and DEGs upon cabazitaxel treatment with (B)/without (C) *HORAS5* overexpression. The criteria used in this figure are FC >2 or <-2 and P value<0.05. **D,E.** RNA sequencing Confirmation of *HORAS5* up-regulation in DU145-OE vs DU145-NC (D) and in cabazitaxel treated cells vs untreated (E). RNA sequencing data are represented as normalized reads (RPM) in figure D and E. FC values are the ratio between reads.

Table 5.2 | Top 25 cabazitaxel-driven genes upregulated in DU145-OE compared to DU145-NC.

Gene-ID	Log$_2$ DU145-OE treated	Log$_2$ DU145-OE untreated	Fold Change (treated vs untreated)	P value (DU145-OE treated vs untreated)	P value (DU145-NC treated vs untreated)
SUMO4	1.6	0.4	2.31	0.0056	0.6321
LTB4R2	1.26	0.15	2.16	0.0094	0.4364
PCDH1	1.03	0	2.05	0.0018	0.4226
FBXO34	1.7	0.15	2.94	0.0029	0.3152
BCL2A1	3.15	1.86	2.45	0.0068	0.2818
BRD8	1.36	0.33	2.04	0.0032	0.2662
TMEM128	2.45	0.98	2.77	0.0099	0.2581
PCDHB19P	1.89	0.33	2.95	0.0086	0.2075
OR2B6	1.17	0	2.25	0.0016	0.1124
IL23A	2.12	0.34	3.42	0.0028	0.112
OAS3	5.71	4.57	2.21	3.67E-05	0.1044
ADCY10P1	1.29	0.08	2.32	0.0079	0.1026
CCNL1	5.65	4.2	2.73	0.0095	0.1025
SF3B4	4.3	3.24	2.09	0.0056	0.0965
HIST1H3J	3.11	1.72	2.63	0.0011	0.0937
CPEB4	4.58	3.52	2.08	0.0065	0.09
LOC100289187	2.02	0.86	2.23	0.0095	0.089
PFN1P2	4.61	3.49	2.17	0.0051	0.0846
SOX9	4.27	2.86	2.67	0.0099	0.0827
USP53	5.74	4.73	2.01	0.0027	0.081
IRF9	4.08	2.69	2.63	0.0018	0.079
TTC18	1.62	0.34	2.43	0.0063	0.0775
DYRK1B	1.95	0.83	2.18	0.0026	0.0767
CCL20	2.61	1.2	2.67	0.0065	0.0738
ALDOC	2.17	0.83	2.54	0.0056	0.0714

Pathway name	Entities				Reactions	
	found	ratio	p-value	FDR*	found	ratio
Leukotriene receptors	2 / 9	4.43e-04	1.22e-04	0.042	1 / 3	2.44e-04
Mitochondrial transcription termination	1 / 2	9.84e-05	0.004	0.393	1 / 1	8.12e-05
Interferon alpha/beta signaling	4 / 369	0.018	0.004	0.393	5 / 20	0.002
Interferon gamma signaling	4 / 406	0.02	0.006	0.393	2 / 15	0.001
Eicosanoid ligand-binding receptors	2 / 72	0.004	0.007	0.393	1 / 12	9.75e-04
Transport of connexins along the secretory pathway	1 / 9	4.43e-04	0.016	0.393	1 / 2	1.62e-04
Transcription from mitochondrial promoters	1 / 17	8.36e-04	0.03	0.393	1 / 3	2.44e-04
Interleukin-10 signaling	2 / 171	0.008	0.037	0.393	1 / 15	0.001
Activation, myristolyation of BID and translocation to mitochondria	1 / 23	0.001	0.04	0.393	4 / 4	3.25e-04
Activation and oligomerization of BAK protein	2 / 26	0.001	0.045	0.393	3 / 3	2.44e-04
Packaging of Eight RNA Segments	1 / 26	0.001	0.045	0.393	1 / 2	1.62e-04
Activation, translocation and oligomerization of BAX	1 / 33	0.002	0.057	0.393	2 / 4	3.25e-04
Unwinding of DNA	1 / 36	0.002	0.062	0.393	2 / 4	3.25e-04
Viral RNP Complexes in the Host Cell Nucleus	1 / 36	0.002	0.062	0.393	1 / 3	2.44e-04
Activation of BAD and translocation to mitochondria	1 / 37	0.002	0.063	0.393	1 / 5	4.06e-04
Activation of BIM and translocation to mitochondria	2 / 38	0.002	0.065	0.393	2 / 2	1.62e-04
RNA Polymerase I Promoter Opening	1 / 38	0.002	0.065	0.393	1 / 2	1.62e-04
Class I peroxisomal membrane protein import	1 / 40	0.002	0.068	0.393	4 / 6	4.87e-04
PRC2 methylates histones and DNA	1 / 46	0.002	0.078	0.393	4 / 4	3.25e-04
Interferon Signaling	4 / 945	0.046	0.085	0.393	9 / 66	0.005
MECP2 regulates transcription of genes involved in GABA signaling	1 / 50	0.002	0.085	0.393	1 / 4	3.25e-04
ABC transporters in lipid homeostasis	1 / 50	0.002	0.085	0.393	1 / 11	8.94e-04
RUNX3 regulates BCL2L11 (BIM) transcription	2 / 51	0.003	0.086	0.393	1 / 2	1.62e-04

Figure 5.3 | Most significant pathways regulated by the top-25 genes mostly upregulated upon HORAS5 overexpression and cabazitaxel treatment.
Most of the pathways shown are associated with immune response. 5 out of the 23 pathways shown in this figure (highlighted in red) are directly linked with programmed cell death (red squares). FDR (false discovery rate): corrected over-representation probability.

Therefore, *SOX9, CCL20* and *BCL2A1* expression was validated in DU145 cells exposed to different doses of cabazitaxel or control. As shown in figure 5.4A, *SOX9* upregulation is not confirmed upon cabazitaxel treatment neither significant differences are found between DU145-NC and DU145-OE. Moreover, in the RT-qPCR experiment a higher drug concentration (10nM) was introduced compared to the RNA sequencing, in order to maximise the observed effects. Even with this additional concentration, a relatively modest and non-significant increase in *SOX9* expression was observed upon treatment (fig.5.4A).

Interestingly, *CCL20* and *BCL2A1* are both significantly upregulated in DU145-OE compared to DU145-NC in response to cabazitaxel treatment, at both concentrations used (fig.5.4 B and C).

BCL2A1 upregulation is particularly significant (fig.5.4C). BCL2A1 function and role in cancer are particularly promising in this context since it is a well-described anti-apoptotic gene (Jenal *et al.*, 2010; Haq *et al.*, 2013; Lionnard *et al.*, 2019). *BCL2A1* is upregulated at the protein level upon cabazitaxel treatment when *HORAS5* is overexpressed (i.e. in DU145-OE) (fig.5.4D).

A

DU145-SOX9

B

DU145-CCL20

C

DU145-BCL2A1
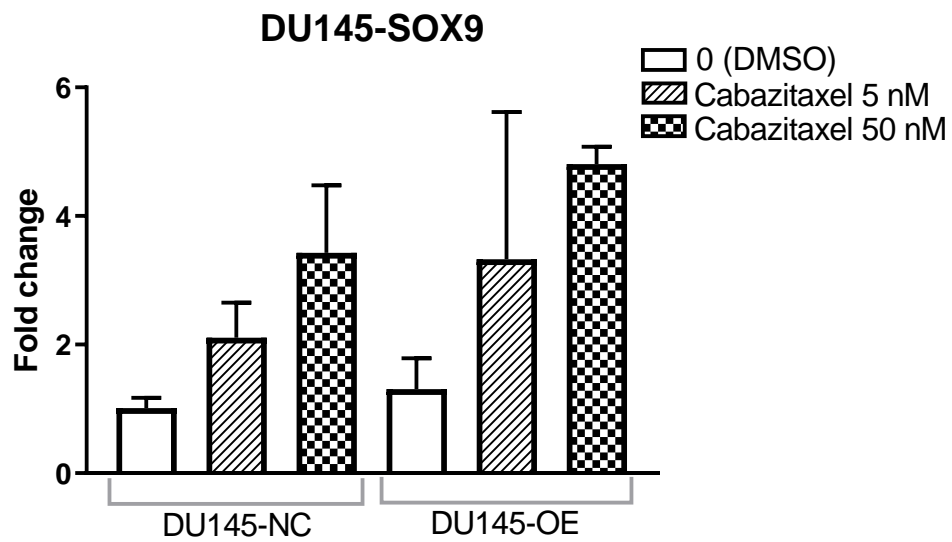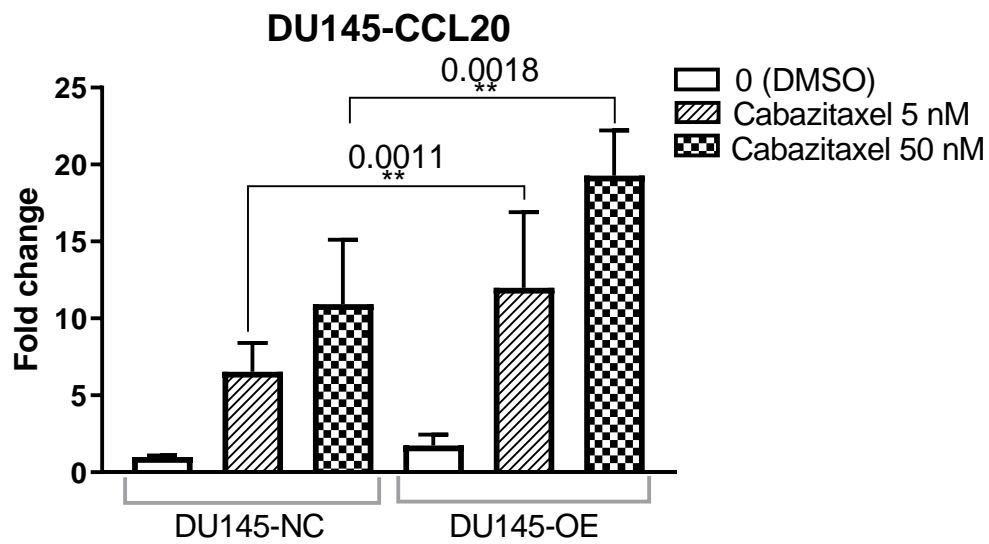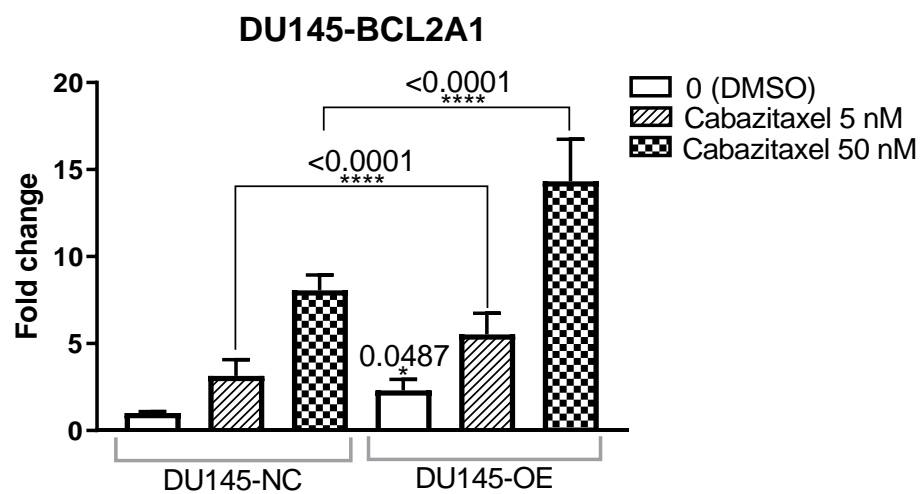
D
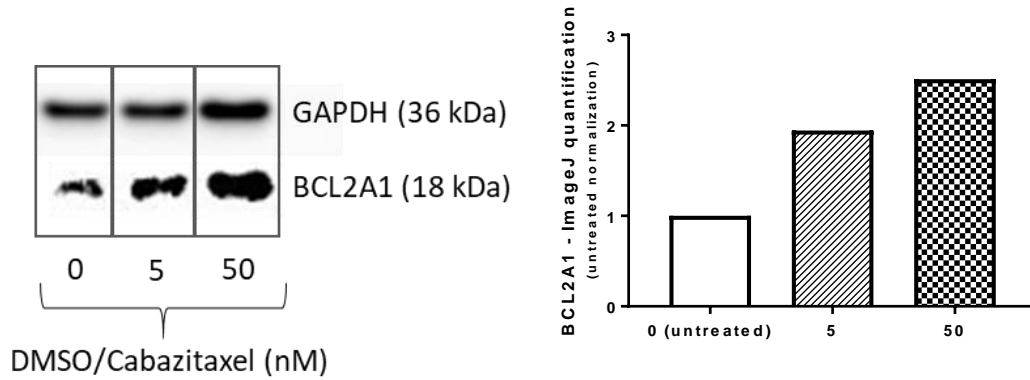
Figure 5.4 | BCL2A1 is the most statistically significantly upregulated gene in prostate cancer cells exposed to cabazitaxel and is induced by HORAS5 overexpression.
A-C. RT-qPCR validation of the 3 genes, shortlisted from RNA sequencing analysis: *SOX9*, *CCL20* and *BCL2A1*. The results are expressed as mean expression relative to negative control (DMSO treated DU145-NC) ± S.D. from three independent replicates. One-way ANOVA with Tukey`s post-test was used in for statistical comparison *P=0.0487, **P<0.002, ****P<0.0001. **D.** BCL2A1 expression is significantly increased at the protein level upon cabazitaxel treatment in the cells that overexpress *HORAS5* (DU145-OE). GAPDH is used as Western blot loading control. Western blots are visualised using Syngene Genesys software and quantified using ImageJ software.

5.2. *BCL2A1* Knock-down

The results obtained so far suggest that the anti-apoptotic protein BCL2A1 could mediate the drug resistance phenotype induced by *HORAS5* in CRPC cells. To test this hypothesis, it was tested whether *BCL2A1* KD rescues *HORAS5* induced drug-resistance in CRPC cells exposed to cabazitaxel. Therefore, DU145-OE cells were transfected with either *BCL2A1*-targeting siRNA (two types tested) or a siRNA control (scramble). As shown in figure 5.5 A, siRNA2 results in higher KD (95%) than siRNA1 (84%) but further experiments were performed using both siRNAs to increase the reliability of these analyses. Moreover, both siRNA1 and siRNA2 decrease BCL2A1 protein expression (fig.5.5B).

A

B
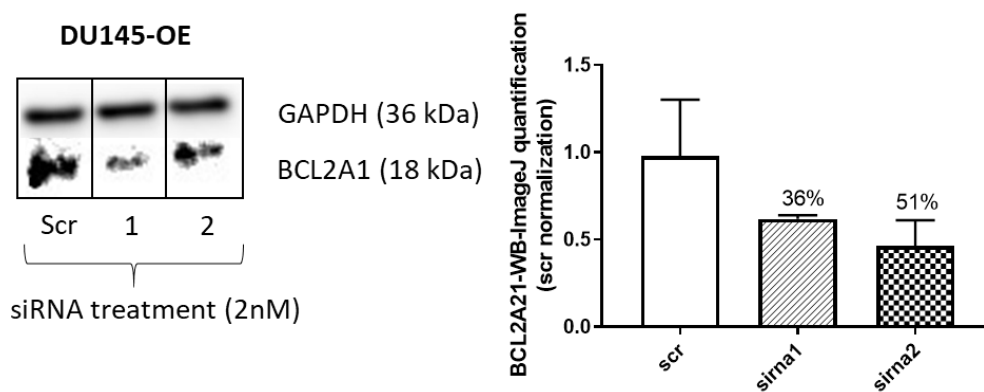
Figure 5.5 |BCL2A1 KD at mRNA and protein level.
A,B. *BCL2A1* expression is significantly reduced at the mRNA (A) and protein (B) level upon KD (GAPDH is used as Western blot loading control). Western blots are visualised using Syngene Genesys software and quantified using ImageJ software.

5.3. Effects of *BCL2A1* KD on cell count in response to cabazitaxel when *HORAS5* is overexpressed

With the use of validated *BCL2A1* targeting siRNA1 and siRNA2, it was sought to assess whether BCL2A1 has any function in the cellular response to cabazitaxel, promoted by *HORAS5* (i.e. in DU145-OE). In particular, according to the data shown, *BCL2A1* KD could partially reverse *HORAS5*-induced cabazitaxel resistance. *BCL2A1* KD significantly reduced DU145-OE cell count upon cabazitaxel treatment (fig.5.6). These findings show

that BCL2A1, which is upregulated upon *HORAS5* overexpression, enhances cabazitaxel

resistance in DU145-OE cells.
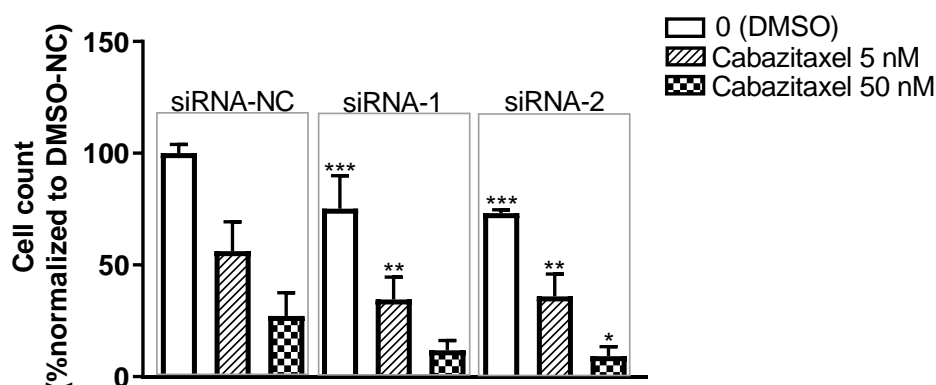
Figure 5.6 |BCL2A1 KD decreases cell count in CRPC cells treated with cabazitaxel.
DU145-OE cell count upon cabazitaxel exposure, with *BCL2A1* KD. The cell count is
expressed as percentage normalized to the untreated (DMSO) control. The results are
reported as means ± S.D. from three independent replicates. One-way ANOVA with
Tukey`s post-test was used in for statistical comparison *P<0.05, **P<0.01, ***P<0.001.

5.4. Effects of *BCL2A1* KD on cell caspase-induced apoptosis in response to cabazitaxel when *HORAS5* is overexpressed

Since *BCL2A1* KD decreases cell count in cabazitaxel-treated cells that overexpress

HORAS5, it was also tested whether the effect of BCL2A1 on cabazitaxel response is a

consequence of its anti-apoptotic activity. As shown in figure 5.7, *BCL2A1* KD results in

a small increase in apoptosis in untreated cells (fig.5.7). But when the cells are treated

with cabazitaxel, *BCL2A1* KD highly increases caspase-induced apoptosis, at both 5 nM

($1.98 \leq FC \leq 2.21$, $p<0.0001$) and 50 nM ($3.06 \leq FC \leq 4.36$, $p<0.0001$) of cabazitaxel (fig.5.7).

These results suggest that BCL2A1 stimulates cabazitaxel resistance by inhibiting

caspase-mediated apoptosis.
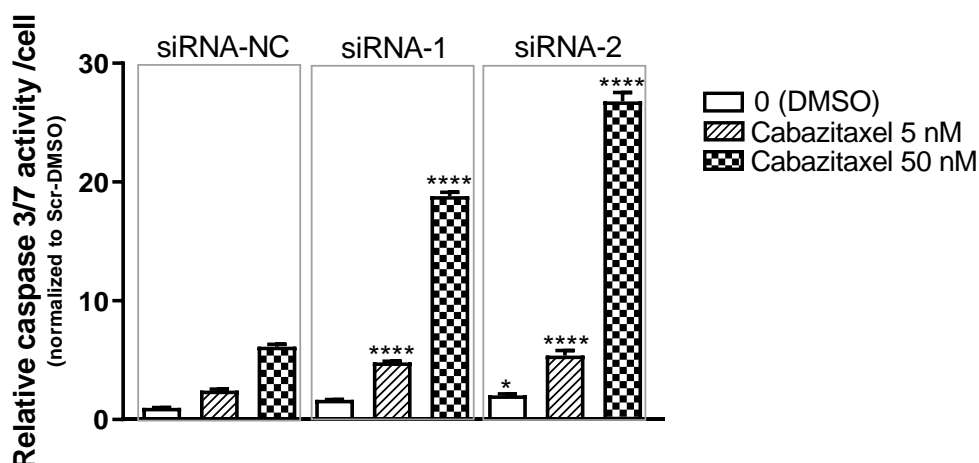
Figure 5.7 | *BCL2A1* KD increases caspase-mediated apoptosis in CRPC cells exposed to cabazitaxel.
The graph represents caspase 3/7 activity normalized to relative cell count number in DU145-OE cells upon BCL2A1 KD and cabazitaxel treatment. The results are expressed as means ± S.D. from three independent replicates. One-way ANOVA with Tukey`s post-test has been used for statistical comparison *$P<0.05$, ****$P<0.0001$.

5.5. Discussion of Chapter 5

In this chapter, the results on *HORAS5* mechanism of action in cabazitaxel resistance in AR⁻ CRPC cells are reported. LncRNAs are able to interact with several cellular pathways via different mechanisms, even in similar cells and conditions.

One possible mechanism of action could be investigated to further study how *HORAS5* promotes cabazitaxel resistance in AR⁻ CRPC cells; evidence on lncRNA pleiotropy suggests that other concurrent mechanisms of action could contribute to the same phenotype.

RNA sequencing analysis was performed on AR⁻ cells with/without *HORAS5* expression, comparing cells treated with cabazitaxel with untreated control cells. This comparative analysis, together with *in silico* pathway analysis and literature research, led us to further focus this work on three genes, among those genes that were most upregulated

on cabazitaxel treatment, in cells that overexpress *HORAS5*, but which were not significantly upregulated in cells lacking detectable *HORAS5* expression. Notably, these three genes were selected according to their described roles in cancer and drug resistance as well as their involvement in the pathways regulated by the 25 genes identified by RNA sequencing. These three genes are *SOX9*, *CCL20* and *BCL2A1*.

SOX9 encodes for a TF that is important during chondrogenesis, embryonic development and adult life and mutations or dysregulation in its expression and activity have been studied in several deseases, including cancer (Jo *et al.*, 2014). Interestingly SOX9 expression correlates with lower PFS and overall survival in mCRPC patients treated with docetaxel (Song *et al.*, 2016) and with prostate cancer aggressiveness (Khurana and Sikka, 2019).

CCL20 is member of the small cytokine CC genes family, characterized by proteins containing two adjacent cysteines in their aminoacidic chain. Proteins belonging to this family are involved in immune and inflammation processes. CCL20 is associated with cancer aggressiveness but conflicting literature exists on CCL20 induction upon taxane treatment. In fact, CCL20 increases upon taxane treatment in breast cancer cells, triggering resistance via upregulation of ABCB1 (W. Chen *et al.*, 2018) while *CCL20* expression decreases after taxane treatment in NSCLC cells (Zhang *et al.*, 2015).

BCL2A1 encodes an anti-apoptotic factor (Jenal *et al.*, 2010; Haq *et al.*, 2013; Lionnard *et al.*, 2019) with oncogenic roles in many cancers, including prostate cancer, where it promotes cancer aggressiveness (Fukuhara *et al.*, 2015). BCL2A1 has been already described to participate in drug resistance phenotypes in different cancers (Vogler, 2012; Haq *et al.*, 2013; Champa *et al.*, 2014). Interestingly no studies have shown its role in taxane resistance before.

From the pathway analysis conducted using Reactome, it has emerged that *HORAS5* seems to be upregulated upon cabazitaxel treatment to act mostly in immune and inflammation response and apoptotic pathways. According to the pathway analysis and to the qPCR validation performed on the expression of the top three genes, *CCL20* and *BCL2A1* were selected as the only genes significantly upregulated upon cabazitaxel treatment and increasing in cells that overexpress *HORAS5*. Although the qPCR on *CCL20* has confirmed its upregulation, the significance is lower than in *BCL2A*1, due to increased variability between independent experiments. Moreover, as mentioned, there is conflicting literature on *CCL20* expression upon taxane treatment in cancer. According to this evidence, further analyses were focussed on BCL2A1. These analyses showed that the increased transcription of *BCL2A1* results in an increase in the protein, in response to cabazitaxel stress, in the AR$^-$ CRPC cells that overexpress *HORAS5*. Differences in the WB bands comparing DU145-NC and DU145-OE were not clearly found, so the WB data are shown for DU145-OE only. Moreover, *BCL2A1* was expressed at low levels in untreated cells, especially at the protein level. This evidence suggests that cabazitaxel stimulates mRNA translation into protein. Moreover, literature evidence suggests that BCL2A1 can promote drug resistance (Vogler *et al.*, 2009; Vogler, 2012; Haq *et al.*, 2013; Champa *et al.*, 2014). Notably, this is the first study linking BCL2A1 to cabazitaxel response. For this reason, further investigation has assessed whether *BCL2A1* KD affects cabazitaxel resistance. Cabazitaxel untreated cells, exposed to *BCL2A1*-siRNAs, showed reduced proliferation and survival and this effect was enhanced by increasing cabazitaxel concentration. These results suggest that BCL2A1 decreases cellular sensitivity to cabazitaxel treatment. Overall, *HORAS5* induces *BCL2A1*

upregulation at both mRNA and protein level and this stimulation promotes cabazitaxel

resistance via apoptosis inhibition, in CRPC AR$^-$ cells.

CHAPTER 6: TRANSLATIONAL POTENTIAL OF *HORAS5* AS FUTURE BIOMARKER AND THERAPEUTIC TARGET FOR CRPC

The *in vitro* work conducted in this project shows that *HORAS5* promotes cabazitaxel resistance in AR$^+$ and AR$^-$ cells. Moreover, when *HORAS5* does not act on the AR pathway (Parolia *et al.*, 2019), it inhibits prostate cancer cell apoptosis by stimulating BCL2A1 mRNA and protein expression, in order to protect the cancer cells from cabazitaxel-induced cell death. This evidence suggests to investigate the role of *HORAS5* as driver of prostate cancer aggressiveness and taxane resistance in clinical samples. This study would support the *in vitro* evidence shown. Moreover, it would clarify *HORAS5* potential in future applications as diagnostic and prognostic biomarker and therapeutic target. *HORAS5* has been already found upregulated in cancer versus normal tissues (L.-C. Xu *et al.*, 2017; Sun *et al.*, 2018). It has been also found upregulated in the exosomes in HCC patients serum. Interestingly, the study of Sun and collaborators (Sun *et al.*, 2018), reveals *HORAS5* potential as non-invasive diagnostic biomarker for HCC patients with high sensitivity and specificity, as indicated from the ROC curve (AUC=0.794) shown in their publication. This evidence suggests that *HORAS5* can have an important role in cancer patients. Particularly, in the context of drug resistance, there are findings showing that *HORAS5* is upregulated in tissues from cisplatin resistant patients compared to sensitive ones (Xu *et al.*, 2019). These promising findings confirm that additional studies are needed in order to characterize the potential of *HORAS5* in cancer, specifically in CRPC, also considering the *in vitro* findings reported in this thesis. *HORAS5* has also been detected in prostate cancer clinical samples (Parolia *et al.*, 2019). Other lncRNAs are upregulated with increased aggressive phenotypes in samples from prostate cancer patients (Lai *et al.*, 2017; W. Li *et al.*, 2018; X. Chen *et al.*, 2018). Some

156

evidence has correlated lncRNAs with taxane resistance in clinical samples, such as *linc00518* which is upregulated in tissues from paclitaxel resistant patients vs sensitive ones (He *et al.*, 2019). This data suggests that further studies on *HORAS5* role in patients could shed light on the correlation of this lncRNA with taxane response and patients' outcome.

In this context, it would be also important to investigate whether *HORAS5* can be targeted with ASOs, to alter CRPC drug response. ASOs should be first studied *in vitro* in order to find novel insights for future *in vivo* studies that could bring *HORAS5* inhibition to a clinical phase. Indeed, the possibility to target and effectively inhibit *HORAS5* with methods that can be translated *in vivo*, paves the way for the development of novel molecular treatments to be used in combination with cabazitaxel in patients who are, or become, resistant to this drug. Furthermore, this study can shed light on molecular mechanisms of lncRNA-mediated cancer drug resistance and identify treatments for other cancers, where *HORAS5* is dysregulated.

All the analyses and experiments described in this chapter are reported and discussed in the next sections and summarized in table 6.1.

Table 6.1 | Summary of experiments, methods and results reported in this Chapter.

Experiments	Methods	Results
Survival analysis	cBio portal analyses	Higher levels of *HORAS5* and *BCL2A1* correlate, with similar trend and significance, with decreased PFS of prostate cancer patients.
HORAS5 expression in clinical samples	cBio portal analyses and data filtering	*HORAS5* is upregulated in metastatic samples from patients treated with taxanes vs samples from untreated patients
HORAS5 KD via ASOs	Eurofins genomics custom designed ASOs transfection with RNAiMax + RNA extraction and RT-qPCR	ASO3 results in the highest inhibition of *HORAS5* expression. It determines a high KD (77%) at 75nM with relative low toxicity (≤50%).
Study of the effect of antisense treatments to target *HORAS5 in vitro* that suggests *HORAS5 in vivo* potential	ASO3 transfection + cabazitaxel treatment + trypan blue exclusion cell count	Cell count show reduction in cell number upon cabazitaxel treatment, when *HORAS5* is knocked down by ASO3, compared to the control.
HORAS5 KD decreases cabazitaxel IC$_{50}$	Non-linear fit from cell count and comparison between *HORAS5* KD and control	This calculation shows that cabazitaxel IC$_{50}$ significantly decreases when *HORAS5* is downregulated in CRPC cells, using ASO3 compared to the control. This suggests that *HORAS5*-targeting ASO increases cell sensitivity to cabazitaxel and confirms that *HORAS5* is a good candidate for future *in vivo* and clinical studies.

6.1. Prognostic value of *HORAS5* and *BCL2A1* in prostate cancer patients

HORAS5 has been shown to promote cabazitaxel resistance via stimulation of *BCL2A1* expression *in vitro*. These molecules could have a prognostic role in prostate cancer patients. In this way, it would be possible to translate the shown *in vitro* findings into clinical applications such as using *HORAS5* as a prognostic and diagnostic biomarker for prostate cancer aggressiveness and treatment response and as a therapeutic target to increase patient survival. Therefore, a TCGA study has been accessed via cBioPortal and analysed.

This study has been already queried in a previous publication in order to determine *HORAS5* prognostic value (fig.6.1A)(Parolia *et al.*, 2019). The same expression criteria were adopted for both *HORAS5* and *BCL2A1*: upregulation in 7% of patients (tables in fig.6.1). *HORAS5* PFS analysis is reported in figure 6.1A, in order to show the similar correlation of the two genes with PFS. As shown in figure 6.1B, *BCL2A1* upregulation correlates with reduced PFS with a similar trend and significance as *HORAS5*. 17.65% of the cases with low *BCL2A1* expression relapsed after prostatectomy compared to the 31.25% of the cases with high *BCL2A1* expression (fig.6.1B), similarly to what has been previously reported for *HORAS5* in the same patients: 17.36% of cases with low *HORAS5* expression relapsed compared to 33.33% of the cases with *HORAS5* upregulation (Parolia *et al.*, 2019) (fig.6.1A).
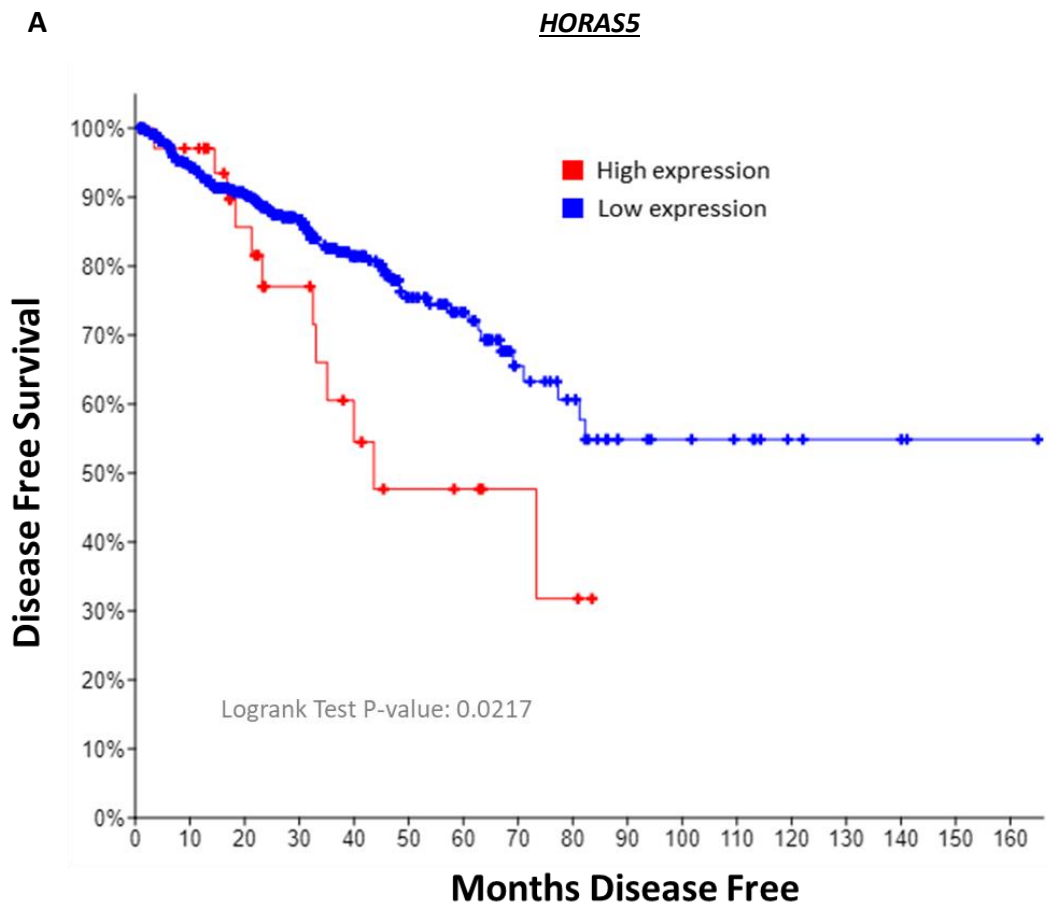
A   <u>*HORAS5*</u>

Group	Total cases	Recurred cases	Recurred cases/total (%)
HORAS5 high expression	36	12	33.33
HORAS5 low expression	455	79	17.36
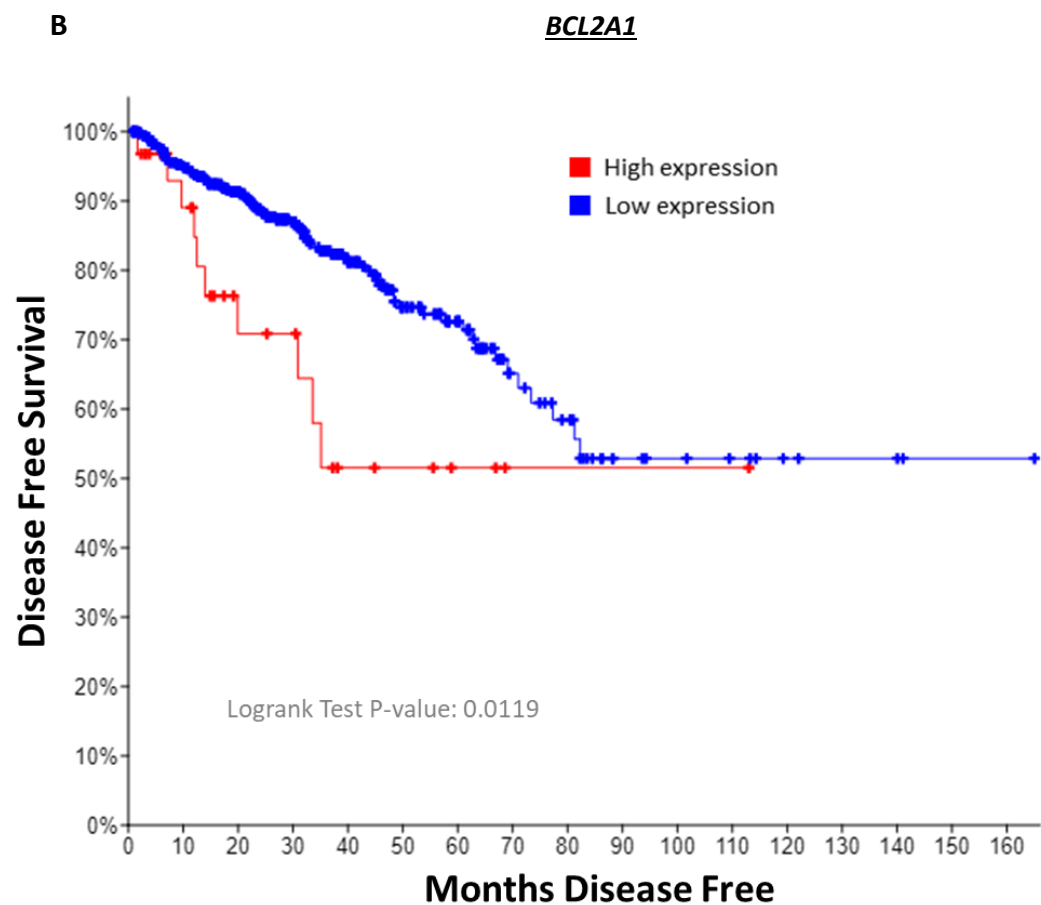
B   *BCL2A1*

Group	Total cases	Recurred cases	Recurred cases/total (%)
BCL2A1 high expression	32	10	31.25
BCL2A1 low expression	459	81	17.65

Figure 6.1 |*HORAS5* and *BCL2A1* have a similar prognostic value in prostate cancer patients.

The graphs show disease free survival data of samples from patients from a TCGA dataset (TCGA Firehose Legacy), who underwent radical prostatectomy, with high or low expression of *HORAS5* (A) and *BCL2A1* (B). **A.** The graph and table in A show the findings from Parolia et al. (Parolia *et al.*, 2019) and are reported here for comparison with *BCL2A1* correlation with disease free survival in the same cohort of patients, in B. **B.** In the cases with *BCL2A1* high expression, 31.25% relapsed after radical prostatectomy vs 17.65% relapsed cases with low *BCL2A1* expression as reported in the table below the graph (cBioportal, TCGA Firehose Legacy).

6.2. *HORAS5* expression in clinical samples from metastatic sites of prostate cancer patients

HORAS5 role in cabazitaxel resistance has been investigated *in vitro* and in patient survival but prostate cancer clinical evidence has not been found yet, on *HORAS5* expression correlation with drug treatment, particularly with taxanes. Hence, the expression of *HORAS5* was analysed in clinical prostate cancer samples from a published study (Kumar *et al.*, 2016), accessed via cBioPortal. As shown in figure 6.2, *HORAS5* expression is significantly higher (P value= 0.0086) in metastatic samples from patients treated with taxanes than in samples from untreated patients. No similar evidence has been found for *BCL2A1* expression.
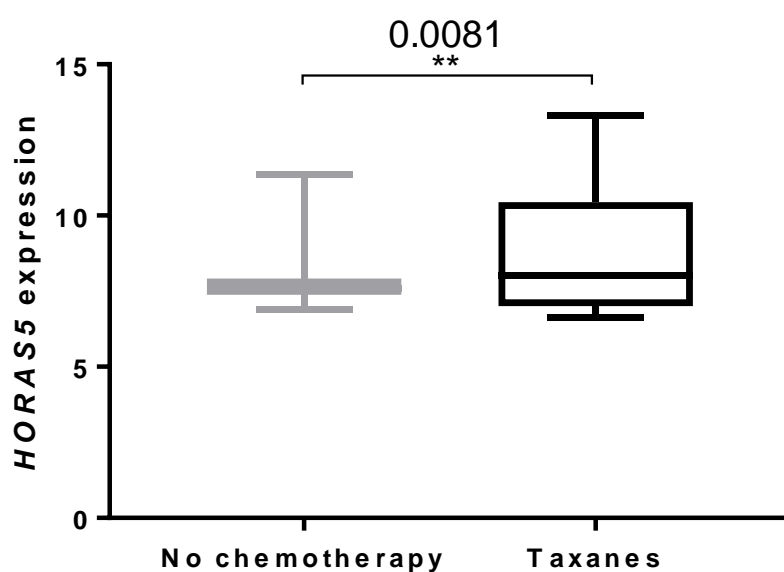
Figure 6.2 | *HORAS5* expression in Prostate cancer clinical samples.
HORAS5 expression from patient metastatic samples treated with taxanes-only (14 samples from 10 patients) compared to samples from untreated patients (46 samples from 15 patients). Student t-test was used for statistical comparison **P=0.0081.

6.3. *HORAS5*-targeting ASOs and effects on cabazitaxel response in prostate cancer cells

Based on the findings on *HORAS5* upregulation in taxane-treated clinical samples, it was analysed if *HORAS5* can effectively be silenced using ASOs. In fact, these compounds can be successfully used *in vivo* and some of them have been tested in clinical trials (Beer *et al.*, 2017; Bellmunt *et al.*, 2017; Yu *et al.*, 2018). These results could highlight the therapeutic potential of targeting lncRNAs like *HORAS5* in the clinical setting. Hence, eight different ASOs were tested in LNCaP cells, which express endogenous detectable levels of *HORAS5*. The results show that ASO3 is the most effective inhibitor of *HORAS5* expression (78.2% KD, as judged by RT-qPCR) (fig.6.3A,B) and reduces by 50 % the cell count when used as the only treatment (fig.6.3C).
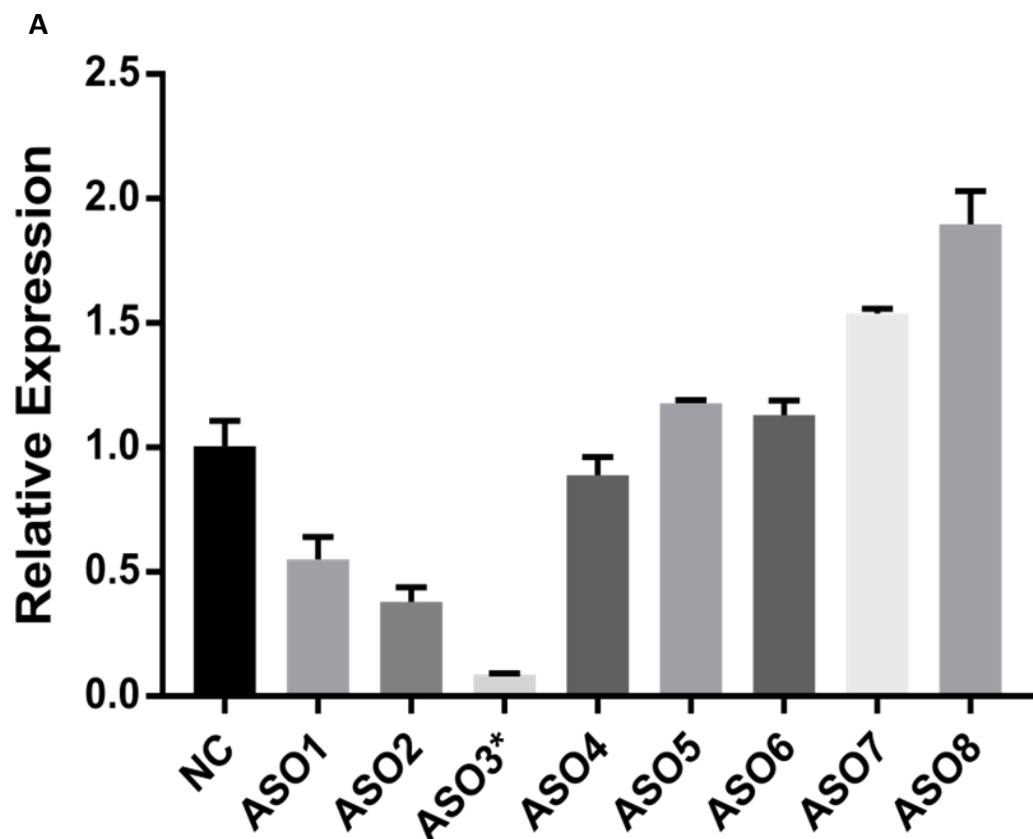
B
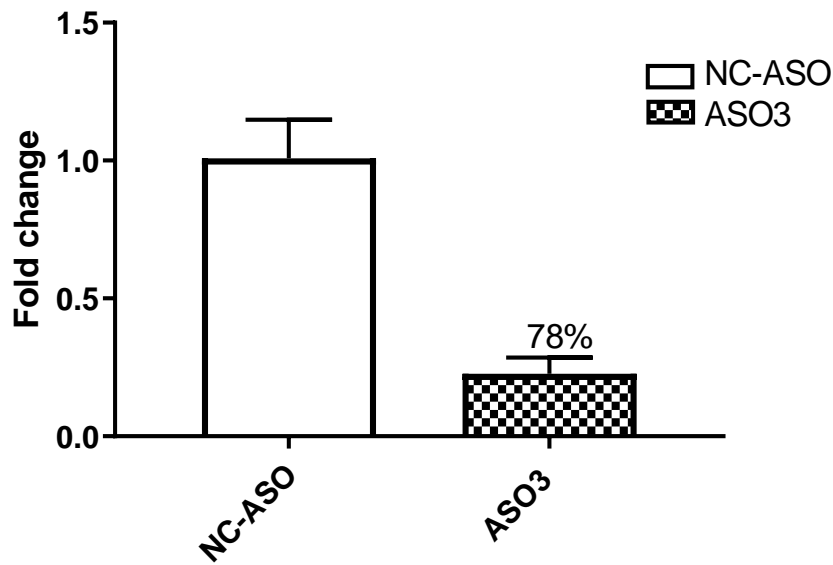
C
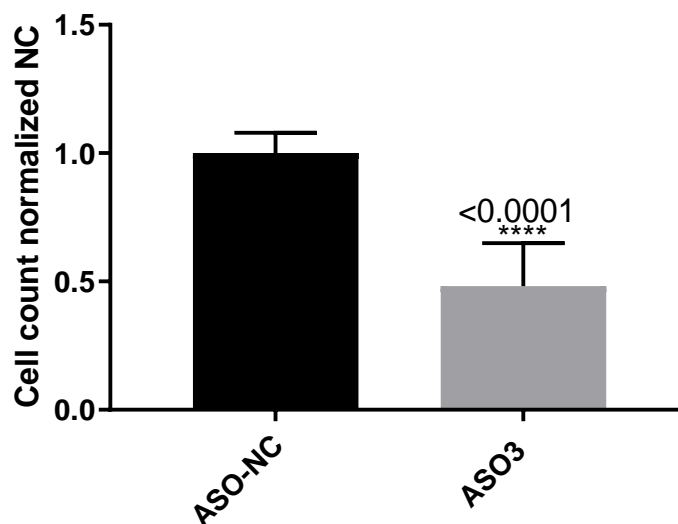
Figure 6.3 | ASO-mediated KD of *HORAS5* and selection of ASO3.
A. RT-qPCR expression of *HORAS5*, upon KD mediated by the 8 tested ASOs, is significantly decreased in LNCaP cells treated with ASO1, ASO2 and ASO3. ASO3 is the most effective inhibitor of *HORAS5* expression. **B**. *HORAS5* KD upon transfection with 75 nM ASO3 is confirmed in LNCaP cells and gives 78% inhibition of *HORAS5* expression measured via RT-qPCR. The results in A and B are expressed as mean expression relative to negative control (NC-ASO) ± S.D. from three independent experimental replicates. All RT-qPCR expression data are normalized for *HPRT1*. One-way ANOVA with Sidak`s post-test was performed for statistical comparison in A ****$P<0.0001$. **C.** ASO3 treatment (75nM) results in LNCaP cell count reduction of around 50% compared to LNCaP cells treated with ASO-NC. The results in C are expressed as mean cell count relative to negative control (NC-ASO) ± S.D. from three independent experimental replicates. Student t-test was used for statistical comparison in C.

Therefore, ASO3 has been tested in combination with cabazitaxel. Cell count decreases when LNCaP cells are treated with *HORAS5*-targeting ASO3 in combination with different concentrations of cabazitaxel (fig.6.4A) (see Chapter 2, Material and Methods for concentrations selection). Moreover, a significant decrease in cabazitaxel IC_{50} (FC=6.55, P=0.0034) was observed in the cells exposed to the cabazitaxel-ASO3 combination treatment compared to cabazitaxel-NC-ASO treatment (fig.6.4B). Hence, ASO-directed *HORAS5* KD increases the sensitivity of LNCaP cells to cabazitaxel.
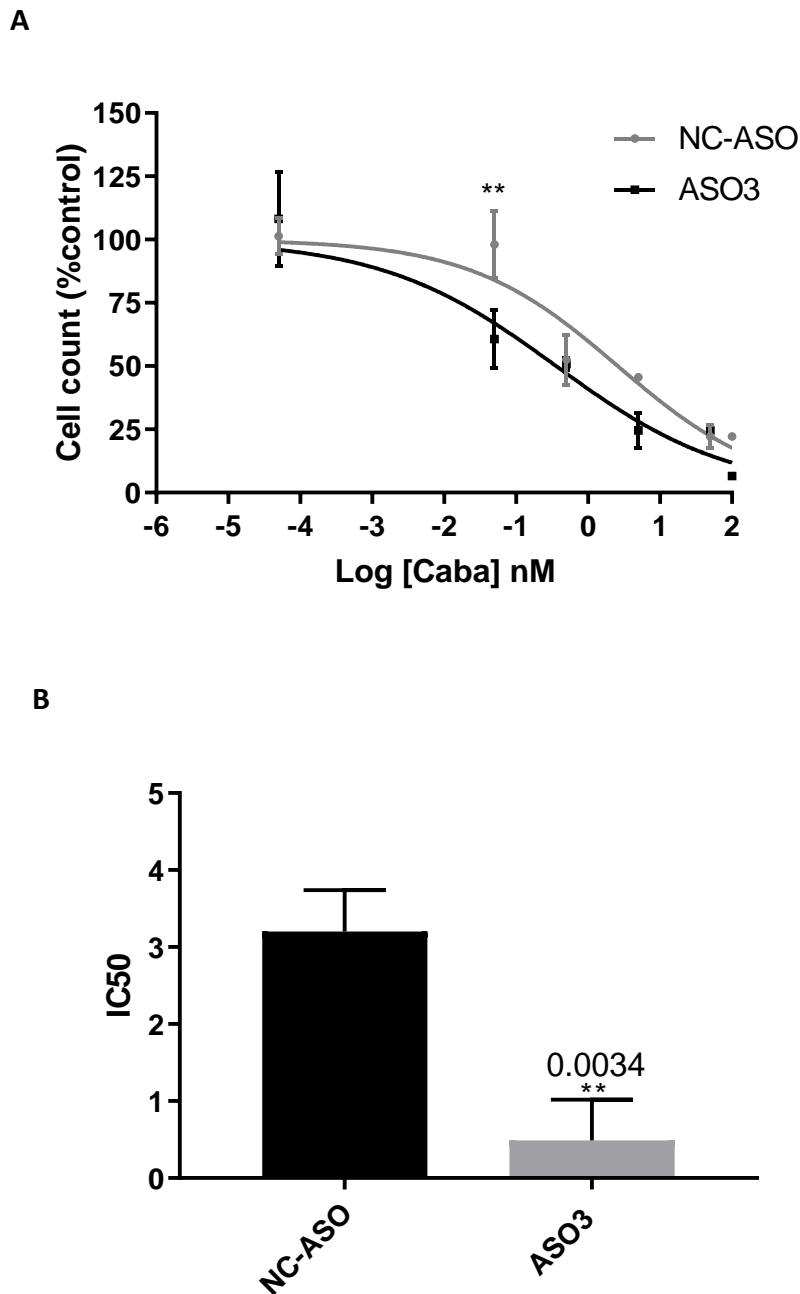
Figure 6.4 | ASO-mediated KD of HORAS5 decreases cabazitaxel resistance.
A, B. *HORAS5* KD mediated by ASO3 induces a decrease in the cell count upon cabazitaxel treatment (A) and a reduction in the IC_{50} (B). Cell count is expressed as nonlinear fit curves of the cell number in percentage, normalized to the untreated (DMSO) control. Results expressed as mean cell count (A) and IC50 (B) relative to the negative control ± S.D. from three independent experimental replicates. Two-way ANOVA with Sidak`s post-test was performed for statistical comparison **P= 0.0056. Student t-test was used for statistical comparison in B **P=0.0034.

6.4. Discussion of Chapter 6

The findings presented in this Chapter suggest that *HORAS5* and *BCL2A1* have a value as prognostic biomarkers for prostate cancer patients and that *HORAS5* expression is affected by taxane treatment in mCRPC clinical samples. Additional experiments reported in this chapter suggest that *HORAS5*-targeting ASO modulation is a successful approach to inhibit this lncRNA and increase cabazitaxel response in prostate cancer cells*.* Therefore, this study paves the way for the translation of the *in vitro* findings described in the previous chapters, into novel knowledge to treat cabazitaxel resistant CRPCs, when *HORAS5* is upregulated. The prognostic value of *BCL2A1* was analysed and compared to some *HORAS5* clinical evidence reported in a published study (Parolia *et al.*, 2019). In this study was shown that high levels of *HORAS5* expression correlates with reduced patient PFS. In the same dataset, *BCL2A1* expression shows the same trend in relation to PFS. Particularly, both *HORAS5* and *BCL2A1* upregulation significantly correlate with increased percentage of cases that relapse after prostatectomy. Although co-expression data, directly linking *HORAS5* and *BCL2A1* expression, have not been found in patient samples, these two molecules have been shown to promote similar effects on patient survival. These findings are fundamental to evaluate the translational potential of *HORAS5* but do not correlate this lncRNA with drug treatment. In order to link *HORAS5* expression with drug treatment in prostate cancer clinical samples, *HORAS5* expression has been analysed in metastatic samples from a cohort of patients treated with taxanes vs untreated, from a published study, accessed via cBioportal (Kumar *et al.*, 2016). *HORAS5* is significantly upregulated in prostate cancer metastatic samples from patients treated with taxanes, compared to untreated patients. This finding is the first clinical confirmation of the *in vitro* evidence shown on *HORAS5*

involvement in taxane-treatment response. The samples considered in this study are tissues from prostate cancer metastases but based on recent evidence (Sun *et al.*, 2018), *HORAS5* could also be detectable in biological fluids (i.e. urine and blood), paving the way for the use of *HORAS5* as a non-invasive biomarker for CRPC. While miRNAs are more stable and can be easily detected in biological fluids (Yun *et al.*, 2015; Berti *et al.*, 2019; Herreros-Villanueva *et al.*, 2019; Ingenito *et al.*, 2019), lncRNAs are less studied in this context and are harder to detect in biological fluids. This can be ascribed to their long sequence which may be harder to pack in extracellular vesicles and more unstable as free sequence in biological fluids, than miRNAs. *HORAS5* increases in the presence of taxane treatment in cells and in patients with metastatic prostate cancer, thereby suggesting that it could be easier to detect this lncRNA in samples from patients treated with these drugs. Moreover, *HORAS5* sequence is shorter than many lncRNAs (long variant is 870bp), suggesting that it could be reasonably stable in blood circulation or other fluids. Future studies could detect *HORAS5* in plasma and urine samples from patients before vs after taxane treatment and could confirm *HORAS5* role in this context.

Due to *HORAS5* function in CRPC cells, further *in vivo* investigation on this lncRNA could also reveal its potential as therapeutic target. Indeed, the inhibition of *HORAS5* in combination with cabazitaxel could decrease cancer resistance to the drug and increase patient response to the treatment. Even though cabazitaxel is effective in CRPC patients and is used when they develop resistance to docetaxel, in some cases the response to this treatment decreases, giving rise to cabazitaxel resistance. In these cases, the introduction of additional treatments, able to restore drug sensitivity, could dramatically increase patient quality of life and survival rate.

With this in mind, *HORAS5*-targeting ASOs have been designed to be capable of effectively reducing *HORAS5* expression. One of the ASOs tested decreases cabazitaxel IC_{50}, when used in combination with this drug to treat CRPC cells. As mentioned, ASOs have been successfully used in clinical trials (Beer *et al.*, 2017; Bellmunt *et al.*, 2017; Yu *et al.*, 2018) and, since lncRNAs are expressed in a tissue and disease-specific manner (Kong *et al.*, 2019), the development of lncRNA-targeting drugs could lead to the production of cancer-specific therapeutic approaches that gives minimal side effects.

LncRNAs can be modulated *in vivo* using several approaches. Lentiviral transduction (B. Zhang *et al.*, 2018; Panda *et al.*, 2018; Somaiah *et al.*, 2019) and CRISPR-Cas9-dependent genome editing (Lavalou *et al.*, 2019) are promising methods to stably modulate lncRNAs expression but their use is at very preliminary stage and needs extensive *in vivo* validation (Lavalou *et al.*, 2019).

Via ASOs it is possible to transiently silence lncRNAs and this method is closer to a clinical application.

HORAS5 has been already inhibited *in vivo* using siRNAs conjugated with a lipidic transfection reagent and has shown significant reduction of CRPC growth (Parolia *et al.*, 2019). Whereas this method is hardly translatable to the clinical setting, *in vivo* studies using *HORAS5*-targeting ASOs, in combination with other treatments, could help identify clinically useful methods to overcome drug resistance.

Notably, ASO structure can be edited to increase their stability in biological fluids and improve their intracellular uptake. Based on this consideration the results obtained in this project are particularly promising since first generation ASOs have been used with efficient results. As underlined in Chapter 1 (1.4.5), chemically modified ASOs such as LNAs and PS-ASOs have shown improved properties, like increased stability and cellular

uptake. In future studies, it would be promising to test ASO3 with specific modifications in order to further increase its potential for *in vivo* studies.

Even if ASOs have been successfully tested in cancer cells and clinical trials (Crea, Quagliata, *et al.*, 2016; Duffy *et al.*, 2016; Chi *et al.*, 2017; Gordon *et al.*, 2019), currently, there is no clinical trial on lncRNA-targeting ASOs.

Therefore, *HORAS5* function in cabazitaxel resistance should be further evaluated *in vivo* using ASOs.

Overall, the findings reported in this Chapter suggest that *HORAS5* is a potential useful biomarker in CRPC and that *HORAS5* inhibition, in combination with taxanes, can increase drug response in CRPC patients, leading to new developments in the fields of personalized medicine and innovative diagnostic strategies.

CHAPTER 7: GENERAL DISCUSSION, FUTURE DEVELOPMENTS AND CONCLUSIONS

7.1. General discussion

This thesis presents the findings on the role of the lncRNA *HORAS5* in advanced prostate cancer response to therapy, highlighting a tight connection between cabazitaxel treatment and a stress response activated by *HORAS5* upregulation, which stimulates *BCL2A1* expression.

This research aims to understand the mechanisms of cancer drug resistance and the role of lncRNAs in this context; the main outcome is to combine commonly used drugs and lncRNA modulation to effectively treat aggressive cancers such as advanced prostate cancer (i.e. CRPC). Current clinical therapies for CRPC can extend patient survival, but are still characterized by short remission times (Nabavi *et al.*, 2017).

Several studies have investigated the modulation of lncRNAs in cancer, in order to assess whether they could be involved in tumour-related pathways and be used as targets for novel therapies (Crea, Watahiki, *et al.*, 2014; Mohanty, Badve and Janga, 2014; Parolia *et al.*, 2015). Previous studies have shown that *HORAS5* is upregulated in CRPC vs. hormone sensitive PDX models and favours cell proliferation and inhibits apoptosis by stabilizing *AR* mRNA in CRPC cells (Parolia *et al.*, 2019).

Wang et al. have shown the involvement of *HORAS5* in osteosarcoma cell response to cisplatin (Wang *et al.*, 2016). They have observed that cisplatin can induce the expression of *HORAS5* and that this lncRNA activates pro-apoptotic pathways. Based on studies recently published (Parolia *et al.*, 2019), the same lncRNA has been hypothesized to trigger an opposite response (i.e. activation of anti-apoptotic pathways) in CRPC cells.

As already mentioned in this thesis, it is well known that lncRNAs are characterized by tissue-specific expression and functions. It is therefore conceivable that *HORAS5* plays opposite roles in CRPC and osteosarcoma. Other important findings have also characterized *HORAS5* in other malignancies suggesting that this lncRNA can play key roles in cancer-associated pathways such as survival, metastasis and drug response, via regulation of different mechanisms and processes (L.-C. Xu *et al.*, 2017; Sun *et al.*, 2018; Xu *et al.*, 2019).

Based on these findings, additional studies could further determine whether *HORAS5* is a novel treatment target for CRPC and for other tumours where it promotes tumour growth and drug resistance.

Sun and collaborators have also shown that *HORAS5* is detectable in serum of HCC patients (Sun *et al.*, 2018). This discovery paves the way for the use of *HORAS5* as a non-invasive biomarker.

For this reason, the specific aims of this project have been to study the correlation between *HORAS5* expression and CRPC drug treatment, to investigate the mechanistic role of *HORAS5* in response to this treatment in prostate cancer cells, and to generate proof of principle on the translational potential of *HORAS5* for future *in vivo* and clinical studies.

To summarize, lentiviral-mediated overexpression and siRNA-mediated KD of *HORAS5* were optimized, in order to obtain efficient stable overexpression and transient silencing of the lncRNA, respectively. *HORAS5* subcellular localization was then assessed in the overexpression model and compared to previously published evidence (Parolia *et al.*, 2019). Afterwards *HORAS5* expression was assessed upon treatment with some

drugs clinically employed for CRPC patient treatment (Fléchon *et al.*, 2011; Scher *et al.*, 2012; Aparicio *et al.*, 2013; Beer *et al.*, 2014; Sissung *et al.*, 2014; Smiyun, Azarenko, Miller, Rifkind, LaPointe, *et al.*, 2017; Hussain *et al.*, 2018). Among the drugs tested, only cabazitaxel induced a consistent and statistically significant increase in *HORAS5* expression, dependent on drug concentration and time of treatment. These findings suggest that there could be a connection between cabazitaxel and *HORAS5.* This connection was further evaluated by modulating *HORAS5* and analysing cell response to cabazitaxel. *HORAS5* expression increases cell count and decreases caspase-induced apoptosis in both AR^+ and AR^- prostate cancer cells, thereby increasing cabazitaxel IC_{50} with decreased cell response to the drug.

Notably, the connection between cabazitaxel treatment and *HORAS5* expression could be explained by (fig.7.1):

- Clonal selection of intrinsically resistant cancer cells, which promotes the expression of *HORAS5* in the overall cancer cell population, without affecting the intracellular modulation of the lncRNA.

- Pro-survival *stimuli* activated in the cells as a downstream response to cabazitaxel stress that promotes *HORAS5* expression, either stimulating its expression or reducing its inhibition.

- Cabazitaxel mechanism of action that promotes *HORAS5* expression, again either stimulating its expression or reducing its inhibition.

Since *HORAS5* is upregulated in prostate cancer cells with both constitutive and exogenous expression of this lncRNA, clonal selection is suggested as the most reliable hypothesis. Moreover, cabazitaxel could also activate a prosurvival stress-response in

the cancer cells, thereby stimulating a post-transcriptional upregulation of *HORAS5* (i.e. decrease of *HORAS5* inhibition mechanisms).

Nevertheless, a connection based on cabazitaxel mechanism of action cannot be excluded. Since taxanes can have several mechanisms of action, from microtubule binding, to ROS and mitochondria metabolism, it could be hard to study this connection. Taxanes main mechanism of action is direct β-tubulin binding with effects on cell division. According to the analysis of the RNA sequencing data performed in this project, a minor involvement of *HORAS5*-upregulated genes has been found in cell cycle. Based on Reactome analysis, *CCNL1* appears of interest since it is involved in DNA unwinding pathways, important for DNA replication. Therefore, it could be interesting to further analyse this interaction even though *HORAS5* is mainly a cytoplasmic lncRNA.

For the reasons discussed so far, *HORAS5* seems to be induced by cabazitaxel-induced clonal selection as well as by cancer cell response to cabazitaxel-triggered downstream *stimuli*. This induction of *HORAS5* is suggested as a defence of the cancer cells from the drug-induced stress, rather than from its mechanism of action. In this way the cancer cells might use *HORAS5* to orchestrate a complex response that inhibits apoptosis and induces cancer cell survival.

As mentioned before, several lncRNAs are upregulated in response to general stress conditions (such as the ones deriving from drug treatment) and the RNA sequencing analyses shown in this thesis reveal that, in response to cabazitaxel, *HORAS5* upregulates prevalently genes involved in inflammation and apoptosis, rather than cell cycle or processes linked to cabazitaxel mechanism of action.

This hypothesis seems also supported by a recent publication on *HORAS5* role in drug response, where *HORAS5* is upregulated upon treatment with another drug (i.e. cisplatin) (Xu *et al.*, 2019); cisplatin has a different mechanism of action from taxanes but still induces a massive stress for the cancer cells.
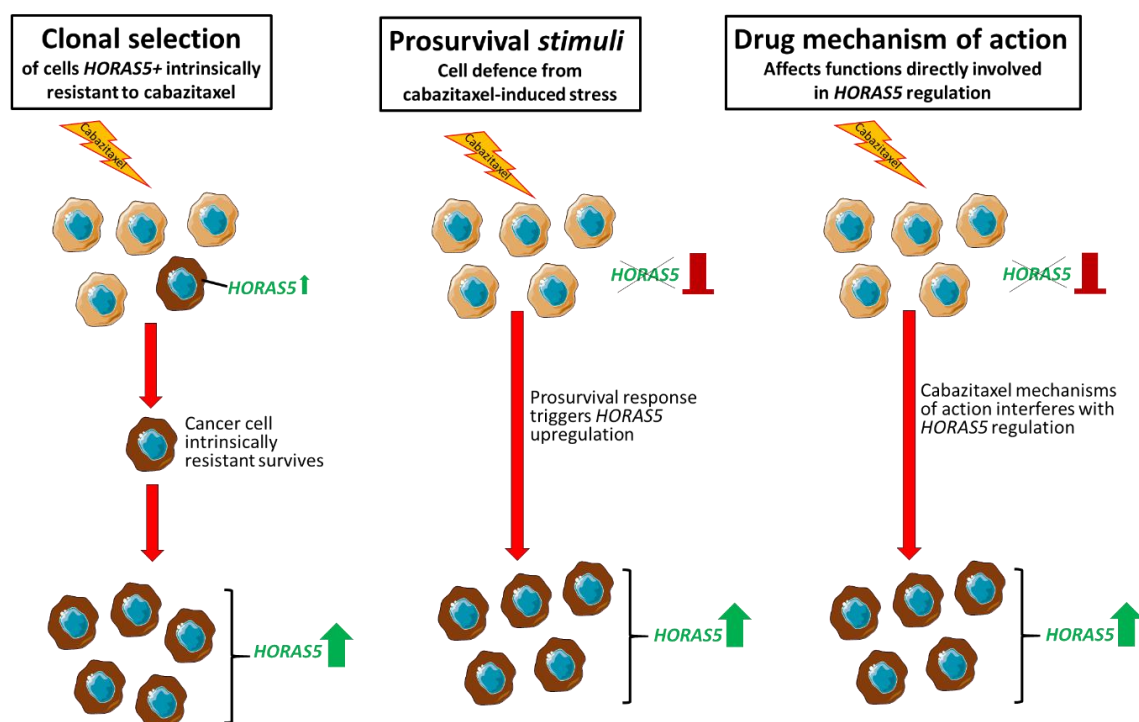
Figure 7.1 | Possible hypotheses of cabazitaxel action in stimulation of *HORAS5* expression.
This figure shows three possible mechanisms of HORAS5 upregulation induced upon cabazitaxel treatment. From the left, clonal selection of cabazitaxel intrinsically resistant cells which express *HORAS5* (dark brown) before drug treatment; cabazitaxel induces a survival stress in cancer cells which, in response, upregulates prosurvival pathways that promote *HORAS5* upregulation in cancer cells; cabazitaxel induces specific effects via its mechanism of action that interfere with *HORAS5* upstream regulation. Orange flash represents cabazitaxel treatment.

Cabazitaxel-induced *HORAS5* stimulation decreases prostate cancer cell response to the drug. High throughput transcriptomic analyses have shown that *HORAS5* stimulates the

expression of the antiapoptotic factor BCL2A1, in response to cabazitaxel treatment. *BCL2A1* KD increases cabazitaxel sensitivity via decrease of cell count and induction of apoptosis.

LncRNAs can have several roles in cancer cells and act in these functions via multifaceted mechanisms of action, such as for *HORAS5*, which can regulate different pathways in the same cancer, according to the expression of *AR*. In fact, in AR⁺ cells *HORAS5* promotes a survival signalling via stabilization of *AR* mRNA (Parolia *et al.*, 2019). In AR⁻ cells, *HORAS5* promotes a similar response by inducing other pro-survival signals (i.e. BCL2A1).

Moreover, lncRNAs can also act in the same cell type and stimulate similar responses and phenotypes via interacting with different molecules. Hence, the findings reported in this thesis describe one mechanism of action via which *HORAS5* promotes AR⁻ CRPC cell survival in response to cabazitaxel treatment. This mechanism does not exclude that *HORAS5* could act via interaction with other molecules and subcellular components. This is very interesting since it paves the way for further investigation on other mechanisms of action of *HORAS5* in drug response. Additionally, since the findings reported in this thesis indicate that *HORAS5* is prevalently cytoplasmic, but a portion is also retained or returned into the nucleus, it is conceivable that this lncRNA could also have nuclear functions. Examples of characterized nuclear functions for lncRNAs are stabilization and recruitment of epigenetic effectors and TFs to specific sites and interaction with splicing complexes (Kong *et al.*, 2016; Qinyu Sun, Qinyu Hao, 2018; Miao *et al.*, 2019).

Based on these *in vitro* findings, it has been investigated whether this model could have a relevance in the clinical setting, where prostate cancer is a heterogeneous disease, characterized by complex interactions of cancer cells with the pathological and physiological environment. *HORAS5* and *BCL2A1* have similar prognostic value in

prostate cancer patients. Moreover, *HORAS5* is upregulated in metastatic prostate cancer samples from taxane-treated patients vs. untreated. This evidence has suggested that *HORAS5* and the reported *in vitro* findings could have a clinical relevance. Therefore, *in vitro* studies have been performed on *HORAS5*-targeting therapies to select a specific 1st generation ASO able to efficiently inhibit *HORAS5* expression and significantly reduce prostate cancer cell count when used both alone and in combination with cabazitaxel (fig.7.2). Moreover, cabazitaxel IC$_{50}$ is decreased when this ASO is employed in combination with this drug. These findings pave the way for the *in vivo* use of *HORAS5*-targeting approaches and for the use of *HORAS5* as therapeutic target and biomarker of tumour progression, recurrence and drug response, as discussed in sections 7.2.4 and 7.2.5. Figure 7.2 schematically summarizes the main *in vitro* findings reported in this thesis.
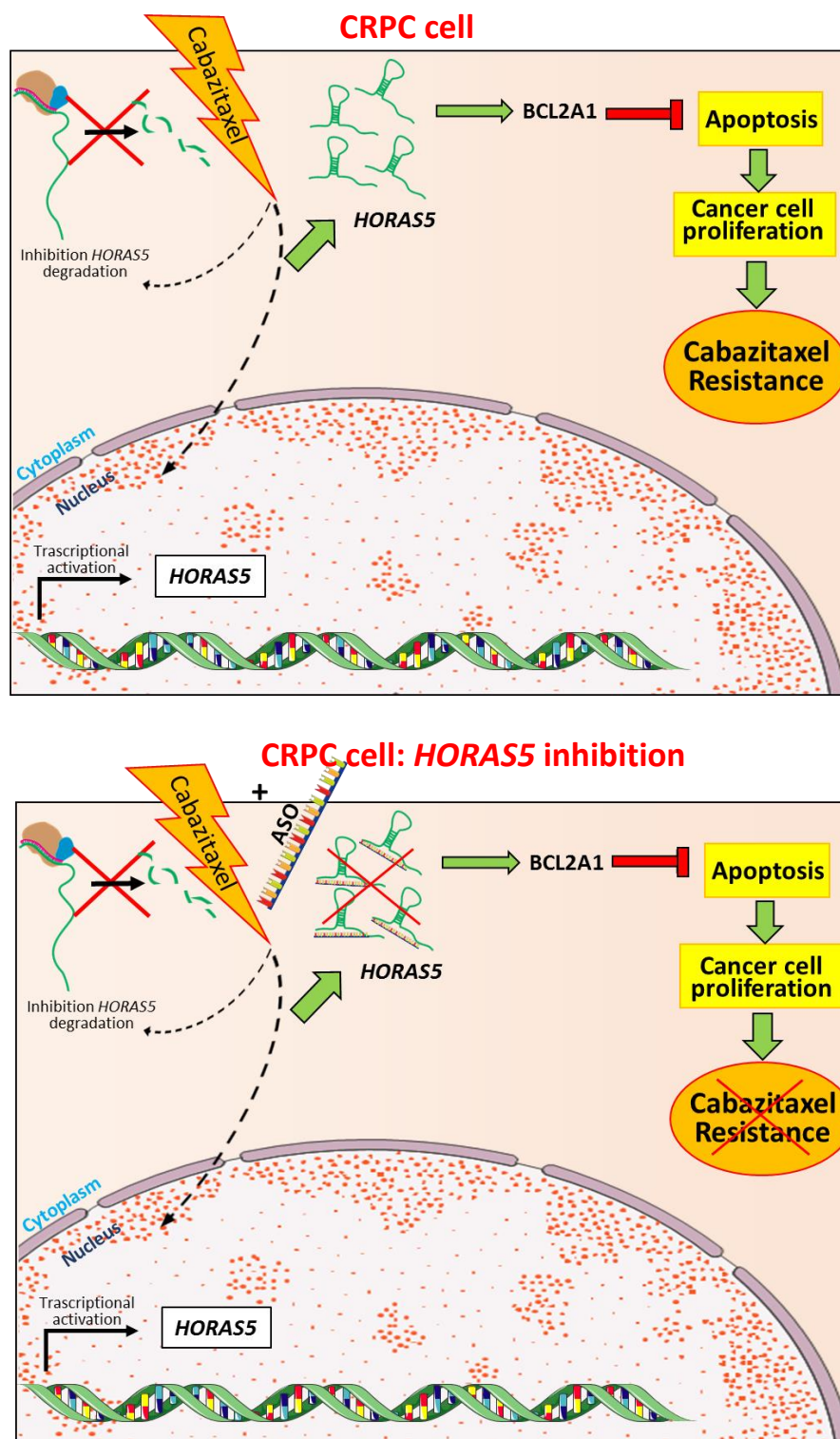
Figure 7.2 | Diagram summarising the *in vitro* findings reported in this thesis.
This figure shows a CRPC cell in the first part that upon treatment with cabazitaxel up-regulates *HORAS5* via either activating *HORAS5* gene transcription or hindering its degradation. *HORAS5* up-regulation stimulates BCL2A1 expression and this decreases apoptosis and increases cell proliferation. This pathway describes the mechanism of cabazitaxel resistance mediated by *HORAS5*. In the bottom picture, is shown the effect of *HORAS5*-targeting ASO that inhibits *HORAS5* expression, thereby reducing cabazitaxel resistance.

7.2. Future developments

This project lays the foundation for further research on *HORAS5* mechanism of action and its potential as biomarker and therapeutic target in the clinical settings. These aspects could be unravelled by future studies that can bring novel developments to the knowledge of lncRNA biology and personalized cancer treatments.

7.2.1. *HORAS5* interaction with miRNAs

HORAS5 has already been involved in drug response in different cancers where it has been shown to act as a miRNA sponge (Xu *et al.*, 2019; Wang *et al.*, 2016). According to the data reported in this thesis, *HORAS5* is prevalently located in prostate cancer cell cytoplasm, thereby suggesting that it can interact with mature miRNAs. *In silico* evidence has shown that *miR-128* is predicted to bind both *HORAS5* and *BCL2A1* RNA sequences (fig.7.3A). Additionally, previous literature has shown that *miR-128* acts as an oncosuppressor, can induce apoptosis via downregulation of anti-apoptotic factors and increases chemosensitivity to drugs, such as the taxane paclitaxel in lung cancer (Koh *et al.*, 2017; T. Liu *et al.*, 2019; Adlakha and Saini, 2011). Since there are two variants of *pre-miR-128* (*pre-miR-128-1* and *pre-miR-128-2*) and each of them originates two mature forms (*-3p* and *-5p*), preliminary experiments have been performed to investigate whether one of these variants is predominantly expressed in the control prostate cancer cell line (DU145-NC) (fig.7.3B). *Pre-miR-128-1* is expressed in prostate cancer cells while *pre-mir-128-2* is not detectable, meaning that future work on *HORAS5* mechanism of action could focus on the mature forms of the former (fig.7.3B). Notably *miR-128* has been also shown to interact with *HORAS5* in ovarian cancer cells (Xu *et al.*, 2019). This enforces the suggestion that *HORAS5* could bind *miR-128* in prostate cancer

cells, establishing a *HORAS5-miR128-BCL2A1* axis that inhibits cabazitaxel-induced apoptosis. Since there is no published evidence of *HORAS5*-miRNAs interaction in prostate cancer, future developments in this context could specifically clarify the type of interaction that connects *HORAS5* and *BCL2A1*, thereby establishing a new regulatory axis in cancer survival and drug response.

A
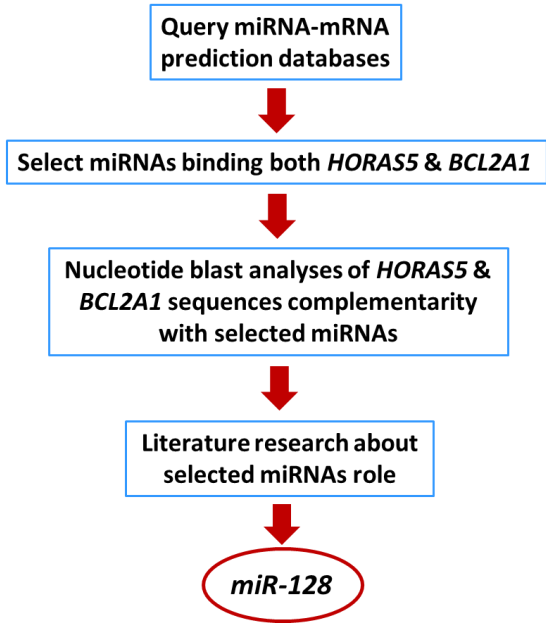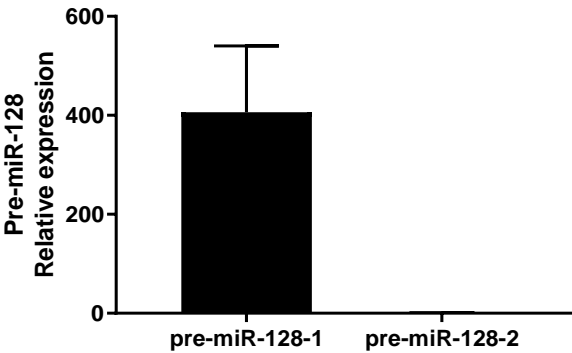
Figure 7.3 | HORAS5 and mir-128.
A. Flowchart showing *in silico* data on *miR-128* interaction with *HORAS5* and *BCL2A1* according to prediction database (i.e. MIRCODE) and nucleotide blast and literature evidence on *miR-128* role in cancer. **B.** Preliminary data on *pre-miR-128* isoforms expression in DU145-NC cells: *pre-miR-128-1* is detectable in the cells and expressed at higher levels than *pre-miR-128-2*.

7.2.2. BCL2A1 in calcium signalling

Future approaches to inhibit *HORAS5* expression seem to be particularly reliable due to expected higher specificity and less side effects, compared to BCL2A1 inhibition. This is due to a broader known effect of this anti-apoptotic factor than HORAS5, on survival pathways. Nevertheless, it would be interesting to test BCL2A1 small-molecule

inhibitors in order to further investigate the downstream mechanism of action activated by *HORAS5*. In this context, it is interesting to consider that BCL2A1 is an antiapoptotic factor of the BCL2 family and retains all 4 BH domains of the BCL2 mature protein. BCL2 was recently shown to suppress apoptosis via regulation of calcium signalling pathways (Distelhorst and Bootman, 2019; Rong *et al.*, 2009). Notably, according to the RNA sequencing data, *BCL2* is not upregulated upon *HORAS5* overexpression neither upon cabazitaxel treatment, suggesting that this key anti-apoptotic factor is not required in this cell type, in these conditions. Therefore, BCL2A1 could resemble BCL2 functions in the cell lines where the latter is not expressed. Further work in this context could clarify some downstream effects triggered by *HORAS5* overexpression (e.g. calcium signalling) that in turn could participate in cabazitaxel response.

7.2.3. Upstream mechanisms of *HORAS5* upregulation by cabazitaxel:

Since *HORAS5* overexpression in AR⁻ prostate cancer cells is driven by the *CMV* promoter, it is not possible to study the up-stream regulation of *HORAS5*. Nevertheless, *HORAS5* expression is also induced by cabazitaxel in LNCaP (AR⁺ cells) under *HORAS5* promoter. Therefore, it would be interesting to study the upstream regulation of *HORAS5* expression upon cabazitaxel treatment in this cell line. First, since cabazitaxel treatment determines *HORAS5* upregulation rather than other drugs tested, this drug could specifically influence *HORAS5* expression, as mentioned in 7.1. Future studies could test this hypothesis. Moreover, preliminary *in silico* data on *HORAS5* putative promoter region have been obtained by using ALGGEN-PROMO a program to predict TF binding sites (TFBSs) in a DNA sequence. LncRNA promoters have been scarcely studied and the concept of "lncRNA promoter" still needs to be defined. For this reason, 200 bp

upstream of the *HORAS5* gene have been selected as the putative promoter. Some studies have suggested this as the region with the highest number of active TFBSs (Guo and Jamison, 2005; Tabach *et al.*, 2007; Fitzgeralda *et al.*, 2008). A region of 10bp has the highest number of predicted TFBSs (fig. 8.2). Among these TFs, CBEP-β is predicted to bind the selected region in two different TFBSs (fig. 8.2). According to a published study, CBEP-β is involved in the activation of senescence upon androgen blockade, thereby promoting CRPC progression (Barakat *et al.*, 2015). Future predictions and experimental validations could elucidate if this TF can have a role in the stimulation of *HORAS5* expression in prostate cancer, upon drug treatment and could establish if there is a link between cabazitaxel mechanism of action and specific TFs predicted to bind *HORAS5* regulatory regions.

7.2.4. *HORAS5* targeting ASOs

As described in Chapter 6, one of the ASOs tested results in efficient *HORAS5* inhibition in prostate cancer cells at clinically achievable concentrations. This ASO increases cabazitaxel-induced cell death, thereby decreasing the drug $IC_{50,}$ with synergistic effect with the drug. As mentioned before, ASOs have an important clinical impact in cancer treatment and no lncRNAs-targeting antisense therapy has yet been approved for cancer patient treatment. Future work could optimize the *HORAS5*-targeting ASO for *in vivo* studies and test it in prostate cancer patients and in other malignancies where *HORAS5* promotes cancer aggressive phenotypes, such as metastasis and drug resistance. This future work could clarify *HORAS5* role as a potential target to increase patient survival when used alone or in combination with other treatments.

7.2.5. *HORAS5* as biomarker in liquid biopsies and CTCs

The *in vitro* and clinical evidence reported in this thesis, together with previous studies, suggest that *HORAS5* is upregulated in prostate cancer, that it increases with taxane treatment and has a prognostic value in PFS of prostate cancer patients. Overall, these findings indicate that further studies are needed to confirm *HORAS5* expression in clinical samples with focus on biological fluids. This would pave the way for the use of *HORAS5* as a diagnostic and prognostic non-invasive biomarker that could be detected in biological fluids such as blood and urine of cancer patients either free, packed in exosomes or in circulating tumour cells (CTCs).

7.3. Conclusions

The novel findings that this PhD project has generated are:

1) Lentiviral-mediated *HORAS5* overexpression does not affect prostate cancer cell morphology and proliferation and maintains *HORAS5* subcellular localization.

2) Cabazitaxel stimulates the expression of *HORAS5* in AR^+ and AR^- prostate cancer cells.

3) *HORAS5* overexpression in AR^- prostate cancer cells decreases cell sensitivity to cabazitaxel and *HORAS5* silencing in AR^+ cells has the opposite effect.

4) *HORAS5* mediates cabazitaxel response in prostate cancer cells via inhibition of apoptosis.

5) The antiapoptotic factor BCL2A1 is upregulated upon cabazitaxel treatment and increases as a consequence of *HORAS5* overexpression. *BCL2A1* KD increases cell sensitivity to cabazitaxel.

6) *HORAS5* and *BCL2A1* have a similar prognostic value in prostate cancer patients.

7) *HORAS5* is upregulated in prostate cancer metastatic samples from patients treated with taxanes compared to untreated.

8) *HORAS5*-targeting ASOs can efficiently silence *HORAS5* in prostate cancer cells and increase cell sensitivity to cabazitaxel.

Overall, this project provides evidence on *HORAS5* role and mechanism of action in prostate cancer response to cabazitaxel and contributes to the research to develop lncRNAs-based personalized treatments and diagnostic screening for incurable diseases, such as CRPC. This and further studies could deepen the knowledge on lncRNA biology, functions and translational potential in prostate cancer and in other malignancies where lncRNAs regulate tumour survival and drug response.
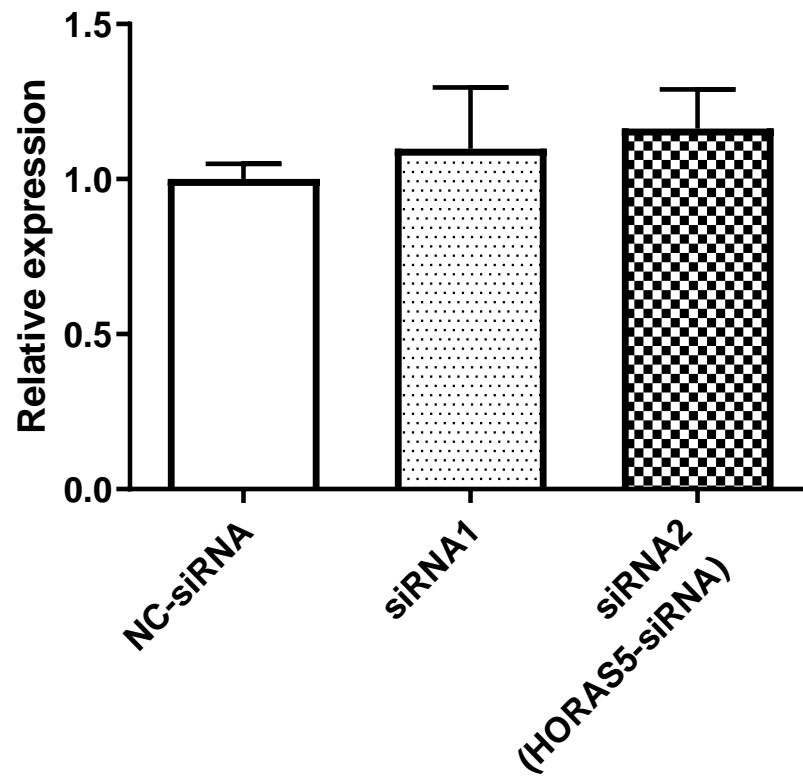
Figure 8.1 | HORAS5 KD in DU145-OE cells.
Expression of *HORAS5* in DU145-OE cells 48h post-treatment with HORAS5-siRNAs and negative control (NC-siRNA), measured via RT-qPCR. Results represented as means ± S.D. from two independent replicates. Referred to on p. 134.

Table 8.1 | List of 87 genes upregulated (FC>2) in cabazitaxel-treated prostate cancer cells overexpressing *HORAS5* (DU145-OE) (P<0.01) but not in cells which do not express *HORAS5* (DU145-NC) (P>0.01). Genes ranked based on P value DU145-NC treated vs untreated, consistently with Table 5.2.

Gene-ID	Log$_2$ DU145-OE treated	Log$_2$ DU145-OE untreated	Fold Change (treated vs untreated)	P value (DU145-OE treated vs untreated)	P value (DU145-NC treated vs untreated)
SUMO4	1.6	0.4	2.31	0.0056	0.6321
LTB4R2	1.26	0.15	2.16	0.0094	0.4364
PCDH1	1.03	0	2.05	0.0018	0.4226
FBXO34	1.7	0.15	2.94	0.0029	0.3152
BCL2A1	3.15	1.86	2.45	0.0068	0.2818
BRD8	1.36	0.33	2.04	0.0032	0.2662
TMEM128	2.45	0.98	2.77	0.0099	0.2581
PCDHB19P	1.89	0.33	2.95	0.0086	0.2075
OR2B6	1.17	0	2.25	0.0016	0.1124
IL23A	2.12	0.34	3.42	0.0028	0.112
OAS3	5.71	4.57	2.21	3.67E-05	0.1044
ADCY10P1	1.29	0.08	2.32	0.0079	0.1026
CCNL1	5.65	4.2	2.73	0.0095	0.1025
SF3B4	4.3	3.24	2.09	0.0056	0.0965
HIST1H3J	3.11	1.72	2.63	0.0011	0.0937
CPEB4	4.58	3.52	2.08	0.0065	0.09
LOC100289187	2.02	0.86	2.23	0.0095	0.089
PFN1P2	4.61	3.49	2.17	0.0051	0.0846
SOX9	4.27	2.86	2.67	0.0099	0.0827
USP53	5.74	4.73	2.01	0.0027	0.081
IRF9	4.08	2.69	2.63	0.0018	0.079
TTC18	1.62	0.34	2.43	0.0063	0.0775
DYRK1B	1.95	0.83	2.18	0.0026	0.0767
CCL20	2.61	1.2	2.67	0.0065	0.0738
ALDOC	2.17	0.83	2.54	0.0056	0.0714

ALPPL2	1,85	0,15	3,26	0,0002	0,0666
N4BP2L2	2,21	0,66	2,94	0,0004	0,0575
IRF7	4,33	2,95	2,6	0,0039	0,051
PPP1R15A	6,1	4,25	3,6	0,0063	0,0488
POU5F1P4	1,87	0,75	2,18	0,0003	0,0486
FAM100B	6,89	5,7	2,27	0,0027	0,046
C19orf77	1,52	0,08	2,71	0,0043	0,046
ROBO4	1,51	0,4	2,17	0,0095	0,0457
CYP26A1	1,72	0,6	2,18	0,0044	0,0453
ZC3H8	4,49	3,35	2,21	0,0068	0,0449
ETV5	6,89	5,79	2,13	0,0039	0,0442
EGR3	1,36	0	2,56	2,47E-05	0,0431
UPF3B	5,03	3,98	2,06	0,0083	0,0411
NPTX2	3,31	1,4	3,77	0,008	0,0398
ENO3	2,67	1,32	2,55	0,0036	0,0397
ZNF107	5,9	4,88	2,02	0,0068	0,0358
PILRB	4,36	3,07	2,44	0,0042	0,035
TMEM158	4,5	3,15	2,54	0,0066	0,0346
GOLGA6L9	2,1	0,99	2,16	0,0065	0,0345
SAMD9	1,97	0,76	2,32	0,0083	0,0337
SNHG1	7,17	5,8	2,58	0,0018	0,033
MMP1	3,35	0,66	6,42	0,0069	0,0325
MCAM	5,87	4,57	2,46	0,0097	0,0322
FOS	3,68	1,39	4,91	0,0067	0,0317
LOC399753	3,97	2,68	2,44	0,0058	0,0314
GADD45A	6,52	4,33	4,58	3,93E-05	0,0311
LOC440354	3,8	2,67	2,19	0,004	0,03
ZFAND2A	6,49	5,18	2,47	0,0064	0,0299
AOC3	1,77	0,06	3,25	0,0052	0,0291
SNAPC1	8,32	7,3	2,04	0,0004	0,0289
NBPF14	4,96	3,61	2,56	4,73E-05	0,0284

SDCBP2	1,3	0,28	2,03	0,0009	0,028
SEMA4A	1,88	0,15	3,33	0,0034	0,028
C2orf78	2,2	0	4,59	0,0054	0,0269
H2AFJ	2,04	0,83	2,32	0,0036	0,0261
LOC646329	3,6	1,98	3,07	0,0026	0,0257
TXNIP	4,97	2,34	6,18	0,0064	0,0252
ECM1	3,95	2,85	2,14	0,0074	0,0245
LOC731275	5,19	3,7	2,82	0,004	0,0242
COL27A1	1,68	0,56	2,17	0,0027	0,0224
CCT6P1	2,54	1,36	2,26	0,0038	0,0222
IFI27	1,83	0,33	2,82	0,0012	0,0215
ARHGAP11B	6,37	5,11	2,4	0,0008	0,0211
ZNF844	4,01	2,11	3,73	0,0085	0,0209
RBM15	2,45	0,9	2,94	0,0073	0,0193
UPP1	3,34	1,48	3,64	0,0099	0,019
JAG1	3,78	2,35	2,69	0,0087	0,0188
LOC100288069	3,75	2,48	2,41	0,0006	0,0185
SESN2	5,48	4,33	2,22	0,0083	0,0185
RRAD	3,12	1,29	3,57	0,0057	0,0175
PI3	1,3	0,22	2,12	0,0086	0,017
NR4A3	5,15	4,04	2,15	0,0043	0,0164
DDR2	1,92	0,08	3,57	0,0073	0,015
AEN	6,17	4,89	2,43	0,0096	0,0146
AKAP17A	6,99	5,87	2,16	0,0048	0,0142
C21orf7	2,74	1,47	2,41	0,0009	0,0139
ZNF790-AS1	1,93	0,56	2,59	0,0001	0,0136
SLC3A2	8,71	7,66	2,07	0,0006	0,0132
NT5E	8,03	6,91	2,18	0,0019	0,0115
NGFR	2,57	0,6	3,91	0,0068	0,0115
PMAIP1	5,52	4	2,88	0,0002	0,0113
DHRS2	3,33	0,18	8,9	0,0047	0,0107

A

GTTTGGCTGAGGTCCACAACTTAAAACAACATTCCAATATAGATTCTCATGATCCCTGAAGAAGTGT
GTCTGATGTGGCTAAACATCATCAAATGAGTAAGTCAACATAGTAAAAGAAAAGAACAGTTCTTTAT
CAGATTAAATGAGCGAAACAGCTAAATGTCAAGTGA`CAAAACATTG`GGACTGACTGTATAAAATGC

B

0	C/EBPbeta [T00581]	1	NF-1 [T00539]	2	ENKTF-1 [T00255]	3	GR-alpha [T00337]
4	TFII-I [T00824]	5	FOXP3 [T04280]	6	c-Myb [T00137]	7	PR B [T00696]
8	PR A [T01661]	9	STAT4 [T01577]	10	c-Ets-1 [T00112]	11	GR-beta [T01920]
12	NFI/CTF [T00094]	13	RBP-Jkappa [T01616]	14	XBP-1 [T00902]	15	RAR-beta:RXR-alpha [T05420]
16	AP-1 [T00029]	17	c-Jun [T00133]	18	TFIID [T00820]	19	STAT5A [T04683]
20	GATA-2 [T00308]	21	GATA-1 [T00306]	22	IRF-2 [T01491]	23	ATF3 [T01313]
24	GR [T05076]	25	C/EBPalpha [T00105]	26	NF-Y [T00150]	27	TBP [T00794]
28	HNF-3alpha [T02512]	29	PU.1 [T02068]	30	EBF [T05427]		

C

D

Figure 8.2 | Putative promoter region of HORAS5 and TBSs.
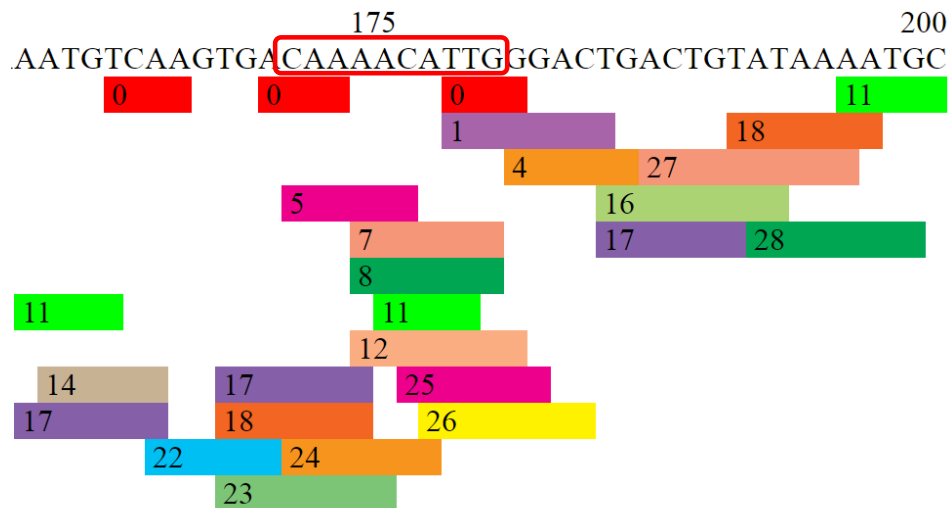**A.** Sequence of 200bp upstream *HORAS5* gene selected for in silico analysis of TBSs. **B.** List of TFs predicted to bind the 200bp upstream *HORAS5* gene. **C.** View of the TFs binding specific 10bp sequences within the 200bp selected. The region 170-180bp contains the highest number of TFBs. **D.** Zoom of the region with the highest number of predicted TBSs.

REFERENCES

Abal, M., Andreu, J. and Barasoain, I. (2003) 'Taxanes: Microtubule and Centrosome Targets, and Cell Cycle Dependent Mechanisms of Action', *Current Cancer Drug Targets*, 3(3), pp. 193–203.

Acharya, S. S. *et al.* (2017) 'Point-of-care ultrasonography (POCUS) in hemophilia A: a commentary on current status and its potential role for improving prophylaxis management in severe hemophilia A', *Therapeutic Advances in Hematology*, 8(4), pp. 153 –156.

Adlakha, Y. K. and Saini, N. (2011) 'MicroRNA-128 downregulates Bax and induces apoptosis in human embryonic kidney cells', *Cellular and Molecular Life Sciences*, 68(8), pp. 1415–1428.

Aggarwal, R. *et al.* (2018) 'Clinical and genomic characterization of treatment-emergent small-cell neuroendocrine prostate cancer: A multi-institutional prospective study', *Journal of Clinical Oncology*, 36(24), pp. 2492–2503.

Aird, J. *et al.* (2018) 'Carcinogenesis in prostate cancer: The role of long non-coding RNAs', *Non-coding RNA Research*. The Authors, 3(1), pp. 29–38.

Ali Zhang, Jonathan C. Zhao, Jung Kim, Ka-wing Fong, Y. A. Y. and Debabrata Chakravarti, Yin-Yuan Mo, J. Y. (2015) 'LncRNA HOTAIR Enhances the Androgen-Receptor-Mediated Transcriptional Program and Drives Castration-Resistant Prostate Cancer', *Cell Rep*, 13(1), pp. 209–221.

American Cancer Society (2016) *Hormone Therapy for Prostate Cancer*. Available at: https://www.cancer.org/cancer/prostate-cancer/treating/hormone-therapy.html.

Ammannagari, N. and George, S. (2014) 'Anti-Androgen Therapies for Prostate Cancer : A Focused Review', *Am J Hematol Oncol.*, 11(2), pp. 15–19.

An, Q., Zhou, L. and Xu, N. (2018) 'Long noncoding RNA FOXD2-AS1 accelerates the gemcitabine-resistance of bladder cancer by sponging miR-143', *Biomedicine and Pharmacotherapy*. Elsevier, 103(42), pp. 415–420.

Antonarakis, E. S. *et al.* (2014) 'AR-V7 and Resistance to Enzalutamide and Abiraterone in Prostate Cancer', *N Engl J Med*, 37(11), pp. 1028–1038.

Antonarakis, E. S. *et al*. (2020) 'Pembrolizumab for Treatment-Refractory Metastatic Castration-Resistant Prostate Cancer: Multicohort, Open-Label Phase II KEYNOTE-199 Study', *J Clin Oncol*, 38(5), pp. 395-405.

Antony, L. *et al.* (2014) 'Androgen Receptor (AR) Suppresses Normal Human Prostate Epithelial Cell Proliferation via AR/β-catenin/TCF-4 Complex Inhibition of c-MYC Transcription', *Prostate*, 74(11), pp. 1118–1131.

Aparicio, A. M. *et al.* (2013) 'Platinum-Based Chemotherapy for Variant Castrate-Resistant Prostate Cancer', *Clin Cancer Res*, 19(13), pp. 3621–3630.

Ayers, D. and Vandesompele, J. (2017) 'Influence of microRNAs and Long Non-Coding RNAs in Cancer Chemoresistance', *Genes,* 8(3), pp.1-34.

Barakat, D. J. *et al.* (2015) 'CCAAT/Enhancer binding protein β controls androgen-deprivation-induced senescence in prostate cancer cells', *Oncogene*, 34(48), pp. 5912–

22.

Bayoumi, A. S. *et al.* (2016) 'Crosstalk between Long Noncoding RNAs and MicroRNAs in Health and Disease', *International Journal of Molecular Sciences, 1*7(3), pp. 1-16.

Bedoya, D. J. and Mitsiades, N. (2012) 'Clinical appraisal of abiraterone in the treatment of metastatic prostatic cancer : patient considerations , novel opportunities , and future directions', *OncoTargets and Therapy*, pp. 9–18.

Beer, T. M. *et al.* (2014) 'Enzalutamide in metastatic prostate cancer patients before chemotherapy', *New England Journal of Medicine*, 371(5), pp. 424–433.

Beer, T. M. *et al.* (2017) 'Custirsen (OGX-011) combined with cabazitaxel and prednisone versus cabazitaxel and prednisone alone in patients with metastatic castration-resistant prostate cancer previously treated with docetaxel (AFFINITY): a randomised, open-label, international, ph', *The Lancet Oncology*, 18(11), pp. 1532–1542.

Beinse, G. *et al.* (2019) 'The NRF2 transcriptional target NQO1 has low mRNA levels in TP53-mutated endometrial carcinomas', *PLoS ONE*, 14(3), pp. 1–19.

Bellmunt, J. *et al.* (2017) 'Borealis-1: A randomized, first-line, placebo-controlled, phase II study evaluating apatorsen and chemotherapy for patients with advanced urothelial cancer', *Annals of Oncology*, 28(10), pp. 2481–2488.

Beltran, H. *et al.* (2014) 'Aggressive Variants of Castration Resistant Prostate Cancer', *Clin Cancer Res*, 20(11), pp. 2846–2850.

Beltran, H. *et al.* (2016) 'Divergent clonal evolution of castration resistant neuroendocrine prostate cancer', *Nat Med*, 22(3), pp. 298–305.

Bennett, H. L. *et al.* (2013) 'Does androgen-ablation therapy (AAT) associated autophagy have a pro-survival effect in LNCaP human prostate cancer cells?', *BJU International*, 111(4), pp. 672–682.

Berti, F. C. B. *et al.* (2019) 'From squamous intraepithelial lesions to cervical cancer: Circulating microRNAs as potential biomarkers in cervical carcinogenesis', *Biochimica et Biophysica Acta (BBA) - Reviews on Cancer*. Elsevier B.V, 1872(2), p. 188306.

Bida, O. *et al.* (2015) 'A novel mitosis-associated lncRNA, MA-linc1, is required for cell cycle progression and sensitizes cancer cells to Paclitaxel', *Oncotarget*, 6(29), pp. 27880–27890.

Block, M. *et al.* (2012) 'Inhibition of the AKT/mTOR and erbB pathways by gefitinib, perifosine and analogs of gonadotropin-releasing hormone I and II to overcome tamoxifen resistance in breast cancer cells', *International Journal of Oncology*, 41(5), pp. 1845–1854.

de Bono, J. S. *et al.* (2010) 'Prednisone plus cabazitaxel or mitoxantrone for metastatic castration-resistant prostate cancer progressing after docetaxel treatment: a randomized open-label trial', *Lancet*, 376(9747), pp. 1147–1154.

Boudny, V. and Nakano, S. (2002) 'Src tyrosine kinase augments taxotere-induced apoptosis through enhanced expression and phosphorylation of Bcl-2', *British Journal of Cancer*, 86, pp. 463–469.

Budman, D. R., Calabro, A. and Kreis, W. (2002) 'Synergistic and antagonistic combinations of drugs in human prostate cancer cell lines in vitro', *Anti-Cancer Drugs*, 13(10), pp. 1011–1016.

Carrieri, C. *et al.* (2015) 'Expression analysis of the long non-coding RNA antisense to Uchl1 (AS Uchl1) during dopaminergic cells ' differentiation in vitro and in neurochemical models of Parkinson ' s disease', *Frontiers in Cellular Neuroscience*, 9, pp. 1–11.

Castro, E. *et al.* (2019) 'Prorepair-B: A prospective cohort study of the impact of germline DNA repair mutations on the outcomes of patients with metastatic castration-resistant prostate cancer', *Journal of Clinical Oncology*, 37(6), pp. 490–503.

Cathcart, P. *et al.* (2015) 'Noncoding RNAs and the control of signalling via nuclear receptor regulation in health and disease', *Clinical Endocrinology & Metabolism*, 29(4), pp. 529–543.

Champa, D. *et al.* (2014) 'Obatoclax overcomes resistance to cell death in aggressive thyroid carcinomas by countering Bcl2a1 and Mcl1 overexpression', *Endocr Relat Cancer*, 21(5), pp. 755–767.

Chen, H. *et al.* (2018) 'Molecular profile of advanced thyroid carcinomas by next-generation sequencing: Characterizing tumors beyond diagnosis for targeted therapy', *Molecular Cancer Therapeutics*, 17(7), pp. 1575–1584.

Chen, J. *et al.* (2016) 'Long noncoding RNA CCAT1 acts as an oncogene and promotes chemoresistance in docetaxel-resistant lung adenocarcinoma cells', *Oncotarget*, 7(38), pp. 62474–62489.

Chen, M. *et al.* (2018) 'LncRNA MALAT1 promotes epithelial-to-mesenchymal transition of esophageal cancer through Ezh2-Notch1 signaling pathway', *Anti-Cancer Drugs*, 29(8), pp. 767–773.

Chen, W. *et al.* (2018) 'CCL20 triggered by chemotherapy hinders the therapeutic efficacy of breast cancer', *PLoS Biology*, 16(7), pp. 1–27.

Chen, X. *et al.* (2018) 'Long non-coding RNA GAS5 and ZFAS1 are prognostic markers involved in translation targeted by miR-940 in prostate cancer', *Oncotarget*, 9(1), pp. 1048–1062.

Chen, X. *et al.* (2019) 'Long noncoding RNA LBCs inhibits self-renewal and chemoresistance of bladder cancer stem cells through epigenetic silencing of SOX2', *Clinical Cancer Research,* 25(4), pp. 1389-1403.

Cheng, N. *et al.* (2015) 'Long non-coding RNA UCA1 induces non-T790M acquired resistance to EGFR-TKIs by activating the AKT/mTOR pathway in EGFR-mutant non-small cell lung cancer', *Oncotarget*, 6(27), pp. 23582–23593.

Chery, J. (2016) 'RNA therapeutics: RNAi and antisense mechanisms and clinical applications', *Postdoc J.*, 4(7), pp. 35–50.

Chi, K. N. *et al.* (2017) 'Custirsen in combination with docetaxel and prednisone for patients with metastatic castration-resistant prostate cancer (SYNERGY trial): a phase 3, multicentre, open-label, randomised trial', *The Lancet Oncology*. Elsevier Ltd, 18(4), pp.

473–485.

Churchill, C. D. M., Klobukowski, M. and Tuszynski, J. A. (2015) 'Elucidating the Mechanism of Action of the Clinically Approved Taxanes: A Comprehensive Comparison of Local and Allosteric Effects', *Chemical Biology and Drug Design*, 86, pp. 1253–1266.

Clark, B. and Blackshaw, S. (2014) 'Long non-coding RNA-dependent transcriptional regulation in neuronal development and disease', *Frontiers in Genetics*, 5, pp. 1–19.

Clermont, P.-L. *et al.* (2015) 'Polycomb-mediated silencing in neuroendocrine prostate cancer', *Clinical Epigenetics*, 7:40.

Corn, P. G. *et al.* (2019) 'Cabazitaxel plus carboplatin for the treatment of men with metastatic castration-resistant prostate cancers: a randomised, open-label, phase 1–2 trial', *The Lancet Oncology*. Elsevier Ltd, 20(10), pp. 1432–1443.

Crea, F., Watahiki, A., *et al.* (2014) 'Identification of a long non-coding RNA as a novel biomarker and potential therapeutic target for metastatic prostate cancer', *Oncotarget*, 5, pp. 764–774.

Crea, F., Clermont, P. L., *et al.* (2014) 'The non-coding transcriptome as a dynamic regulator of cancer metastasis', *Cancer and Metastasis Reviews*, 33, pp. 1–16.

Crea, F., Quagliata, L., *et al.* (2016) 'Integrated analysis of the prostate cancer small-nucleolar transcriptome reveals SNORA55 as a driver of prostate cancer progression', *Molecular Oncology*, 10(5), pp. 693–703.

Crea, F., Venalainen, E., *et al.* (2016) 'The role of epigenetics and long noncoding RNA MIAT in neuroendocrine prostate cancer', *Epigenomics*, 8(5), pp. 721–731.

Crea, F., Serrat, M. A. D. and Hurt, E. M. (2011) 'BMI1 Silencing Enhances Docetaxel Activity and Impairs Antioxidant Response in Prostate Cancer', *Int J Cancer*, 128(8), pp. 1946–1954.

Crick, F. (1970) 'Central dogma of molecular biology', *Nature*, 227.

Cui, Z. *et al.* (2013) 'The prostate cancer-up-regulated long noncoding RNA PlncRNA-1 modulates apoptosis and proliferation through reciprocal regulation of androgen receptor', *Urologic Oncology: Seminars and Original Investigations*, 31(7), pp. 1117–1123.

Das, V. *et al.* (2015) 'Role of tumor hypoxia in acquisition of resistance to microtubule-stabilizing drugs', *Biochimica et Biophysica Acta*, 1855(2), pp. 172–182.

Datta, S. *et al.* (2017) 'Paclitaxel resistance development is associated with biphasic changes in reactive oxygen species, mitochondrial membrane potential and autophagy with elevated energy production capacity in lung cancer cells: A chronological study', *Tumor Biology*, 39(2), pp. 1–14.

Deng, X. *et al.* (2019) 'Long noncoding RNA CCAL transferred from fibroblasts by exosomes promotes chemoresistance of colorectal cancer cells', *International Journal of Cancer*.

Denning, W. *et al.* (2013) 'Optimization of the transductional efficiency of lentiviral vectors: effect of sera and polycations.', *Mol Biotechnol*, 53(3), pp. 308–314.

Diéras, V. *et al.* (2013) 'Cabazitaxel in patients with advanced solid tumours: Results of a Phase i and pharmacokinetic study', *European Journal of Cancer*, 49(1), pp. 25–34.

Distelhorst, C. W. and Bootman, M. D. (2019) 'Creating a new cancer therapeutic agent by targeting the interaction between Bcl-2 and IP3 receptors', *Cold Spring Harbor Perspectives in Biology*, 11(9).

Duffy, A. G. *et al.* (2016) 'Modulation of tumor eIF4E by antisense inhibition: A phase I/II translational clinical trial of ISIS 183750—an antisense oligonucleotide against eIF4E—in combination with irinotecan in solid tumors and irinotecan-refractory colorectal cancer', *International Journal of Cancer*, 139(7), pp. 1648–1657.

Elizabeth Newcomb, B. T. Y. H. T. C. T. M. (1993) 'Tumour-suppressor activity of H19 RNA', *Nature*, 365, pp. 764–767.

Fan Liancheng, Wang Yanqing, Chi Chenfei, Pan Jiahua, Shangguan Xun, Xin Zhixiang, Hu Jianian, Zhou Lixin, Dong Baijun, X. W. (2017) 'Chromogranin A and neurone-specific enolase variations during the first three months of abiraterone therapy predict outcomes in patients with metastatic castration-resistant prostate cancer', *BJU Int,* 120(2), pp.226-232.

Fitzgeralda, L. A. *et al.* (2008) 'Putative Gene Promoter Sequences in the Chlorella viruses', *Virology*, 380(2), pp. 388–393.

Fléchon, A. *et al.* (2011) 'Phase II study of carboplatin and etoposide in patients with anaplastic progressive metastatic castration-resistant prostate cancer (mCRPC) with or without neuroendocrine differentiation: Results of the French Genito-Urinary Tumor Group (GETUG) P01 trial', *Annals of Oncology*, 22, pp. 2476–2481.

Fukuda, Minoru *et al.* (1999) 'Phase I study of Irinotecan combined with carboplatin in previously untreated solid cancers', *Clin Cancer Res.*, 5(12), pp. 3963–3969.

Fukuhara, S. *et al.* (2015) 'Functional role of DNA mismatch repair gene PMS2 in prostate cancer cells', *Oncotarget*, 6(18), pp. 16341–16351.

Galletti, G. *et al.* (2017) 'Mechanisms of resistance to systemic therapy in metastatic castration-resistant prostate cancer', *Cancer Treatment Reviews*, 57, pp. 16–27.

Ganansia-Leymarie, V. *et al.* (2003) 'Signal transduction pathways of taxanes-induced apoptosis.', *Current Medicinal Chemistry - Anti-Cancer Agents*, 3(4), pp. 291–306.

Gibbons, J. A. *et al.* (2015) 'Clinical Pharmacokinetic Studies of Enzalutamide', *Clinical Pharmacokinetics*, 54(10), pp. 1043–1055.

Hager, S., Ackermann, CJ., Joerger, M., Gillessen, S., Omlin A., (2016) 'Antitumour activity of platinum compounds in advanced prostate cancer – a systematic literature review', *Annals of Oncology Advance*, 27(6), pp. 975-984.

Gonzalez, I. *et al.* (2015) 'A lncRNA regulates alternative splicing via establishment of a splicing-specific chromatin signature.', *Nature structural & molecular biology*, 22, pp. 370–379.

Gordon, M. A. *et al.* (2019) 'The long non-coding RNA MALAT1 promotes ovarian cancer progression by regulating RBFOX2-mediated alternative splicing', *Molecular Carcinogenesis*, 58(2), pp. 196–205.

Gradishar, W. J. (2006) 'Albumin-bound paclitaxel : a next-generation taxane', *Expert Opin Pharmacother*, 7(8), pp. 1041-53.

Guo, C. *et al.* (2017) 'Targeting Androgen Receptor versus Targeting Androgens to suppress Castration Resistant Prostate Cancer', *Cancer Letters*, 397, pp.133-143.

Guo, Y. and Jamison, D. C. (2005) 'The distribution of SNPs in human gene regulatory regions.', *BMC genomics*, 6:140.

Gupta, R. a *et al.* (2010) 'Long noncoding RNA HOTAIR reprograms chromatin state to promote cancer metastasis', *Nature*, 464(7291), pp. 1071–1076.

Han, S. *et al.* (2019) 'Downregulation of long noncoding RNA CRNDE suppresses drug resistance of liver cancer cells by increasing microRNA-33a expression and decreasing HMGA2 expression', *Cell Cycle*. Taylor & Francis, 18(19), pp. 2524–2537.

Haq, R. *et al.* (2013) 'BCL2A1 is a lineage-specific antiapoptotic melanoma oncogene that confers resistance to BRAF inhibition ', *Proceedings of the National Academy of Sciences*, 110(11), pp. 4321–4326.

Harland, S. *et al.* (2013) 'Effect of abiraterone acetate treatment on the quality of life of patients with metastatic castration-resistant prostate cancer after failure of docetaxel chemotherapy', *European Journal of Cancer*. Elsevier Ltd, 49(17), pp. 3648–3657.

Hattori, Y. *et al.* (2017) 'Evaluation of Small Interfering RNA Delivery into Cells by Reverse Transfection in Suspension with Cationic Liposomes', *Pharmacology & Pharmacy*, 08(5), pp. 129–139.

He, J. *et al.* (2019) 'Long non-coding RNA Linc00518 promotes paclitaxel resistance of the human prostate cancer by sequestering miR-216b-5p', *Biology of the Cell*, 111(2), pp. 39–50.

Herbst, R. S. and Khuri, F. R. (2003) 'Mode of action of docetaxel - A basis for combination with novel anticancer agents', *Cancer Treatment Reviews*, 29, pp. 407–415.

Herreros-Villanueva, M. *et al.* (2019) 'Plasma MicroRNA Signature Validation for Early Detection of Colorectal Cancer', *Clinical and translational gastroenterology*, 10(1), p. e00003.

Higgins, C. F. (2007) 'Multiple molecular mechanisms for multidrug resistance transporters', *Nature*, 446(7137), pp. 749–757.

Hsu, C. *et al.* (2017) 'Characterization of a novel androgen receptor (AR) coregulator RIPK1 and related chemicals that suppress AR-mediated prostate cancer growth via peptide and chemical screening', *Oncotarget*, 8(41), pp. 69508-69519.

Hsu, J.-L. *et al.* (2012) 'Pim-1 knockdown potentiates paclitaxel-induced apoptosis in human hormone-refractory prostate cancers through inhibition of NHEJ DNA repair', *Cancer Lett*, 319(2), pp. 214–222.

Huang, W. *et al.* (2019) 'Long noncoding RNA PCAT6 inhibits colon cancer cell apoptosis by regulating anti-apoptotic protein ARC expression via EZH2', *Cell Cycle*, 18(1), pp. 69–83.

Hussain, M. *et al.* (2018) 'Enzalutamide in Men with Nonmetastatic, Castration-Resistant

Prostate Cancer', *The new england journal of medicine*, 378(26), pp. 2465–2474.

Hwang, J. J. *et al.* (2012) 'A novel histone deacetylase inhibitor, CG200745, potentiates anticancer effect of docetaxel in prostate cancer via decreasing Mcl-1 and Bcl- XL', *Investigational New Drugs*, 30(4), pp. 1434–1442.

Iida, S., Shimada, J. and Sakagami, H. (2013) 'Cytotoxicity induced by docetaxel in human oral squamous cell carcinoma cell lines', *In vivo*, 27(3), pp. 321–332.

Ingenito, F. *et al.* (2019) 'The Role of Exo-miRNAs in Cancer: A Focus on Therapeutic and Diagnostic Applications', *International Journal of Molecular Sciences*, 20(19), p. 4687.

Jaiyesimi, I. A. *et al.* (1995) 'Use of tamoxifen for breast cancer: Twenty-eight years later', *Journal of Clinical Oncology*, 13(2), pp. 513–529.

James, N. D. *et al.* (2016) 'Addition of docetaxel, zoledronic acid, or both to first-line long-term hormone therapy in prostate cancer (STAMPEDE): Survival results from an adaptive, multiarm, multistage, platform randomised controlled trial', *The Lancet*, 387(10024), pp. 1163–1177.

Jenal, M. *et al.* (2010) 'The anti-apoptotic gene BCL2A1 is a novel transcriptional target of PU.1', *Leukemia*, 24(5), pp. 1073–1076.

Ji, P. *et al.* (2003) 'MALAT-1, a novel noncoding RNA, and thymosin β4 predict metastasis and survival in early-stage non-small cell lung cancer', *Oncogene*, 22(39), pp. 8031–8041.

Jia, J. *et al.* (2019) 'KLF5 downregulation desensitizes castration-resistant prostate cancer cells to docetaxel by increasing BECN1 expression and inducing cell autophagy', *Theranostics*, 9(19), pp. 5464–5477.

Jiang, H. *et al.* (2019) 'Electrochemical Monitoring of Paclitaxel-Induced ROS Release from Mitochondria inside Single Cells', *Small*, 15(48), p. 1901787.

Jiang, Q. *et al.* (2016) 'Long non-coding RNA-MIAT promotes neurovascular remodeling in the eye and brain', *Oncotarget*, 7(31), pp. 49688-49698.

Jo, A. *et al.* (2014) 'The versatile functions of Sox9 in development, stem cells, and human diseases', *Genes and Diseases*. Elsevier Ltd, 1(2), pp. 149–161.

Kern, W. *et al.* (2001) 'Carboplatin pharmacokinetics in patients receiving carboplatin and paclitaxel/docetaxel for advanced lung cancers: Impact of age and renal function on area under the curve', *Journal of Cancer Research and Clinical Oncology*, 127(1), pp. 64–68.

Khurana, N. and Sikka, S. C. (2019) 'Interplay Between SOX9, Wnt/β-Catenin and Androgen Receptor Signaling in Castration-Resistant Prostate Cancer', *International journal of molecular sciences*, 20(9), p. E2066.

Kim, J. *et al.* (2017) 'FOXA1 inhibits prostate cancer neuroendocrine differentiation', *Oncogene*, 36(28), pp. 4072-4080.

Kim, J. *et al.* (2018) 'Long non-coding RNA MALAT1 suppresses breast cancer metastasis', *Nat Genet*, 50(12), pp. 1705–1715.

Kim, Y. *et al.* (2017) 'Downregulation of androgen receptors by NaAsO 2 via inhibition of AKT-NF- κ B and HSP90 in castration resistant prostate cancer', *Prostate*, 77(10), pp.

1128-1136.

Koh, H. *et al.* (2017) 'MicroRNA-128 suppresses paclitaxel-resistant lung cancer by inhibiting MUC1-C and BMI-1 in cancer stem cells', *Oncotarget*, 8(66), pp. 110540–110551.

Kong, J. *et al.* (2016) 'Long non-coding RNA LINC01133 inhibits epithelial–mesenchymal transition and metastasis in colorectal cancer by interacting with SRSF6', *Cancer Letters*. Elsevier Ireland Ltd, 380(2), pp. 476–484.

Kong, Y. *et al.* (2019) 'Long Noncoding RNA: Genomics and Relevance to Physiology', *Comprehensive Physiology*, 9(3), pp. 933–946.

Kosaka, T. *et al.* (2017) 'Reactive oxygen species induction by cabazitaxel through inhibiting Sestrin-3 in castration resistant prostate cancer', *Oncotarget*, 8, pp. 87675–87683.

Kotake, Y. *et al.* (2017) 'Long noncoding RNA PANDA positively regulates proliferation of osteosarcoma cells', *Anticancer Research*, 37(1), pp. 81–86..

Kumar, A. *et al.* (2016) 'Substantial inter-individual and limited intra-individual genomic diversity among tumors from men with metastatic prostate cancer', *Nature Medicine*, 22(4), pp. 369–378.

Lai, J. *et al.* (2017) 'A microsatellite repeat in PCA3 long non-coding RNA is associated with prostate cancer risk and aggressiveness', *Scientific Reports*, 7(1), pp. 1–14.

Lavalou, P. *et al.* (2019) 'Strategies for genetic inactivation of long noncoding RNAs in zebrafish', *Rna*, 25(8), pp. 897–904.

Lee, A. R. *et al.* (2017) 'Alternative RNA splicing of the MEAF6 gene facilitates neuroendocrine prostate cancer progression', *Oncotarget*, 8(17), pp. 27966–27975.

Li, L. *et al.* (2015) 'Infiltrating mast cells enhance prostate cancer invasion via altering LncRNA-HOTAIR / PRC2-androgen receptor (AR) -MMP9 signals and increased stem / progenitor cell population', *Oncotarget*, 6(16), pp. 14179-14190.

Li, Ling *et al.* (2017) 'Long noncoding RNA SFTA1P promoted apoptosis and increased cisplatin chemosensitivity via regulating the hnRNP-U-GADD45A axis in lung squamous cell carcinoma', *Oncotarget*, 8(57), pp. 97476–97489.

Li, Li-juan *et al.* (2017) 'The effects of the long non-coding RNA MALAT-1 regulated autophagy-related signaling pathway on chemotherapy resistance in diffuse large B-cell lymphoma', *Biomedicine et Pharmacotherapy*, 89, pp. 939–948.

Li, W. *et al.* (2018) 'Long noncoding RNA BDNF-AS is associated with clinical outcomes and has functional role in human prostate cancer', *Biomedicine and Pharmacotherapy*, 102, pp. 1105–1110.

Li, W. *et al.* (2019) 'LncRNA SNHG1 contributes to sorafenib resistance by activating the Akt pathway and is positively regulated by miR-21 in hepatocellular carcinoma cells', *Journal of Experimental and Clinical Cancer Research*. Journal of Experimental & Clinical Cancer Research, 38(1), pp. 1–13.

Li, X. *et al.* (2016) 'Long non-coding RNA UCA1 enhances tamoxifen resistance in breast

cancer cells through a miR-18a-HIF1α feedback regulatory loop', *Tumor Biology*. Tumor Biology, 37(11), pp. 14733–14743.

Li, Y. *et al.* (2018) 'Long noncoding RNA SChLAP1 accelerates the proliferation and metastasis of prostate cancer via targeting miR-198 and promoting the MAPK1 pathway', *Oncology Research*, 26(1), pp. 131–143.

Li, Z. *et al.* (2014) 'Long non-coding RNA UCA1 promotes glycolysis by upregulating hexokinase 2 through the mTOR-STAT3/microRNA143 pathway', *Cancer Science*, 105(8), pp. 951–955.

Li, Z. *et al.* (2017) 'Long non-coding RNA H19 promotes the proliferation and invasion of breast cancer through upregulating DNMT1 expression by sponging miR-152', *JBiochem Mol Toxicol,* 31(9).

Liang, X. H. *et al.* (2017) 'RNase H1-Dependent Antisense Oligonucleotides Are Robustly Active in Directing RNA Cleavage in Both the Cytoplasm and the Nucleus', *Molecular Therapy*. Elsevier Ltd., 25(9), pp. 2075–2092.

Lin, D. *et al.* (2014) 'Identification of DEK as a potential therapeutic target for neuroendocrine prostate cancer', *Oncotarget*, 6(3), pp. 1806-1820.

Lin, T. H. *et al.* (2013) 'Differential androgen deprivation therapies with anti-androgens casodex/bicalutamide or MDV3100/Enzalutamide versus anti-androgen receptor ASC-J9® lead to promotion versus suppression of prostate cancer metastasis', *Journal of Biological Chemistry*, 288(27), pp. 19359–19369.

Lin, Y.-C. *et al.* (2017) 'MAOA-a novel decision maker of apoptosis and autophagy in hormone refractory neuroendocrine prostate cancer cells', *Scientific Reports*, 7, p. 46338.

Ling, Z. *et al.* (2017) 'Involvement of aberrantly activated HOTAIR/EZH2/miR-193a feedback loop in progression of prostate cancer', *Journal of Experimental and Clinical Cancer Research*. Journal of Experimental & Clinical Cancer Research, 36(1), pp. 1–15.

Lionnard, L. *et al.* (2019) 'TRIM17 and TRIM28 antagonistically regulate the ubiquitination and anti-apoptotic activity of BCL2A1', *Cell Death and Differentiation*, 26(5), pp. 902–917.

Lipianskaya, J. *et al.* (2014) 'Androgen - deprivation therapy - induced aggressive prostate cancer with neuroendocrine differentiation', *Asian Journal of Andrology*, 16(4), pp. 541–544.

Liu, H. *et al.* (2017) 'Long noncoding RNA TUG1 is a diagnostic factor in lung adenocarcinoma and suppresses apoptosis via epigenetic silencing of BAX', *Oncotarget*, 8(60), pp. 101899–101910.

Liu, J. *et al.* (2019) 'Ambra1 induces autophagy and desensitizes human prostate cancer cells to cisplatin', *Bioscience Reports*, 39(8), p. BSR20170770.

Liu, T. *et al.* (2019) 'Exosome-transmitted miR-128-3p increase chemosensitivity of oxaliplatin-resistant colorectal cancer', *Molecular Cancer*. Molecular Cancer, 18(1), pp. 1–17.

Liu, W. *et al.* (2017) 'Long non - coding RNA MALAT1 contributes to cell apoptosis by

sponging miR - 124 in Parkinson disease', *Cell & Bioscience*, 7:19.

Lombard, A. P. *et al.* (2017) 'ABCB1 mediates cabazitaxel-docetaxel cross-resistance in advanced prostate cancer', *Mol Cancer Ther.*, 16(10), pp. 2257–2266.

Lombard, A. P. *et al.* (2019) 'Overexpressed ABCB1 Induces Olaparib-Taxane Cross-Resistance in Advanced Prostate Cancer', *Translational Oncology*. The Authors, 12(7), pp. 871–878.

Lorch, J. H. *et al.* (2011) 'Long term results of TAX324, a randomized phase III trial of sequential therapy with TPF versus PF in locally advanced squamous cell cancer of the head and neck', *The Lancet.Oncology*, 12(2), pp. 153–159.

Lu, N. Z. *et al.* (2006) 'The Pharmacology and Classification of the Nuclear Receptor Superfamily: Glucocorticoid, Mineralocorticoid, Progesterone, and Androgen Receptors', *Journal of Biological Chemistry*, 58(4), pp. 782–797.

Luo, J. *et al.* (2019) 'LncRNA-p21 alters the antiandrogen enzalutamide-induced prostate cancer neuroendocrine differentiation via modulating the EZH2/STAT3 signaling', *Nature Communications*. Springer US, 10(1), pp. 1–17.

Lyakhovich, A. and Lleonart, M. E. (2016) 'Bypassing Mechanisms of Mitochondria-Mediated Cancer Stem Cells Resistance to Chemo- and Radiotherapy', *Oxidative Medicine and Cellular Longevity*. Hindawi Publishing Corporation, 2016, pp. 1–10.

Machioka, K. *et al.* (2018) 'Establishment and characterization of two cabazitaxel-resistant prostate cancer cell lines', *Oncotarget*, 9(22), pp. 16185–16196.

Mahmoodi Chalbatani, G. *et al.* (2019) 'Small interfering RNAs (siRNAs) in cancer therapy: a nano-based approach', *International journal of nanomedicine*, 14, pp. 3111–3128.

Majidinia, M. *et al.* (2016) 'The roles of non-coding RNAs in Parkinson' s disease', *Mol Biol Rep.* , 43(11), pp. 1193-1204.

Martin, S. K. *et al.* (2015) 'N-terminal targeting of androgen receptor variant enhances response of castration resistant prostate cancer to taxane chemotherapy', *Molecular Oncology*, 9(3), pp. 628–639.

Matsunaga, T. *et al.* (2016) 'Roles of aldo-keto reductases 1B10 and 1C3 and ATP-binding cassette transporter in docetaxel tolerance', *Free Radical Research*, 50(12), pp. 1296–1308.

Maurano, M. T. *et al.* (2012) 'Systematic Localization of Common Disease-Associated Variation in Regulatory DNA', *Science*, 337(6099).

McPherson, R. A. C., Galettis, P. T. and de Souza, P. L. (2009) 'Enhancement of the activity of phenoxodiol by cisplatin in prostate cancer cells.', *British journal of cancer*, 100(4), pp. 649–55.

Mercer, T. R. and Mattick, J. S. (2013) 'Structure and function of long noncoding RNAs in epigenetic regulation', *Nature Structural & Molecular Biology*, 20(3), pp. 300–307.

Miao, H. *et al.* (2019) 'A long noncoding RNA distributed in both nucleus and cytoplasm operates in the PYCARD-regulated apoptosis by coordinating the epigenetic and

translational regulation', *PLOS Genetics*, 15(5), p. e1008144.

Misawa, A. *et al.* (2017) 'Androgen-induced lncRNA POTEF-AS1 regulates apoptosis-related pathway to facilitate cell survival in prostate cancer cells', *Cancer Science*, 108(3), pp. 373–379.

Mizokami, A. *et al.* (2017) 'Therapies for castration-resistant prostate cancer in a new era: The indication of vintage hormonal therapy, chemotherapy and the new medicines', *International Journal of Urology*, 24(8) pp. 566-572.

Mohanty, V., Badve, S. and Janga, S. C. (2014) 'Role of lncRNAs in health and disease-size and shape matter', *BRIEFINGS IN FUNCTIONAL GENOMICS*.

Montero, A. *et al.* (2005) 'Docetaxel for treatment of solid tumours: a systematic review of clinical data', *The Lancet. Oncology*, 6(4), pp. 229–239.

Mukhtar, E. *et al.* (2016) 'Fisetin enhances chemotherapeutic effect of cabazitaxel against human prostate cancer cells', *Mol Cancer Ther*, 15(12), pp. 2863–2874.

Muro, K. *et al.* (2016) 'Subgroup analysis of East Asians in RAINBOW: A phase 3 trial of ramucirumab plus paclitaxel for advanced gastric cancer', *Journal of Gastroenterology and Hepatology*, 31(3), pp. 581–589.

Nabavi, N. *et al.* (2017) 'miR-100-5p inhibition induces apoptosis in dormant prostate cancer cells and prevents the emergence of castration-resistant prostate cancer', *Scientific Reports*, 7(4079), pp. 1-10.

Narita, S. *et al.* (2012) 'Outcome, clinical prognostic factors and genetic predictors of adverse reactions of intermittent combination chemotherapy with docetaxel, estramustine phosphate and carboplatin for castration-resistant prostate cancer', *International Journal of Clinical Oncology*, 17(3), pp. 204–211.

National Cancer Institute (2014) *Hormone Therapy for Prostate Cancer*. Available at: https://www.cancer.gov/types/prostate/prostate-hormone-therapy-fact-sheet.

Needleman, D. J. *et al.* (2005) 'Radial compression of microtubules and the mechanism of action of taxol and associated proteins', *Biophysical Journal*, 89(5), pp. 3410–3423.

Němcová-Fürstová, V. *et al.* (2016) 'Characterization of acquired paclitaxel resistance of breast cancer cells and involvement of ABC transporters', *Toxicology and Applied Pharmacology*, 310, pp. 215–228.

Nikolaou, M. *et al.* (2018) 'The challenge of drug resistance in cancer treatment: a current overview', *Clinical and Experimental Metastasis*, 35(4), pp. 309–318.

Nouri, M. *et al.* (2017) 'Therapy-induced developmental reprogramming of prostate cancer cells and acquired therapy resistance', *Oncotarget*, 8(12), pp. 18949–18967.

Ojima, I. *et al.* (1999) 'A common pharmacophore for cytotoxic natural products that stabilize microtubules.', *Proceedings of the National Academy of Sciences of the United States of America*, 96, pp. 4256–4261.

Ozcan, G. *et al.* (2015) 'Preclinical and clinical development of siRNA-based therapeutics', *Adv Drug Deliv Rev.*, 87, pp. 108–119.

Pan, B. *et al.* (2014) 'HMGB1-mediated autophagy promotes docetaxel resistance in

human lung adenocarcinoma', *Molecular Cancer*, 13, pp. 165–182.

Pan, Y. *et al.* (2017) 'Long noncoding RNA ROR regulates chemoresistance in docetaxel-resistant lung adenocarcinoma cells via epithelial mesenchymal transition pathway', *Oncotarget*, 8(20), pp. 33144–33158.

Panda, S. *et al.* (2018) 'Noncoding RNA Ginir functions as an oncogene by associating with centrosomal proteins', *PLoS biology*, 16(10), p. e2004204.

Parolia, A. *et al.* (2015) 'The long non-coding RNA PCGEM1 is regulated by androgen receptor activity in vivo', *Molecular Cancer*, 14:46.

Parolia, A. *et al.* (2019) 'The long noncoding RNA HORAS5 mediates castration-resistant prostate cancer survival by activating the androgen receptor transcriptional program', *Molecular Oncology*, 13(5), pp. 1121–1136.

Peng, X. *et al.* (2014) 'Autophagy promotes paclitaxel resistance of cervical cancer cells: involvement of Warburg effect activated hypoxia-induced factor 1-α-mediated signaling.', *Cell death & disease*, 5, pp. 1367–1378.

Pennisi, E. (2012) 'ENCODE Project Writes Eulogy for Junk DNA', *Science*, 337(6099), pp. 1159–1161.

Perla Pucci, Wallace Yuen, Erik Venalainen, David Roig Carles, Yuzhuo Wang, F. C. (2019) 'Long non-coding RNAs and cancer cells' drug resistance: an unexpected connection. (Accepted).', in *THE CHEMICAL BIOLOGY OF LONG NONCODING RNAs*. Springer.

Petrioli, R. *et al.* (2003) 'Weekly low-dose docetaxel in advanced hormone-resistant prostate cancer patients previously exposed to chemotherapy.', *Oncology*, 64, pp. 300–305.

Pezaro, C., Woo, H. H. and Davis, I. D. (2014) 'Prostate cancer: Measuring PSA', *Internal Medicine Journal*, 44(5), pp. 433–440.

Pignata, S. *et al.* (2014) 'Carboplatin plus paclitaxel once a week versus every 3 weeks in patients with advanced ovarian cancer (MITO-7): A randomised, multicentre, open-label, phase 3 trial', *The Lancet Oncology*, 15(4), pp. 396–405.

Pilling, A. B. and Hwang, C. (2019) 'Targeting prosurvival BCL2 signaling through Akt blockade sensitizes castration-resistant prostate cancer cells to enzalutamide', *Prostate*, 79(11), pp. 1347–1359.

Poliseno, L. *et al.* (2010) 'A coding-independent function of gene and pseudogene mRNAs regulates tumour biology', *Nature*, 465(7301), pp. 1033–1038.

Poller, W. *et al.* (2017) 'Non-coding RNAs in cardiovascular diseases : diagnostic and therapeutic perspectives', *European Heart Journal*, 39(29), pp. 2704–2716.

Pomerantz MM, Spisák S, Jia L, Cronin AM, Csabai I, Ledet E, Sartor AO, Rainville I, O'Connor EP, H. Z. *et al.* (2017) 'The association between germline BRCA2 variants and sensitivity to platinum-based chemotherapy among men with metastatic prostate cancer', *Cancer*, 123(18), pp. 3532–3539.

Ponjavic, J., Ponting, C. P. and Lunter, G. (2007) 'Functionality or transcriptional noise? Evidence for selection within long noncoding RNAs', *Genome Research*, 17(5), pp. 556–

565.

Poruchynsky, M. S. *et al.* (2015) 'Microtubule-targeting agents augment the toxicity of DNA-damaging agents by disrupting intracellular trafficking of DNA repair proteins', *Proceedings of the National Academy of Sciences*, 112, pp. 1571–1576.

Pratt, A. J. and MacRae, I. J. (2009) 'The RNA-induced silencing complex: A versatile gene-silencing machine', *Journal of Biological Chemistry*, 284(27), pp. 17897–17901.

Pucci, P. *et al.* (2018) 'Hypoxia and Noncoding RNAs in Taxane Resistance', *Trends in Pharmacological Sciences*, 39(8), pp. 695–709.

Qi, H. *et al.* (2018) 'Long noncoding RNA SNHG7 accelerates prostate cancer proliferation and cycle progression through cyclin D1 by sponging miR-503', *Biomedicine and Pharmacotherapy*. Elsevier, 102(1), pp. 326–332.

Qinyu Sun, Qinyu Hao, K. V. P. (2018) 'Nuclear long noncoding RNAs: key regulators of gene expression', *Trends Genet*, 34(2), pp. 142–157.

Quoix, E. *et al.* (2011) 'Carboplatin and weekly paclitaxel doublet chemotherapy compared with monotherapy in elderly patients with advanced non-small-cell lung cancer: IFCT-0501 randomised, phase 3 trial', *The Lancet*, 378, pp. 1079–1088.

Qureshi, I. and Mehler, M. (2010) 'The Emerging Role of Epigenetics in Stroke', *Arch Neurol*, 67(12), pp. 1435–1441.

Rapicavoli, N. A., Poth, E. M. and Blackshaw, S. (2010) 'The long noncoding RNA RNCR2 directs mouse retinal cell specification', *BMC Developmental Biology*, 10:49.

Regan, M. M. *et al.* (2010) 'Efficacy of carboplatin – taxane combinations in the management of castration-resistant prostate cancer : a pooled analysis of seven prospective clinical trials', *Annals of Oncology*, 21(2), pp. 312–318.

Ren, S. *et al.* (2013) 'Long noncoding RNA MALAT-1 is a new potential therapeutic target for castration resistant prostate cancer', *Journal of Urology*, 190(6), pp. 2278–2287.

Ríos-Colón, L. *et al.* (2017) 'Targeting the stress oncoprotein LEDGF/p75 to sensitize chemoresistant prostate cancer cells to taxanes', *Oncotarget*, 8(15), pp. 24915–24931.

Rong, Y. P. *et al.* (2009) 'The BH4 domain of Bcl-2 inhibits ER calcium release and apoptosis by binding the regulatory and coupling domain of the IP3 receptor', *Proceedings of the National Academy of Sciences of the United States of America*, 106(34), pp. 14397–14402.

Rosenberg, J. E. *et al.* (2007) 'Activity of second-line chemotherapy in docetaxel-refractory hormone-refractory prostate cancer patients: Randomized phase 2 study of ixabepilone or mitoxantrone and prednisone', *Cancer*, 110(3), pp. 556–563.

Ryan, C. J. *et al.* (2013) 'Abiraterone in Metastatic Prostate Cancer without Previous Chemotherapy', *The new england journal of medicine*, 368(2), pp. 138–148.

Ryan, C. J. *et al.* (2015) 'Abiraterone acetate plus prednisone versus placebo plus prednisone in chemotherapy-naive men with metastatic castration-resistant prostate cancer (COU-AA-302): fi nal overall survival analysis of a randomised , double-blind , placebo-controlled phase 3', *Lancet Oncol*, 2045(14), pp. 1–9.

Rybak, A. P., Bristow, R. G. and Kapoor, A. (2014) 'Prostate cancer stem cells: deciphering the origins and pathways involved in prostate tumorigenesis and aggression', *Oncotarget*, 6(4), pp. 1900-1919.

Sarkadi, B. *et al.* (2006) 'Human multidrug resistance ABCB and ABCG transporters: Participation in a chemoimmunity defense system', *Physiological Reviews*, 86(4), pp. 1179–1236.

Scher, H. *et al.* (2012) 'Increased Survival with Enzalutamide in Prostate Cancer after Chemotherapy', *The new england journal of medicine*, 367(13), pp. 1187–1197.

Schmitt, A. M. and Chang, H. Y. (2016) 'Long Noncoding RNAs in Cancer Pathways', *Cancer Cell*, 29(4), pp. 452–463.

Schroder, F. H. (2008) 'Progress in Understanding Androgen-Independent Prostate Cancer (AIPC): A Review of Potential Endocrine-Mediated Mechanisms', *European Urology*, 53(6), pp. 1129–1137.

Sedelaar, J. P. M. and Isaacs, J. T. (2009) 'Tissue culture media supplemented with 10% fetal calf serum contains a castrate level of testosterone', *Prostate*, 69(16), pp. 1724–1729.

Sekino, Y. *et al.* (2019) 'TUBB3 reverses resistance to docetaxel and cabazitaxel in prostate cancer', *International Journal of Molecular Sciences*, 20(16), p. e3936.

Shan, Y. *et al.* (2018) 'LncRNA SNHG7 sponges MIR-216b to promote proliferation and liver metastasis of colorectal cancer through upregulating GALNT1', *Cell Death and Disease*. Springer US, 9(7), p. 722.

Shen, M. and Abate-Shen, C. (2010) 'Molecular genetics of prostate cancer: new prospects for old challenges', *Genes & development*, 24 (18), pp. 1967–2000.

Shen, X. and Corey, D. R. (2018) 'Chemistry, mechanism and clinical status of antisense oligonucleotides and duplex RNAs', *Nucleic Acids Research*. Oxford University Press, 46(4), pp. 1584–1600.

Shiota, M. *et al.* (2013) 'Interaction between docetaxel resistance and castration resistance in prostate cancer: Implications of Twist1, YB-1, and androgen receptor', *Prostate*, 73(12), pp. 1336–1344.

Shtivelman, E., Beer, T. M. and Evans, C. P. (2014) 'Molecular pathways and targets in prostate cancer', *Oncotarget*, 5(17), pp. 7217–7259.

Sissung, T. M. *et al.* (2014) 'Genetic variation : effect on prostate cancer', *Biochim Biophys Acta*, 1846(2), pp. 446–456.

Smiyun, G., Azarenko, O., Miller, H., Rifkind, A., Lapointe, N. E., *et al.* (2017) 'β III - tubulin enhances efficacy of cabazitaxel as compared with docetaxel', *Cancer Chemotherapy and Pharmacology*, 80(1), pp. 151–164.

Smolle, M. A. *et al.* (2017) 'Current Insights into Long Non-Coding RNAs (LncRNAs) in Prostate Cancer', *International Journal of Molecular Sciences*, 18(2), p. e473.

Somaiah, N. *et al.* (2019) 'First-in-Class, First-in-Human Study Evaluating LV305, a Dendritic-Cell Tropic Lentiviral Vector, in Sarcoma and Other Solid Tumors Expressing

NY-ESO-1', *Clinical Cancer Research*, 25(19), pp. 5808-5817.

Song, J. *et al.* (2019) 'Long noncoding RNA SNHG12 promotes cell proliferation and activates Wnt/β-catenin signaling in prostate cancer through sponging microRNA-195', *Journal of Cellular Biochemistry*, 120(8), pp. 13066–13075.

Song, W. *et al.* (2016) 'Immunohistochemical staining of ERG and SOX9 as potential biomarkers of docetaxel response in patients with metastatic castration-resistant prostate cancer', *Oncotarget*, 7(50), pp. 83735–83743. doi: 10.18632/oncotarget.13407.

Stice, J. P. *et al.* (2017) 'CDK4 / 6 Therapeutic Intervention and Viable Alternative to Taxanes in CRPC .', *Mol Cancer Res.*, pp. 660–669.

Stinchcombe, T. E. (2007) 'Nanoparticle albumin-bound paclitaxel: a novel Cremphor-EL -free formulation of paclitaxel', *Nanomedicine*, 2(4), pp. 415–423.

Su, W. *et al.* (2017) 'Long noncoding RNA ZEB1-AS1 epigenetically regulates the expressions of ZEB1 and downstream molecules in prostate cancer', *Molecular Cancer*. Molecular Cancer, 16(1), pp. 1–10.

Sun, L. *et al.* (2018) 'Serum and exosome long non coding RNAs as potential biomarkers for hepatocellular carcinoma', *Journal of Cancer*, 9(15), pp. 2631–2639.

Sun, X. and Wong, D. (2016) 'Long non-coding RNA-mediated regulation of glucose homeostasis and diabetes', *Am J Cardiovasc Dis*, 6(2), pp. 17–25.

SunnyHanna, S. (2018) 'HOTAIR-mediated reciprocal regulation of EZH2 and DNMT1 contribute to polyphyllin I-inhibited growth of castration-resistant prostate cancer cells in vitro and in vivo', *Biochimica et Biophysica Acta*, 1862(3), pp. 589–599.

Swanton, C. *et al.* (2009) 'Chromosomal instability determines taxane response', *Proceedings of the National Academy of Sciences*, 106(21), pp. 8671–8676.

Tabach, Y. *et al.* (2007) 'Wide-Scale Analysis of Human Functional Transcription Factor Binding Reveals a Strong Bias towards the Transcription Start Site', *PLoS ONE*, 2(8), p. e807.

Takashima, T. *et al.* (2018) 'Safety and Efficacy of Low-dose Nanoparticle Albumin-bound Paclitaxel for HER2-negative Metastatic Breast Cancer', *Anticancer Research*, 38(1), pp. 379–383.

Tang, Q. and Hann, S. S. (2018) 'HOTAIR: An oncogenic long non-coding RNA in human cancer', *Cellular Physiology and Biochemistry*, 47(3), pp. 893–913.

The Cleveland Clinic Foundation (2017) *Benign Prostatic Enlargement (BPH)*. Available at: https://my.clevelandclinic.org/health/articles/benign-enlargement-of-the-prostate.

Toledo-pereyra, L. H. (2001) 'Discovery in Surgical Investigation: The Essence of Charles Brenton Huggins', *Journal of Investigative Surgery*, 14(5), pp. 251–252.

Tran, C. et al. (2009) 'Development of a Second-Generation Antiandrogen for Treatment of Advanced Prostate Cancer', *Science*. 324(5928), pp. 787-790.

Tsaur, I. *et al.* (2019) 'Aggressive variants of prostate cancer – Are we ready to apply specific treatment right now?', *Cancer Treatment Reviews*, 75, pp. 20–26.

Varbiro, G *et al.* (2001) 'Direct effect of Taxol on free radical formation and mitochondrial permeability transition.', *Free Radic Biol Med.*, 31(4), pp. 548–58.

Varbiro, Gabor *et al.* (2001) 'Direct effect of Taxol on free radical formation and mitochondrial permeability transition', *Free Radical Biology and Medicine*, 31(4), pp. 548–558.

Vogel, A. *et al.* (2016) 'Efficacy and safety profile of nab-paclitaxel plus gemcitabine in patients with metastatic pancreatic cancer treated to disease progression: A subanalysis from a phase 3 trial (MPACT)', *BMC Cancer*. BMC Cancer, 16(1), p. 817.

Vogler, M. *et al.* (2009) 'Concurrent up-regulation of BCL-XL and BCL2A1 induces approximately 1000-fold resistance to ABT-737 in chronic lymphocytic leukemia', *Blood*, 113(18), pp. 4403–4413.

Vogler, M. (2012) 'BCL2A1: The underdog in the BCL2 family', *Cell Death and Differentiation*, 19(1), pp. 67–74.

Wang, L. G. *et al.* (1999) 'The effect of antimicrotubule agents on signal transduction pathways of apoptosis: A review', *Cancer Chemotherapy and Pharmacology*, 44(5), pp. 355–361.

Wang, N. *et al.* (2019) 'Pivotal prognostic and diagnostic role of the long non-coding RNA colon cancer-associated transcript 1 expression in human cancer (Review)', *Molecular Medicine Reports*, 19(2), pp. 771–782.

Wang, Q. *et al.* (2019) 'Long noncoding RNA Linc02023 regulates PTEN stability and suppresses tumorigenesis of colorectal cancer in a PTEN-dependent pathway', *Cancer Letters*. Elsevier, 451, pp. 68–78.

Wang, X., Yang, B. and Ma, B. (2016) 'The UCA1/miR-204/Sirt1 axis modulates docetaxel sensitivity of prostate cancer cells', *Cancer Chemotherapy and Pharmacology*, 78(5), pp. 1025–1031.

Wang, Y. *et al.* (2016) 'Long non-coding RNA LINC00161 sensitises osteosarcoma cells to cisplatin-induced apoptosis by regulating the miR-645-IFIT2 axis', *Cancer Letters*, 382(2), pp. 137–146.

Wang, Yingjun *et al.* (2017) 'Discovery and validation of the tumor-suppressive function of long noncoding RNA PANDA in human diffuse large B-cell lymphoma through the inactivation of MAPK/ERK signaling pathway', *Oncotarget*, 8(42), pp. 72182–72196.

Wani, M. C. *et al.* (1971) 'Plant Antitumor Agents.VI.The Isolation and Structure of Taxol, a Novel Antileukemic and Antitumor Agent from Taxus brevifolia', *Journal of the American Chemical Society*, 93(9), pp. 2325–2327.

Weaver, B. A. (2014) 'How Taxol/paclitaxel kills cancer cells', *Molecular Biology of the Cell*, 25(18), pp. 2677–2681.

Wei, J. *et al.* (2018) 'Long non-coding RNA H19 promotes TDRG1 expression and cisplatin resistance by sequestering miRNA-106b-5p in seminoma', *Cancer Medicine*, 7(12), pp. 6247–6257.

de Wit, R. *et al.* (2019) 'Cabazitaxel versus Abiraterone or Enzalutamide in Metastatic Prostate Cancer', *New England Journal of Medicine*, pp. 1–13.

206

Wu, C. and Luo, J. (2016) 'Long non-coding RNA (lncRNA) urothelial carcinoma-associated 1 (UCA1) enhances tamoxifen resistance in breast cancer cells via inhibiting mTOR signaling pathway', *Medical Science Monitor*, 22, pp. 3860–3867.

Wu, G. *et al.* (2017) 'Mp99-17 Circularrna-C17 Alters the Anti Androgen-Enzalutamide Resistance in Castration-Resistant Prostate Cancer Via Regulating Androgen Receptor Variant Arv7 Expression', *The Journal of Urology*, 197(4), pp. 1326–1327.

Wu, Q. *et al.* (2017) 'Long noncoding RNA PVT1 inhibits renal cancer cell apoptosis by up-regulating Mcl-1', *Oncotarget*, 8(60), pp. 101865–101875.

Wu, X. *et al.* (2018) 'Long noncoding RNA BLACAT1 modulates ABCB1 to promote oxaliplatin resistance of gastric cancer via sponging miR-361', *Biomedicine and Pharmacotherapy*. Elsevier, 99(December 2017), pp. 832–838.

Xia, L. *et al.* (2006) 'Upregulation of Bfl-1/A1 in leukemia cells undergoing differentiation by all-trans retinoic acid treatment attenuates chemotherapeutic agent-induced apoptosis', *Leukemia*, 20(6), pp. 1009–1016.

Xin, L. (2013) 'Cells of origin for cancer: an updated view from prostate cancer', *Oncogene*, 32(32), pp. 3655–3663.

Xu, C. G. *et al.* (2016) 'Exosomes mediated transfer of lncRNA UCA1 results in increased tamoxifen resistance in breast cancer cells', *European review for medical and pharmacological sciences*, 20(20), pp. 4362–4368.

Xu, L.-C. *et al.* (2017) 'Up-regulation of LINC00161 correlates with tumor migration and invasion and poor prognosis of patients with hepatocellular carcinoma.', *Oncotarget*, 8(34), pp. 56168–56173.

Xu, M. *et al.* (2019) 'Linc00161 regulated the drug resistance of ovarian cancer by sponging microRNA-128 and modulating MAPK1', *Molecular Carcinogenesis*, 58(4), pp. 577–587.

Xu, X. *et al.* (2017) 'Potential therapeutic effect of epigenetic therapy on treatment -induced neuroendocrine prostate cancer', *Asian Journal of Andrology*, 19(6), pp. 686-693.

Xu, Y. *et al.* (2018) 'Predictive value of BRCA1/2 mRNA expression for response to neoadjuvant chemotherapy in BRCA negative breast cancers.', *Cancer science*, 109(1), pp. 166–173.

Xue, D. *et al.* (2018) 'Long noncoding RNA MALAT1 enhances the docetaxel resistance of prostate cancer cells via miR-145-5p-mediated regulation of AKAP12', *Journal of Cellular and Molecular Medicine*, 22(6), pp. 3223–3237.

Yadav, S. S. *et al.* (2016) 'Combination effect of therapies targeting the PI3K- and ARsignaling pathways in prostate cancer', *Oncotarget*, 7(46), pp. 76181–76196.

Yadav, S. S. *et al.* (2017) 'Induction of Neuroendocrine Differentiation in Prostate Cancer Cells by Dovitinib (TKI-258) and its Therapeutic Implications', *Translational Oncology*, 10(3), pp. 357–366.

Yang, C. C., Hsu, C. P. and Yang, S. Der (2000) 'Antisense suppression of proline-directed protein kinase F(A) enhances chemosensitivity in human prostate cancer cells', *Clinical*

Cancer Research, 6(3), pp. 1024–1030.

Yang, C., Pan, Y. and Deng, S. P. (2019) 'Downregulation of lncRNA CCAT1 enhances 5-fluorouracil sensitivity in human colon cancer cells', *BMC Molecular and Cell Biology*. BMC Molecular and Cell Biology, 20(1), pp. 1–11.

Yap, K. L. *et al.* (2010) 'Molecular Interplay of the Non-coding RNA ANRIL and Methylated Histone H3 Lysine 27 by Polycomb CBX7 in Transcriptional Silencing of INK4a', *Mol Cell.*, 38(5), pp. 662–674.

Ying, L. *et al.* (2012) 'Upregulated MALAT-1 contributes to bladder cancer cell migration by inducing epithelial-to-mesenchymal transition', *Molecular BioSystems*, 8(9), pp. 2289–2294.

Yoshimizu, T. *et al.* (2008) 'The H19 locus acts in vivo as a tumor suppressor', *Proc Natl Acad Sci*, 105(34), pp. 12417–12422.

Yu, E. Y. *et al.* (2018) 'A randomized phase 2 study of a HSP27 targeting antisense, apatorsen with prednisone versus prednisone alone, in patients with metastatic castration resistant prostate cancer', *investigational New Drugs*. Investigational New Drugs, 36(2), pp. 278–287.

Yun, S. J. *et al.* (2015) 'Urinary MicroRNAs of Prostate Cancer: Virus-Encoded hsv1-miR-H18 and hsv2-miR-H9-5p Could Be Valuable Diagnostic Markers', *International Neurourology Journal*, 19(2), pp. 74–84.

Zaffuto, E. *et al.* (2017) 'Contemporary Incidence and Cancer Control Outcomes of Primary Neuroendocrine Prostate Cancer: A SEER Database Analysis', *Clinical Genitourinary Cancer*, 15(5), pp. e793-e800.

Zhang, B. *et al.* (2018) 'Long non-coding RNA EPIC1 promotes human lung cancer cell growth', *Biochemical and Biophysical Research Communications*, 503(3), pp. 1342–1348.

Zhang, C. yang *et al.* (2015) 'The role of CCL20/CCR6 axis in recruiting Treg cells to tumor sites of NSCLC patients', *Biomedicine and Pharmacotherapy*, 69, pp. 242–248.

Zhang, L. *et al.* (2019) 'A multi-functional therapy approach for cancer: targeting Raf1-mediated inhibition of cell motility, growth and interaction with the microenvironment', *Molecular Cancer Therapeutics*, pp. 1-42.

Zhang, Y. *et al.* (2018) 'Androgen deprivation promotes neuroendocrine differentiation and angiogenesis through CREB-EZH2-TSP1 pathway in prostate cancers', *Nature Communications*, 9(4080).

Zheng, P. *et al.* (2019) 'Long noncoding RNA CASC2 promotes paclitaxel resistance in breast cancer through regulation of miR-18a-5p/CDK19', *Histochemistry and Cell Biology*, 152(4), pp. 281-291.

Zhu, F. *et al.* (2017) 'Downregulation of lncRNA TUBA4B is Associated with Poor Prognosis for Epithelial Ovarian Cancer', *Pathol. Oncol. Res.*, 24(2), pp. 419-425.

Zhu, W., Li, Y. and Gao, L. (2015) 'Cisplatin in combination with programmed cell death protein 5 increases antitumor activity in prostate cancer cells by promoting apoptosis', *Molecular Medicine Reports*, 11(6), pp. 4561–4566.

Zielinski, C. *et al.* (2016) 'Bevacizumab plus paclitaxel versus bevacizumab plus capecitabine as first-line treatment for HER2-negative metastatic breast cancer (TURANDOT): primary endpoint results of a randomised, open-label, non-inferiority, phase 3 trial', *The Lancet Oncology*, 17(9), pp. 1230–1239.

Zong, L. *et al.* (2019) 'LINC00162 confers sensitivity to 5-Aza-2'-deoxycytidine via modulation of an RNA splicing protein, HNRNPH1', *Oncogene*, 38(26), pp. 5281–5293.